RICE UNIVERSITY

Steric Considerations in Copper(I)-olefin Complexes Incorporating Substituted *Bis*(2-pyridyl)amines

by

JOHN J. ALLEN

A THESIS SUBMITTED
IN PARTIAL FULFILLMENT OF THE
REQUIREMENTS FOR THE DEGREE OF
DOCTOR OF PHILOSOPHY

APPROVED, THESIS COMMITTEE

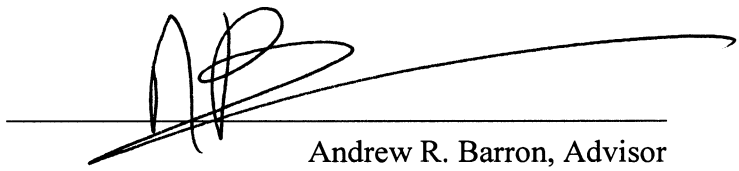

Andrew R. Barron, Advisor
Charles W. Duncan, Jr. - Welch Chair of Chemistry
Professor of Chemistry and Materials Science

Kenton H. Whitmire
Associate Dean for Academic Affairs, Weiss School of Natural Sciences
Professor of Chemistry

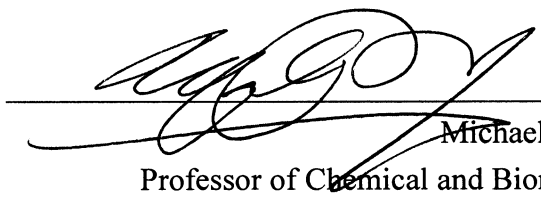

Michael S. Wong
Professor of Chemical and Biomolecular
Engineering and Chemistry

Houston, TX
January, 2011

Abstract

Steric Considerations in Copper(I)-olefin Complexes Incorporating Substituted *Bis*(2-pyridyl)amines

by

John J. Allen

The separation of olefin isomers by traditional methods (e.g., distillation) is generally a costly process, as the range of phase-transition temperatures for a given set of isomers is usually quite small. Complexes of the type [Cu(H-dpa)(η^2-olefin)]BF_4 have been prepared for numerous aliphatic/aromatic α-olefins, internal *cis-*/*trans*-aliphatic/aromatic olefins, as well as for cyclic olefins (2-norbornylene and 1,5-cyclooctadiene). Preparation of complexes and characterization via ^1H and ^{13}C NMR, FT-IR, and TG/DTA reveals clear trends amongst compounds in the different spectroscopic methods. Of particular note is the direct relation between olefin dissociation temperature (TG/DTA) and upfield NMR shifts, Δδ, for olefin signals, giving a convenient means of assessing complex strength. Molecular structures of several such olefin complexes have been determined via single crystal X-ray diffraction. Features in the determined structural geometries are discussed. Theoretical models served to predict advantageous structural changes (i.e., steric preference for a given isomer) in complexes having functionalized ancillary ligands. Aryl substitution at the amine nitrogen yielded subtle distortions to calculated geometries, loosely indicating preferential binding of terminal and *cis*-olefin isomers. The synthesis of several novel di(pyridyl)amine [ArN(2-py)$_2$: Ar = Ph, Mes, 2,6-$Et_2C_6H_3$, 2-^{i}PrC_6H_4, 2,6-$^i Pr_2C_6H_3$, and 1-naph] and di(quinolyl)amine [ArN(2-quin)$_2$: Ar = Mes and 2,6-$^i Pr_2C_6H_3$] ligands was accomplished via Buchwald-Hartwig type palladium-catalyzed cross-coupling of the appropriate halogenated heterocycle with substituted anilines (2:1 molar ratio). Asymmetric (pyridyl)(quinolyl)amines [ArN(2-

py)(2-quin): Ar = H, Ph, Mes, 2,6-$^{i}Pr_2C_6H_3$] were prepared in a similar manner, with two steps in the coupling reactions: (1) initial 1:1 molar ratio of 2-bromopyridine:aniline allowed the isolation of aryl(pyridyl)amine compounds [ArN(H)py: Ar = Ph, Mes, 2,6-$Et_2C_6H_3$, 2-$^{i}PrC_6H_4$, 2,6-$^{i}Pr_2C_6H_3$, and 1-naph]. A second cross-coupling with 2-chloroquinoline resulted in the desired ArN(2-py)(2-quin) ligand. Characterization of new ligands was performed via ^{1}H and ^{13}C NMR, EI-MS, FT-IR, TG/DTA, and X-ray crystallography; the resulting trends from spectroscopic and structural data are discussed. Synthesis and spectroscopic/structural investigations of complexes incorporating novel ligands were initially performed on protonated salts, e.g., [H(Ar-dpa)]BF_4, in addition to dimeric copper(II) complexes [Cu(Ar-dpa)(Cl)(μ-Cl)]$_2$. Structural data confirmed theoretical predictions concerning distortions in complexed-ligand geometry. Thus, complexes [Cu(R-dpa)(η^2-olefin)]BF_4 (where R = Ph, Mes, 2-$^{i}PrC_6H_4$, and 1-naph) were then prepared for styrene, as well as several internal *cis*/*trans*-octenes. TG/DTA and ^{13}C NMR data indicate an increasing difference in complex strength between *cis*/*trans*-3-octene complexes as the substituent is varied from R = H (smallest difference in strength), to R = Mes, to R = 2-$^{i}PrC_6H_4$ (largest difference in strength). Thus, the identity of the remote ligand substituent (Ar) controls the differentiation of binding between *cis*- and *trans*-isomers, as a consequence of increased ligand geometric distortion.

Acknowledgements

When I first started in July of 2006, my advisor, Professor Andrew R. Barron, described graduate school as "...the only time you will ever get to tell your boss what you want to do." I soon found that statement was made in complete sincerity; as I was looking for a research project with a focus on inert synthesis, crystallography, and/or kinetic studies, I was unable to motivate myself to acid-wash SWNT's for the remainder of my graduate career. Three months into my first semester, Dr. Barron came to me with the initial ideas for the present study. Above all, I would like to thank him for his patience, humor, and wisdom, which have allowed me to go my own pace, develop the skills of a well-rounded organometallic chemist, and enjoy myself at the same time.

I would also like to thank the two other members of my defense committee, Professor Kenton H. Whitmire and Professor Michael S. Wong, for their time and consideration (considering the length of this document).

I need also to thank my wife, for her patience and love, as I'm sure that any other woman in her right mind would have cast me aside by now. I thank my son, who can put a smile on my face on the darkest of days, for everything that he does.

Additionally, I have to thank all group members, both past and present, as it never hurts to be surrounded by bright minds. I owe Dr. Christopher E. Hamilton a tremendous debt for the role he played in ligand synthesis, about half of which he made. Last, but certainly not least, without the hard work and dedication of Dr. Lawrence B. Alemany and Richard Crouse to their respective instrument laboratories, I would have little to show for the last four years. I am forever grateful for their efforts.

Table of Contents

List of Figures

List of Tables

List of Compounds

1.1	[Cu(H-dpa)(η^2-ethylene)]BF_4
1.2	[Cu(H-dpa)(η^2-propylene)]BF_4
1.3	[Cu(H-dpa)(η^2-1-butene)]BF_4
1.4	[Cu(H-dpa)(η^2-1-hexene)]BF_4
1.5	[Cu(H-dpa)(η^2-1-octene)]BF_4
1.6	[Cu(H-dpa)(η^2-*cis*-2-octene)]BF_4
1.7	[Cu(H-dpa)(η^2-*trans*-2-octene)]BF_4
1.8	[Cu(H-dpa)(η^2-*cis*-3-octene)]BF_4
1.9	[Cu(H-dpa)(η^2-*trans*-3-octene)]BF_4
1.1	[Cu(H-dpa)(η^2-norbornylene)]BF_4
1.11	[Cu(H-dpa)(η^2,$\eta^{2'}$-1,5-cyclooctadiene)]BF_4
1.12	[Cu(H-dpa)(η^2-styrene)]BF_4
1.13	[Cu(H-dpa)(η^2-*cis*-stilbene)]BF_4
1.14	[Cu(H-dpa)(η^2-*trans*-stilbene)]BF_4
1.15	[Cu(H-dpa)(η^2-$Ph_2C{=}CH_2$)]BF_4
2.1	MesN(H)py
2.2	2,6-$Et_2C_6H_3$N(H)py
2.3	2-^{i}PrC_6H_4N(H)py
2.4	Ph_3CN(H)py
2.5	MesN$(py)_2$ / Mes-dpa
2.6	2,6-$Et_2C_6H_3$N$(py)_2$ / 2,6-Et_2Ph-dpa
2.7	2-^{i}PrC_6H_4N$(py)_2$ / 2-^{i}PrPh-dpa
2.8	2,6-^{i}Pr$_2C_6H_3$N$(py)_2$ / 2,6-^{i}Pr$_2$Ph-dpa
2.9	1-naphN$(py)_2$ / naph-dpa
2.1	HN(py)quin / H-pqa
2.11	PhN(py)quin / Ph-pqa

2.12	MesN(py)quin / Mes-pqa
2.13	2,6-$^{i}Pr_2C_6H_3$N(py)quin / 2,6-$^{i}Pr_2$Ph-pqa
2.14	MesN(quin)$_2$ / Mes-dqa
2.15	2,6-$^{i}Pr_2C_6H_3$N(quin)$_2$ / 2,6-$^{i}Pr_2$Ph-dqa
2.16	MesN{2-quin-[N-(2'-quin)]}
3.1	[H(Mes-dpa)]BF_4
3.2	[H(2-$^{i}PrC_6H_4$-dpa)]BF_4
3.3	[H(Ph-pqa)]BF_4
3.4	[H(Mes-pqa)]BF_4
3.5	[H(2,6-$^{i}Pr_2C_6H_3$-dqa)]BF_4
3.6	[Cu{MesN(H)py}$_2$]BF_4
3.7	[Cu(Ph-dpa)Cl_2]$_2$
3.8	[Cu(2-$^{i}PrC_6H_4$-dpa)Cl_2]$_2$
3.9	[Cu(naph-dpa)Cl_2]$_2$
3.1	[Cu(Ph-pqa)Cl_2]
3.11	[Cu(Mes-dpa)(μ-OH)(H_2O)]$_2$[BF_4]$_2$
3.12·(MeOH)	[Cu(2,6-$^{i}Pr_2C_6H_3$-dqa)$_2$]BF_4·(MeOH)
3.12·(tol)	[Cu(2,6-$^{i}Pr_2C_6H_3$-dqa)$_2$]BF_4·(tol)
4.1	[Cu(Ph-dpa)(η^2-styrene)]BF_4
4.2	[Cu(Mes-dpa)(η^2-styrene)]BF_4
4.3	[Cu(2-$^{i}PrC_6H_4$-dpa)(η^2-styrene)]BF_4
4.4	[Cu(1-naph-dpa)(η^2-styrene)]BF_4
4.5	[Cu(Mes-dpa)(η^2-norbornylene)]PF_6
4.6	[Cu(2-$^{i}PrC_6H_4$-dpa)(η^2-norbornylene)]BF_4
4.7	[Cu(Mes-dpa)(η^2-*cis*-3-octene)]BF_4
4.8	[Cu(Mes-dpa)(η^2-*trans*-3-octene)]BF_4
4.9	[Cu(2-$^{i}PrC_6H_4$-dpa)(η^2-*cis*-3-octene)]BF_4

4.1	[Cu(2-^{i}PrC$_6$H$_4$-dpa)(η^2-*trans*-3-octene)]BF$_4$
4.11	[Cu(2-^{i}PrC$_6$H$_4$-dpa)(η^2-*cis*-4-octene)]BF$_4$
4.12	[Cu(2-^{i}PrC$_6$H$_4$-dpa)(η^2-*trans*-4-octene)]BF$_4$
5.1	[Ag(H-dpa)(η^2-styrene)]BF$_4$
6.1	[Cu$_2$(μ-tpy)$_2$(MeCN)$_2$][BPh$_4$]$_2$
D.1	Methylated Meerwin's ester: C$_{18}$H$_{22}$O$_{10}$

Abbreviations and Glossary

Å	Angstroms, 10^{-10} m
ADP	atomic displacement parameter
Ar	aryl group (general)
ATR	attenuated total reflectance
br	broad
bu	1-butene
$Cg_{(R)}$	center of gravity of specified group, R
*c*2o / *c*2oct	*cis*-2-octene
cod	1,5-cyclooctadiene
csbn	*cis*-1,2-diphenylethylene (*cis*-stilbene)
δ	chemical shift
$\delta_{C=C}$	aromatic ring deformation/stretching
Δδ	change in chemical shift (i.e., free L to complexed L)
Δ_{MPLN}	mean-plane angle difference
$\Delta\rho_{max,min}$	maximum/minimum residual electron density
dba	dibenzylideneacetone
D_{calc}	calculated density
dpa	*bis*(2-pyridyl)amine
dpe	1,1-diphenylethylene
DPPF	*bis*(diphenylphosphino)ferrocene
dqa	*bis*(2-quinolyl)amine
esd	estimated standard deviation
et	ethylene
FT-IR	fourier transform infrared spectroscopy
GC-MS	gas chromatography mass spectrometry
η^2	hapticity of 2; coordination via two C atoms

hx	1-hexene
^{i}Pr	isopropyl
J(H-H)	coupling constant for ^{1}H-^{1}H
λ	wavelength of radiation
L_n	chelate ligand of n coordination sites
(μ-X)	atom/ligand (X) bridging metal centers
μ	absorption coefficient; micro (10^{-6}), as unit prefix
M^+	molecular ion
Mes	mesityl
M_w	molecular weight
naph	1-naphthyl
$\nu_{C\text{-}H}$	C-H stretching mode (FT-IR)
nbn	2-norbornene
NCS	non-crystallographic symmetry
neat	pure compound (i.e., no solvent/mulling agent)
NMR	nuclear magnetic resonance spectroscopy
p-, *m*-, *o*-C*H*, Ar	designation of *para*-, *meta*-, or *ortho*-H in aryl group, Ar
ppm	parts per million
ppn	propylene
pqa	N-(2-pyridyl)-N-(2-quinolyl)amine
py	pyridyl
quin	quinolyl
s.o.f.	site occupancy factor (crystallographic disorder)
sty	styrene
*t*2o / *t*2oct	*trans*-2-octene
TG/DTA	thermogravimetric/differential thermal analysis
tpy	2,2':6',6"-terpyridine

tsbn	*trans*-1,2-diphenylethylene (*trans*-stilbene)
w, m, s, vs	weak, medium, strong, very strong (FT-IR bands)
Z	formula units per unit cell

Introduction

As the largest volume feedstock in the chemical and petrochemical industry, olefins are used in the production of polymers, acids, alcohols, esters, and ethers. Unfortunately, olefin production is extremely energy intensive, generally requiring separation from their alkane counterparts (olefin/paraffin separation).[1] More problematic is the separation of particular olefins from an isomeric mixture, considering the range of phase-transition temperatures for a given set of isomers is usually small. For instance, the seven n-octene isomers, as well as a number of branched C_8 isomers, are reported[2] to have boiling points that fall within only a 4.5 °C range (see Table I.1).[3] As a distillation process operates based upon differences in relative volatilities, it is only reasonable that some other means of separation is needed to achieve the desired increase in efficiency.

Table I.1. Boiling points (°C) for several isomers of C_8H_{16}.

1-octene	121.3	2-methyl-2-heptene	122.6
cis-2-octene	125.6	3-methyl-2-heptene	122.3
trans-2-octene	125.0	4-methyl-3-heptene	122.4
cis-3-octene	122.9	3-ethyl-2-hexene	121.1
trans-3-octene	123.3	2,3-dimethyl-2-hexene	121.7
cis-4-octene	122.5	2-ethyl-1-hexene	121.1
trans-4-octene	122.3		

The simplest of olefins, ethylene ($H_2C=CH_2$), has been shown to take part in a variety of biological processes; specifically, ethylene is of some importance regarding plant development, ranging in use from germination and growth to sex expression and fruit ripening.[4] Moreover, considering the multitude of transition metals thought to be present in biological systems, the only known metal-ethylene interaction is with copper.[5]

This assortment of naturally occurring processes has inspired a great deal of work dedicated to understanding this interaction, which has found applications in catalysis[6] as well as industrial processing of hydrocarbon feedstocks.[7] The large volumes of olefins produced and the required purity for most applications provide strong incentives for novel purification approaches.

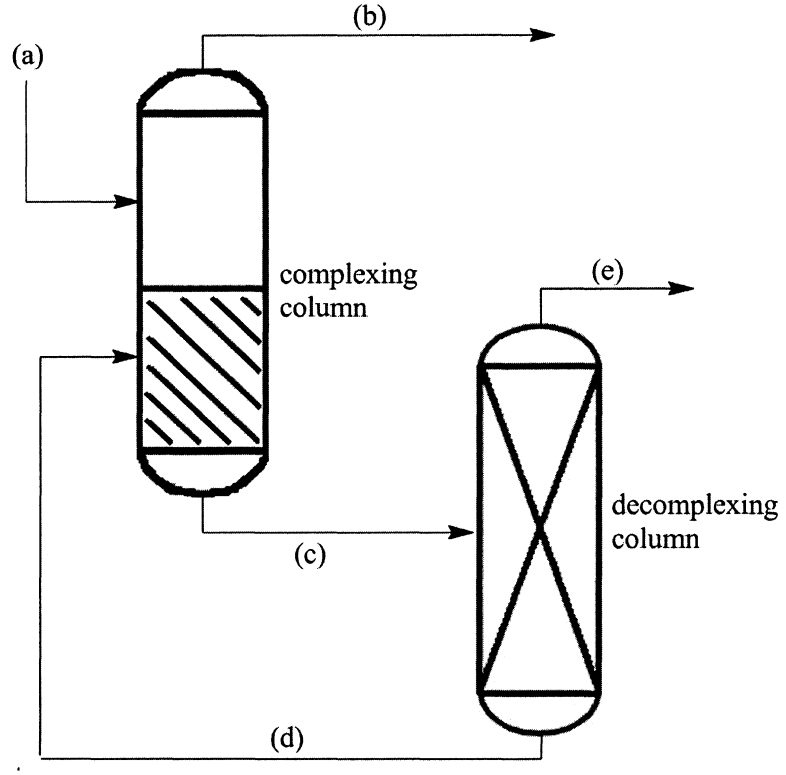

Figure I.1. Extractive distillation process flow diagram: (a) hydrocarbon feedstock-olefin mixture; (b) *cis-/trans*-olefin rich stream for further processing; (c) polar layer-(L^n)M-[α-olefin]; (d) recycle (L^n)M-[solvent]; (e) purified α-olefin stream. Adapted from A. E. Wentink, et al., *Sep. Purif. Technol.*, 2005, **43**, 149.

The development of metal complexes incorporating sterically directive ancillary ligands tailored to the selective removal of olefins from their isomeric counterparts is currently of great interest in the petroleum/petrochemical industries.[8] To this end, various

complexing reagents have been described,[9] where the function of the complexing agent is to coordinate one particular isomer of an olefin in preference to another.[10] A great deal of effort has been put forth in the study of simple copper(I) and silver(I) salts, serving as olefin-complexing agents. Proposed processes for these separations range from membrane applications[11] and ionic-liquids[6i] to LLE and reactive extractive distillation (see Figure I.1).[12]

Past synthetic studies have shown the Cu-olefin bond to be rather labile, but enhanced stability can be achieved incorporating chelate ligands that encourage metal to olefin back-donation. The most widely accepted model for the metal-olefin interaction is that developed by Dewar, Chatt, and Duncanson.[13] The Dewar-Chatt-Duncanson (DCD) model (Figure I.2)[14] describes the metal-olefin interaction as two-fold: (1) a σ-donation from the filled olefin π-bonding orbital to an empty metal 4s orbital (for the case of copper), and (2) a π back-donation from a filled metal 3d orbital to the empty π^* anti-bonding olefin orbital.[15] The contribution of each interaction towards overall complex stability remains a subject of debate, with reports that π back-donation contributes from 1/6 to 1/3 of the covalent bond character.[16]

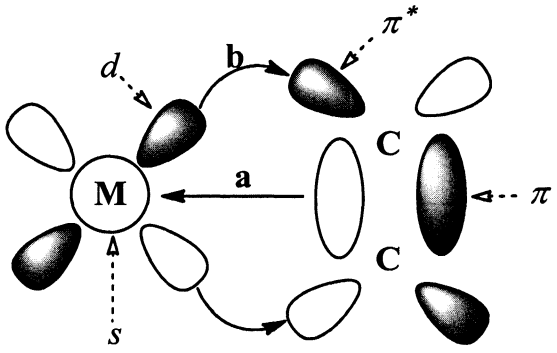

Figure I.2. Molecular orbital representation of the Dewar-Chatt-Duncanson model for the interaction between metal and olefin. Adapted from N. N. Greenwood and A. Earnshaw, *Chemistry of the Elements,* 2nd Ed, Reed Educational and Professional Publishing, Ltd., London, 2001.

A physical consequence of this interaction can be seen in lengthening of the C=C bond. This is due, in part, to depletion of C=C π-bonding electron density to form the metal-olefin σ-bond. The primary cause of lengthening, however, is the degree of metal back-donation.[17] As the olefin π^*-antibonding orbitals gain electron density, the alkene carbons partially shift from sp^2 to sp^3 hybridization, causing a partial decrease in C=C bond order. This shift in hybridization also causes alkene substituents to bend slightly out of plane, away from the metal (Figure I.3).

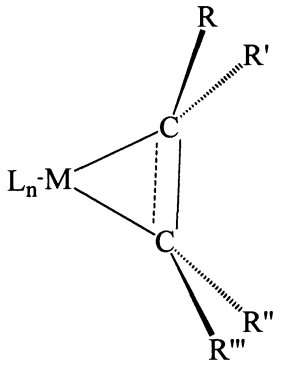

Figure I.3. Generalized geometry for metal olefin π-complexes, illustrating the shift in C_{olefin} hybridization from sp^2 to some intermediate between sp^2 and sp^3, as can be seen by olefin substituents deviation from co-planarity. Adapted from R. H. Crabtree, *The Organometallic Chemistry of the Transition Metal Elements*. 3rd ed., New York: John Wiley and Sons, Inc., (2001).

The primary factors that influence the overall stability of a given metal complex include: (1) basicity of the donor atom; (2) covalent tendency of the metal ion; (3) charge neutralization (if present) on complexation; (4) increase in translational enthalpy, i.e., the classical chelate effect; (5) steric effects; and (6) ligand pre-organization.[18] Complexes in which the metal center is electron rich and the olefin substituents are electron withdrawing exhibit a large degree of □back-bonding, creating more shared electron density between metal and olefin, and therefore a stronger interaction. In particular, low

oxidation state metals, e.g., Ni(0), Pd(0), Pt(0), result in a high degree of back-donation. Conversely, metals such as Hg(II), Ag(I), and Cu(I) are notorious in forming rather labile π-complexes.

The degree of back-donation is also affected by the nature of any substituents present on the olefin; specifically, electron withdrawing groups have been shown to promote back-donation. A direct comparison can be seen for C=C bond lengthening in coordinated ethylene [2.358(9) Å] and tetrafluoroethylene [1.405(7) Å] within the same molecule [$(C_5H_5)Rh(C_2H_4)(C_2F_4)$].[19] The archetypical case of extreme back-donation is found in complexes of tetracyanoethylene,[20] in which, the cyano- groups of the olefin sufficiently draw electrons from the metal center to create a so-called metallocyclopropane.[21] Complexes toward this extreme have such a high degree of C=C lengthening, bond lengths can approach those expected for a C-C single bond.[22] As a result of the combined C=C bond lengthening and shortened M-C distances for strong interactions, the C-M-C bond angle also increases with the degree of interaction.

It has been well-established that the nature of the ancillary ligand in a given metal-olefin complexes has an impact on the various donor/acceptor orbitals, and thus affects the amount of electron sharing (Figure I.4)[15]. Consequently, this is reflected in complex geometry and overall stability.[23]

Nominally, the most stable complexes have been prepared with chelating, strongly Lewis-basic ancillary ligands, in which the enhanced chelate-to-metal σ-donation creates an electron-rich copper-center, thereby promoting π back-donation. Thus, the most robust of complexes often incorporate anionic ancillary ligands, such as the O-donor hexafluoro(acac) or trifluoroacetate chelates,[24] iminophosphinamide,[25] β-diketiminato;[26] or one of the several previously reported fluorinated *tris*(pyrazolyl)borate derivatives,[27] some of which are reported as stable towards atmospheric conditions, as well as towards olefin loss under reduced pressure.[27a]

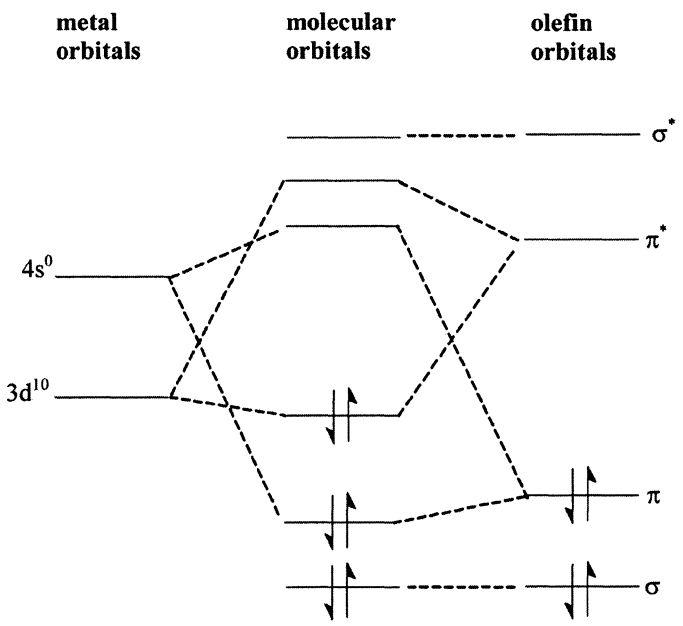

Figure I.4. Energy level diagram proposed for the Dewar-Chatt type copper(I)-olefin interaction. Adapted from R. G. Salomon and J. K. Kochi, *J. Organomet. Chem.*, 1974, **64**, 135.

More recently, stable complexes of ethylene, 1-hexene, allyl ethyl ether, cyclohexene, and styrene have been reported incorporating a more sterically demanding hydro-*tris*((3-mesityl)pyrazolyl)borate ligand.[27a] This report presents the case in which steric limitations dominate over electronic factors in the overall complex stability. Furthermore, the paper cautions against conclusions drawn from NMR spectral data alone, as the complexes reported therein have deceptively large $\Delta\delta(^1H)$ and $\Delta\delta(^{13}C)$ values, resulting from aromatic ring anisotropy from the ancillary ligand. Midway between strongly σ-donating anionic ligands and weakly donating heterocyclic chelates lie neutral, tridentate amino-ligands. For example, pentamethyldiethylenetriamine, has been used to prepare copper(I) complexes of several olefin monomers.[6,28,29] Similarly, various copper(I) complexes incorporating 1,4-diaza-1,3-diene-type di(imine) chelates of ethylene and cyclohexene have been reported to be moderately stable.[30]

On the opposite side of the N-donor chelate spectrum, ancillary ligands with a softer character (i.e., less basic) generally result in complexes with a more labile metal-olefin bond. In spite of their increased stability, the incorporation of strong σ-donor chelate ligands into complexes intended for olefin separations is undesirable, as a complexed olefin needs also to be removed with relative ease. Ultimately, the choice of ancillary ligand is a delicate balance between complex stability and relative ease of olefin recovery. Complexes observed to most closely approximate this desired behavior have been reported using neutral chelating heterocyclic compounds, including *bis*(pyrazolyl)methanes,[31] dipyridylamine,[32] and bipyridines.[33,34] The report by Thompson and Whitney demonstrating that *bis*(2-pyridyl)amine (R-dpa, **I** where R = H), can produce stable, yet reversibly bound copper(I)-olefin complexes (**II**), has formed the basis for our efforts towards alternative methods in olefin separations.[35]

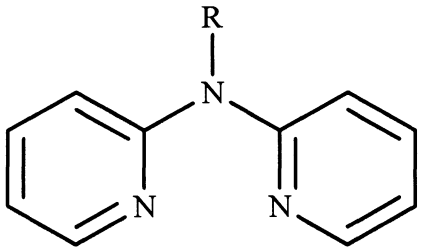

(I)

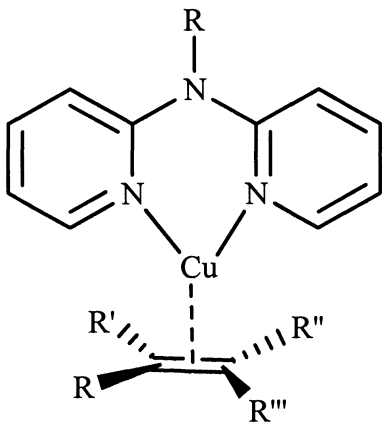

(II)

R = H, Ph, Mes, 2-^{i}PrPh, and 1-naph

References

1 J. L. Humphrey, A. F. Seibert and R. A. Koort, *Separation Technologies: Advances and Priorities*, DOE/ID/12920-1, Washington, DC 1001.

2 K. N. Campbell and L. T. Eby, *J. Am. Chem. Soc.*, 1941, **63**, 216.

3 L. Berg and R. W. Wytcherley, *Separation of 1-octene from its isomers by azeotropic and extractive distillation*, US Patent 5,262,015, 1993.

4 (a) J. R. Ecker, *Science*, 1995, **268**, 667. (b) J. S. Thompson, R. L. Harlow, and J. F. Whitney, *J. Am. Chem. Soc.*, 1983, **105**, 3522. (c) F. I. Rodriguez, J. J. Esch, A. E. Hall, B. M. Binder, G. E. Schaller, and A. B. Bleeker, *Science*, 1999, **283**, 996. (d) G. E. Schaller, and A. B. Bleeker, *Science*, 1995, **270**, 1809.

5 F. A. Cotton, G. Wilkinson, C. A. Murillo, and M. Bochmann, *Advanced Inorganic Chemistry*. 6th ed., John Wiley & Sons, Inc, 1999.

6 (a) W. A. Braunecker, T. Pintauer, N. V. Tsarevsky, G. Kickelbick, and K. Matyjaszewski, *J. Organomet. Chem.*, 2005, **690**, 916. (b) L. Cavallo, M. E. Cucciolito, A. De Martino, F. Giordano, I. Orabona, and A. Vitagliano, *Chem. Eur. J.*, 2000, **6**, 1127. (c) Rios, R.; Liang, J.; Lo, M. M.-C.; Fu, G. C. *Chem. Comm.*, 2000, 377.

7 (a) G. C. Blytas, *Concentrated Cuprous Nitrate/Propionitrile Solutions as Complexing Agents for Olefin Separations*, US Patent Office, Editor. 1974, Shell Oil Company: United States. (b) R. E. Brown and R. L. Hair, *Monoolefin/Paraffin Separation by Selective Absorption*, 1993, Phillips Petroleum Company: United States. (c) J. B. Cooper and K. Small, *Process for Recovering Olefins from Gaseous Mixtures*, 1997, BP Chemicals Limited: United States. (d) J. C. Davis and R. J. Valus, *Removal of Olefins from Fluids*, EP Office, Editor, 1998, BP Chemicals Limited: England. (e) T. W. Evans, B. O. Blackburn, and J. R. Scheibli, *Recovery of Olefins*, US Patent Office, Editor, 1945, Shell Development Company: United States. (f) H. S. Kim, Y. J. Kim, J. J. Kim, S. D. Lee, Y. S. Kang, and C. S. Chin, *Chem. Mater.*, 2001, **13**, 1720. (g) J. F. Knifton, *Process for Separating Liquid Olefin-Paraffin Mixtures*, Texaco Inc., United States, 1979.

(h) C. L. Munson, L. C. Boudreau, M. S. Driver, and W. L. Schinski, *Separation of Olefins from Paraffins Using Ionic Liquid Solutions*, US Patent Office, Editor. Chevron U.S.A. Inc., 2002.

8 National Research Council, *Separation and Purification: Critical Needs and Opportunities*, National Academy Press, Washington, DC, 1987.

9 (a) E. R. Brown and R. L. Hair, *Monoolefin/paraffin separation by selective adsorption*, Phillips Petroleum Company, 1993. (b) H. Y. Huang, J. Padin, and R. T. Yang, *J. Phys. Chem. B*, 1999, **103**, 3206.

10 (a) K. Wang and E. I. Stiefel, *Science*, 2001, **291**, 106. (b) A. E. Wentink, D. Kockman, N. J. M. Kuipers, A. B. de Haan, J. Scholtz, and H. Mulder, *Chem. Eng. Proc. Des.*, 2007, **85**, 88. (c) M. E. Cucciolito, G. Flores, and A. Vitagliano, *Organomet.*, 2004, **23**, 15.

11 (a) W. S. W. Ho, *Polymeric Membrane and Process for Separating Aliphatically Unsaturated Hydrocarbons*, US Patent 5,015,268, 1991. (b) *Handbook of Membrane Separations*, Ed. By A. K. Pabby, S. S. H. Rizvi, and A. M. Sastre, 2009, Boca Raton, FL.

12 (a) A. E. Wentink, D. Kockman, N. J. M. Kuipers, A. B. de Haan, J. Scholtz, and H. Mulder, *Chem. Eng. Proc.*, 2007, **46**, 800. (b) D. J. Sarafik and R. B. Eldridge, *Ind. Eng. Chem. Res.*, 1998, **37**, 2571. (c) A. E. Wentink, D. Kockman, N. J. M. Kuipers, A. B. de Haan, J. Scholtz, and H. Mulder, *Ind. Eng. Chem. Res.*, 2005, **44**, 9221. (d) A. E. Wentink, D. Kockman, N. J. M. Kuipers, A. B. de Haan, J. Scholtz, and H. Mulder, *Sep. Purif. Technol.*, 2005, **43**, 149.

13 (a) M. J. S. Dewer, *Bull. Soc. Chim. Fr.*, 1951, **18**, C79. (b) J. Chatt and L. A. Duncanson, *J. Chem. Soc.*, 1953, 2939.

14 N. N. Greenwood and A. Earnshaw, *Chemistry of the Elements*. 2nd Ed., Reed Educational and Professional Publishing Ltd., London, 2001.

15 R. G. Salomon and J. K. Kochi, *J. Organomet. Chem.*, 1974, **64**, 135.

16 (a) M. S. Nachaev, V. M. Rayon, and G. Frenking, *J. Phys Chem. A*, 2004, **108**, 3134. (b) H. V. Rasika-Dias and J. Wu, *Eur. J. Inorg. Chem.*, 2008, 509.

17 R. H. Crabtree, *The Organometallic Chemistry of the Transition Metal Elements*. 3rd Ed., John Wiley and Sons Inc., New York, 2001.

18 A. E. Martelli, R. D. Hancock, and R. J. Motekaitis, *Coord. Chem. Rev.*, 1994, **133**, 39-65.

19 L. J. Guggenberger and R. Cramer, *J. Am. Chem. Soc.*, 1972, **94**, 3779.

20 (a) L. Manojlovic-Muir, K. W. Muir, and J. A. Ibers, *Discuss. Faraday Soc.*, 1969, 84. (b) F. R. Hartley, *Angew. Chem. Int. Ed.*, 1972, **11**, 596.

21 J. E. Huheey, E. A. Keiter, and R. L. Keiter, *Inorganic Chemistry: Principles of Structure and Reactivity*. 4th ed., HarperCollins College Publishers, NY, 1993..

22 G. Bombieri, E. Forsellini, C. Panattoni, R. Graziani, and G. Bandoli, *J. Chem. Soc. A*, 1970, 1313.

23 R. Mason, *Chem. Soc. Revs.*, 1972, **1**, 431.

24 G. Pampaloni, R. Peloso, C. Graiff, and A. Tripicchio, *Organometallics*, 2005, **24**, 4475.

25 B. F. Straub, F. Eisentrager, and P. Hofmann, *Chem. Commun.*, 1999, 2507.

26 P. O. Oguadinma and F. Schaper, *Organometallics*, 2009, **28**, 6721.

27 (a) C. Martín, J. M. Muñoz-Molina, A. Locati, E. Alvarez, F. Maseras, T. R. Belderrain, and P. J. Pérez. *Organometallics*, 2010, **29**, 3481. (b) H. V. R Dias, H.-L. Lu, H.-J. Kim, S. A. Polach, T. K. H. Goh, R. G. Browning, and C. J. Lovely, *Organometallics*, 2002, **21**, 1466. (c) H. V. R. Dias, X. Wang, and H. V. K. Diyabalanage, *Inorg. Chem.*, 2005, **44**, 7322.

28 T. Pintauer, *J. Organomet. Chem.*, 2006, **691**, 3948.

29 X. Dai and T. H. Warren, *Chem. Commun.*, 2001, 1998.

30 L. Stamp and H. T. Dieck, *Inorg. Chim. Acta*, 1987, **129**, 107.

31 A. Boni, G. Pampaloni, R. Peloso, D. Belleti, C. Graiff, and A. Tiripicchio, *J. Organomet. Chem.,* 2006, **691**, 5602.

32 (a) J. S. Thompson and J. F. Whitney, *Inorg. Chem.,* 1984, **23**, 2813. (b) J. S. Thompson, J. C. Calabrese, and J. F. Whitney, *Acta Cryst.,* 1985, **C41**, 890.

33 (a) C. Ricardo and T. Pintauer, *J. Organomet. Chem.*, 2007, **692**, 5165. (b) B. F. Straub, F. Eisentrager, and P. Hofmann, *Chem. Commun.,* 1999, 2507. (c) J. Zhang, R.-G. Xiong, J.-L. Zuo, and X.-Z. You, *Chem. Commun.*, 2000, 1495; (d) J. Zhang, R.-G. Xiong, J.-L. Zuo, C.-M. Che, and X.-Z. You, *J. Chem. Soc., Dalton Trans.*, 2000, 2898.

34 M. Munakata, S. Kitagawa, S. Kosome, and A. Asahara, *Inorg. Chem.,* 1986, **25**, 2622.

35 J. J. Allen and A. R. Barron, *Dalton Trans.*, 2009, 878.

Chapter 1.

Olefin Coordination in Copper(I) Complexes of *Bis*(2-pyridyl)amine

Introduction

Olefins are the largest volume feedstock in the chemical and petrochemical industry, and are widely used in the production of polymers, acids, alcohols, esters, and ethers. The lightest olefin, ethylene, is the largest volume organic chemical. While demand is increasing, production is lagging, primarily because the cost of producing olefins has escalated dramatically in the past several years. One part of this is due to the fact that olefin production is extremely energy intensive, generally requiring the separation of these molecules from their alkane counterparts (olefin/paraffin separation) via cryogenic distillation. Over a decade ago it was estimated that these two separations accounted for 6.3% (about 0.15 quadrillion BTUs) of the energy used by the chemical and petrochemical industries,[1] leading to the suggestion that less energy-intensive separations would be useful for the petroleum refining industry.[2] Another reason for increased production costs is the fact that feedstock (natural gas liquids) prices have soared in recent years. Since there is little that can be done to control the price of natural gas in the current market, the large volume of olefins produced and the requisite purity for most applications provide strong incentives for novel alternative separation approaches. The use of chemically specific separation reagents is a potentially inexpensive and efficient approach for separation.[3]

With respect to complex formation, various complexing reagents have been described,[4] but in all cases the function of the complexing agent is to coordinate the olefin under one condition, and liberate it under another (Eq. 1.1).[5] Thus, the olefin coordination must be easily reversible upon change in ambient conditions (heat or reduced pressure) in order to release the olefin when desired. It follows that the solvent and the metal complex must be of sufficiently high boiling points that the olefin is

removed upon heating without loss of complexing agent. The latter can be accomplished through the use of a salt rather than a neutral complex.

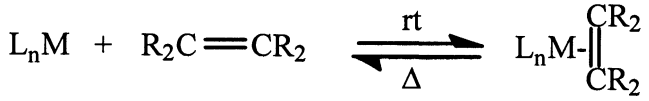

(1.1)

In designing a suitable coordination system for olefins, we are interested in a metal···olefin interaction that is sufficiently strong to allow for isolation, but will allow for recovery of the olefin after extraction. Although redox-active metal salts such as copper[6,7] have been reported to reversibly coordinate olefins they do not allow for selectivity. Unfortunately, in general, Cu···olefin complexes are not strong and dissociation occurs under ambient conditions; however, interest in the copper(I)···ethylene interaction present in biological systems has resulted in the synthesis of several potential ligand systems. Ethylene plays a variety of roles in plant development, ranging from germination and growth to sex expression and fruit ripening.[8,9] Considering all of the metals present in biological systems, copper is the only metal known to interact with ethylene. This assortment of naturally occurring processes has inspired a great deal of work, which has found applications in catalysis[6b] and industrial processing of hydrocarbon feedstocks.[10]

These studies have also demonstrated that Cu···olefin complex stability can be tailored by choice of the ancillary ligand. Incorporation of chelating, strongly Lewis-basic N-donor ligands have proven to yield the most robust complexes. The most stable complexes have been reported as having anionic ancillary ligands,[11,12] of which the olefin remains complexed even under vacuum. Moreover, The tridentate ligand, pentamethyldiethylenetriamine, has been used to prepare copper(I) complexes of several olefin monomers.[13] For a process in which the complexed olefin needs to be readily recovered, however, this type of ancillary ligand is not ideal. The class of ligands more commonly used for reversible olefin binding is the neutral N-donor heterocyclic chelates,

including *bis*(pyrazolyl)methanes, [14] dipyridylamine, [15, 16] phenanthroline, [17] and bipyridines.[15,18] Of all these studies, it is the report by Thompson and Whitney that reversible binding in complexes with ethylene are formed when stabilized with the chelate ligand *bis*(2-pyridyl)amine (H-dpa), that has formed the basis for the present study.

We are interested in using *bis*(2-pyridyl)amine-type ligands to effect the binding propensity of various olefins. But prior to this work we desire to have a detailed understanding of the structural trends observed with terminal versus internal olefin's coordination, as well as using spectroscopic and computational methods as a tool in ligand design. Herein we report the first part of this study: a structural, spectroscopic, and computational study of olefin coordination in copper(I) complexes of *bis*(2-pyridyl)amine.

Results and Discussion

The reaction of $[Cu(MeCN)_4]BF_4$ with H-dpa in the presence of the appropriate olefin results in the formation of the olefin complex, $[Cu(H\text{-}dpa)(olefin)]BF_4$ (Eq. 1.2) where olefin = ethylene (**1.1**), propylene (**1.2**), 1-butene (**1.3**), 1-hexene (**1.4**), 1-octene (**1.5**), *cis*-2-octene (**1.6**), *trans*-2-octene (**1.7**), *cis*-3-octene (**1.8**), *trans*-3-octene (**1.9**), 2-norbornylene (**1.10**), 1,5-cyclooctadiene (**1.11**), styrene (**1.12**), *cis*-stilbene (**1.13**), *trans*-stilbene (**1.14**), and $Ph_2C{=}CH_2$ (**1.15**). Compounds **1.1 - 1.15** are soluble in alcohols and show instability in air. All of the compounds have been characterized by ^1H and ^{13}C NMR, FT-IR, and TG/DTA. The crystal structures have been determined for the compounds of 1-octene (**1.5**), *cis*-2-octene (**1.6**), *cis*-3-octene (**1.8**), and 2-norbornene, styrene, and *cis*-stilbene (**1.10 - 1.13**).

$$[Cu(MeCN)_4]BF_4 + \text{H-dpa} + \text{olefin} \longrightarrow [Cu(\text{H-dpa})(\text{olefin})]BF_4 + 4\ \text{MeCN} \qquad (1.2)$$

The structures for the complex cations in **1.5**, **1.6**, **1.8**, and **1.10 - 1.13** are shown in Figures 1.1 – 1.7, respectively. Selected bond lengths and angles are given in Table 1.1.

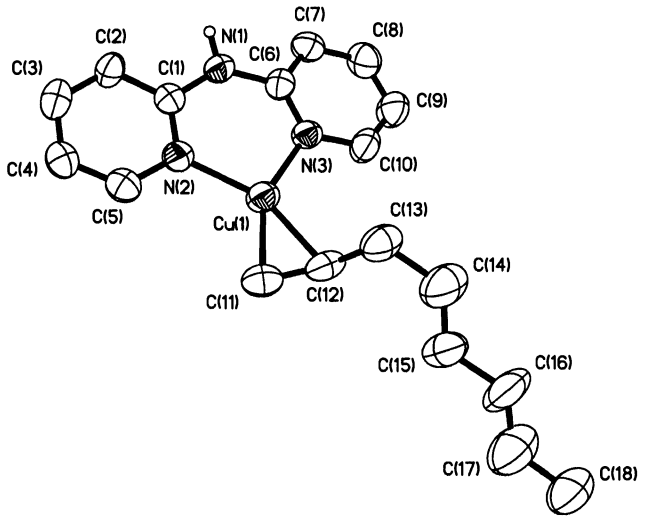

Figure 1.1. Structure of the $[Cu(H\text{-}dpa)(1\text{-octene})]^+$ cation in compound **1.5**. Thermal ellipsoids are shown at the 30% level and hydrogen atoms attached to carbon are omitted for clarity.

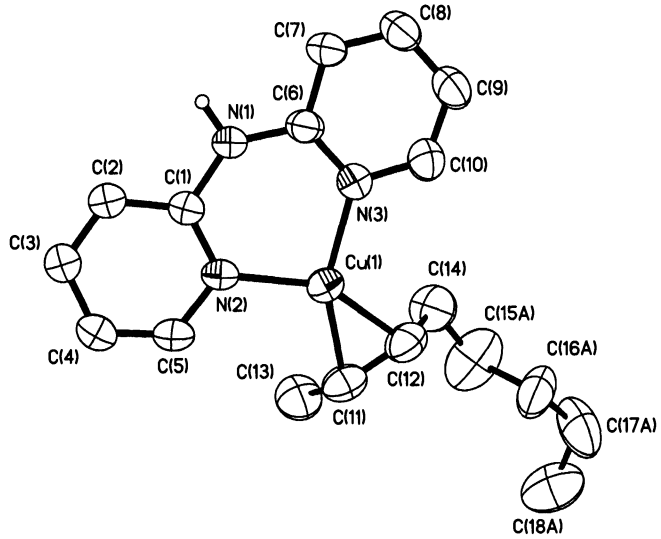

Figure 1.2. Structure of the $[Cu(H\text{-}dpa)(cis\text{-}2\text{-octene})]^+$ cation in compound **1.6**. Thermal ellipsoids are shown at the 30% level and hydrogen atoms attached to carbon are omitted for clarity.

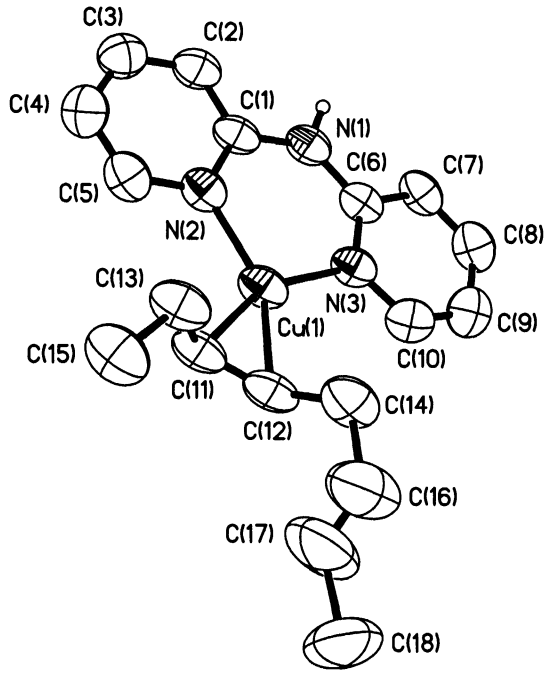

Figure 1.3. Structure of the [Cu(H-dpa)(*cis*-3-octene)]$^+$ cation in compound **1.8**. Thermal ellipsoids are shown at the 30% level and hydrogen atoms attached to carbon are omitted for clarity.

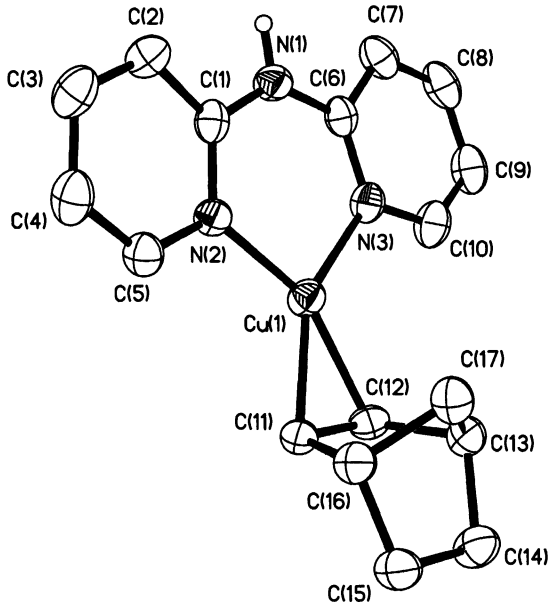

Figure 1.4. Structure of the [Cu(H-dpa)(2-norbornylene)]$^+$ cation in compound **1.10**. Thermal ellipsoids are shown at the 30% level and hydrogen atoms attached to carbon are omitted for clarity.

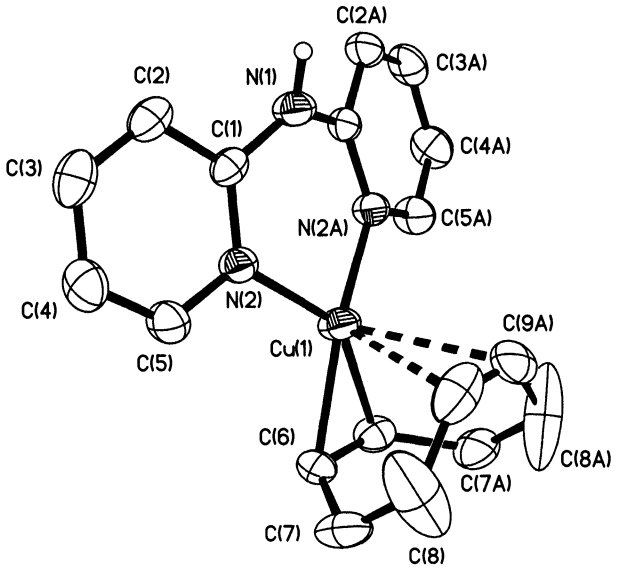

Figure 1.5. Structure of the $[Cu(H\text{-}dpa)(1,5\text{-}cyclooctadiene)]^+$ cation in compound **1.11**. Thermal ellipsoids are shown at the 30% level and hydrogen atoms attached to carbon are omitted for clarity.

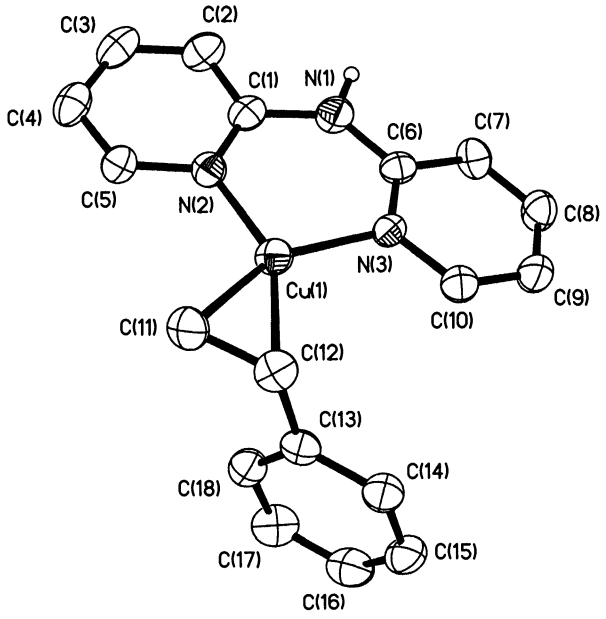

Figure 1.6. Structure of the $[Cu(H\text{-}dpa)(styrene)]^+$ cation in compound **1.12**. Thermal ellipsoids are shown at the 30% level and hydrogen atoms attached to carbon are omitted for clarity.

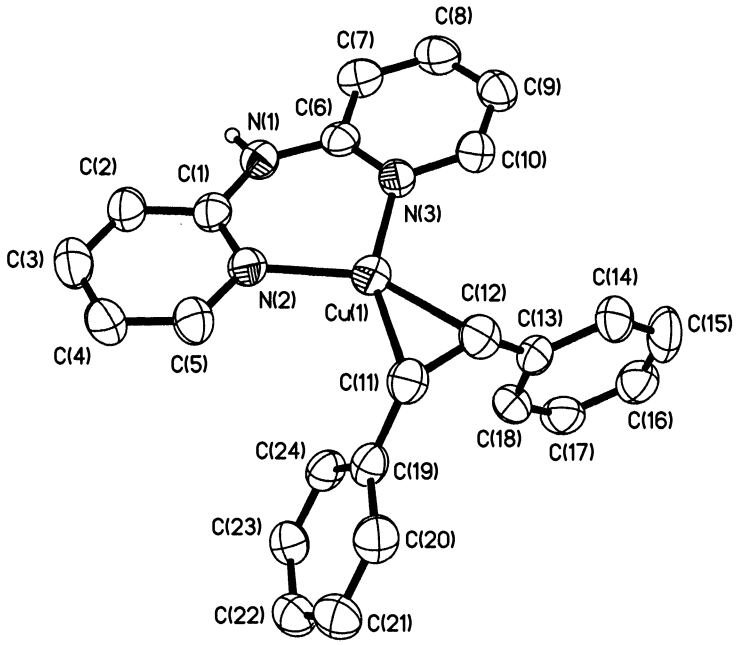

Figure 1.7. Structure of the [Cu(H-dpa)(*cis*-stilbene)]$^+$ cation in compound **1.13**. Thermal ellipsoids are shown at the 30% level and hydrogen atoms attached to carbon are omitted for clarity.

It is interesting to note that complexes **1.6**, **1.8**, and **1.13** represent, to the best of our knowledge, the first structurally characterized complexes of these olefins with any metal, while **1.5** is only the second 1-octene metal π-complex to be reported.[12] The copper atoms in compounds **1.5**, **1.6**, **1.8**, **1.10**, **1.12**, and **1.13** are each coordinated to two pyridine nitrogen atoms and the appropriate olefin; consistent with three-coordinate Cu(I) cation. The Cu-N distances [1.957(5) - 1.996(3) Å] are within experimental error of the analogous ethylene and cyclohexene complexes [1.963(2) - 1.973(3) Å].[16,17] In a similar manner the Cu-C distances [1.990(6) - 2.087(4) Å] overlap the range for the previously reported derivatives [2.019(3) - 2.032(4) Å].[16,17] The copper atom in compound **1.11** is situated on a crystallographic mirror plane, and is coordinated to two pyridine nitrogen atoms and the 1,5-cyclooctadiene via two distinct interactions.

Table 1.1. Selected bond lengths (Å) and angles (°) in compounds of the type [Cu(H-dpa)(η^2-olefin)]BF_4.

	1.5	**1.6**	**1.8**	**1.10**	**1.11**[a]	**1.12**	**1.13**
Cu-C	1.997(6)	2.024(6)	2.026(4)	2.030(6)	2.087(4)	1.990(6)	2.011(6)
Cu-C'	2.024(6)	2.034(6)	2.038(4)	2.026(6)	-	2.044(5)	2.013(5)
Cu-N	1.963(5)	1.959(4)	1.974(3)	1.962(5)	1.996(3)	1.959(5)	1.959(5)
Cu-N'	1.965(5)	1.979(4)	1.978(3)	1.957(5)	-	1.967(5)	1.964(4)
C=C'	1.374(8)	1.373(9)	1.363(6)	1.388(7)	1.358(10)	1.387(8)	1.380(7)
N-Cu-N'	97.0(2)	96.5(1)	96.2(1)	97.7(2)	95.3(1)	96.7(2)	96.9(2)
C-Cu-C'	39.9(2)	39.5(2)	39.2(1)	40.0(2)	38.0(3)	40.2(2)	40.1(2)
C_{py}-N-$C_{py'}$	135.0(5)	135.5(4)	135.2(3)	135.1(5)	132.3(5)	133.5(5)	134.4(5)
N'···N···C=C'	5.4(5)	2.5(4)	2.1(3)	1.6(3)	0	6.8(4)	2.6(4)
$\Delta MPLN_{[py...py']}$	10.3(3)	4.4(3)	7.7(2)	7.2(4)	23.1(2)	12.3(3)	6.5(3)

[a] secondary metal-olefin interaction (η^2,$\eta^{2'}$-cod coordination): Cu-C = 2.560(5) Å; C=C' = 1.33(1) Å; C-Cu-C' = 30.0(3)°.

As has been observed for the 2,2'-bipyridine analog [19] and the neutral hexafluoroacetylacetonato derivative, [20] the geometry about the Cu atom, which is coordinated to the two pyridine nitrogen atoms and two olefinic moieties of the 1,5-cyclooctadiene, is that of a very distorted tetrahedron.

The angle between the Cu(1)-C(6)-C(6a) plane, and the Cu(1)-N(2)-N(2a) plane is 158.7(2)°, which is close to the 2,2'-bipyridine derivative (154.3°). In a similar manner, the angle between the plane Cu(1)-C(9)-C(9a) plane, and the Cu(1)-N(2)-N(2a) plane is 118.7(2)° compared to 118° in the 2,2'-bipyridine analog.[20] The primary Cu···olefin interaction [2.087(4) Å] is slightly weaker than those observed for our other structures, while the secondary interaction involves a significantly longer distance [2.560(5) Å].

It should be noted that in compound **1.11** the stronger Cu···olefin interaction is shorter, and the weaker interaction is longer as compared to [Cu(bipy)(1,5-cyclooctadiene)]PF_6 [2.113(8) and 2.105(9) Å, and 2.47(1) and 2.40(1) Å, respectively].[20] The C=C bond and C-Cu-C angle determined for **1.5** [1.374(8) Å and 39.9(2)°, respectively] are slightly larger than those for the pentamethyldiethylenetriamine (PMDETA) derivative reported by Braunecker *et al.* [1.35(1) Å and 38.3(3)°],[12] suggesting a weaker Cu-olefin interaction in the latter; however, the PMDETA acts as a tridentate ligand giving a pseudo-tetrahedral coordination geometry around Cu(I) which may account for the variation.

The C=C bond determined for compound **1.10** [1.388(7) Å] is lengthened compared to free norbornylene [1.334(1) Å],[21] and is slightly longer than those observed in the neutral iminophosphanamide-norbornylene and diethylenetriamine (detn) complexes [1.37(2) and 1.38(2) Å, respectively].[12,22]

The C(6)-C(6A) distance of 1.35(1) Å for the strongest interaction in compound **1.11** is shorter than the C=C distance observed for the other compounds reported here,

consistent with the longer Cu-C distance. Furthermore, the C(9)-C(9A) distance associated with the secondary Cu···olefin interaction [1.33(1) Å] is within experimental error to that reported for free 1,5-cyclooctadiene (1.34 Å), consistent with a very weak Cu···olefin interaction and little or no π-back donation.[23] The C=C bond in compound **1.12** [1.387(8) Å] is longer than in free styrene [1.325(2) Å],[24] as well as compared to the PMDETA, bipy, and neutral β-diketiminato complexes [1.35(1) - 1.373(6) Å].[11,12,25]

It is worth noting that, the C=C bond lengthening in **1.10** as compared to free norbornylene (0.06 Å), as well as the shift in the ^{1}H and ^{13}C NMR signal upon complexation (see below) are amongst the largest for any olefin examined. As a result of the rigid nature of the uncomplexed cyclic norbornylene molecule, the alkene C-C-C angles (106.5°)[21] are constrained to less than ideal for sp^2 hybridization. Partial rehybridization to sp^3 upon coordination results in a relief of this angle strain, thereby accounting for a stronger interaction than observed for unconstrained *cis*-olefins.

Even assuming a coplanar structure (i.e., coplanar H-dpa and C=C olefin bond), there will be steric hindrance between the ligands for any olefin above ethylene. The structural consequence of such a steric interaction would be to expect twisting of the olefin out of the plane of the H-dpa ligand (Figure 1.8).

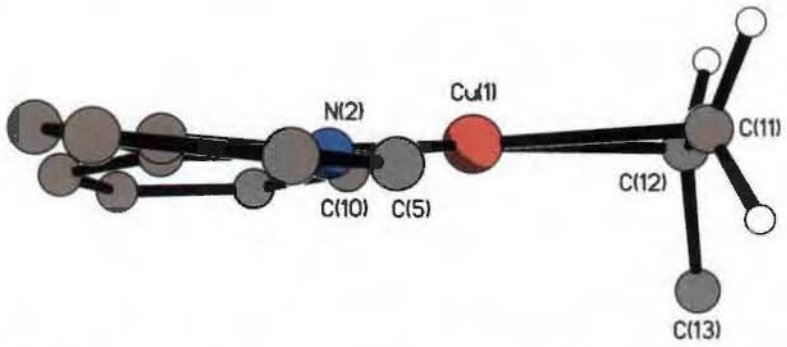

Figure 1.8. Partial coordination sphere of $[Cu(H\text{-}dpa)(styrene)]^+$ cation in compound **1.12** showing the twisting of the olefin out of the CuN_2 plane, and the folding of the H-dpa ligand.

Quantifying this twist as the dihedral angle between the olefin C=C bond and the plane of the H-dpa ligand (i.e., N'-N-C-C') allows for comparison with different steric bulks of the olefin substituents. As may be seen from Figure 1.9, this twist is largest for terminal olefins and smallest for constrained olefins, including the previously reported cyclohexene derivative (0.81°).[16]

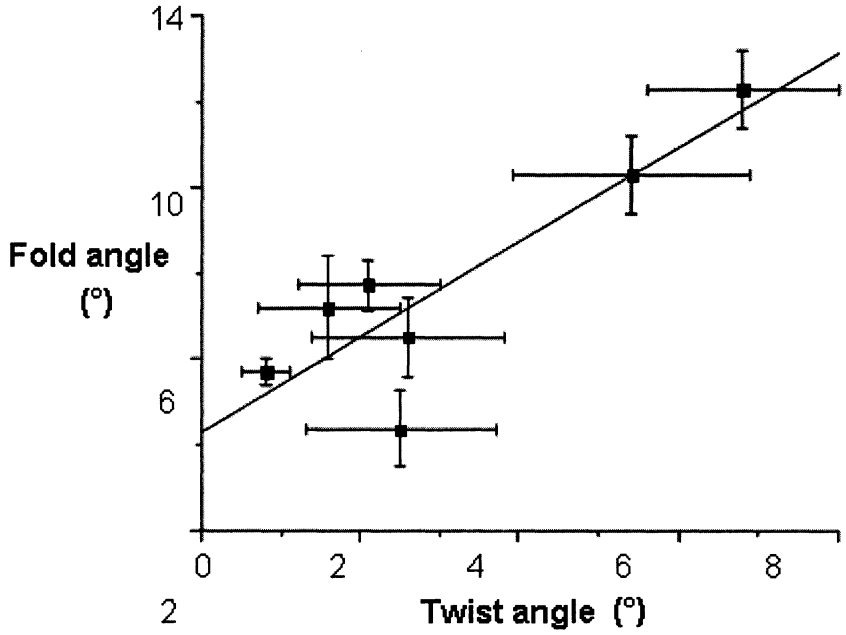

Figure 1.9. Plot of folding of the H-dpa ligand as measured by the angle between the mean planes for each pyridine ring [fold angle = $MPLN_{py(1)}$ - $MPLN_{py(2)}$] as a function of the dihedral angle between the olefin C=C bond and the plane of the H-dpa ligand (twist angle = N'-N-C-C') for [Cu(H-dpa)(olefin)]BF_4 (R^2 = 0.764).

Associated with the twisting of the olefin out of the CuN_2 plane is a folding of the H-dpa ligand (Table 1.1), such that the pyridyl rings are no longer co-planar. Figure 1.9 illustrates the relation between these parameters for different olefin substituents. We note that the twist angle observed for [Cu(H-dpa)(ethylene)]ClO_4 (9.91°)[15] is significantly larger than other examples. While the fold observed in compound **1.11** is large [23.1(2)°]

the twist is 0° due to the crystallographic mirror plane and the secondary olefin interaction. We propose that the combination of a folding of the H-dpa ligand and a rotation of the olefin out of the CuN_2 plane (as measured by the twist) provide the relief of inter-ligand/intra-molecular steric strain for terminal and *cis*-olefins. It should be noted that while we have been unable to structurally characterize any of the *trans*-isomers, the folding of the H-dpa ligand would not provide relief of steric strain. We propose that this may be a method for differentiating the binding of *cis*-and *trans*-olefins. A common feature of the crystal packing is that the counter ion, BF_4^-, interacts with the amine hydrogen of the H-dpa ligand (Figure 1.10).

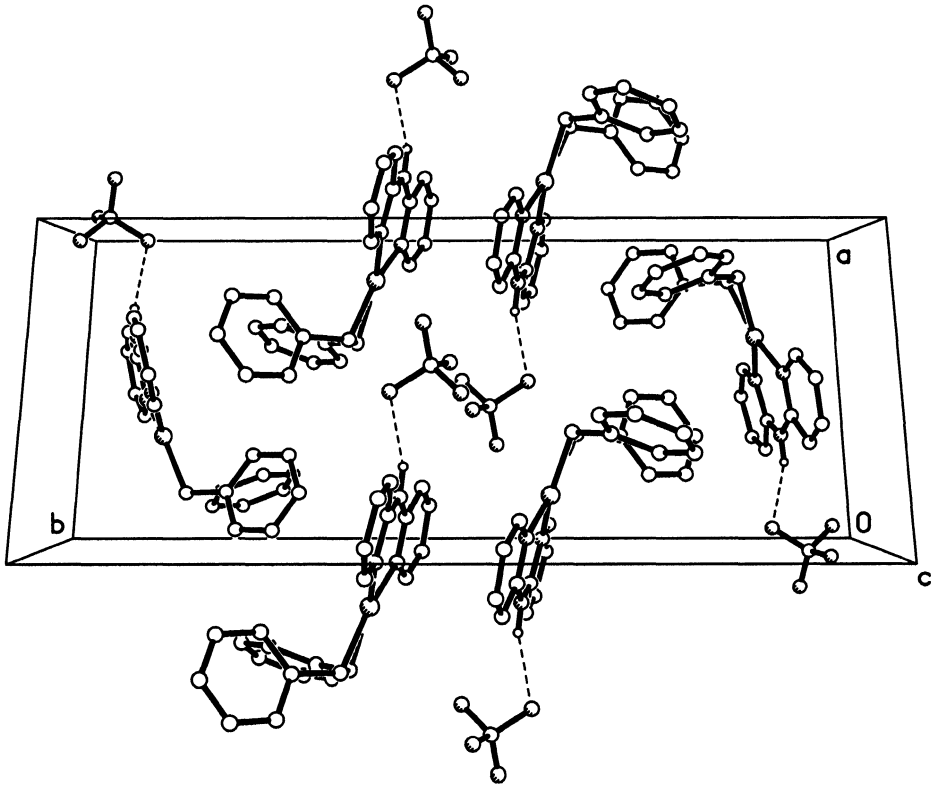

Figure 1.10. Crystal packing diagram of [Cu(H-dpa)(*cis*-stilbene)]BF_4 (**1.13**) showing the cation···anion hydrogen bonding interaction. Hydrogen atoms attached to carbon are omitted for clarity.

The N···F distances (2.80 – 3.00 Å) are within the range previously observed (2.77 – 3.31 Å),[26] and hence consistent with N-H···F hydrogen bonding. This cation···anion interaction is in contrast to the perchlorate derivatives [Cu(H-dpa)(ethylene)]ClO4[15] and [Cu(H-dpa)(cyclohexene)]ClO4[16] that show clear separation of the cation and anion in the solid state.

The presence of N-H···F hydrogen bonding is confirmed by the IR spectra of compounds **1.1** - **1.15** by the observation of a medium strength bands for each complex (3340 - 3353 cm^{-1}). These bands are shifted to a higher wavenumber than the corresponding band in the free ligand (3263 cm^{-1}) in which there is strong intermolecular N-H···N hydrogen bonding; however, the observed shifts in N-H stretching and bending bands are indicative of association of the amine hydrogen. A second aspect of packing shared amongst complexes is that the cations pair up, appearing to have a π-π stacking interaction between the pyridyl rings, with mean-plane angle differences of 0 - 12.3(3)°. However, only complex **1.8** exhibits a stacking distance [3.651(3) Å] consistent with that accepted for the sum of the van der Waals' half-thickness of an aromatic nucleus (3.70 Å).[27]

The distances in the other complexes [3.719(4) - 4.334(4) Å] likely result in very little or no interaction between rings. Metal···aromatic π-interactions are found in **1.5** and **1.10**, between the copper center and one of the pyridyl rings [3.547(9) and 3.633(9) Å], as well as in complex **1.12** between the copper center and the phenyl ring of styrene [3.586(8) Å]. These distances are all within the sum of van der Waals' half radii for Cu and an aromatic nucleus (4.02 Å).[28] Crystal packing diagrams for the two complexes of *cis*-octenes (i.e., **1.6** and **1.8**) reveals a weak interaction of the copper center with the tetrafluoroborate anion (Figure 1.11), having Cu···F distances of 2.699(5) and 2.823(8) Å, respectively.

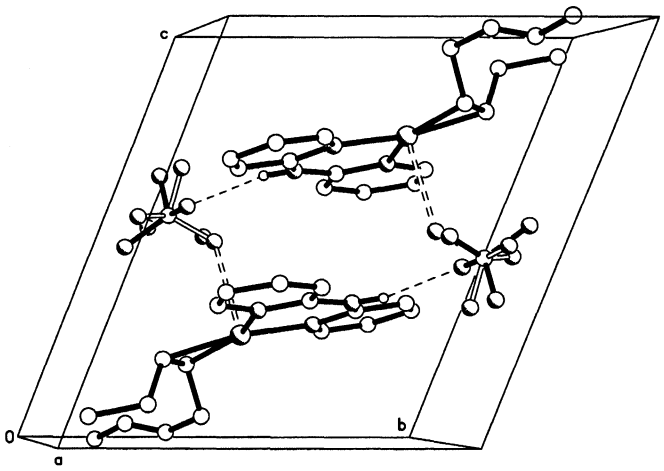

Figure 1.11. Crystal packing diagram of [Cu(H-dpa)(*cis*-3-octene)]BF_4 (**1.8**) showing the pyridyl ring π-π stacking and the Cu···F interaction. Hydrogen atoms attached to carbon are omitted for clarity.

The aromatic (3260 - 3120 cm^{-1}) and alkene (3080 - 3000 cm^{-1}) C-H stretching bands in the IR spectra yielded relatively weak signals in each case, while aliphatic C-H stretching (2980 - 2850 cm^{-1}) in **1.1**, **1.2**, and **1.7** gave medium strength bands. Bands caused by N-H bending in complexes (1640 - 1650 cm^{-1}) are shifted to higher wavenumber than in the free ligand (1592 cm^{-1}). Assignment of the olefin C=C stretch was obscured by the presence of several strong bands caused by aromatic C=C and C=N ring stretching (1580 - 1440 cm^{-1}) from the H-dpa ligand. As a result, no conclusions can be drawn concerning the shift in C=C stretch.

Munakata et al. have previously demonstrated that ^1H NMR can be used to assess the binding efficacy of various ligand/olefin combinations in Cu(I) olefin complexes.[18] We have previously used similar methods for Lewis acid-base complexes.[29] The ^1H NMR spectra of [Cu(H-dpa)(olefin)]BF_4 exhibits an upfield shift in the olefin signal as compared to free olefin (consistent with the difference between complexed and free olefin). In simple terms, the further upfield (lower δ) peaks are, the more complexed the olefin (Table 1.2).

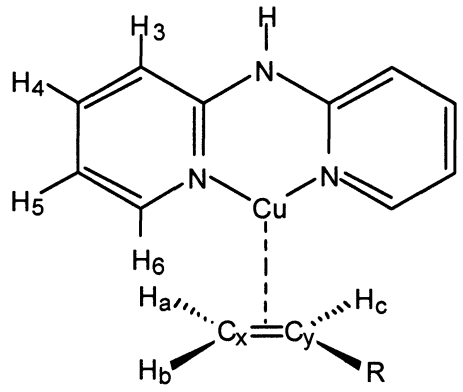

Figure 1.12. Schematic representation of $[Cu(H\text{-}dpa)(olefin)]^+$ showing the atom labels used in Table 1.2 and 1.3.

Table 1.2. Change in ^1H and ^{13}C NMR chemical shift (ppm) for olefins upon coordination to copper in $[Cu(H\text{-}dpa)(olefin)][BF_4]$.[a,b]

Complex	$\Delta\delta H_a$	$\Delta\delta H_b$	$\Delta\delta H_c$	$\Delta\delta C_x$	$\Delta\delta C_y$
1.1	0.91	-	-	39.4	-
1.2	0.67	0.64	0.53	34.2	33.3
1.3	0.68	0.62	0.50	34.1	33.1
1.4	0.64	0.66	0.50	33.9	33.0
1.5	0.59	0.64	0.47	32.7	32.2
1.6	0.29	-	-	27.7	27.0
1.7	0.32	-	-	23.2	22.9
1.8	0.29	-	-	27.8	27.4
1.9	0.32	-	-	24.8	25.0
1.10	0.93	-	-	33.9	-
1.11	0.03	-	-	7.2	-
1.12	0.68	0.82	0.55	32.9	36.1
1.13	0.34	-	-	22.8	-
1.14	0.29	-	-	7.7	-
1.15	0.10	-	-	6.1	7.7

[a] NMR collected at 298 K in CD_3OD. [b] H_a, H_b, H_c, C_x, and C_y are defined as shown in Figure 1.12.

A consideration of the data in Table 1.2 shows that the change in both ^{1}H and ^{13}C NMR shifts upon coordination is greatest for sterically unhindered and constrained olefins (i.e., ethylene and 2-norbornylene) and least for internal olefins. This trend is consistent with the expected binding stability of the olefin complex (c.f., Eq 1.3).

$$[Cu(H\text{-}dpa)(olefin)]^{+} + solvent \rightleftharpoons [Cu(H\text{-}dpa)(solvent)]^{+} + olefin \quad (1.3)$$

Table 1.3. Changes in ^{1}H NMR chemical shifts of the H-dpa ligand in [Cu(H-dpa)(olefin)]BF_4 as compared to the free ligand and the ethylene complex (**1.1**).[a,b]

Compound	$\Delta\delta_{free}$ (ppm)				$\Delta\delta_{1.1}$ (ppm)			
	$H_{3,3'}$	$H_{4,4'}$	$H_{5,5'}$	$H_{6,6'}$	$H_{3,3'}$	$H_{4,4'}$	$H_{5,5'}$	$H_{6,6'}$
1.1	0.33	-0.27	-0.23	-0.05	-	-	-	-
1.2	0.38	-0.24	-0.22	-0.03	0.05	0.03	0.01	0.02
1.3	0.38	-0.23	-0.22	-0.02	0.05	0.04	0.01	0.03
1.4	0.36	-0.25	-0.24	-0.03	0.03	0.02	-0.01	0.02
1.5	0.35	-0.26	-0.25	-0.04	0.02	0.01	-0.02	0.01
1.6	0.39	-0.24	-0.24	-0.02	0.06	0.03	-0.01	0.03
1.7	0.39	-0.23	-0.21	-0.03	0.06	0.04	0.02	0.02
1.8	0.38	-0.23	-0.23	-0.01	0.05	0.04	0.00	0.04
1.9	0.39	-0.23	-0.21	-0.04	0.06	0.04	0.02	0.01
1.10	0.36	-0.26	-0.26	-0.16	0.03	0.01	-0.03	-0.11
1.11	0.42	-0.19	-0.14	0.12	0.09	0.08	0.09	0.17
1.12	0.43	-0.14	0.01	0.27	0.10	0.13	0.24	0.32
1.13	0.52	-0.12	-0.08	0.13	0.19	0.15	0.15	0.18
1.14	0.47	-0.15	-0.11	0.10	0.14	0.12	0.12	0.15
1.15	0.34	-0.27	-0.28	0.04	0.01	0.00	-0.05	0.09

[a] NMR collected at 298 K in CD_3OD. [b] $H_{n,n'}$ (n = 3 - 6) are defined as shown in Figure 1.12.

Given the ionic nature of the complex, the solvent must be solvating enough to allow formation of a non-coordinating cation···anion pair, but not so coordinating as to inhibit olefin binding. The relative shift of the olefin protons is dependent on the donor ability of the solvent used. The difference in chemical shifts with respect to change in solvent is a measure of the competition between the olefin and the solvent, i.e., Eq. 1.3.

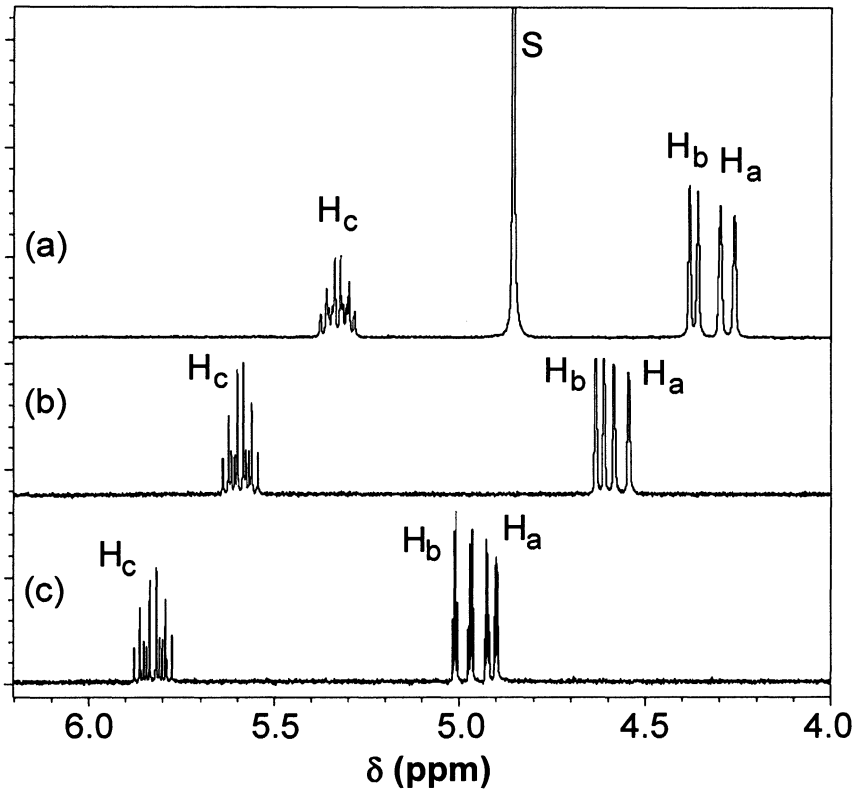

Figure 1.13. Comparison of ^{1}H NMR shift in resonances for the olefin region for [Cu(H-dpa)(1-octene)]BF_4 as a function of solvent in (a) CD_3OD, (b) d_6-acetone, and (c) CD_3CN. H_a, H_b, and H_c are defined as shown in Figure 1.12. Solvent peak is designated by "S".

Thus, from Figure 1.13 it may be seen that MeCN competes strongly (Eq. 1.3 is shifted to the right) while MeOH shows little competition (Eq. 1.3 is shifted to the left). As a consequence we used CD_3OD for all subsequent measurements. We note, however,

that the use of MeOH is also a model for the choice of the solvent for suitable for olefin separation.

A comparison of the Δδ values (and thus binding ability) for terminal olefins shows that ethylene binds significantly better than substituted olefins, but there is little effect of increasing chain length (Figure 1.14).

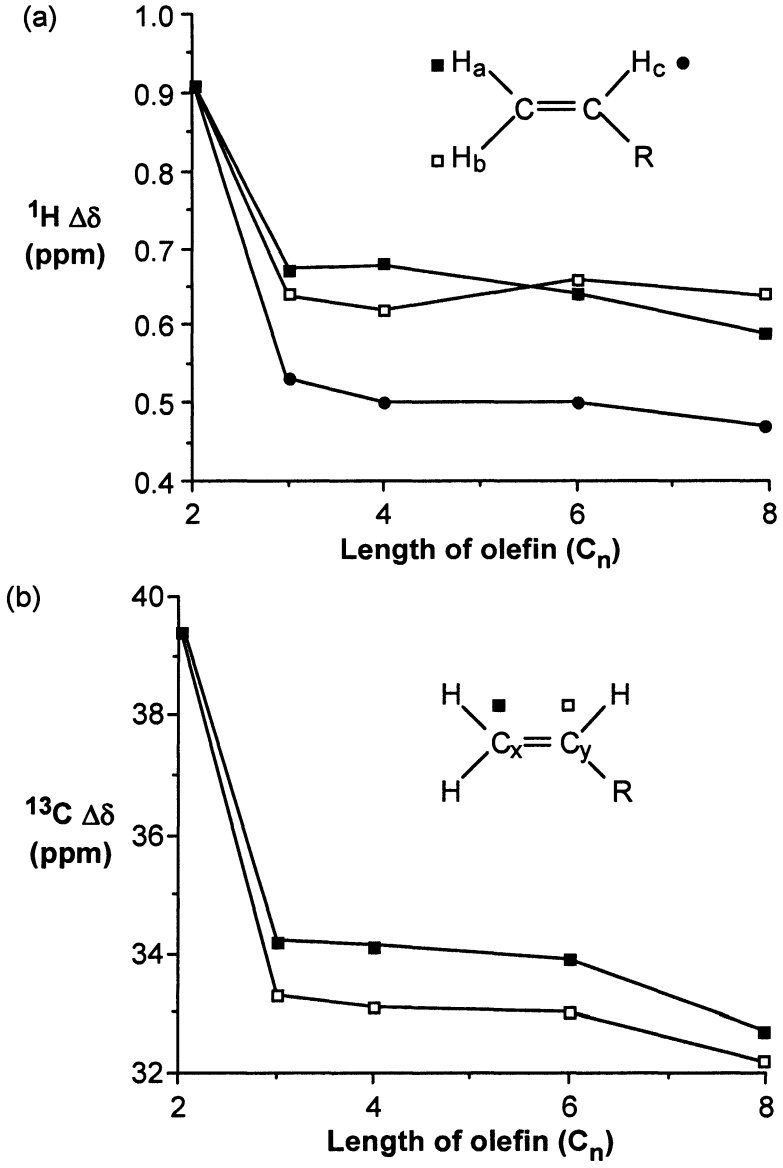

Figure 1.14. Plots of difference in chemical shift (Δδ) for the olefin (a) ^{1}H and (b) ^{13}C NMR spectra between the free olefin and [Cu(H-dpa)(olefin)]BF_4 for terminal olefins.

This result suggests that while the H-dpa parent complex may allow for differentiation of ethylene from other terminal olefins, the preferential complexation of various terminal olefins is not possible with the H-dpa ligand.

Using the alteration in the ^{13}C NMR shift of the C=C unit upon coordination, it is possible to compare the binding efficiency as a function of the position of the C=C group. For example, a comparison of the ^{13}C $\Delta\delta$ values for 1-octene, 2-octene and 3-octene. Figure 1.15 shows that while there is a significant difference in binding between a terminal and internal olefin (irrespective of *cis* or *trans* isomer), there is much less preference between binding for different internal olefin, i.e., there is only a small difference between *cis*-2-octene versus *cis*-3-octene or *trans*-2-octene versus *trans*-3-octene.

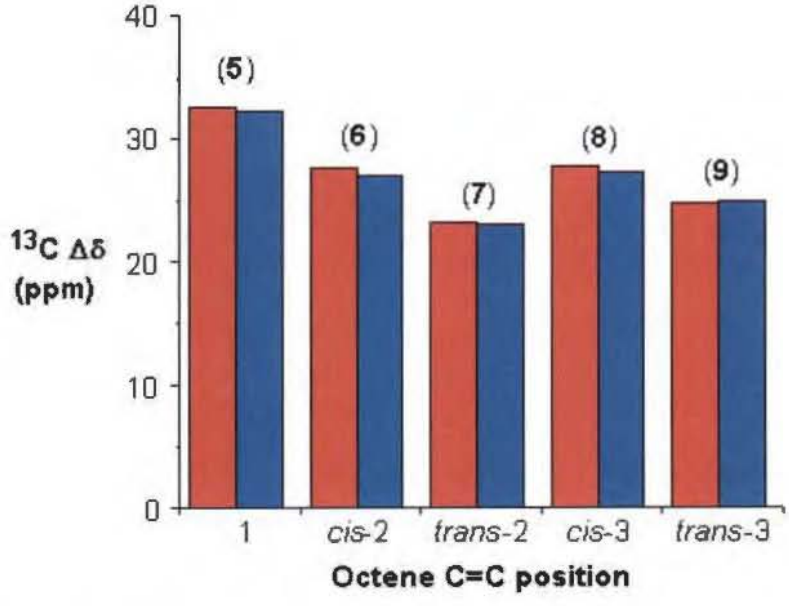

Figure 1.15. ^{13}C NMR $\Delta\delta$ for C_x (■) and C_y (■) as a function of octene double bond position in $[Cu(H\text{-}dpa)(olefin)]BF_4$ for compounds **1.5 – 1.9**.

There is, however, a modest difference between the *cis* and *trans* isomers of the same olefin (i.e., *cis*-2-octene versus *trans*-2-octene). This suggests that while differential

complexation of *cis* and *trans* isomers is possible for the H-dpa ligand, the parent ligand will not allow for separation of different internal olefins by their C=C position.

In a similar manner to the shift of the olefin signals in the ^{1}H NMR spectrum of [Cu(H-dpa)(olefin)]BF_4 versus free olefin, the chemical shifts of the ligand protons are shifted in comparison with free H-dpa. While the shifts in this case are not indicative of a comparison with the solvent complex, i.e., [Cu(H-dpa)(solvent)]BF_4, they can be used to compare the effective changes with different olefins.

As may be seen from Table 1.3, Given the ionic nature of the complex, the solvent must be solvating enough to allow formation of a non-coordinating cation···anion pair changes in the olefin result in the largest range of shifts for $H_{3,3'} > H_{4,4'} = H_{5,5'} > H_{6,6'}$. This is consistent with the binding of the H-dpa to the copper and breaking of the strong inter-molecular dimer in free H-dpa. A comparison of the difference in chemical shift for the H-dpa protons between the ethylene complex (**1.1**) and the sterically more demanding olefins (compounds **1.2 - 1.15**) provides a measure of the electronic and potentially steric effects of the olefin on the H-dpa ligand. We have previously demonstrated that ^{1}H and ^{13}C NMR may be used as a measure of changes in structure as a consequence of ligand binding.[30,31] Unfortunately, as may be seen from Table 1.3, there are only small differences (except for aromatic substituted olefins where ring current effects are possibly in force) between different olefins. This suggests that the electronic effects of different olefins on the H-dpa ligand are minimal.

We have also shown that thermogravimetric/differential thermal analysis (TG/DTA) of Lewis acid-base complexes provides information as to the relative strength of the M···L interaction.[30,32] The TG/DTA of compounds **1.1 – 1.15** is consistent with their decomposition resulting via the loss of the olefin. It should be noted that in all cases the boiling point of the olefin is lower than the temperature of decomposition of the respective [Cu(H-dpa)(olefin)][BF_4] derivative, thus any mass loss is related to the strength Cu···olefin interaction rather than the boiling point of the olefin. This is also

confirmed by the DTA that shows decomposition to be exothermic rather than the endothermic process of boiling/evaporation. As with the ^{1}H and ^{13}C NMR $\Delta\delta$ measurements the temperature associated with olefin dissociation (see Experimental) indicates a significant difference in binding of ethylene versus substituted olefins.

Importantly, Figure 1.16 shows a good correlation between the ^{1}H NMR $\Delta\delta$ values and the TGA data, validating the assumption that the shift of the olefin NMR resonances upon coordination is associated with the binding strength of the complex (see above). Also following the NMR data, the similarity of the T_{dec} for *cis*-2-octene (146 °C) and *cis*-3-octene (143 °C), as well as that for *cis*-3-octene and *trans*-3-octene (144 °C) suggest that separation of various olefin isomers through differentiation of binding to the Cu(I) H-dpa complex is not feasible and that alternative ligands must be explored.

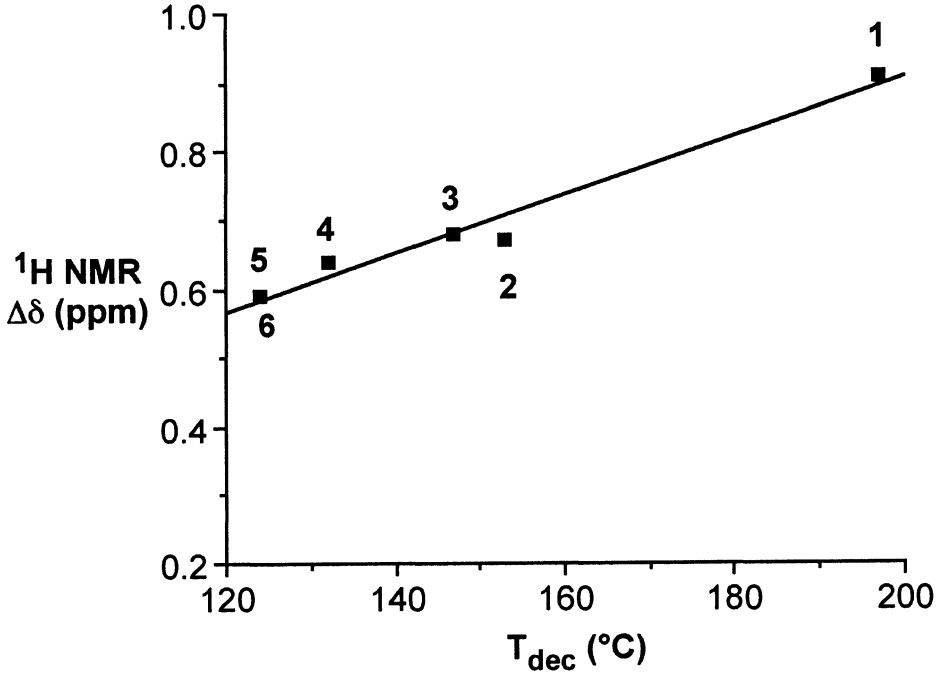

Figure 1.16. Plot of the change in chemical shift of H_a as compared to the free olefin (ppm) versus the temperature of terminal olefins dissociation in [Cu(H-dpa)(olefin)][BF_4] (n = alkyl chain length, 0 - 6) as determined from TGA (R^2 = 0.965).

Molecular Modeling. As part of our efforts to determine the viability of modeling for comparing how various olefins interact with the copper H-dpa unit, we have calculated the structure of the $[Cu(H\text{-}dpa)(1\text{-octene})]^+$ cation using four different method/basis set combinations. A comparison with the experimentally determined structure will indicate which method most faithfully replicates observed structural trends; in particular, we are interested in choosing an appropriate computational method for predicting the conformational interactions. Unfortunately, the most difficult structural features to replicate (and therefore use reliably in future predictions) is the twist angle between the H-dpa ligand and the olefin [N(3)-N(2)-C(11)-C(12)] and the folding of the H-dpa ligand $\{\Delta MPLN_{[py(1)\cdots py(2)]}\}$.

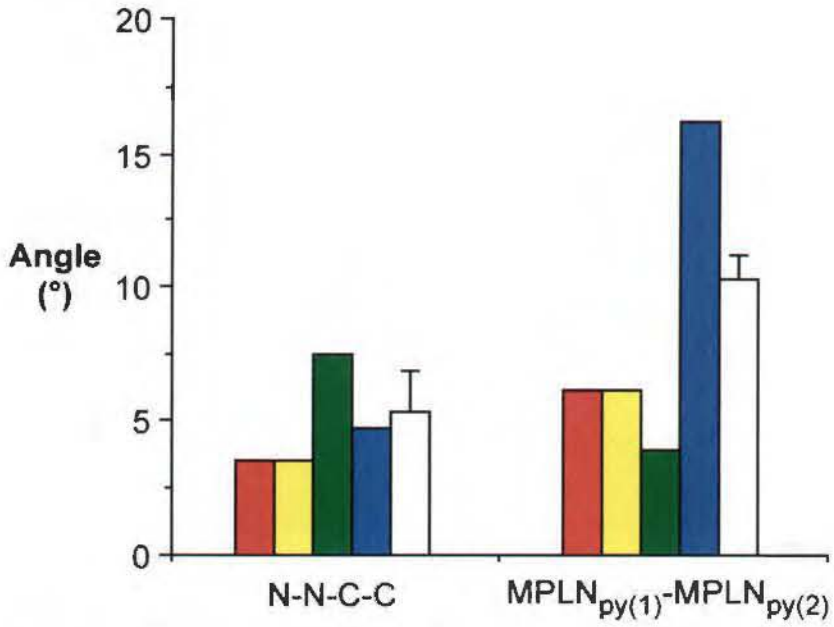

Figure 1.17. Plot of torsion angles for calculated structure of $[Cu(H\text{-}dpa)(1\text{-octene})]^+$, using MOPAC (■), RHF/STO-3G (□), RB3LYP/LANL2DZ/6-311++G* (■), and RMP2-FC/LANL2DZ/6-311++G* (■) and experimentally determined values (□).

This is in part a function of inter-molecular crystal packing forces on the organic tail of the 1-octene that may overshadow intra-molecular interactions. As may be seen

from Figure 1.17, MOPAC and RHF STO-3G equally underestimate both values. In contrast, RB3LYP (LANL2DZ/6-311++G*) overestimates the twisting between the ligands, but underestimates the folding of the H-dpa. The converse is true for RMP2-FC using the same basis set. For any individual olefin the greater the twist angle (the further away from ideal planar geometry around the copper) the less the steric interactions between the olefin and the pyridine rings of the H-dpa ligand, and consequently the more planar the H-dpa ligand will be.

Table 1.4. Comparison of bond lengths (Å) and angles (°) for $[Cu(H\text{-}dpa)(1\text{-}octene)]^+$ as determined through computational modeling and crystallographically.[a]

	Calc. Method/Basis Set				
	MOPAC	RHF	RB3LYP	RMP2-FC	
		STO-3G	LANL2DZ/6-311++G*		Exper.
Cu-C	2.078	2.080	2.096	2.062	1.997(6)
Cu-C'	2.119	2.115	2.161	2.060	2.024(6)
Cu-N	2.044	2.043	2.012	1.982	1.963(5)
Cu-N'	2.029	2.029	2.004	1.982	1.965(5)
C=C'	1.406	1.406	**1.391**	1.427	1.374(8)
N-Cu-N'	90.49	90.49	**97.70**	97.92	97.0(2)
C-Cu-C'	39.14	39.14	38.11	40.49	39.9(2)
Cu-C'-C_β	**112.20**	**112.21**	111.81	110.72	112.3(4)
twist [b]	3.52	3.52	7.48	**4.70**	5.4(5)
fold [c]	6.18	6.18	3.91	16.27	10.3(3)

[a] Values in bold are within 3σ of experimental values, while those underlined are the closest to experimental but outside 3σ. [b] Dihedral angle between the olefin C=C bond and the plane of the H-dpa ligand, i.e., N(3)-N(2)-C(11)-C(12). [c] Mean plane angle difference between pyridyl rings, i.e., $\Delta MPLN_{[py(1)\text{-}py(2)]}$.

Table 1.5. Comparison of bond lengths (Å) and angles (°) for [Cu(H-dpa)(*cis*-2-octene)]$^+$ as determined through computational modeling and crystallographically.

	Calc. Method/Basis Set				
	MOPAC	RHF	RB3LYP	RMP2-FC	
		STO-3G	LANL2DZ/6-311++G*		Exper.
Cu-N	2.041	2.017	2.017	1.986	1.959(4)
Cu-N'	2.046	2.016	2.016	1.987	1.979(4)
Cu-C	2.107	2.140	2.140	2.074	2.024(6)
Cu-C'	2.102	2.139	2.139	2.060	2.034(6)
C=C'	1.410	1.396	1.396	1.430	1.373(9)
N-Cu-N'	89.46	96.56	96.56	96.88	96.5(1)
C-Cu-C'	39.15	38.08	38.08	40.43	39.5(2)
TWIST	0.10	0.13	0.13	0.39	2.1(3)
FOLD	15.91	11.57	11.57	23.71	4.4(3)

Table 1.6. Comparison of bond lengths (Å) and angles (°) for [Cu(H-dpa)(*cis*-3-octene)]$^+$ as determined through computational modeling and crystallographically.

	Calc. Method/Basis Set			
	RHF	RB3LYP	RMP2-FC	Exper.
	STO-3G	LANL2DZ/6-311++G*		
Cu-N	2.046	2.017	1.984	1.974(3)
Cu-N'	2.041	2.017	1.985	1.978(3)
Cu-C	2.102	2.140	2.065	2.026(4)
Cu-C'	2.107	2.140	2.062	2.038(4)
C=C'	1.410	1.396	1.431	1.363(6)
N-Cu-N'	89.46	96.56	97.04	96.2(1)
C-Cu-C'	39.15	38.09	40.58	39.2(1)
TWIST	0.11	0.05	1.08	2.1(3)
FOLD	15.91	11.72	22.83	7.7(2)

Figure 1.18 shows a plot of twist angle [N(3)-N(2)-C(11)-C(12)] as a function of the folding of the H-dpa ligand [$MPLN_{py(1)}$-$MPLN_{py(2)}$]. The linear relationship between the crystal structural determined value and the values calculated using RB3LYP and RMP2-FC suggest that while neither of the latter provide exact replication of the crystal structure, they do replicate the steric relationship between intra-molecular inter-ligand interactions.

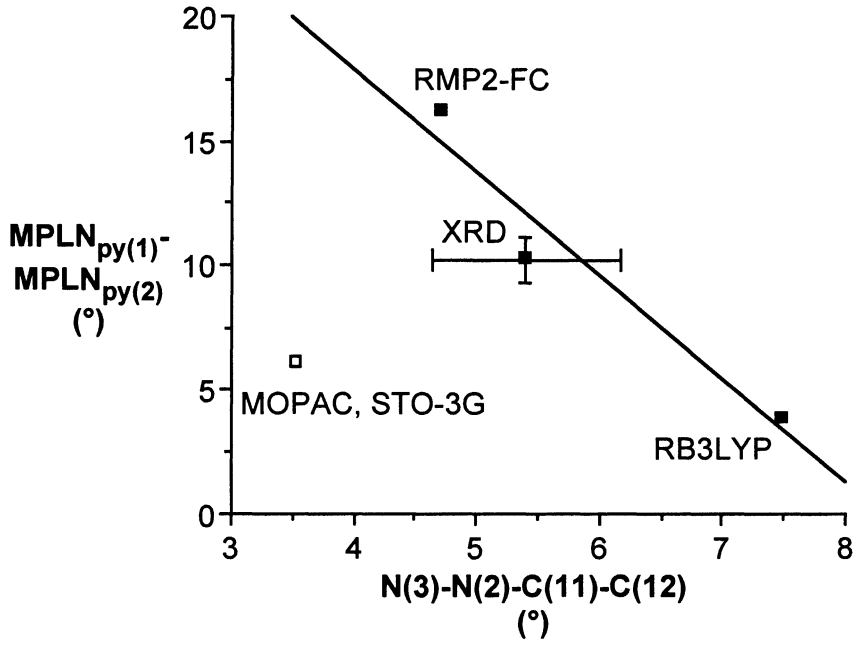

Figure 1.18. Plot of calculated and experimental twist angle [N(3)-N(2)-C(11)-C(12)] as a function of the folding of the H-dpa ligand [$MPLN_{py(1)}$-$MPLN_{py(2)}$] for [Cu(H-dpa)(1-octene)]$^+$ (■) using RB3LYP LANL2DZ/6-311++G*, RMP2-FC LANL2DZ/6-311++G*, and X-ray crystallography (R^2 = 0.934). The values calculated using MOPAC and RHF STO-3G are shown for comparison (□).

None of the method/basis set combinations replicate all of the parameters exactly. They all overestimate the Cu-X distances; however, the highest-level calculation studied (RMP2-FC LANL2DZ/6-311++G*) is consistently the closest. Interestingly, despite

significantly overestimating the olefin C=C distance, this does replicate the C-Cu-C angle associated with the olefin.

The C=C distance is faithfully predicted (within 3σ) using RB3LYP at the LANL2DZ/6-311++G* level, as is the chelate angle of the H-dpa ligand. It is also worthy of note that the lowest level calculations (MOPAC and RHF STO-3G) are clearly sufficient to predict the extent of distortion from planar of the olefin substituents, since this out-of-plane distortion is usually used as a measure of the extent of π-back bonding from a metal to an olefin. Tabulated atomic coordinates for calculated structures are located in Appendix B, in addition to figures comparing the distortions in pyridyl rings brought on by functionalization of the bridging amine nitrogen atom.

Conclusions

We have shown that the *bis*(2-pyridyl)amine ligand allows for the isolation and structural characterization of a wide range of ionic copper···olefin complexes. Interestingly we have been unable to crystallographically characterize any of the *trans* isomer complexes. Unfortunately, there appears to be no correlation of the binding strength of the olefin with Cu-C or C=C bond lengths. We have observed that a twisting of the olefin out of the plane of the H-dpa ligand and a related folding of the H-dpa ligand provide relief of inter-ligand/intra-molecular steric strain for terminal and *cis*-olefins.

The difference in the ^{1}H and ^{13}C NMR shift values between free and complexed olefins can be used to compare binding interactions. While there is a significant difference in binding between a terminal and internal olefin, there is much less preference between binding for different internal olefins. There is also a modest difference between the *cis* and *trans* isomers of the same olefin. These trends are also mimicked by the temperature of dissociation of the olefin in the solid state as determined by TGA. Our results suggest that while differential complexation of *cis* and *trans* isomers is possible

using a H-dpa type ligand, separation of different internal olefins by their C=C position will not be possible. However, the use of pre-folded *bis*(2-pyridyl)amine ligands should allow for differentiation of coordination of olefin isomers. We are presently investigating the synthesis and complexation of alkyl substituted *bis*(2-pyridyl)amine ligands.

Experimental

All reagents in this study were used as received from commercial suppliers and were stored under an argon atmosphere in a drybox. The precursor complex $[Cu(MeCN)_4]BF_4$ was prepared according to the literature.[33] All solvents were distilled and degassed via freeze-pump-thaw immediately prior to use. Glassware was thoroughly cleaned and dried prior to use. All manipulations were performed under an argon atmosphere using standard schlenk line techniques. ^1H NMR and ^{13}C NMR spectra were obtained at room temperature using Bruker Avance 400 and 500 MHz spectrometers. Spectra were collected at 298 K in CD_3OD unless otherwise stated. Chemical shifts are reported relative to internal solvent resonances. IR spectra were obtained using a Nicolet FTIR spectrometer equipped with ATR accessory. Thermogravametric analyses were performed on a Seiko I TG/DTA 200 under an argon gas flow of 10 - 15 $mL.min^{-1}$.

[Cu(H-dpa)(ethylene)]BF_4 (1.1). $[Cu(MeCN)_4]BF_4$ (1.0 mmol) and H-dpa (1.0 mmol) were charged to separate 100 mL schlenk flasks in a dry box. MeOH (10 mL) was added to the flask containing the H-dpa, which was stirred to dissolve solids. To the flask containing the copper precursor was added ethylene saturated MeOH (20mL), which was stirred for two hours at room temperature before adding the H-dpa solution. The mixture was allowed to stir under an atmosphere of ethylene for two hours, after which, ethylene was bubbled through the solution on a medium porosity glass frit until the volume had reduced by half. The solution was then filtered, and n-pentane (10 mL) was added to precipitate the complex. Filtration afforded 3.76 g (60%). Mp: 196 - 199 °C (dec.). IR

(ATR, cm^{-1}): 3347 (m, ν_{N-H}), 3261 (w, aromatic ν_{C-H}), 3225 (w, aromatic ν_{C-H}), 3158 (w, aromatic ν_{C-H}), 3115 (w, aromatic ν_{C-H}), 3082 (w, alkene ν_{C-H}), 3052 (w, alkene ν_{C-H}), 1640 (s, δ_{N-H}), 1584 (s), 1530 (s), 1478 - 1380 (s, aromatic $\delta_{C=C}$), 1233 (s, aromatic $\delta_{C=N}$), 1006 (br vs). ^{1}H NMR: δ 8.24 (2H, br d, *6,6'*-py), 7.93 (2H, br t, *4,4'*-py), 7.25 (2H, br d, *3,3'*-py), 7.12 (2H, br t, *5,5'*-py), 4.48 (4H, br s, CH_2). ^{13}C NMR: δ 154.04 (*2,2'*-py), 150.27 (*6,6'*-py), 141.94 (*4,4'*-py), 118.83 (*5,5'*-py), 116.28 (*3,3'*-py), 84.22 (CH_2).

[Cu(H-dpa)(propylene)]BF_4 (1.2). This compound was prepared in an analogous manner to that of compound **1**. Yield: 64% . Mp: 152 - 154 °C (dec.). IR (ATR, cm^{-1}): 3342 (m, ν_{N-H}), 3258 (w, aromatic ν_{C-H}), 3223 (w, aromatic ν_{C-H}), 3156 (w, aromatic ν_{C-H}), 3122 (w, aromatic ν_{C-H}), 3084 (w, alkene ν_{C-H}), 3048 (w, alkene ν_{C-H}), 2968 (w, alkyl ν_{C-H}), 2929 (w, alkyl ν_{C-H}), 1637 (s, δ_{N-H}), 1585 (s), 1531 (s), 1475 - 1375 (s, aromatic $\delta_{C=C}$), 1230 (s, aromatic $\delta_{C=N}$), 1067 - 993 (br vs). ^{1}H NMR: δ 8.22 (2H, br d, *6,6'*-py), 7.90 (2H, br t, *4,4'*-py), 7.20 (2H, br d, *3,3'*-py), 7.11 (2H, br t, *5,5'*-py), 5.29 [1H, ddq, *J*(H-H) = 15.0 Hz, *J*(H-H) = 8.9 Hz. *J*(H-H) = 6.1 Hz, H_2CCH], 4.34 [1H, d, *J*(H-H) = 8.9 Hz, *trans*-C*H*], 4.27 [1H, d, *J*(H-H) = 15.0 Hz, *cis*-C*H*], 1.76 [3H, d, *J*(H-H) = 6.1 Hz, $CHCH_3$]. ^{13}C NMR: δ 154.19 (*2,2'*-py), 149.74 (*6,6'*-py), 141.66 (*4,4'*-py), 118.97 (*5,5'*-py), 116.10 (*3,3'*-py), 100.59 ($CHCH_2$), 82.87 ($CHCH_2$), 19.69 ($CHCH_3$).

[Cu(H-dpa)(1-butene)]BF_4 (1.3). This compound was prepared in an analogous manner to that of compound **1**. Yield: 32%. Mp: 146 - 148 °C (dec.). IR (ATR, cm^{-1}): 3346 (m, ν_{N-H}), 3261 (w, aromatic ν_{C-H}), 3224 (w, aromatic ν_{C-H}), 3157 (w, aromatic ν_{C-H}), 3122 (w, aromatic ν_{C-H}), 3081 (w, alkene ν_{C-H}), 3049 (w, alkene ν_{C-H}), 2969 (w, alkyl ν_{C-H}), 2934 (w, alkyl ν_{C-H}), 2871 (w, alkyl ν_{C-H}), 1637 (s, δ_{N-H}), 1584 (s), 1531 (s), 1477 - 1379 (s, aromatic $\delta_{C=C}$), 1231 (s, aromatic $\delta_{C=N}$), 1063 - 986 (br vs). ^{1}H NMR: δ 8.21 (2H, br d, *6,6'*-py), 7.89 (2H, br t, *4,4'*-py), 7.20 (2H, br d, *3,3'*-py), 7.11 (2H, br t, *5,5'*-py), 5.36 [1H, ddt, *J*(H-H) = 15.2 Hz, *J*(H-H) = 9.0 Hz. *J*(H-H) = 7.3 Hz, H_2CCH], 4.31

[1H, d, *J*(H-H) = 9.0 Hz, *trans*-C*H*], 4.27 [1H, dd, *J*(H-H) = 15.2 Hz, *cis*-C*H*], 2.09 (2H, br quint, CHCH_2), 1.08 [3H, t, *J*(H-H) = 7.3 Hz, CH_2CH_3]. ^{13}C NMR: δ 154.22 (*2,2'*-py), 149.72 (*6,6'*-py), 141.67 (*4,4'*-py), 118.88 (*5,5'*-py), 116.11 (*3,3'*-py), 107.63 (*C*HCH_2), 80.73 (CH*C*H_2), 27.97 (CH_2CHCH_2), 14.98 (CH_2CH_3).

[Cu(H-dpa)(1-hexene)]BF_4 (1.4). [Cu(MeCN)$_4$]BF_4 (0.314 g, 1.00 mmol) and H-dpa (0.172g, 1.0 mmol) were charged to separate 100 mL Schlenk flasks in a dry box. MeOH (10 mL) was added to the flask containing the H-dpa, which was stirred to dissolve solids. To the flask containing the copper complex was added 1-hexene (5 mL) in MeOH (20 mL). The mixture was allowed to stir for 1 hr at room temperature before adding the H-dpa/methanol solution. After, the combined solutions were stirred another three hours at room temperature; the solution volume was reduced under vacuum by approximately half. The solution was gently warmed with a water bath to redissolve the product, and then filtered through a medium porosity glass frit to remove insoluble impurities. Argon was vigorously bubbled through the resulting pale green solution to further reduce its volume to ca. 10 mL. The solution was gently warmed to dissolve any precipitate, and upon cooling to –12 °C for several days, the solution yielded 0.231 g (57%) colorless needles. Mp: 131 - 134 °C (dec.). IR (ATR, cm^{-1}): 3339 (m, ν_{N-H}), 3260 (w, aromatic ν_{C-H}), 3225 (w, aromatic ν_{C-H}), 3158 (w, aromatic ν_{C-H}), 3122 (w, aromatic ν_{C-H}), 3087 (w, alkene ν_{C-H}), 3051 (w, alkene ν_{C-H}), 2954 (w, alkyl ν_{C-H}), 2925 (w, alkyl ν_{C-H}), 2862 (w, alkyl ν_{C-H}), 1641 (s, δ_{N-H}), 1583 (s), 1532 (s), 1478 - 1340 (s, aromatic $\delta_{C=C}$), 1231 (s, aromatic $\delta_{C=N}$), 1070 - 985 (br vs). ^{1}H NMR: δ 8.22 (2H, br d, *6,6'*-py), 7.91 (2H, br t, *4,4'*-py), 7.22 (2H, br d, *3,3'*-py), 7.13 (2H, br t, *5,5'*-py), 5.30 [1H, ddt, *J*(H-H) = 15.2 Hz, *J*(H-H) = 9.0 Hz. *J*(H-H) = 7.2 Hz, H_2CCH], 4.34 [1H, d, *J*(H-H) = 9.0 Hz, *trans*-C*H*], 4.25 [1H, d, *J*(H-H) = 15.2 Hz, *cis*-C*H*], 2.06 (2H, br q, CHCH_2), 1.47 (2H, br mult, C$H_2CH_2CH_3$), 1.38 (2H, br mult, $CH_2CH_2CH_3$), 0.90 [3H, t, *J*(H-H) = 7.2 Hz, CH_2CH_3]. ^{13}C NMR: δ 154.08 (*2,2'*-py), 149.75 (*6,6'*-py), 141.78 (*4,4'*-py), 118.96

(*5,5'*-py), 116.17 (*3,3'*-py), 106.30 (*C*HCH$_2$), 81.87 (CH*C*H$_2$), 34.65 (CH$_2$CH*C*H$_2$), 33.79 (CH$_2$*C*H$_2$CH$_2$), 23.27 (*C*H$_2$CH$_3$), 14.31 (CH$_2$*C*H$_3$).

[Cu(H-dpa)(1-octene)]BF$_4$ (1.5). This compound was prepared in an analogous manner to that of compound **4**. Yield: 56%. Mp: 123 - 125 °C (dec.). IR (ATR, cm^{-1}): 3333 (m, ν_{N-H}), 3259 (w, aromatic ν_{C-H}), 3224 (w, aromatic ν_{C-H}), 3127 (w, aromatic ν_{C-H}), 3083 (w, alkene ν_{C-H}), 3053 (w, alkene ν_{C-H}), 2922 (w, alkyl ν_{C-H}), 2853 (w, alkyl ν_{C-H}), 1643 (m, δ_{N-H}), 1581 (s), 1479 - 1396 (s, aromatic $\delta_{C=C}$), 1256 (m, aromatic $\delta_{C=N}$), 1056 - 1006 (br vs). ^{1}H NMR: δ 8.23 (2H, br d, *6,6'*-py), 7.92 (2H, br t, *4,4'*-py), 7.23 (2H, br d, *3,3'*-py), 7.14 (2H, br t, *5,5'*-py), 5.32 [1H, ddt, *J*(H-H) = 15.0 Hz, *J*(H-H) = 9.0 Hz, *J*(H-H) = 6.8 Hz, H$_2$C=C*H*], 4.36 [1H, d, *J*(H-H) = 9.0 Hz, *trans*-C*H*], 4.26 [1H, d, *J*(H-H) = 15.0 Hz, *cis*-C*H*], 2.05 (2H, br q, CHC*H*$_2$), 1.49 (2H, br quint, CHCH$_2$C*H*$_2$), 1.35 (2H, br m, C*H*$_2$Pr), 1.28 (4H, br m, C*H*$_2$C*H*$_2$CH$_3$) 0.88 [3H, t, *J*(H-H) = 6.8 Hz, CH$_2$C*H*$_3$]. ^{13}C NMR: δ 154.11 (*2,2'*-py), 149.78 (*6,6'*-py), 141.85 (*4,4'*-py), 118.96 (*5,5'*-py), 116.23 (*3,3'*-py), 107.40 (*C*HCH$_2$), 82.77 (CH*C*H$_2$), 34.89 (*C*H$_2$CHCH$_2$), 32.89 (CH$_2$*C*H$_2$CH$_2$), 31.38 (CH$_2$*C*H$_2$CH$_2$), 29.94 (CH$_2$*C*H$_2$CH$_2$), 23.74 (CH$_2$*C*H$_2$CH$_2$), 14.51 (CH$_2$*C*H$_3$).

[Cu(H-dpa)(*cis*-2-octene)]BF$_4$ (1.6). This compound was prepared in an analogous manner to that of compound **4**. Yield: 47%. MP (TGA; decomp.) 145 - 147 °C. IR (ATR, cm^{-1}): 3352 (m, ν_{N-H}), 3261 (w, aromatic ν_{C-H}), 3226 (w, aromatic ν_{C-H}), 3160 (w, aromatic ν_{C-H}), 3123 (w, aromatic ν_{C-H}), 3083 (w, alkene ν_{C-H}), 3048 (w, alkene ν_{C-H}), 2937 (w, alkyl ν_{C-H}), 2857 (w, alkyl ν_{C-H}), 1640 (s, δ_{N-H}), 1583 (s), 1531 (m), 1479 - 1381 (s, aromatic $\delta_{C=C}$), 1234 (m, aromatic $\delta_{C=N}$), 1090 - 997 (br vs). ^{1}H NMR: δ 8.21 (2H, br d, *6,6'*-py), 7.90 (2H, br d, *4,4'*-py), 7.19 (2H, br d, *3,3'*-py), 7.13 (2H, br d, *5,5'*-py), 5.10 (2H, m, *H*C=C*H*), 2.07 (2H, br q, CHC*H*$_2$), 1.66 [3H, d, *J*(H-H) = 5.4 Hz, CHC*H*$_3$], 1.47 (2H, br quin, CHCH$_2$C*H*$_2$), 1.34 (4H, br m, C*H*$_2$C*H*$_2$CH$_3$), 0.91 [3H, t, *J*(H-H) = 7.0

Hz, CH_2CH_3]. ^{13}C NMR: δ 154.34 (*2,2'*-py), 149.39 (*6,6'*-py), 141.56 (*4,4'*-py), 118.98 (*5,5'*-py), 116.08 (*3,3'*-py), 104.10 ($CHCHCH_2$), 97.54 ($CHCH_3$), 32.75 (CH_2Et), 30.81 (CH_2CH_2CH), 28.94 (CH_2CH), 23.73 (CH_2CH_3), 14.48 (CH_2CH_3), 13.59 ($CHCH_3$).

[Cu(H-dpa)(*trans*-2-octene)]BF_4 (1.7). This compound was prepared in an analogous manner to that of compound **4**. Yield: 53%. Mp: 126 - 129 °C (dec.). IR (ATR, cm^{-1}): 3347 (m, ν_{N-H}), 3257 (w, aromatic ν_{C-H}), 3223 (w, aromatic ν_{C-H}), 3158 (w, aromatic ν_{C-H}), 3091 (w, alkene ν_{C-H}), 3047 (w, alkene ν_{C-H}), 2940 (w, alkyl ν_{C-H}), 2867 (w, alkyl ν_{C-H}), 1635 (s, δ_{N-H}), 1584 (s), 1532 (s), 1474 - 1377 (s, aromatic $\delta_{C=C}$), 1231 (m, aromatic $\delta_{C=N}$), 1058 - 1000 (br vs). ^1H NMR: δ 8.22 (2H, br s, *6,6'*-py), 7.89 (2H, br s, *4,4'*-py), 7.19 (2H, br d, *3,3'*-py), 7.10 (2H, br s, *5,5'*-py), 5.09 (2H, br m, *H*C=C*H*), 2.01 (2H, br q, $CHCH_2$), 1.73 (3H, br d, $CHCH_3$), 1.45 (2H, br quin, $CHCH_2CH_2$), 1.31 (4H, br m, $CH_2CH_2CH_3$), 0.89 (3H, br t, CH_2CH_3). ^{13}C NMR: δ 154.41 (*2,2'*-py), 149.31 (*6,6'*-py), 141.58 (*4,4'*-py), 119.02 (*5,5'*-py), 116.08 (*3,3'*-py), 109.59 ($CHCHCH_2$), 102.79 ($CHCHCH_2$), 34.07 ($CHCHCH_2$), 32.56 ($CH_2CH_2CH_3$), 31.50 ($CHCH_2CH_2$), 23.65 ($CH_2CH_2CH_3$), 18.67 ($CH_2CH_2CH_3$), 14.47 (CH_3CH).

[Cu(H-dpa)(*cis*-3-octene)]BF_4 (1.8). This compound was prepared in an analogous manner to that of compound **4**. Yield: 47%. Mp: 142 - 145 °C (dec.). IR (ATR, cm^{-1}): 3344 (m, ν_{N-H}), 3257 (w, aromatic ν_{C-H}), 3224 (w, aromatic ν_{C-H}), 3154 (w, aromatic ν_{C-H}), 3123 (w, aromatic ν_{C-H}), 3077 (w, alkene ν_{C-H}), 3047 (w, alkene ν_{C-H}), 2955 (w, alkyl ν_{C-H}), 2927 (w, alkyl ν_{C-H}), 2871 (w, alkyl ν_{C-H}), 1639 (s, δ_{N-H}), 1583 (s), 1531 (m), 1478 - 1377 (s, aromatic $\delta_{C=C}$), 1233 (m, aromatic $\delta_{C=N}$), 1060 - 992 (br vs). ^1H NMR: δ 8.20 (2H, br d, *6,6'*-py), 7.89 (2H, br d, *4,4'*-py), 7.20 (2H, br d, *3,3'*-py), 7.12 (2H, br d, *5,5'*-py), 5.04 (2H, m, *H*C=C*H*), 2.05 (4H, m, $CHCH_2$), 1.49-1.34 (4H, m, $CH_2CH_2CH_3$), 1.07 [2H, t, *J*(H-H) = 7.5 Hz, $CHCH_2CH_3$], 0.93 [3H, t, *J*(H-H) = 7.2 Hz, $CH_2CH_2CH_3$]. ^{13}C NMR: δ 154.41 (*2,2'*-py), 149.35 (*6,6'*-py), 141.54 (*4,4'*-py), 119.01

(*5,5'*-py), 116.04 (*3,3'*-py), 104.80 (*C*H), 102.89 (*C*HCH$_2$), 34.14 (*C*H$_2$Et), 28.84 (CH*C*H$_2$CH$_2$), 23.66 (CH$_2$*C*H$_2$CH$_3$), 22.43 (CH*C*H$_2$CH$_3$), 15.47 (CHCH$_2$*C*H$_3$), 14.41 (CH$_2$CH$_2$*C*H$_3$).

[Cu(H-dpa)(*trans*-3-octene)]BF$_4$ (1.9). This compound was prepared in an analogous manner to that of compound **4**. Yield: 46%. Mp: 143 - 145 °C (dec.). IR (ATR, cm^{-1}): 3349 (m, ν_{N-H}), 3265 (w, aromatic ν_{C-H}), 3230 (w, aromatic ν_{C-H}), 3164 (w, aromatic ν_{C-H}), 3086 (w, alkene ν_{C-H}), 3051 (w, alkene ν_{C-H}), 2961 (w, alkyl ν_{C-H}), 2923 (w, alkyl ν_{C-H}), 2869 (w, alkyl ν_{C-H}), 1646 (s, δ_{N-H}), 1586 (s), 1534 (s), 1481 - 1383 (s, aromatic $\delta_{C=C}$), 1231 (m, aromatic $\delta_{C=N}$), 1054 - 996 (br vs). ^{1}H NMR: δ 8.23 (2H, br d, *6,6'*-py), 7.89 (2H, br t, *4,4'*-py), 7.19 (2H, br d, *3,3'*-py), 7.10 (2H, br t, *5,5'*-py), 5.08 (2H, br m, *H*C=C*H*), 2.04 (4H, br m, C*H*$_2$CHCHC*H*$_2$), 1.49-1.32 (4H, br m, C*H*$_2$C*H*$_2$CH$_3$), 1.07 [3H, t, *J*(H-H) = 7.3 Hz, CHC*H*$_3$], 0.91 [3H, t, *J*(H-H) = 7.2 Hz, CH$_2$C*H*$_3$]. ^{13}C NMR: δ 154.33 (*2,2'*-py), 149.43 (*6,6'*-py), 141.66 (*4,4'*-py), 118.94 (*5,5'*-py), 116.16 (*3,3'*-py), 108.14 (*C*HCH$_2$CH$_3$), 105.73 (*C*HCH$_2$CH$_2$), 34.37 (CH*C*H$_2$CH$_2$), 33.74 (*C*H$_2$CH$_2$CH$_3$), 27.33 (CH*C*H$_2$CH$_3$), 23.23 (CH$_2$*C*H$_2$CH$_3$), 15.76 (CHCH$_2$*C*H$_3$), 14.35 (CH$_2$CH$_2$*C*H$_3$).

[Cu(H-dpa)(2-norbornene)]BF$_4$ (1.10). This compound was prepared in an analogous manner to that of compound **4**. Yield: 77%. Mp: 169 - 172 °C. IR (ATR, cm^{-1}): 3341 (m, ν_{N-H}), 3262 (w, aromatic ν_{C-H}), 3224 (w, aromatic ν_{C-H}), 3159 (w, aromatic ν_{C-H}), 3121 (w, aromatic ν_{C-H}), 3055 (w, alkene ν_{C-H}), 2982 (w, alkyl ν_{C-H}), 2944 (w, alkyl ν_{C-H}), 2878 (w, alkyl ν_{C-H}), 2853 (w, alkyl ν_{C-H}), 1643 (s, δ_{N-H}), 1582 (s), 1530 (m), 1478 - 1379 (s, aromatic $\delta_{C=C}$), 1232 (s, aromatic $\delta_{C=N}$), 1087 - 965 (br vs). ^{1}H NMR: δ 8.35 (2H, br d, *6,6'*-py), 7.92 (2H, br t, *4,4'*-py), 7.22 (2H, br d, *3,3'*-py), 7.15 (2H, br t, *5,5'*-py), 5.05 (2H, br s, C*H*=C*H*), 3.17 (2H, s, C*H*CH$_2$C*H*), 1.65 (2H, m, C*H*$_2$), 1.27 (1H, m, CHC*H*$_2$CH), 1.12 (2H, m, C*H*$_2$), 0.99 (1H, m, CHC*H*$_2$CH). ^{13}C NMR: δ 153.87 (*2,2'*-

py), 150.07 (*6,6'*-py), 141.88 (*4,4'*-py), 118.95 (*5,5'*-py), 116.18 (*3,3'*-py), 102.44 (*C*H=*C*H), 44.45 (CH*C*H$_2$CH), 44.41 (*C*HCH$_2$*C*H), 25.62 (*C*H$_2$*C*H$_2$).

[Cu(H-dpa)(1,5-cyclooctadiene)]BF_4 (1.11). This compound was prepared in an analogous manner to that of compound **4**. Yield: 79%. Mp: 182 - 185 °C (dec.). IR (ATR, cm^{-1}): 3339 (m, ν_{N-H}), 3256 (w, aromatic ν_{C-H}), 3220 (w, aromatic ν_{C-H}), 3156 (w, aromatic ν_{C-H}), 3125 (w, aromatic ν_{C-H}), 3086 (w, alkene ν_{C-H}), 3013(w, alkene ν_{C-H}), 2982 (w, alkyl ν_{C-H}), 2949 (w, alkyl ν_{C-H}), 2886 (w, alkyl ν_{C-H}), 2849 (w, alkyl ν_{C-H}), 1634 (s, δ_{N-H}), 1582 (s), 1523 (s), 1469 - 1361 (s, aromatic $\delta_{C=C}$), 1229 (s, aromatic $\delta_{C=N}$), 1076 - 979 (br vs). ^{1}H NMR: δ 8.23 (2H, br d, *6,6'*-py), 7.93 (2H, br t, *4,4'*-py), 7.24 (2H, br d, *3,3'*-py), 7.17 (2H, br t, *5,5'*-py), 5.50 (4H, br m, C*H*), 2.40 (8H, br m, C*H*$_2$). ^{13}C NMR: δ 154.40 (*2,2'*-py), 149.42 (*6,6'*-py), 141.94 (*4,4'*-py), 122.46 (*C*H), 119.45 (*5,5'*-py), 116.22 (*3,3'*-py), 29.18 (*C*H$_2$).

[Cu(H-dpa)(styrene)]BF_4 (1.12). This compound was prepared in an analogous manner to that of compound **4**. Yield: 82%. Mp: 173 - 176 °C (dec.). IR (ATR, cm^{-1}): ν 3346 (m, ν_{N-H}), 3265 (w, aromatic ν_{C-H}), 3228 (w, aromatic ν_{C-H}), 3162 (w, aromatic ν_{C-H}), 3083 (w, alkene ν_{C-H}), 3056 (w, alkene ν_{C-H}), 1641 (s, δ_{N-H}), 1584 (s), 1530 (s), 1477 - 1378 (s, aromatic $\delta_{C=C}$), 1231 (s, aromatic $\delta_{C=N}$), 1076 - 988 (br vs). ^{1}H NMR: δ 8.07, (2H, br d, *6,6'*-py), 7.85 (2H, br t, *4,4'*-py), 7.54 (2H, d, *o*-C*H*, Ph), 7.30, (2H, t, *m*-C*H*, Ph), 7.24 (1H, t, *p*-C*H*, Ph), 7.16 (2H, br d, *3,3'*-py), 7.03 (2H, br t, *5,5'*-py), 6.11 [1H, dd, *J*(H-H) = 15.6 Hz, *J*(H-H) = 9.7 Hz, C*H*Ph], 4.88 [1H, d, *J*(H-H) = 15.6 Hz, *cis*-C*H*], 4.48 [1H, d, *J*(H-H) = 9.7 Hz, *trans*-C*H*]. ^{13}C NMR: δ 153.99 (*2,2'*-py), 149.65 (*6,6'*-py), 141.70 (*4,4'*-py), 138.79 (*1*-Ph), 130.20 (*m-C*H, Ph), 129.40 (*p-C*H, Ph), 127.28 (*o-C*H, Ph), 118.80 (*5,5'*-py), 116.03 (*3,3'*-py), 105.20 (H$_2$C=*C*H), 77.97 (H$_2$*C*=CH).

[Cu(dpa)(*cis*-stilbene)]BF_4 (1.13). This compound was prepared in an analogous manner to that of compound **4**. Yield: 33%. Mp: 157 - 159 °C (dec.). IR (ATR, cm^{-1}): 3341 (m, ν_{N-H}), 3263 (w, aromatic ν_{C-H}), 3224 (w, aromatic ν_{C-H}), 3161 (w, aromatic ν_{C-H}), 3093 (w, alkene ν_{C-H}), 3051 (w, alkene ν_{C-H}), 1640 (s, δ_{N-H}), 1585 (s), 1531 (s), 1477 - 1379 (s, aromatic $\delta_{C=C}$), 1232 (s, aromatic $\delta_{C=N}$), 1053 - 1014 (br vs). ^1H NMR: δ 7.92 (2H, br s, *6,6'*-py), 7.80 (2H, br s, *4,4'*-py), 7.27 (4H, m, *o*-C*H*), 7.14 (8H, br m + s, *m*-C*H*, *p*-C*H* + *3,3'*-py), 6.88 (2H, br s, *5,5'*-py), 6.25 (2H, s, C*H*Ph). ^{13}C NMR: δ 154.32 (*2,2'*-py), 149.32 (*6,6'*-py), 141.47 (*1,1'*-Ph), 138.25 (*4,4'*-py), 130.44 (*o*-*C*H, Ph), 129.47 (*m*-*C*H, Ph), 128.71 (*p*-*C*H, Ph), 118.80 (*5,5'*-py), 115.99 (*3,3'*-py), 108.50 (*C*H).

[Cu(H-dpa)(*trans*-stilbene)]BF_4 (1.14). This compound was prepared in an analogous manner to that of compound **4**. Yield: 25%. Mp: 126 - 128 °C (dec.). IR (ATR, cm^{-1}): 3348 (m, ν_{N-H}), 3263 (w, aromatic ν_{C-H}), 3227 (w, aromatic ν_{C-H}), 3163 (w, aromatic ν_{C-H}), 3078 (w, alkene ν_{C-H}), 3059 (w, alkene ν_{C-H}), 3021 (w, alkene ν_{C-H}), 1642 (s, δ_{N-H}), 1583 (m), 1532 (m), 1478 - 1423 (s, aromatic $\delta_{C=C}$), 1234 (m, aromatic $\delta_{C=N}$), 1073 - 1014 (br vs). ^1H NMR: δ 8.06 (2H, br d, *6,6'*-py), 7.78 (2H, br t, *4,4'*-py), 7.57 (4H, br d, *o*-C*H* Ph), 7.32 (4H, br t, *m*-C*H* Ph), 7.23 (2H, br t, *p*-C*H*, Ph), 7.06 (2H, br d, *3,3'*-py), 6.97 (2H, br t, *5,5'*-py), 6.88 (2H, s, C*H*Ph). ^{13}C NMR (298 K; CD_3OD): δ 154.58 (*2,2'*-py), 149.50 (*6,6'*-py), 141.32 (*4,4'*-py), 138.80 (*1,1'*-Ph), 129.98 (*m*-*C*H, Ph), 128.87 (*p*-*C*H, Ph), 127.64 (*o*-*C*H, Ph), 122.19 (C*H*), 118.73 (*5,5'*-py), 115.88 (*3,3'*-py).

[Cu(H-dpa)($Ph_2C=CH_2$)]BF_4 (1.15). This compound was prepared in an analogous manner to that of compound **4**. Yield: 25%. Mp: 131 - 133 °C (dec.). IR (ATR, cm^{-1}): 3348 (m, ν_{N-H}), 3257 (w, aromatic ν_{C-H}), 3225 (w, aromatic ν_{C-H}), 3157 (w, aromatic ν_{C-H}), 3128 (w, aromatic ν_{C-H}), 3084 (w, alkene ν_{C-H}), 3047 (w, alkene ν_{C-H}), 1635 (s, δ_{N-H}), 1583 (s), 1532 (s), 1472 - 1377 (s, aromatic $\delta_{C=C}$), 1231 (s, aromatic $\delta_{C=N}$),

1055 - 998 (br vs). ^{1}H NMR: δ 8.09 (2H, br d, *6,6'*-py), 7.81 (2H, br t, *4,4'*-py), 7.32 (10H, m, C*H* Ph), 7.11 (2H, br d, *3,3'*-py), 7.00 (2H, br t, *5,5'*-py), 5.29 (2H, s, CH_2). ^{13}C NMR: δ 154.83 (*2,2'*-py), 149.14 (*6,6'*-py), 145.82 (*C*CH$_2$), 142.64 (*1,1'*-Ph), 140.99 (*4,4'*-py), 129.50 (*o*-*C*H, Ph), 129.36 (*m*-*C*H, Ph), 129.09 (*p*-*C*H, Ph), 118.50 (*5,5'*-py), 115.85 (*3,3'*-py), 106.92 (*C*H$_2$).

Computational Methods. A modified literature procedure [34] was used for modeling complex cations at different method/basis set levels. Gaussian input files were prepared using MOPAC[35] semi-empirical energy minimizations. Second pass modeling was performed at the RHF/STO-3G level.[36,37] Subsequent modeling was performed using effective electron core potentials for Cu at the B3LYP/LanL2DZ [38,39] basis set level. The 6-311++G* basis set[40] was used for N, C, and H atoms. Final calculations were then performed at the RMP2-FC/LanL2DZ level.[41] Gaussian 03 Package was used for all calculations.[42]

Crystallographic Study. X-ray data for compounds **1.5**, **1.6**, **1.8**, and **1.10 - 1.13** were collected at room temperature on a Bruker SMART 1000 CCD diffractometer equipped with graphite monochromated Mo-K_α radiation (λ = 0.71073 Å) and corrected for Lorentz and polarization effects. The samples were prepared by suspension in mineral oil under an inert atmosphere (facilitating separation and selection of a single crystal), followed by sealing in a thin layer of epoxy resin and securing to the end of a glass fiber. Fibers were fastened onto brass pins and mounted onto a fixed-χ 3-circle goniometer head. Data collection and unit cell refinement were carried out according to established methods[43] using the program SMART.[44] The program SAINT[45] was used for data reduction, and absorption correction was applied using SADABS.[46] Pertinent details are given in Table 1.5. Heavy atom sites were located by Patterson[47] methods for complexes **1.8** and **1.11**; all other structures were solved by direct methods, and models were refined

using full-matrix least squares techniques.[48] All non-hydrogen atoms were initially refined as having isotropic thermal parameters, and subsequent refinement was then performed with anisotropic thermal parameters: shift/error less than 0.01.

All hydrogen atoms were placed in calculated positions [C-H (alkene) = 0.98 Å, C-H (methylene) = 0.97 Å, C-H (methyl) = 0.96 Å, N-H = 0.86 Å, and C-H (aromatic) = 0.93 Å] and refined using a riding model with fixed isotropic displacement parameters. Neutral-atom scattering factors were taken from the usual source.[49] Refinement of positional and anisotropic displacement parameters led to convergence for all data. The program used for structure solution and refinement was SHELXTL Version 6.14.[50] The program PLATON was employed for structure validation.[51] Selected bond lengths and angles are given in Table 1.1.

Refinement of compound **1.6** indicated that the C_5H_{11} groups [C(14)-C(18)] showed a site occupancy disorder. While the first methylene carbon [C(14)] has a fixed position, the remainder of the alkyl chain exhibits a reversal of the conformation of the substituent with a 60:40 site occupancy (Figure 1.19).

Disordered atoms C(15) through C(18) were refined with site occupancies of 60:40 [C(15a)-C(18a):C(15b)-C(18b)], with adjacent C-C distances restrained to 1.54(0.025) Å and alternating C-C distances, i.e. C(15a)-C(17a), restrained to 2.60(0.05) Å. H atoms for C(18a) and C(18b) were placed in idealized positions for a disordered methyl group.

This form of static disorder is sometimes observed for "floppy" ligands.[52,53] Such disorder is seen to a lesser extent in the other two complexes having long alkyl chains (**1.5** and **1.8**), as shown by their relatively large thermal ellipsoids. These disorders are likely a result of room temperature data collection. Refinement of **1.5** and **1.8** as having site occupancy disorder in the alkyl chains did not result in better agreement of data, so refinement was performed without the disorder. The tetrafluoroborate anions present in the [Cu(H-dpa)(*cis*-3-octene)]BF_4 and [Cu(H-dpa)(cod)]BF_4 complexes were also found

to exhibit a site occupancy disorder of the fluorine atoms. Refinement details of disordered BF_4^- anions in compounds **1.8** and **1.11** are located in chapter 7.

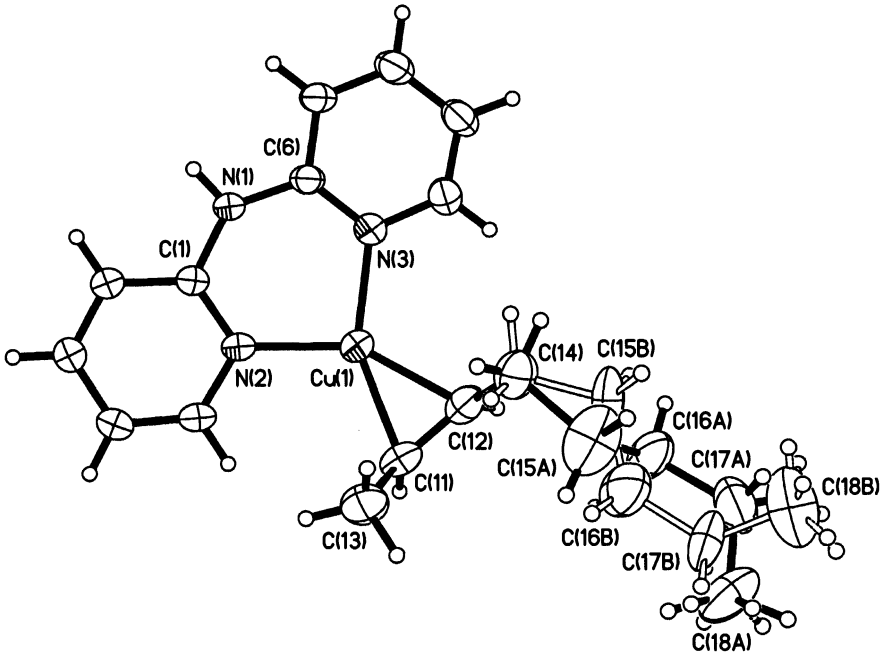

Figure 1.19. Molecular structure for the complex cation of (**1.6**) with both parts of the disordered alkyl chain present. For clarity, thermal ellipsoids are shown at the 20 % level.

Table 1.7. Summary of X-ray diffraction data for [Cu(H-dpa)(η^2-olefin)]BF_4 compounds.

compound	**1.5**	**1.6**	**1.8**
empir. formula	$CuC_{18}H_{25}N_3BF_4$	$CuC_{18}H_{25}N_3BF_4$	$CuC_{18}H_{25}N_3BF_4$
M_W	433.76	433.76	433.76
cryst. system	monoclinic	monoclinic	triclinic
space group	C2/c	$P2_1/n$	P-1
a, Å	17.770(4)	8.885(1)	9.652(1)
b, Å	10.399(2)	10.554(2)	10.106(2)
c, Å	23.290(5)	21.729(4)	11.396(2)
α, deg.	-	-	69.02(3)
β, deg.	108.98(3)	92.36(3)	77.70(3)
γ, deg.	-	-	80.75(3)
V, $Å^3$	4069 (1)	2035.9(7)	1009.7(3)
Z	8	4	2
D_{calc}, g/cm^3	1.416	1.415	1.427
μ, mm^{-1}	1.115	1.115	1.124
2θ range, deg.	3.70 - 56.50	3.76 - 56.62	3.88 - 56.64
No. collected	24172	24020	12398
No. ind. (R_{int})	4921 (0.1494)	4942 (0.0551)	4798 (0.0419)
No. obsd. ($\|F_o\| > 4.0\sigma \|F_o\|$)	1475	1921	1900
R	0.0702	0.0556	0.0495
R_w	0.1501	0.1536	0.1258
$\Delta\rho_{max/min}$ ($eÅ^{-3}$)	0.413, -0.340	0.549, -0.343	0.269, -0.229
weights	0.0671, 0	0.1113, 0.9024	0.0825, 0
CCDC Deposit No.	692443	692444	693280

Table 1.7. contd.

compound	**1.10**	**1.11**	**1.12**
empir. formula	$CuC_{17}H_{19}N_3BF_4$	$CuC_{18}H_{21}N_3BF_4$	$CuC_{18}H_{17}N_3BF_4$
M_W	415.7	429.73	425.7
cryst. system	monoclinic	monoclinic	monoclinic
space group	C2/c	$P2_1/m$	$P2_1/n$
a, Å	21.438(4)	7.217(1)	12.503(3)
b, Å	14.935(3)	11.797(2)	10.368(2)
c, Å	14.510(3)	10.771(2)	13.827(3)
α, deg.	-	-	-
β, deg.	130.56(3)	95.30(3)	92.70(3)
γ, deg.	-	-	-
V, $Å^3$	3530(1)	913.0(3)	1790.5(6)
Z	8	2	4
D_{calc}, g/cm^3	1.565	1.563	1.579
μ, mm^{-1}	1.283	1.242	1.266
2θ range, deg.	3.70 - 56.86	3.80 - 56.58	4.30 - 56.86
No. collected	20570	7472	21029
No. ind. (R_{int})	4279 (0.0860)	2289 (0.0258)	4329 (0.1717)
No. obsd. ($\|F_o\| > 4.0\sigma \|F_o\|$)	2401	1699	1505
R	0.0883	0.0656	0.0656
R_w	0.2193	0.1796	0.1529
$\Delta\rho_{max/min}$ ($eÅ^{-3}$)	1.523, -0.623	1.456, -0.955	0.696, -0.843
weights	0.0575, 0	0.0977, 1.5308	0.0920, 0
CCDC Deposit No.	692446	698583	692447

Table 1.7. contd.

compound	**1.13**
empir. formula	$CuC_{24}H_{21}N_3BF_4$
M_W	501.79
cryst. system	monoclinic
space group	$P2_1/n$
a, Å	10.324(2)
b, Å	22.671(5)
c, Å	10.923(2)
α, deg.	-
β, deg.	116.92(3)
γ, deg.	-
V, $Å^3$	2279.8(8)
Z	4
D_{calc}, g/cm^3	1.462
μ, mm^{-1}	1.007
2θ range, deg.	3.60 - 56.68
No. collected	27790
No. ind. (R_{int})	5568 (0.1147)
No. obsd.	
($\|F_o\| > 4.0\sigma \|F_o\|$)	2098
R	0.0713
R_w	0.1584
$\Delta\rho_{max/min}$ ($eÅ^{-3}$)	0.629, -0.310
weights	0.0820, 0.7302
CCDC Deposit No.	692445

References

1 J. L. Humphrey, A. F. Seibert and R. A. Koort, *Separation Technologies: Advances and Priorities*, DOE/ID/12920-1, Washington, DC 1001.

2 National Research Council, *Separation Technologies for the Industries of the Future*, Publication NMAB-487-3, National Academy Press, Washington, DC 1998.

3 National Research Council, *Separation and Purification: Critical Needs and Opportunities* (National Academy Press, Washington, DC, 1987).

4 E. R. Brown and R. L. Hair, *Monoolefin/paraffin separation by selective adsorption*, Phillips Petroleum Company, 1993.

5 K. Wang and E. I. Stiefel, *Science*, 2001, **291**, 106.

6 G. C. Blytas, in *Separation and Purification Technology*, N. N. Li, J. M. Calo, Eds. Dekker, New York, 1992, pp. 19-57.

7 T. Suzuki, R. D. Nobel, and C. A. Koval, *Inorg. Chem.*, 1997, **36**, 136.

8 J. S. Thompson, R. L. Harlow, and J. F. Whitney, *J. Am. Chem. Soc.*, 1983, **105**, 3522.

9 (a) F. I. Rodriguez, J. J. Esch, A. E. Hall, B. M. Binder, G. E. Schaller, and A. B. Bleeker, *Science*, 1999, **283**, 996; (b) G. E. Schaller and A. B. Bleeker, *Science*, 1995, **270**, 1809; (c) J. R. Ecker, *Science*, 1995, **268**, 667.

10 (a) H. S. Kim, Y. J. Kim, J. J. Kim, S. D. Lee, Y. S. Kang, and C. S. Chin, *Chem. Mater.*, 2001, **13**, 1720; (b) H. Y. Huang, J. Padin, and R. T. Yang, *J. Phys. Chem. B*, 1999, **103**, 3206.

11 X. Dai and T. H. Warren, *Chem. Comm.*, 2001, 1998.

12 B. F. Straub, F. Eisentrager, and P. Hofmann, *Chem. Comm.*, 1999, 2507.

13 W. A. Braunecker, T. Pintauer, N. V. Tsarevsky, G. Kickelbick, and K. Matyjaszewski, *J. Organomet. Chem.*, 2005, **690**, 916.

14 A. Boni, G. Pampaloni, R. Peloso, D. Belleti, C. Graiff, and A. Tiripicchio, *J. Organomet. Chem.*, 2006, **691**, 5602.

15 J. S. Thompson and J. F. Whitney, *Inorg. Chem.*, 1984, **23**, 2813.

16 J. S. Thompson, J. C. Calabrese, and J. F. Whitney, *Acta Cryst.*, 1985, **C41**, 890.

17 (a) J. Zhang, R.-G. Xiong, J.-L. Zuo, and X.-Z. You, *Chem. Commun.*, 2000, 1495; (b) J. Zhang, R.-G. Xiong, J.-L. Zuo, C.-M. Che and X.-Z. You, *J. Chem. Soc., Dalton Trans.*, 2000, 2898.

18 M. Munakata, S. Kitagawa, S. Kosome, and A. Asahara, *Inorg. Chem.*, 1986, **25**, 2622.

19 M. Munakata, S. Kitagawa, H. Shimono, and H. Masuda, *Inorg. Chem.*, 1991, **30**, 2610.

20 K. M. Chi, H.-K. Shin, M. J. Hampden-Smith, E. N. Duesler, and T. T. Kodas, *Polyhedron*, 1991, **10**, 2293.

21 J. Min, J. Benet-Buchholz, and R. Boese, *Chem. Comm.*, 1998, 2751.

22 M. Pasquali, C. Floriani, A. Gaetani-Manfredotti, and A. Chiesi-Villa, J. Am. *Chem. Soc.,* 1978, **100**, 4918.

23 (a) L. Cavallo, M. E. Cucciolito, A. De Martino, F. Giordano, I. Orabona, and A. Vitagliano, *Chem. Eur. J.*, 2000, **6**, 1127; (b) R. Rios, J. Liang, M. M.-C. Lo, and G. C. Fu, *Chem. Comm.*, 2000, 377.

24 N. Yasuda, H. Uekusa, and Y. Ohasi, *Acta Cryst.,* 2001, **E57**, o1189.

25 H. Masuda, K. Machida, M. Munakata, S. Kitagawa, and H. Shimono, *J. Chem. Soc., Dalton Trans.,* 1988, 1907.

26 T. Steiner, *J. Chem. Cryst.*, 1997, **27**, 673.

27 *CRC Handbook of Chemistry and Physics*, 60th Ed. CRC Press, Inc. Boca Raton, FL, **1980**, D-194.

28 A. Bondi, *J. Phys. Chem.*, 1964, **68**, 441.

29 M. B. Power, J. R. Nash, M. D. Healy, and A. R. Barron, *Organometallics*, 1992, **11**, 1830.

30 (a) A. R. Barron, *J. Chem. Soc., Dalton Trans.*, 1988, 3047; (b) D. Ogrin, L. H. van Poppel, S. G. Bott and A. R. Barron, *Dalton Trans.*, 2004, 3689; (c) C. S. Branch, L. G. van Poppel, S. G. Bott, and A. R. Barron, *J. Chem. Cryst.*, 1999, **29**, 993; (d) C. S. Branch, S. G. Bott, and A. R. Barron, *J. Organomet. Chem.*, 2003, **666**, 23.

31 L. H. van Poppel, S. G. Bott and A. R. Barron, *J. Chem. Soc., Dalton Trans.*, 2002, 3327.

32 L. H. van Poppel, S. G. Bott, and A. R. Barron, *J. Am. Chem. Soc.*, 2003, **125**, 11006.

33 B. J. Hathaway, D. G. Holah, and J. D. Postlethwaite, *J. Chem. Soc.*, 1961, 3215.

34 H. Y. Huang, J. Padin, and R. T. Yang, *J. Phys. Chem. B,* 1999, **103**, 3206.

35 *CS MOPAC Pro*. v6.0, 2000, CambridgeSoft Corporation: Cambridge, MA.

36 W. J. Hehre, R. F. Stewart, and J. A. Pople, *J. Chem. Phys.* 1969, **51**, 2657.

37 J. B. Collins, P. Schleyer, J. S. Binkley, and J. A. Pople, *J. Chem. Phys.* 1976, **64**, 5142.

38 P. J. Hay and W. R. Wadt, *J. Chem. Phys.,* 1985, **82**, 270.

39 W. R. Wadt and P. J. Hay, *J. Chem. Phys.*, 1985, **82**, 284.

40 (a) R. Krishnan, J. S. Binkley, R. Seeger, and J. A. Pople, *J. Chem. Phys.,* 1980, **72**, 650; (b) A. D. McLean and G. S. Chandler, *J. Chem. Phys.,* 1980, **72**, 5639; (c) C. Moller and M. S. Plesset, *Phys. Rev. Lett.,* 1934, **46**, 618.

41 J. B. Foresman and A. Frisch, *Exploring Chemistry with Electronic Structure Methods* 2nd Ed. 1994, Gaussian Inc.: Wallingtonford, CT.

42 M. J. Frisch, G. W. Trucks, H. B. Schlegel, G. E. Scuseria, M. A. Robb, J. R. Cheeseman, J. A. Montgomery, Jr., T. Vreven, K. N. Kudin, J. C. Burant, J. M.

Millam, S. S. Iyengar, J. Tomasi, V. Barone, B. Mennucci, M. Cossi, G. Scalmani, N. Rega, G. A. Petersson, H. Nakatsuji, M. Hada, M. Ehara, K. Toyota, R. Fukuda, J. Hasegawa, M. Ishida, T. Nakajima, Y. Honda, O. Kitao, H. Nakai, M. Klene, X. Li, J. E. Knox, H. P. Hratchian, J. B. Cross, V. Bakken, C. Adamo, J. Jaramillo, R. Gomperts, R. E. Stratmann, O. Yazyev, A. J. Austin, R. Cammi, C. Pomelli, J. W. Ochterski, P. Y. Ayala, K. Morokuma, G. A. Voth, P. Salvador, J. J. Dannenberg, V. G. Zakrzewski, S. Dapprich, A. D. Daniels, M. C. Strain, O. Farkas, D. K. Malick, A. D. Rabuck, K. Raghavachari, J. B. Foresman, J. V. Ortiz, Q. Cui, A. G. Baboul, S. Clifford, J. Cioslowski, B. B. Stefanov, G. Liu, A. Liashenko, P. Piskorz, I. Komaromi, R. L. Martin, D. J. Fox, T. Keith, M. A. Al-Laham, C. Y. Peng, A. Nanayakkara, M. Challacombe, P. M. W. Gill, B. Johnson, W. Chen, M. W. Wong, C. Gonzalez, and J. A. Pople, *Gaussian 03, Rev. D.01*. 2004, Gaussian, Inc.: Wallingtonford, CT.

43 S. Ruhl and M. Bolte, *Z. Kristallogr.*, 2000, **215**. 499.

44 Bruker AXS. *SMART v5.050; Bruker Molecular Analysis Research Tool*, Bruker AXS Inc., Madison, WI, 1999b.

45 Bruker AXS. *SAINT v6.06. Integration Software for Single Crystal Data.* Bruker AXS Inc., Madison, WI, 1999a.

46 Sheldrick, G. M. *SADABS, Bruker Area Detector Absorption Corrections*. Bruker AXS Inc., Madison, WI; R. H. Blessing, *Acta Crystallogr.,* 1995, **A51**, 33.

47 A. L. Patterson, *Z. Kristallogr.*, 1935, **A90**, 517.

48 G. M. Sheldrick, *Acta Crystallogr.*, 2008, **A64**, 112-122.

49 F. H. Allen, O. Kennard, D. G. Watson, L. Brammer, A. G. Orpen, R. Taylor, *International Tables for Crystallography*, 1995, Volume C, edited by A. J. C. Wilson, pp. 685-706. Dordrecht: Kluwer.

50 G. M. Sheldrick, *SHELXTL v6.14*, 2000, Bruker AXS Inc., Madison, WI.

51 (a) A. L. Spek, *PLATON, Molecular Geometry Program*, 2008, Utrecht, The Netherlands. (b) A. L. Spek, *J. Appl. Cryst.*, 2003, **36**, 380-388.

52 (a) J. L. Atwood, S. G. Bott, C. Eaborn, M. N. A. El-Khali, and J. D. Smith, *J. Organomet. Chem.*, 1985, **294**, 23; (b) K. A. Abboud, E. J. Eaborn, and A. Trivellas, *Acta Cryst.*, 1992, **C48**, 1695.

53 (a) C. L. Aitken and A. R. Barron, *J. Chem. Cryst.*, 1996, **26**, 297; (b) C. J. Harlan, E. G. Gillan, S. G. Bott, and A. R. Barron, *Organometallics,* 1996, **15**, 5479; (c) A. W. Apblett and A. R. Barron, *J. Cryst. Spec. Res.*, 1993, **23**, 529.

Chapter 2

N-Aryl Substituted (2-Pyridyl), *Bis*(2-Pyridyl), (2-Pyridyl)(2-quinolyl), and *Bis*(2-quinolyl)amines

Introduction

Through the structural comparisons between observed and calculated data in the previous chapter, it would seem that functionalization of the amine nitrogen bridging the two pyridyl rings could potentially offer some degree of steric selectivity without adding bulk in the immediate vicinity of the metal center. The control over the selective binding of olefins to a metal center has the potential as a simple route to overcoming the inherent difficulty in the separation of different olefins with near identical boiling points.[1] Various complexing reagents have been described[2] in which the olefin will coordinate the metal center under one condition, and dissociate under another (see Chapter 1, Eq. 1.1).[3]

Past studies have demonstrated that stable, yet reversible, Cu···olefin interactions can be achieved using chelating N-donor ligands.[4,5,6] In general, ligands that have proven effective in this regard are neutral, N-donor heterocyclic chelates. This includes *bis*(pyrazolyl)methanes,[7] *bis*(2-pyridyl)amine,[8,9] phenanthroline,[10] and bipyridines.[11] The work done by Thompson and Whitney with reversible binding of ethylene to cuprous complexes incorporating *bis*(2-pyridyl)amine (H-dpa) has formed the basis for our studies.

In Chapter 1, it was demonstrated that the *bis*(2-pyridyl)amine ligand (**I**, where Ar = H) allows for the isolation and structural characterization of a wide range of ionic copper(I)···olefin complexes. Moreover, it was observed that a twisting of the olefin out of the plane of the H-dpa ligand and a related folding of the H-dpa ligand provide relief of inter-ligand/intramolecular steric strain for terminal and *cis*-olefins. Using ^{1}H and ^{13}C NMR it was shown that there is a significant difference in binding between a terminal and internal olefin, but much less preference between different internal olefins, with only

modest difference between the *cis* and *trans* isomers of the same olefin. These results suggest that while differential complexation of *cis* and *trans* isomers is possible using *bis*(2-pyridyl)amine-type ligands, but the separation of different internal olefins by their C=C position is unlikely. The use of pre-folded *bis*(2-pyridyl)amine ligands, however, should allow for an enhanced differentiation between isomer coordination.

Molecular mechanics calculations on aryl substituted *bis*(2-pyridyl)amine ligands (with R = H, Ph, Mes, 2,6-Et_2Ph, 2-^{i}PrPh, 2,6-$^i Pr_2$Ph, and 1-naph) suggests that the presence of the aryl substituent results in a folding of the *bis*(2-pyridyl)amine unit. Based on these initial calculations, substitution remotely from the metal center could have the desired pre-folding effect on the pyridyl rings of the ancillary ligand.

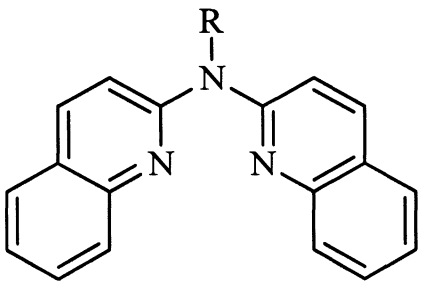

(I)

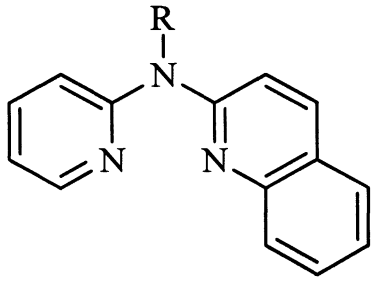

(II)

More traditional methods of altering steric interactions about a metal center involve increasing the steric bulk of ligands in the immediate vicinity of the metal, or alternatively, modification of the ligand chelate size and dentate number.[12] In this regard, increased steric effects can be obtained using quinolyl versus pyridyl heterocycles, *i.e.*, **I** and **II**.

As part of our study towards the development of novel chelate N-donor heterocycles to prepare stable, yet reversibly bound, Cu(I)-olefin complexes, we have prepared a series of novel N-functionalized dipyridylamine and diquinolylamine ligands via Buchwald-Hartwig amination[13,14] of 2-bromopyridine and 2-chloroquinoline with

substituted anilines. Where the synthesis of aryl substituted asymmetrical N-(2-pyridyl)-N-(2-quinolyl)amines (**II**) is desired, convenient starting materials for the reactions are the corresponding N-(2-pyridyl)amines. Four of these N-(2-pyridyl)amines, RN(H)py [R = Mes (**2.1**), 2,6-Et_2Ph (**3.2**), 2-^{i}PrPh (**2.3**), and $(Ph)_3C$ (**2.4**)], have been prepared and structurally characterized, and the results are presented herein.

Results and Discussion

Aryl Substituted (2-pyridyl)amines. The molecular structures of the secondary aromatic amines **2.1** - **2.4** are shown in Figures 2.1 - 2.4, and selected bond lengths and angles are given in Tables 2.1 and 2.2.

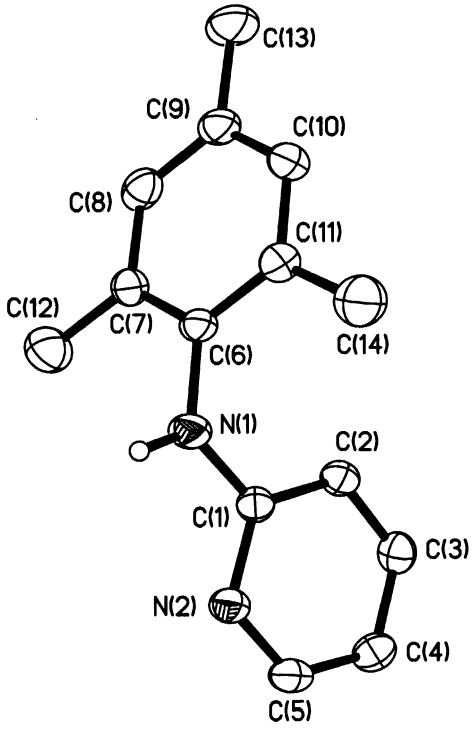

Figure 2.1. Molecular structure of MesN(H)py (**2.1**). Thermal ellipsoids are shown at the 30% level, and hydrogen atoms attached to carbon are omitted for clarity.

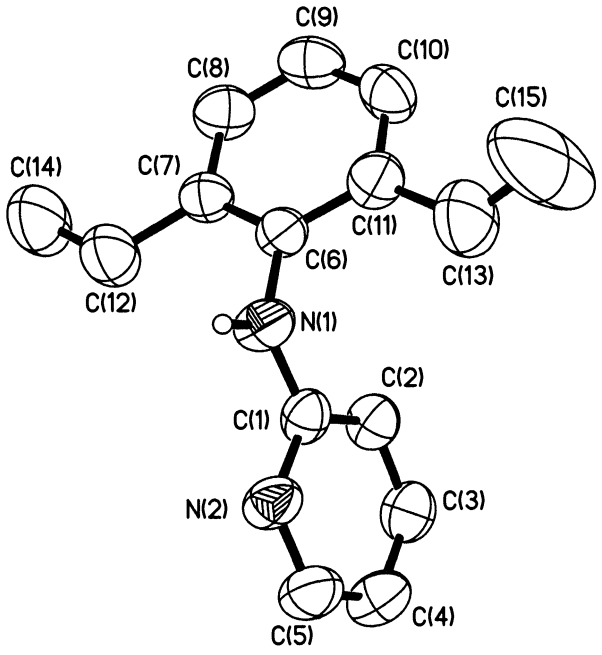

Figure 2.2. Molecular structure of (2,6-Et_2Ph)N(H)py (**2.2**). Thermal ellipsoids are shown at the 30% level, and hydrogen atoms attached to carbon are omitted for clarity.

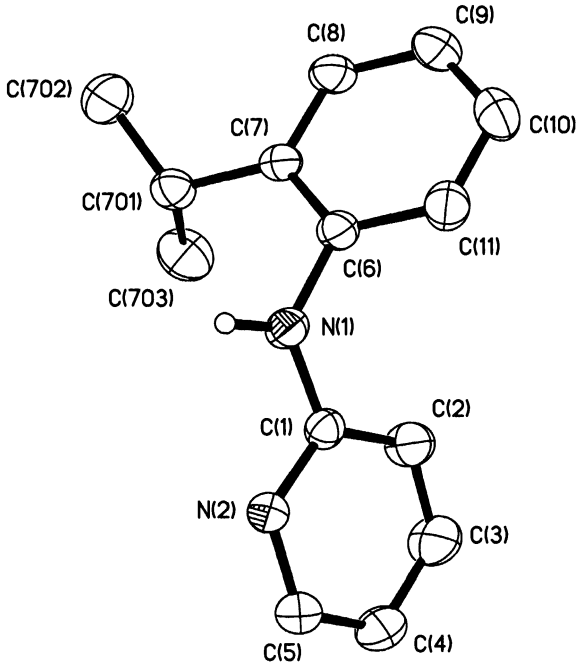

Figure 2.3. Molecular structure of (2-^{i}PrPh)N(H)py (**2.3**). Thermal ellipsoids are shown at the 30% level, and hydrogen atoms attached to carbon are omitted for clarity.

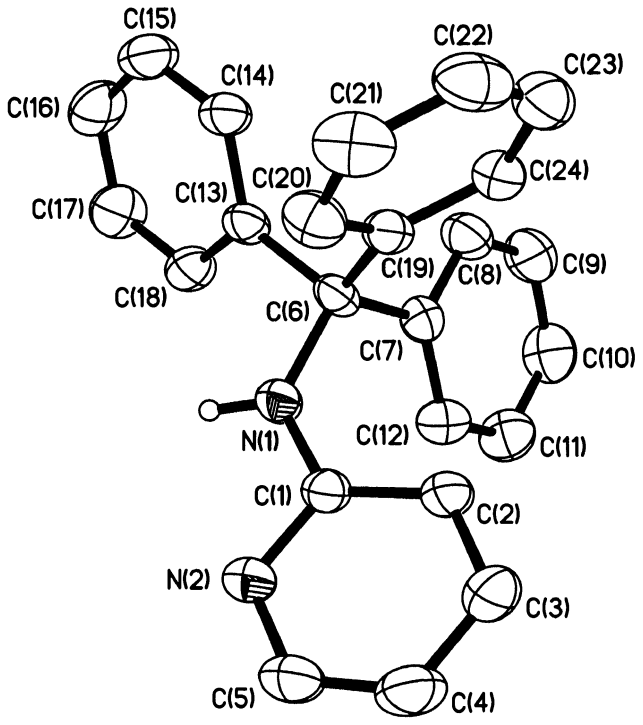

Figure 2.4. Molecular structure of one of the crystallographically independent molecules of $(Ph_3C)N(H)py$ (**2.4**). Thermal ellipsoids are shown at the 30% level, and hydrogen atoms attached to carbon are omitted for clarity.

Table 2.1. Selected bond lengths (Å) and angles (°) for compounds **2.1 - 2.3**.

	2.1	**2.2**	**2.3**
C(1)-N(1)	1.368(2)	1.362(4)	1.363(2)
C(6)-N(1)	1.427(2)	1.416(4)	1.419(2)
C(1)-N(1)-C(6)	122.7(1)	124..8(3)	125.5(1)
$\Delta MPLN_{[py\text{-}Ar]}$	72.82(2)	73.58(4)	66.01(2)

Bond distances and angles measured between the amine nitrogen, N(1), and its substituent carbon atoms are within the ranges of those reported for ArN(H)py (Ar = 2,6-$^{i}Pr_2Ph$, and 1-naph) [N-C_{py} = 1.355(3) - 1.370(6) Å; N-C_{Ar} = 1.415(6) - 1.435(3) Å; C_{py}-N-C_{Ar} = 122.4(1) - 126.6(4)°].[15,16]

Table 2.2. Selected bond lengths (Å) and bond angles (°) for each of the unique molecules in compound **2.4**.

Molecule	a	b	c	d
N(1)-C(1)	1.372(5)	1.374(5)	1.366(5)	1.372(5)
N(1)-C(6)	1.471(5)	1.466(5)	1.464(5)	1.469(5)
N(2)-C(1)	1.345(5)	1.339(5)	1.347(5)	1.340(5)
$N_a \cdots N_{py'}$	3.078(5)	3.201(5)	3.097(5)	3.121(5)
C(1)-N(1)-C(6)	126.1(4)	125.3(4)	126.8(4)	126.4(4)
N(1)-C(1)-N(2)	114.1(4)	114.8(4)	113.9(4)	113.9(4)
$\Delta MPLN_{[py\text{-}Ar(1)]}$	73.1(2)	76.4(2)	72.9(2)	67.7(2)
$\Delta MPLN_{[py\text{-}Ar(2)]}$	55.2(2)	51.6(2)	48.2(2)	49.7(2)
$\Delta MPLN_{[py\text{-}Ar(3)]}$	78.5(2)	71.3(2)	79.9(2)	83.4(2)

Each of the structures crystallize in a centrosymmetric space group. For compounds **2.1 - 2.3** this results in the formation of hydrogen-bonded head-to-tail dimers (e.g., Figure 2.5.). In compound **2.4** the asymmetric unit contains four independent molecules (a-d), in which (a) pairs with (b) and (c) pairs with (d) to form non-centrosymmetric hydrogen bonded dimers. The observed formation of dimers is typical of compounds of the type RN(H)py.[15]

The resulting N(1)···N(2') distances (Tables 2.1 and 2.2) are comparable to those previously reported at 2.998 Å for (2,6-^{i}Pr$_2$Ph)N(H)py, 2.929(6) and 3.039(6) Å for (1-naph)N(H)py, as well as 3.014(3) Å for PhN(H)py. In addition, the N-H···N interaction for (2,6-^{i}Pr$_2$Ph)N(H)py, (1-naph)N(H)py, and PhN(H)py are slightly bent, with angles 166.6°, 171(3)° and 174(3)°, and 172(2)°, respectively. The corresponding values determined for **2.1 - 2.3** match reasonably well, having N-H···N angles of 155.5°, 173(2)°,

and 160.1°, respectively. In contrast, compound **2.4** exhibits a much larger deviation from linearity between dimers, with angles ranging 131.6 - 147.1° (see Figure 2.6).

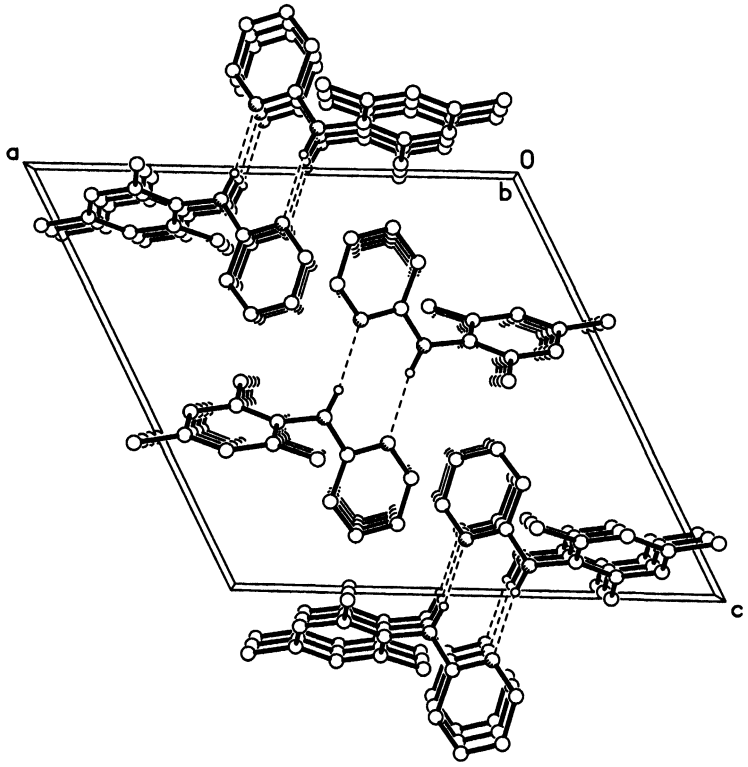

Figure 2.5. Molecular packing diagram of MesN(H)py (**2.1**) viewed along the *b*-axis. Hydrogen atoms attached to carbon are omitted for clarity.

Due to the head-to-tail structure the N(2)-C(1)-N(1)-C(6) torsion angle is controlled by the N-H···N interactions rather than the steric bulk of the aryl substituent. Increased steric bulk of the *ortho*-groups on the aryl substituent does result in a defined change in the twist of the aryl group with regard the hydrogen bonded core [i.e., C(1)-N(1)-C(6)-C(7)] suggesting that inter-dimer molecular packing offers more control (c.f., Figure 2.5).

It is interesting to note that for symmetrically substituted aryl derivatives, the N-C_{Ph} distances [N(1)-C(6)] increase with increased steric bulk of the substituents on the

phenyl group in an manner expected from steric factors. However, the N-C_{py} distances [N(1)-C(1)] undergo a concomitant decrease (Figure 2.7).

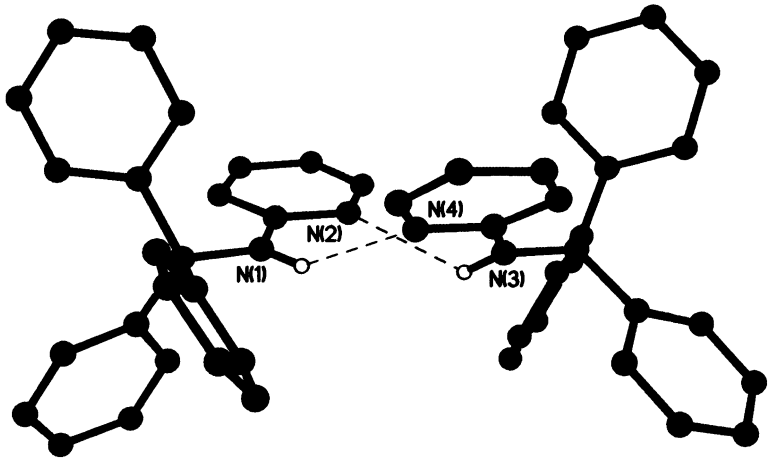

Figure 2.6. Conformation of hydrogen bonding between unique molecules in $(Ph_3C)N(H)py$. Hydrogen atoms attached to carbon are omitted for clarity.

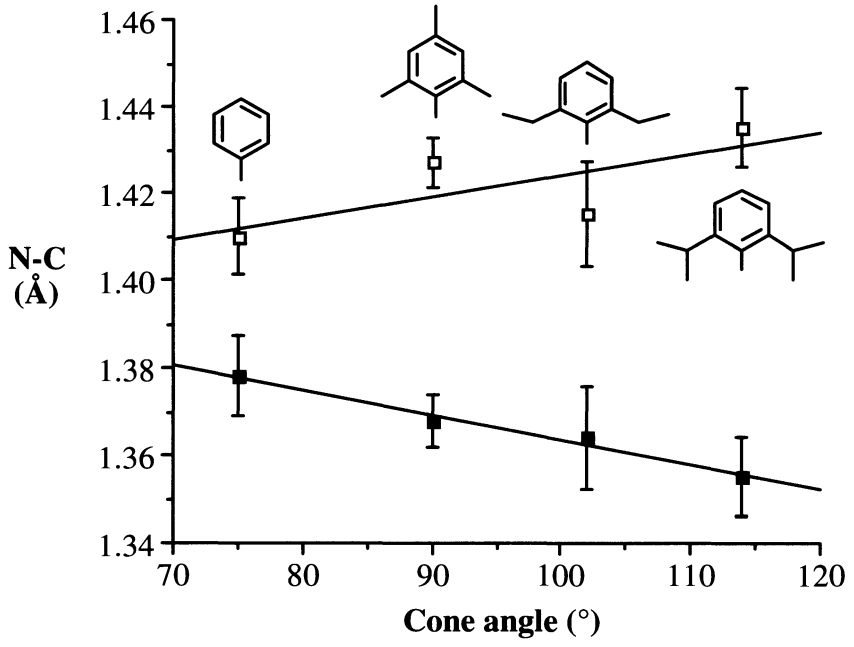

Figure 2.7. Plot of the N-C_{py} (■, R^2 = 0.984) and N-C_{Ph} (□, R^2 = 0.529) versus the steric bulk of the *ortho*-substituents.

As noted above, the asymmetric unit for compound **2.4** contains four independent molecules. The difference between each crystallographically unique molecule is associated with the orientation of the phenyl rings with respect to the pyridyl ring. As may be seen from Figure 2.8, the differences may be assigned to changes in "pitch" of the three-bladed propeller.

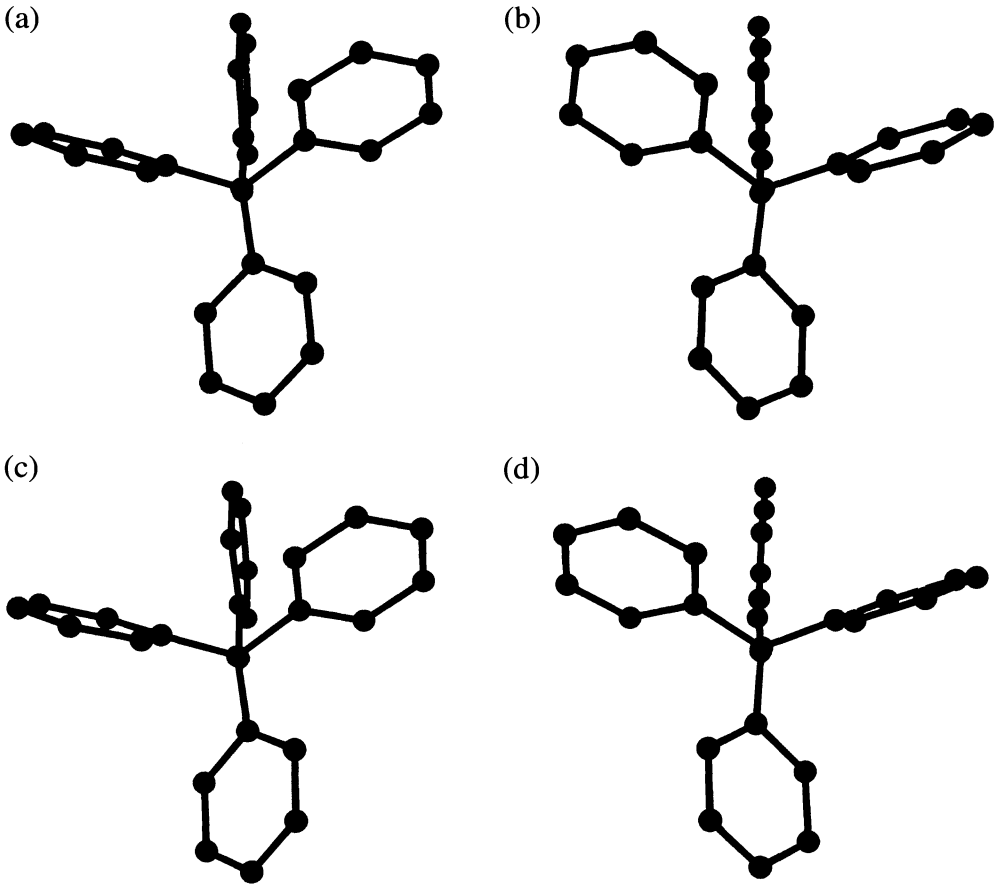

Figure 2.8. Orientation of phenyl rings for each of the crystallographically independent molecules of $(Ph_3C)N(H)py$ (**2.4**) viewed along the C(6)-N(1) vector. Hydrogen atoms are omitted for clarity.

The $N\text{-}C_{py}$ and $N\text{-}C_{Trit}$ bond lengths found in **2.4** match fairly well with those reported for the dichloro-*bis*{2-[(triphenylmethyl)amino]pyridyl}cobalt(II) complex

[1.362(3) and 1.486(3) Å] reported by Fang et al.,[17] while the C_{py} - N - C_{Trit} bond angles in the latter are slightly larger in the complex [127.4(1) and 127.6(1)°].

Aryl Substituted *Bis*(2-pyridyl)amines. The direct reaction of an aniline with 2-bromopyridine yields the appropriate mono-pyridyl amine derivatives, i.e., ArN(H)py. We have found that in order to prepare the associated dipyridylamine derivatives, $ArN(py)_2$ (hereafter referred to as Ar-dpa), it is better to isolate the mono-pyridyl amine and react with additional 2-bromopyridine in the presence of a catalyst, see Scheme 2.1 and Experimental. Using these methods we have prepared the new di-(2-pyridyl)amines, Ar-dpa, where Ar = Mes (**2.5**), 2,6-$Et_2C_6H_3$ (**2.6**), 2-^{i}PrC$_6$H$_4$ (**3.7**), 2,6-^{i}Pr$_2$C$_6$H$_3$ (**2.8**), and 1-naph (**2.9**).

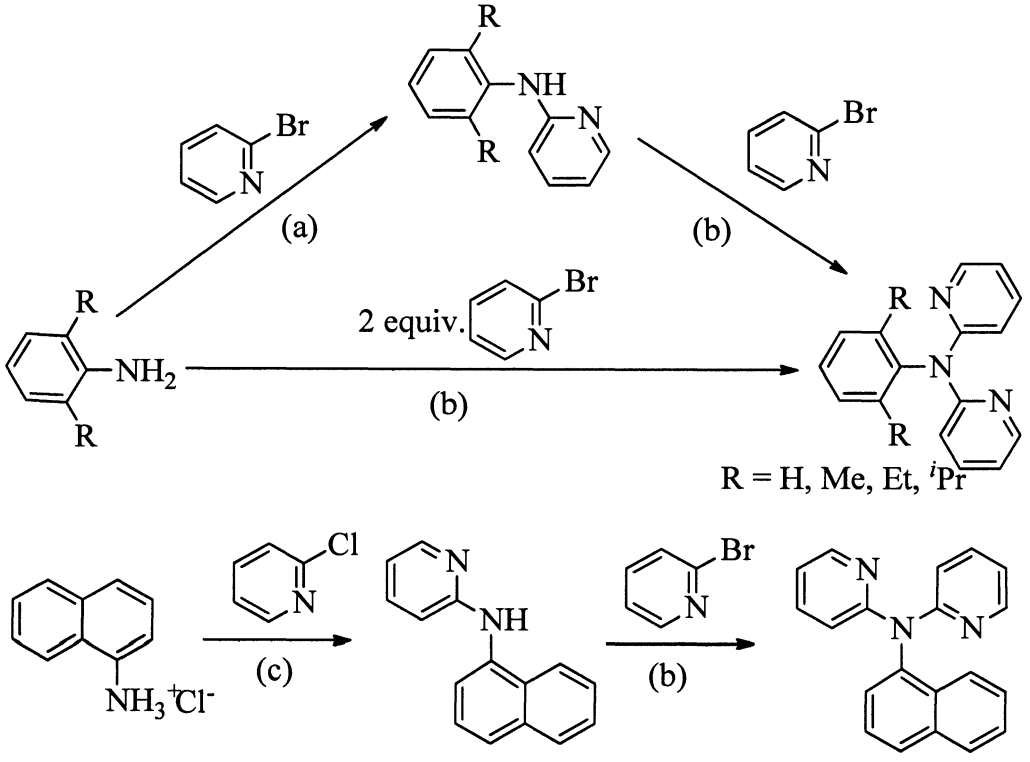

Scheme 2.1. Synthesis routes to Ar-dpa. (a) neat, reflux 2h, (b) NaO^{t}Bu, Pd cat., toluene 90 °C, and (c) neat, 180 °C, 2h.

Compounds **2.5** – **2.9** have been characterized by NMR and IR spectroscopy, as well as mass spectrometry. The molecular structures for compounds have each been determined by single crystal X-ray diffraction. Details of data collection and structure solution and refinement are outlined in the experimental section. Highlighted geometrical parameters are given in Table 2.3.

The molecular structures for Ar-dpa (Ar = Mes, 2,6-Et_2Ph, 2-^{i}PrPh, 2,6-$^i P_2$rPh, and 1-naph) ligands are shown in Figure 2.9 (**2.5**), Figure 2.10 (**2.6**), Figure 2.12 (**2.7**), Figure 2.14 (**2.8**), and Figure 2.16 (**2.9**). Compounds **2.6** – **2.8** crystallize with two independent molecules in the asymmetric unit; comparisons between conformers are given in Figure 2.11, Figure 2.13, and Figure 2.15, respectively. The most significant differences observed between the two conformers are the orientation of alkyl substituents on the phenyl rings, the degree of pitch between the planes of the rings, and C-N-C bond angles between rings.

The N-C bond lengths and the bond angles between the amine nitrogen and the heterocycles in the compounds **2.5** - **2.9** [1.398(3) - 1.416(4) Å and 123.2(3) - 124.6(1)°, respectively] are within the ranges to previously reported aryl-substituted dipyridylamines [1.400(2) - 1.435(3) Å, 118.8(1) - 123.8(1)°],[18,19] as well as N-alkyl pyridyl- and quinolyl- amines [1.378(4) - 1.415(4) Å, 123.7(3)°].[20,21]

The N-C bond lengths [1.438(5) - 1.454(3) Å] and the angles between the tertiary amine nitrogen and the aryl substituent [116.4(3) -120.4(3)°] also seem to match well with similar compounds [1.415(3) - 1.463(4) Å and 117.2(1) - 121.3(2)°, respectively]. The geometry about the amine nitrogen atom in compounds **2.5** – **2.9** is essentially planar ($\sum_{C\text{-}N\text{-}C}$ = 359.3 – 360°); consequently the pyridyl and aryl rings are forced to twist out of plane due to the steric bulk of the *ortho*-substituents. Thus, as proposed, the presence of the aryl group's substituents forces the pyridyl rings out of plane from the NC_3 core.

Table 2.3. Selected bond lengths (Å) and angles (°) for Ar-dpa.

Compound	**2.5**	**2.6**[a]	**2.7**[a]	**2.8**[a]	**2.9**
$N\text{-}C_{py}$	1.398(3)	1.402(5), 1.402(5)	1.403(4), 1.395(4)	1.405(3), 1.405(3)	1.411(1)
$N\text{-}C_{py'}$	1.411(3)	1.403(5), 1.413(5)	1.411(4), 1.416(4)	1.387(3), 1.400(3)	1.410(1)
$N\text{-}C_{Ar}$	1.439(3)	1.442(5), 1.438(5)	1.445(5), 1.453(4)	1.454(3), 1.451(3)	1.442(1)
$C_{py}\text{-}N\text{-}C_{py'}$	124.0(2)	123.4(3), 123.2(3)	123.7(3), 124.6(3)	124.0(1), 124.5(2)	124.6(1)
$C_{py}\text{-}N\text{-}C_{Ar}$	118.3(2)	117.8(3), 120.4(3)	118.2(3), 118.7(3)	117.5(2), 117.3(1)	117.0(1)
$C_{py'}\text{-}N\text{-}C_{Ar}$	117.6(1)	118.6(3), 116.4(3)	117.8(3), 116.6(3)	117.8(1), 118.0(1)	117.9(1)
$\Delta MPLN_{[py\text{-}py']}$	48.7(1)	47.5(2), 46.5(2)	43.3(2), 41.8(2)	46.4(1), 40.7(1)	42.17(7)
$\Delta MPLN_{[py\text{-}Ar]}$	82.0(1)	87.3(2), 82.1(2)	85.8(2), 84.9(2)	88.9(1), 85.1(1)	84.02(7)
$\Delta MPLN_{[py'\text{-}Ar]}$	81.1(1)	87.3(2), 86.5(2)	88.8(2), 85.4(2)	81.7(1), 79.7(1)	69.49(7)

[a] two unique conformations in the asymmetric unit.

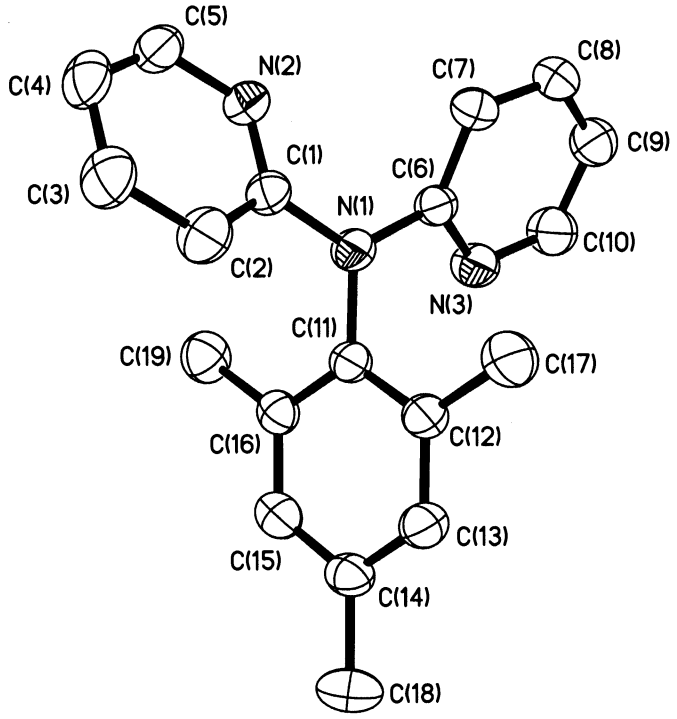

Figure 2.9. Molecular structure of Mes-dpa (**2.5**). Thermal ellipsoids are shown at the 30% level, and all hydrogen atoms are omitted for clarity.

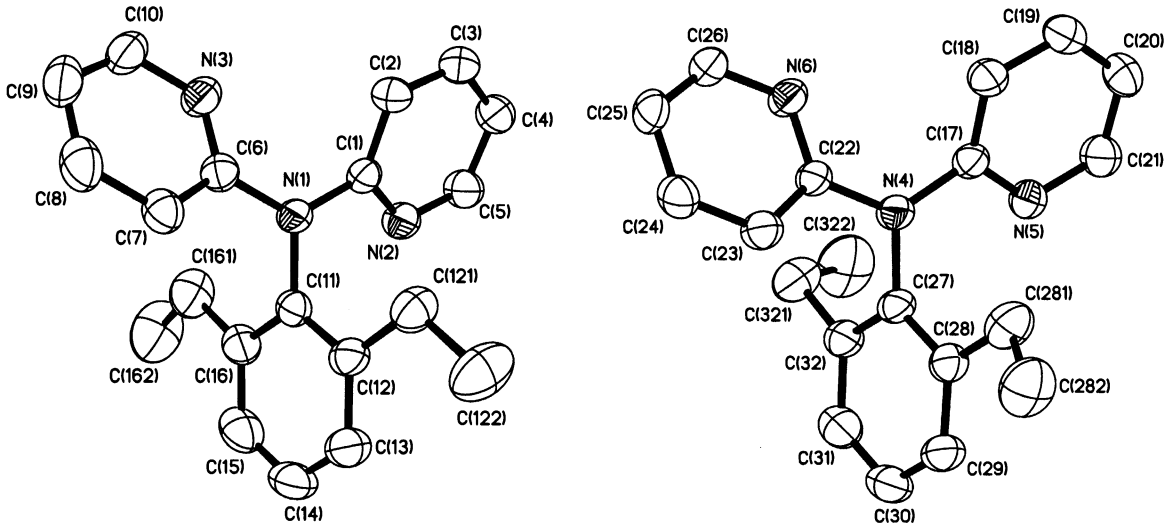

Figure 2.10. Molecular structures of the two crystallographically independent molecules of 2,6-Et_2Ph-dpa (**2.6**). Thermal ellipsoids are shown at the 30% level, and all hydrogen atoms are omitted for clarity.

Interestingly, the trend is the opposite of what may be expected, i.e., the greater the steric bulk of the *ortho*-substituents the more co-planar the pyridyl rings. This may be seen from a consideration of either the N(2)-C(1)···C(6) - N(3) torsion angle or the angle between the mean plane of each pyridyl ring ($MPLN_{[py\text{-}py']}$) for compounds **2.5** (R = Me), **2.6** (R = Et), and **2.7** (R = ^{i}Pr). In part, this may be explained by a greater twisting of the aryl ring with respect to the amine's NC_3 core with larger substituents. As may be seen from Table 2.3, the pyridyl rings appear more coplanar for asymmetrically substituted aryl groups.

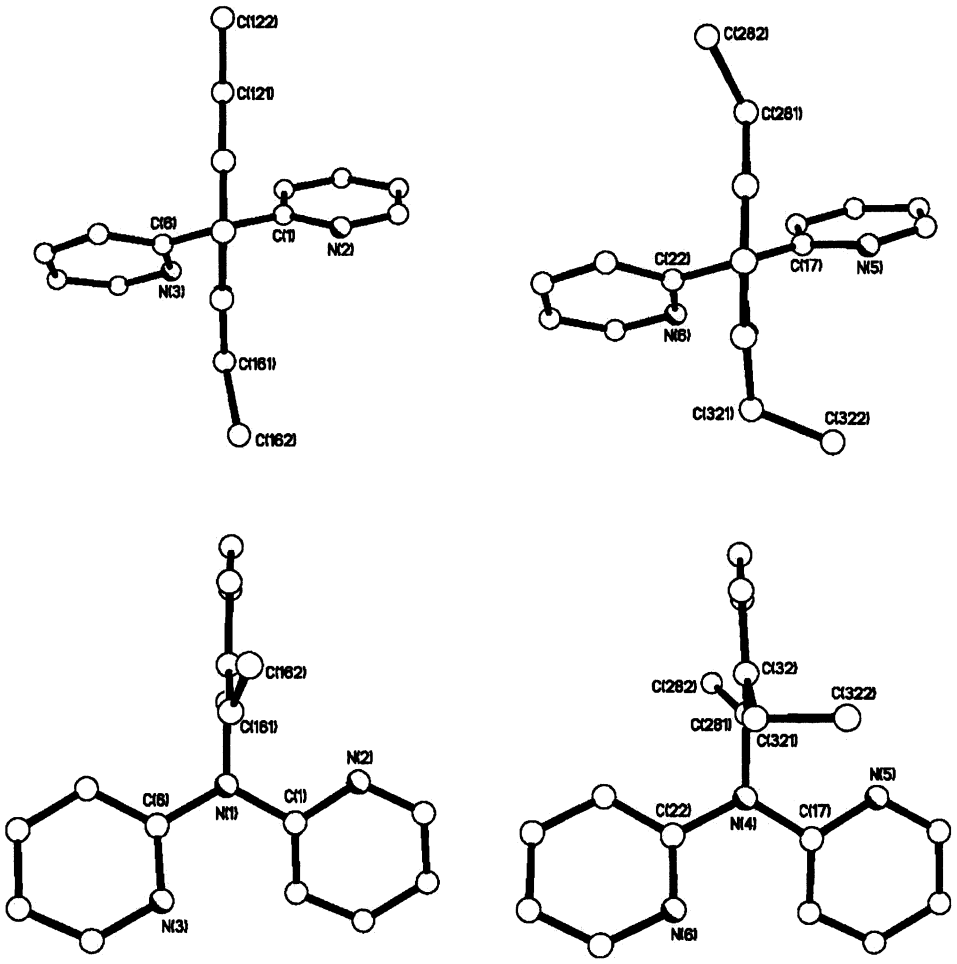

Figure 2.11. Comparison of unique conformers present in the asymmetric unit of compound **2.6**.

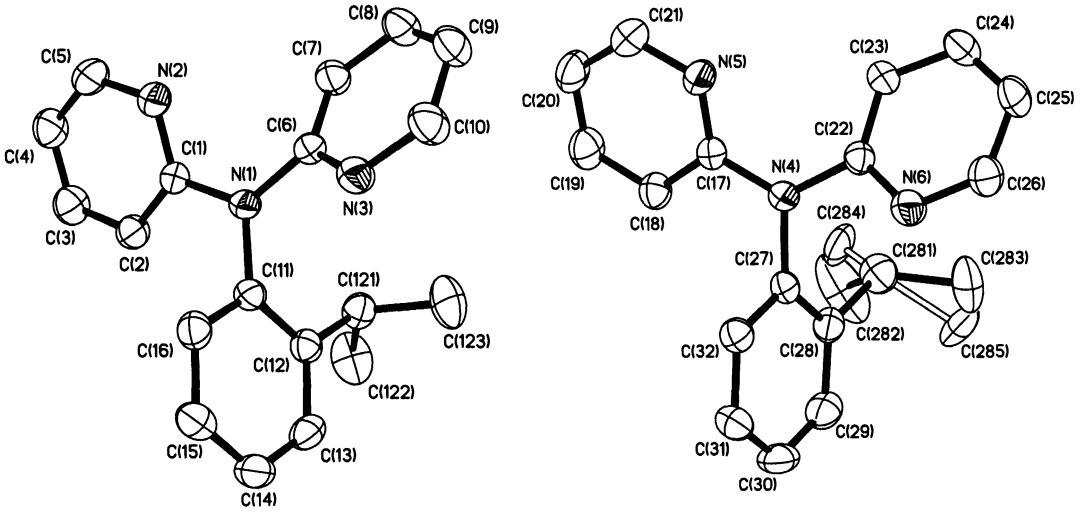

Figure 2.12. Molecular structures of the two crystallographically independent molecules of 2-^{i}PrPh-dpa (**2.7**). Thermal ellipsoids are shown at the 30% level, and all hydrogen atoms are omitted for clarity.

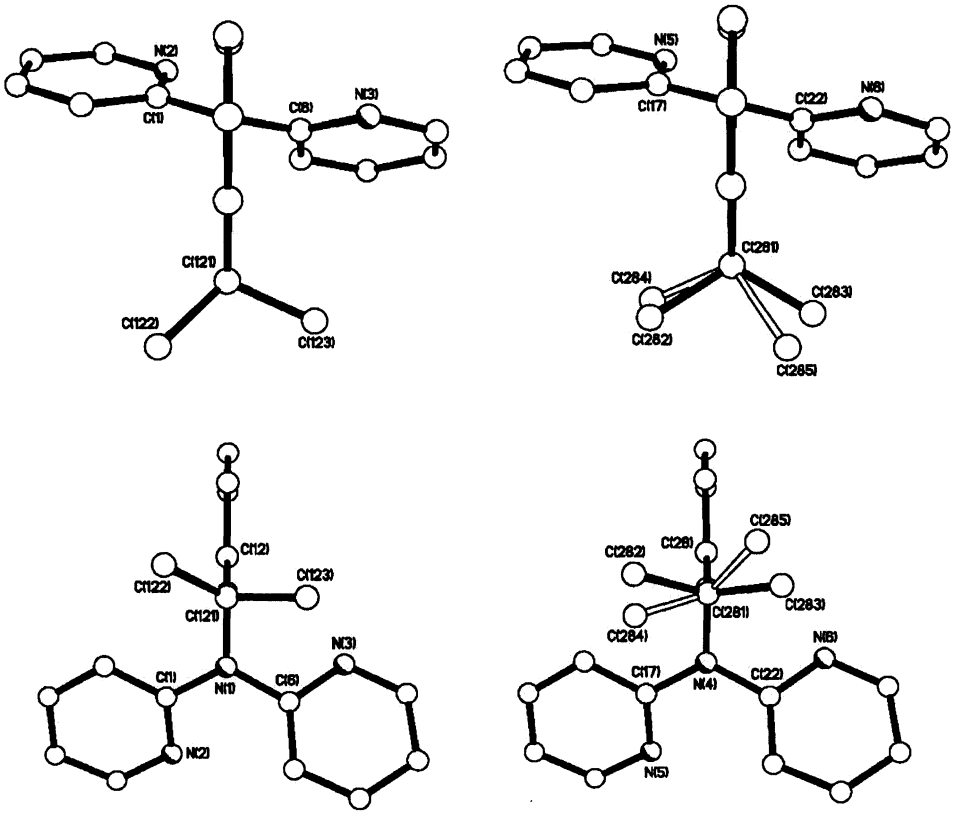

Figure 2.13. Comparison of unique conformers present in the asymmetric unit of compound **2.7**.

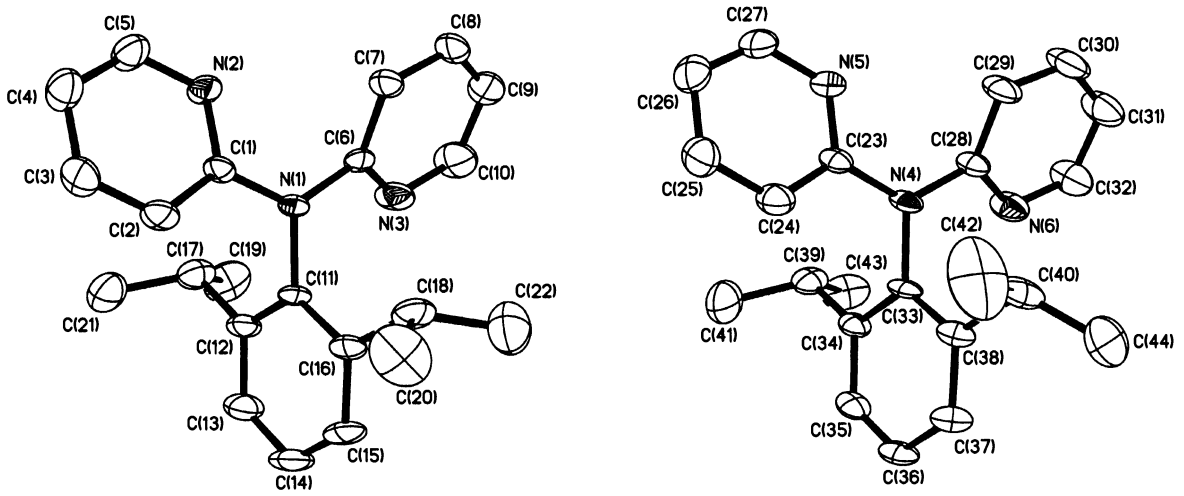

Figure 2.14. Molecular structures of the two crystallographically independent molecules of 2,6-$^{i}Pr_2$Ph-dpa (**2.8**). Thermal ellipsoids are shown at the 30% level, and all hydrogen atoms are omitted for clarity.

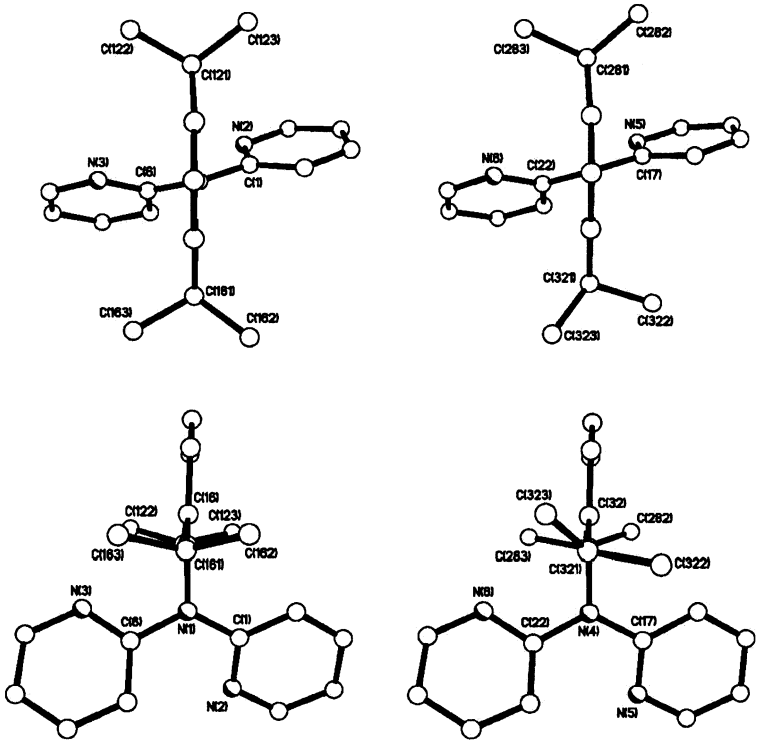

Figure 2.15. Comparison of unique conformers present in the asymmetric unit of compound **2.8**.

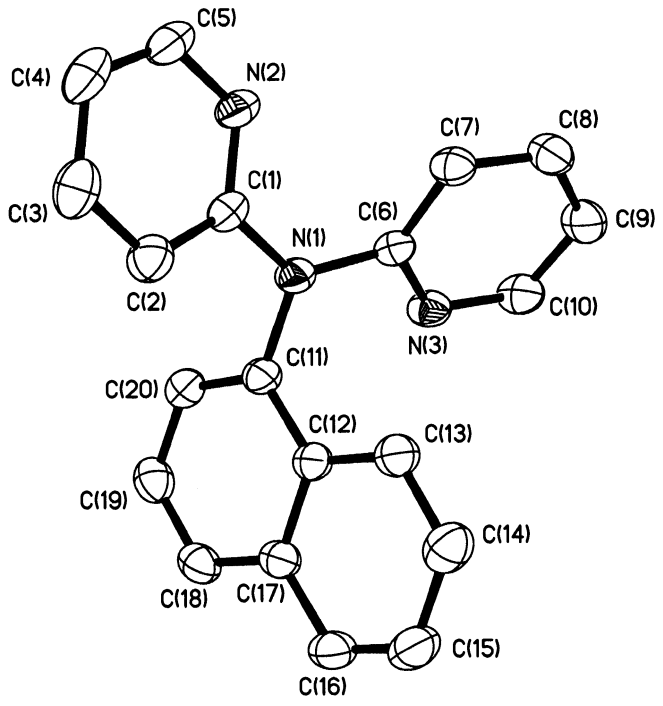

Figure 2.16. Molecular structure of (1-naph)-dpa (**2.9**). Thermal ellipsoids are shown at the 30% level, and all hydrogen atoms are omitted for clarity.

A plot of N_a-C_{Ar} bond distance versus the mean plane difference ($\Delta MPLN_{[py\text{-}py']}$) for compounds **2.5** – **2.9**, as well as previously reported analogs, shows a distinct trend (Figure 2.17a). The inter-pyridyl angle (C_{py}-N_a-$C_{py'}$) is also dependent on the N_a-C_{Ar} distance (Figure 2.17b). However, a closer consideration of the *ortho*- versus *para*-substitution suggests that electronic factors also influence geometrical parameters. Specifically, *ortho*-substituents result in longer bond lengths and larger bond angles. Based upon the forgoing, the presence of *ortho*-substitution in the uncomplexed Ar-dpa compounds results in a significant distortion of the coordination around the amine nitrogen and twisting of the two pyridyl rings with respect to each other.

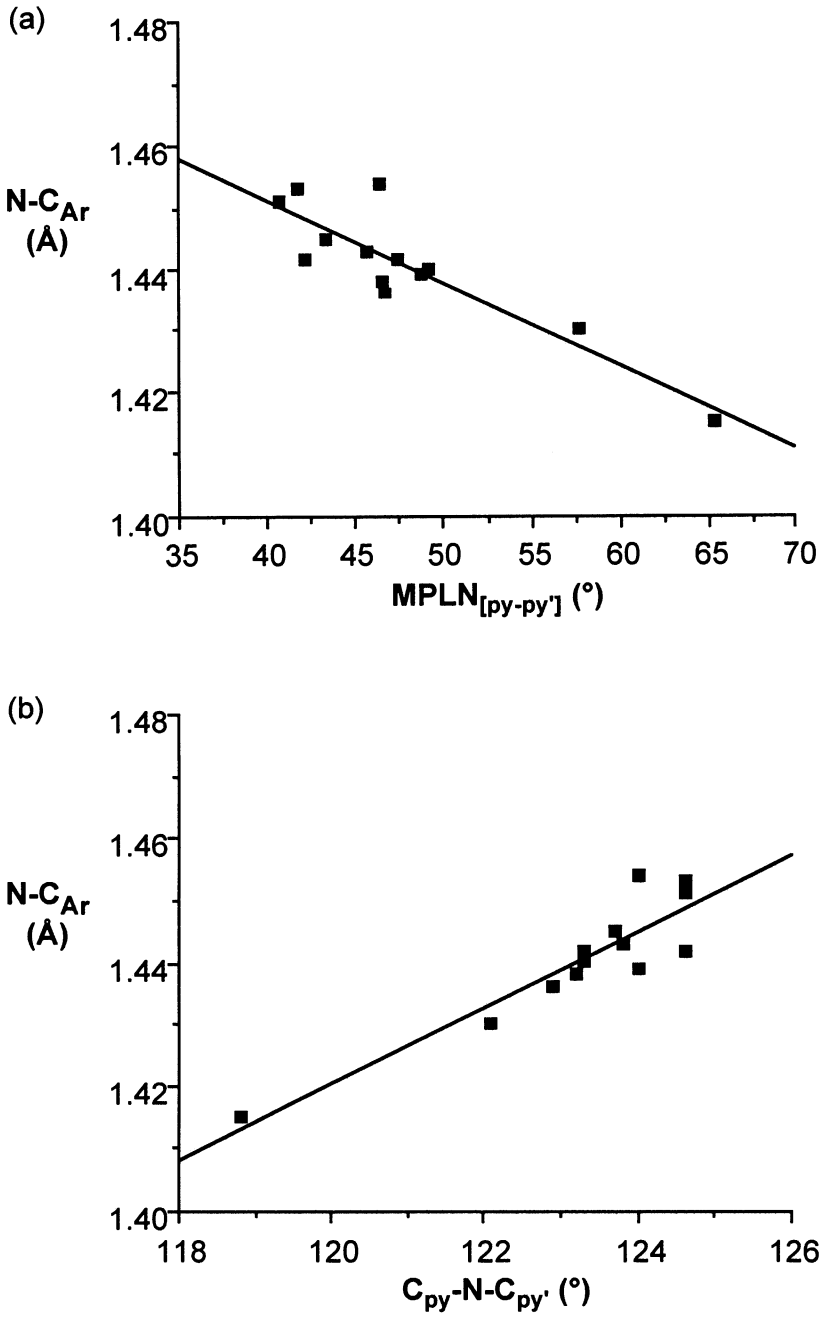

Figure 2.17. Plot of the N-C_{Ar} bond lengths versus (a) the mean-plane-difference between pyridyl rings (R^2 = 0.793) and (b) C_{py}-N-$C_{py'}$ bond angle (R = 0.828) for compounds **2.5** – **2.9**, as well as previously reported Ar-dpa derivatives.

Cross Coupling of Substituted Anilines with Quinoline. N-(2-pyridyl)-N-(2-quinolyl)amines [Ar-pqa, where Ar = H (**2.10**), Ph (**2.11**), Mes (**2.12**), and 2,6-$^{i}Pr_2Ph$

(**2.13**)] were prepared by the palladium catalyzed cross-coupling of 2-chloroquinoline with the appropriate 2-aminopyridine.[19,22] IR and NMR spectroscopic characterization and mass spectrometry are all consistent with the formulation. The molecular structures for compounds **2.10** - **2.13** have been confirmed by single crystal X-ray diffraction (Figures. 2.18 – 2.21). Selected bond lengths and angles can be found in Table 2.4.

The bond lengths and angles in compound **2.10** are comparable to those reported by Polyakova et al., for the hydroxylated analog.[23] A more beneficial comparison, however, can be drawn with the aforementioned aryl substituted secondary amines (**2.1** - **2.3**) and others from past works.[15] Bond distances and angles measured between the amine nitrogen, N_a in compound **2.10**, and its substituents are within the ranges of the secondary pyridyl amines (Mes)N(H)py (**2.1**), (2,6-Et_2Ph)N(H)py (**2.2**), (2,6-$^i Pr_2$Ph)N(H)py (**2.3**), and (1-naph)N(H)py [N-C_{py} = 1.355(3) - 1.370(6) Å; C_{py}-N-C_{Ar} = 122.4(1) - 126.6(4)°].[15,16]

As is typical for compounds of the type ArN(H)py, compound **2.10** crystallizes in a hydrogen-bonded head-to tail dimer structure (Figure 2.18). The N-H···N interaction observed in **2.10** has an N(1)-H(1)···N(2') angle (171°) within the range reported for analogous compounds [155.5 - 174(3)°], but a noticeably longer N(1)···N(2') distance [3.277(2) Å] compared to its homologs [2.929(6) - 3.041(2) Å].

This difference in hydrogen-bonding interaction is evident from the associated IR spectra. The N-H stretching frequency observed for **2.10** (3271 cm^{-1}) is shifted to a higher wavenumber compared to that found for (*o*-^{i}PrPh)N(H)py (3201 cm^{-1}), which is consistent with a weaker hydrogen bonded interaction in compound **2.10**. Crystal packing in **2.10** (Figure 2.22) shows the quinolyl ring stacking is close to parallel [Δ_{MPLN} = 2.30(8)°] along the *c*-axis with dimers alternating along the *a*-axis.

A comparison of the distances between stacked-ring centers of gravity for the quinolyl stacks [3.827(1) Å] and the sum of the van der Waals' half-thickness for an aromatic nucleus (3.70 Å),[24] suggests the π···π stacking is relatively weak. Additionally,

from Figure 2.22, there appears to be pyridyl rings stack along the c-axis with dimers alternating along the *b*-axis; however while the rings are parallel (ΔMPLN = 0°), the large py···py' distances [4.094(1) Å] precludes significant π···π interactions. Similar π···π stacking between quinolyl rings is also observed in the crystal packing diagrams of **2.11** - **2.13**.

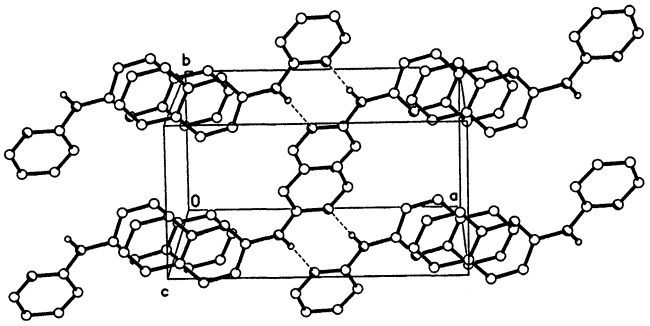

Figure 2.18. Molecular packing diagram of HN(py)quin (**2.10**), viewed perpendicular to the *a*-axis. Hydrogen atoms attached to carbon are omitted for clarity.

Table 2.4. Selected bond lengths (Å) and angles (°) for compounds **2.10** – **2.13**.

Compound	**2.10**	**2.11**[a]	**2.12**	**2.13**[a]
N-C_{py}	1.385(2)	1.414(2), 1.408(2)	1.400(4)	1.409(2), 1.418(2)
N-$C_{py'}$	1.387(2)	1.409(2), 1.409(2)	1.406(4)	1.411(2), 1.398(2)
N-C_{Ar}	0.91(2)	1.440(2), 1.439(2)	1.443(4)	1.451(2), 1.453(2)
C_{py}-N-$C_{py'}$	129.7(2)	124.8(1), 125.5(1)	124.3(3)	122.2(1), 122.6(1)
C_{py}-N-C_{Ar}	115(1)	117.6(1), 118.1(1)	118.6(3)	116.9(1), 117.5(1)
$C_{py'}$-N-C_{Ar}	116(1)	116.9(1), 116.0(1)	116.9(3)	117.2(1), 119.2(1)
$\Delta MPLN_{[py\text{-}py']}$	12.5(2)	31.9(1), 31.3(1)	48.5(2)	50.2(1), 42.0(1)
$\Delta MPLN_{[py\text{-}Ar]}$	-	76.3(1), 75.2(1)	88.8(2)	84.8(1), 89.6(1)
$\Delta MPLN_{[py'\text{-}Ar]}$	-	77.2(1), 74.6(1)	89.6(2)	75.4(1), 86.8(1)

[a]Two unique conformers in the asymmetric unit.

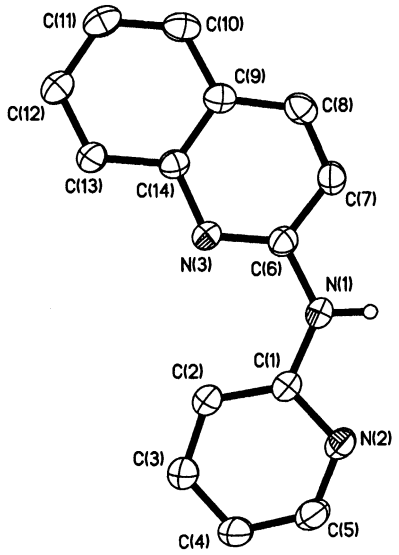

Figure 2.19. Molecular structure of HN(py)quin (**2.10**). Thermal ellipsoids are shown at the 30% level, and hydrogen atoms attached to carbon are omitted for clarity.

The effect of the nitrogen heterocycle in **2.10** can directly be seen by comparison with (1-1-naph)N(H)py, where the N(1)-C(6) distance in **2.10** [1.387(2) Å] is closer to the N-C_{py} distances than the N-C_{Ar} distance in (1-naph)N(H)py [1.415(6) Å].

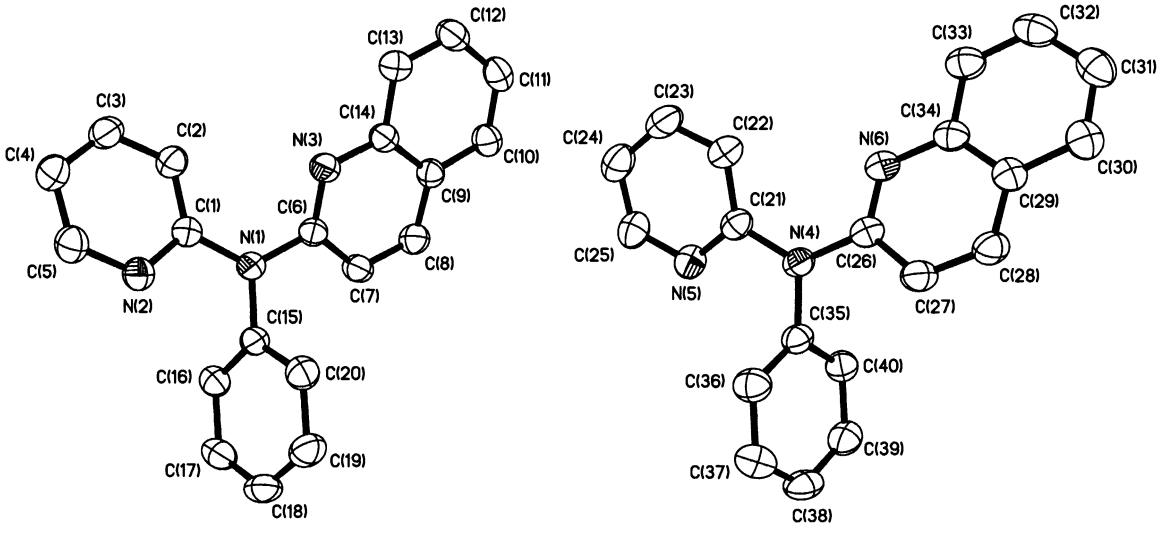

Figure 2.20. Molecular structure of the two unique conformers in PhN(py)quin (**2.11**). Thermal ellipsoids are shown at the 30% level, and all hydrogen atoms are omitted for clarity.

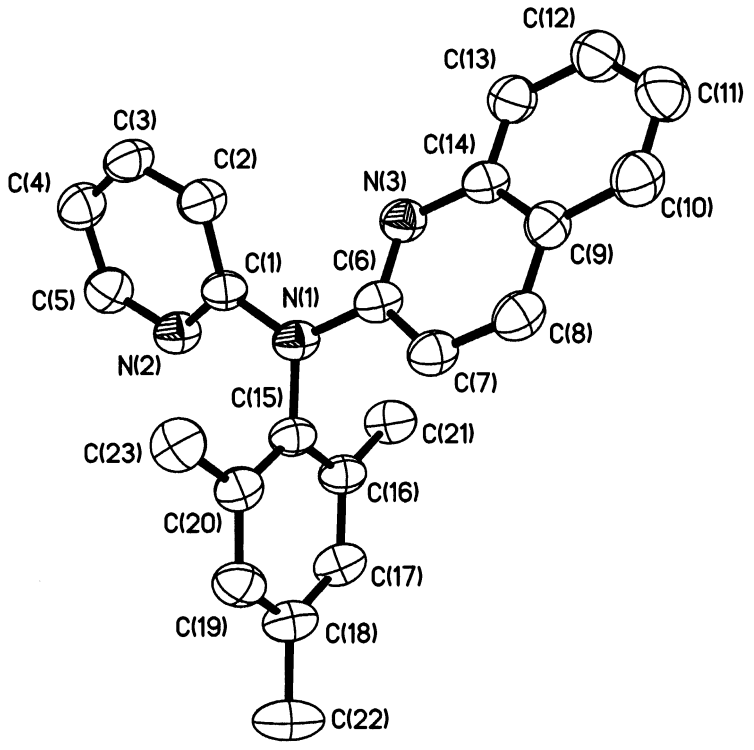

Figure 2.21. Molecular structure of MesN(py)quin (**2.12**). Thermal ellipsoids are shown at the 30% level, and all hydrogen atoms are omitted for clarity.

The N-C bond lengths and the bond angles between the amine nitrogen and the heterocycles in the compounds **2.11** - **2.13** (Table 2.4) are similar to previously reported aryl-substituted dipyridylamines [1.400(2) - 1.435(3) Å, 118.8(1) - 123.8(1)°],[19,20] as well as N-alkyl pyridyl- and quinolyl- amines [1.378(4) - 1.415(4) Å, 123.7(3)°].[20,21] Similarly to their dipyridyl analogs, compounds **2.11** - **2.13** crystallize in a three bladed propeller conformation, with varying degrees of pitch between the planes of the rings.

The sum of the bond angles about the amine nitrogen, $\sum$(C-N-C), are found to range 359.3-359.8° (with the exception of **2.13a**), indicating that the amine nitrogen, N(1), and three carbons bonded to it are nearly planar. The mean-plane-angle difference between the NC_3 plane and each heterocycle [12.4(1) - 28.8(2)°] are smaller those observed for the aryl substituent [67.3(1) - 78.0(2)°].

(a)

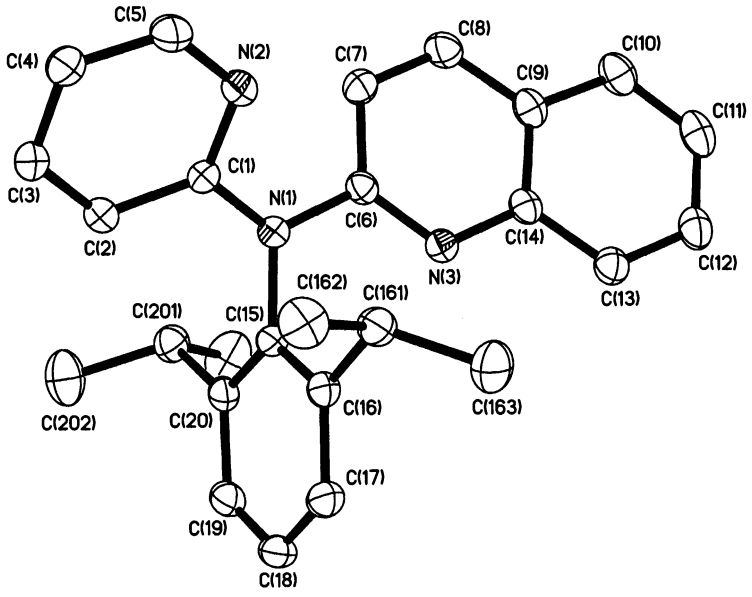

(b)

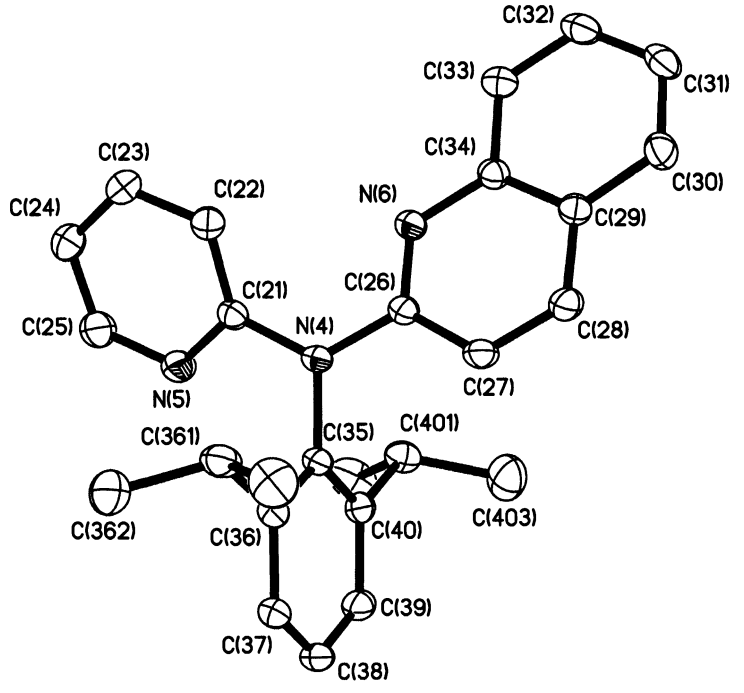

Figure 2.22. Molecular structure of the two unique conformers in **2.13**. Thermal ellipsoids are shown at the 30% level, and all hydrogen atoms are omitted for clarity.

Compound **2.11** crystallizes with two crystallographically independent molecules within the unit cell. As may be seen from Table 2.4, the bond lengths associated with the

amine nitrogen are within experimental error. The only significant geometric differences are with regard to the orientation of the phenyl ring (Figure 2.24). There is a slight bending of the phenyl ring away or towards the pyridyl substituent which may be ascribed to differences in the crystal packing interactions for each of the molecules.

Compound **2.13** also crystallizes with two unique conformations in the asymmetric unit (see Figure 2.22), having most prominent differences in the orientation of the quinolyl heterocycles with respect to the rest of the molecule. Specifically, rotation of the quinolyl group 180° about the N_a-C_{quin} bond in the first conformer approaches the conformation of the second.

A second apparent difference regarding the quinolyl heterocycles is seen in the mean plane angle difference (ΔMPLN), with the respective pyridyl ring, which is larger in the first conformer [50.2(1)°] than in the second [42.0(1)°]. These are both significantly larger than those observed in the phenyl derivative (**2.11**) [31.9(1)° and 31.3(1)°], while the mesityl analog (**2.12**) yields a value [48.5(2)°] more akin to that in **2.13a**. Furthermore, the ΔMPLN values between pyridyl rings in structurally similar Ar-dpa ligands (Ar = Mes, 2,6-Et_2Ph, 2-^{i}PrPh, 2,6-iPr2Ph, 1-naph, and Ph[19]) are found to exhibit values [40.7(1)° - 48.7(1)°] primarily within the range spanned by the two extremes seen in **2.13**. The only dipyridyl analogs that clearly lie outside of this range are those reported with substitution in the *para-* position, (*p*-OMe)Ph-dpa and (*p*-CN)Ph-dpa, having values of 57.7(1)° and 49.2(1)° in the former, and 65.3(1)° in the latter.[18]

The analogous ΔMPLN angle in Mes-dqa (**2.14**; see below) between the two heterocycles is observed to be intermediate [44.9(1)°] between **2.13**a and **2.13**b, while the 2,6-^{i}Pr_2Ph-dqa compound (**2.15**) exhibits a value [41.2(1)°] closer to that of **2.13**b. Furthermore, the ΔMPLN values between pyridyl rings in structurally similar Ar-dpa ligands (Ar = Mes, 2,6-Et_2Ph, 2-^{i}PrPh, 2,6-iPr_2Ph, 1-naph, and Ph[19]) are found to exhibit values [40.7(1)° - 48.7(1)°] primarily within the range spanned by the two extremes seen in **2.13**. The only dipyridyl analogs that clearly lie outside of this range are those reported

with substitution in the para- position, (*p*-OMe)Ph-dpa and (*p*-CN)Ph-dpa, having values of 57.7(1)° and 49.2(1)° in the former, and 65.3(1)° in the latter.

Another more subtle difference between the conformers of **2.13** is seen in the geometry about the amine nitrogen atom. More specifically, the deviation from planarity, i.e. the departure of the sum of the three C_i-N_a-C_j bond angles ($\Sigma_{Ci\text{-}Na\text{-}Cj}$) from 360°, in **2.13**a [356.3(1)°] is significantly larger than that in **2.13**b [359.4(1)°] (see Table 2.4). Surprisingly, the value in **2.13**a seems to exist at the lower extreme for $\Sigma_{Ci\text{-}Na\text{-}Cj}$, in structurally similar compounds, including the other aforementioned ArN(py)quin compounds (Ar = Ph and Mes), the diquinolyl compounds, **2.14** and 2,6-^{i}Pr$_2$Ph-dqa, as well as all of the Ar-dpa ligands. In fact, of those mentioned above, the only other compound that features a $\Sigma < 359°$ is the (*p*-CN)Ph-dpa derivative, in which the angles sum to 357.7°.

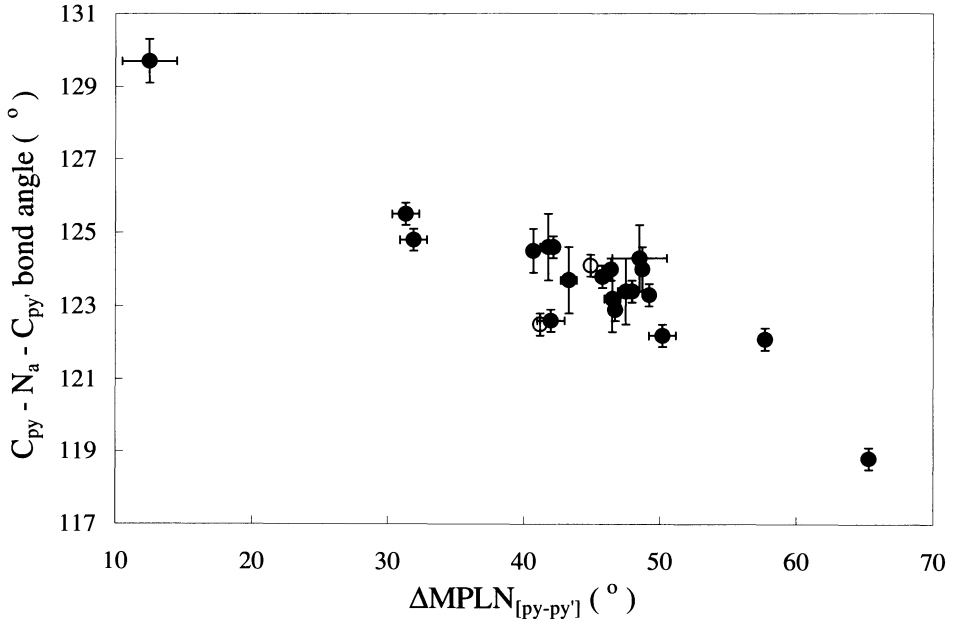

Figure 2.23. Plot of C_{py}-N-C_{quin} bond angle as a function of the mean plane angle difference between heterocycles [$\Delta MPLN_{(py\text{-}py/quin)}$] for ArN(py)quin (●), ArN(py)$_2$ (●), and ArN(quin)$_2$ (○).

There is also a similarity with N-alkyl pyridyl quinolyl amines.[33] An analysis of the bond lengths and angles as a function of substituent (i.e., H < Me < Ph < Mes < 2,6-$^{i}Pr_2Ph$) shows that increasing steric bulk of the alkyl/aryl substituent is accompanied by a lengthening of the N-C_{Ar} bond, a closing of the C_{py}-N-C_{quin} bond angle, and, generally, an increased mean-plane angle difference [$\Delta MPLN_{(py\text{-}quin)}$] between the two heterocycles. Figure 2.23 shows the correlation between $\Delta MPLN_{(py\text{-}quin)}$ and C_{py}-N-C_{quin} bond angle.

Figure 2.24. Overlay of the two independent molecules of (Ph)N(py)quin (**2.11**).

Figure 2.25. Overlay of the two independent molecules of (2,6-$^{i}Pr_2Ph$)N(py)quin (**2.13**).

Synthesis and Structural Characterization of ArN(quin)$_2$. The catalyzed reaction of 2,4,6-trimethyl aniline with an excess of 2-chloroquinoline in toluene yielded the desired di(2-quinolyl)amine, MesN(quin)$_2$ (**2.14**) in a surprisingly low yield (19 %), caused by the formation of an unexpected imine side-product, quinolin-1-(2-quinolyl)-2-one mesitylimine (**2.16**).[25] In contrast, the same catalyzed reaction, using (2,6-diisopropyl)aniline, rendered the clean formation of (2,6-^{i}Pr$_2$Ph)N(quin)$_2$ (**2.15**) in moderate yield (49 %).

Compounds **2.14** & **2.15** were characterized by mass spectrometry, and IR and NMR spectroscopy. The molecular structures of each compound has been determined by single crystal X-ray diffraction (Figure 2.26 and Figure 2.27). Selected bond lengths and angles are given in Table 2.5. Details of data collection and structure solution and refinement are outlined in the experimental section.

Table 2.5. Selected bond lengths (Å) and angles (°) for compounds **2.14** and **2.15**.

	(2.14)	**(2.15)**
N-C_{quin}	1.412(3)	1.400(2)
N-$C_{quin'}$	1.401(2)	1.410(2)
N-C_{Ar}	1.443(2)	1.442(2)
C_{quin}-N-$C_{quin'}$	124.1(1)	122.5(1)
C_{quin}-N-C_{Ar}	117.1(1)	118.7(1)
$C_{quin'}$-N-C_{Ar}	118.8(1)	118.5(1)
$\Delta MPLN_{[quin-quin']}$	44.9(1)	41.2(1)
$\Delta MPLN_{[quin-Ar]}$	81.6(1)	84.4(1)
$\Delta MPLN_{[quin'-Ar]}$	75.5(1)	86.7(1)

The N-C bond lengths and the bond angles between the amine nitrogen and the heterocycles in compounds **2.14** and **2.15** are similar to previously reported aryl-substituted dipyridylamines [1.398(3) - 1.435(3) Å, 118.8(1) - 124.6(1)°],[2,18] as well as N-alkyl pyridyl- and quinolyl-amines [1.378(4) - 1.415(4) Å, 123.7(3)°].[20,21] The N(1)-C(19) bond length and the C(1)-N(1)-C(6) bond angle also match well with similar compounds.

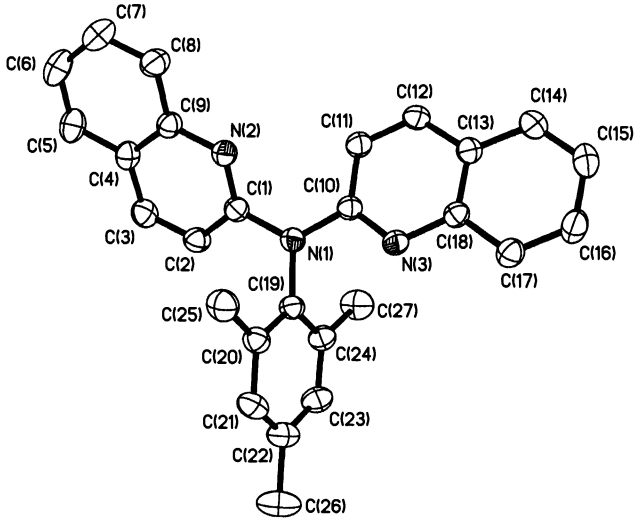

Figure 2.26. Molecular structure of MesN(quin)$_2$ (**2.14**). Thermal ellipsoids are set at the 30% level, and all H-atoms are omitted for clarity.

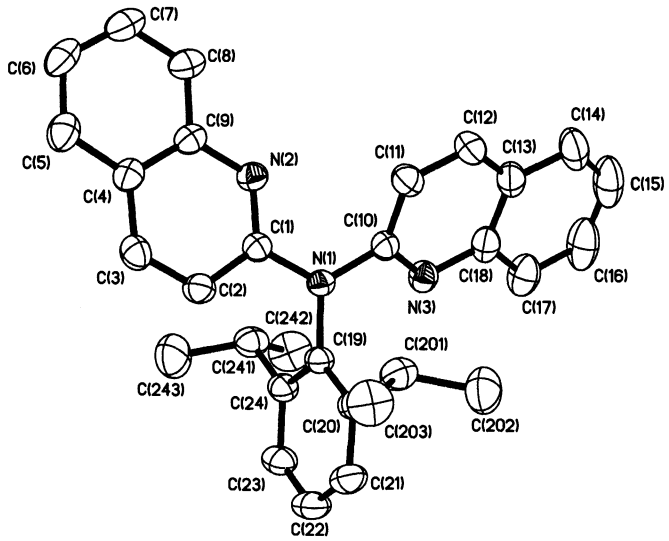

Figure 2.27. Molecular structure of 2,6-^{i}Pr$_2$PhN(quin)$_2$ (**2.15**). Thermal ellipsoids are set at the 30% level, and all H-atoms are omitted for clarity.

The ΔMPLN angle in **2.14** between the two heterocycles is observed to be intermediate [44.9(1)°] between **2.13a** and **2.13b**, while **2.15** exhibits a value [41.2(1)°] closer to that of **2.13b**. The sum of the bond angles about the amine nitrogen, $\sum(C\text{-}N_a\text{-}C)$ = 359.7(1)°, indicates that N(1) and three carbons bonded to it are nearly planar. While the most electronically favorable conformation of the rings would be coplanar to allow maximum overlap with the nitrogen lone pair, however, such a conformation is sterically undesirable, and thus, compound **2.15** crystallizes in a propeller conformation.

The mean-plane-angle difference between the NC_3 plane and each heterocycle [16.1(1) and 31.0(1)°] is smaller that observed for the aryl substituent [77.2(1)°], presumably as a consequence of the *ortho*-^{i}Pr substituents. There is expected relationship between the N(1)-C(1) and N(1)-C(10) distances with the twist of the quinolyl group from the NC_3 plane is consistent with greater conjugation with the nitrogen lone pair the less the twist.

The quinolyl rings adopt *anti-syn* (C_{Ar}-N-C-N_{quin}) conformation (see Figure 2.26 and Figure 2.27) in the absence of a metal to constrain an *anti-anti* the N(2)-conformation. The twist angle of the two quinolyl rings with respect to each other, as defined by C(1)-C(10)-N(3) torsion angle, is 122.6(3)°. This conformation is in part due to solid-state packing. The crystal packing diagram for **2.15** suggests the presence of π-π stacking between quinolyl rings, with the quin···quin' distance of 3.710(1) Å (equal to the van der Waals' distance for an aromatic half nucleus (3.70 Å). In addition, the stacked quinolyl rings are almost co-planar with the angle between the mean-planes of 1.6(1)°.

Imine side-product formation. Interestingly, through the course of the synthesis and characterization of Mes-dqa (**2.14**), the main product to be isolated from the reaction mixture was not the expected *bis*(2-quinolyl)amine, as was the case in the more sterically hindered 2,6-^{i}Pr$_2$Ph-dqa (**2.15**), but an imine (compound **2.16**; Scheme 2.2).

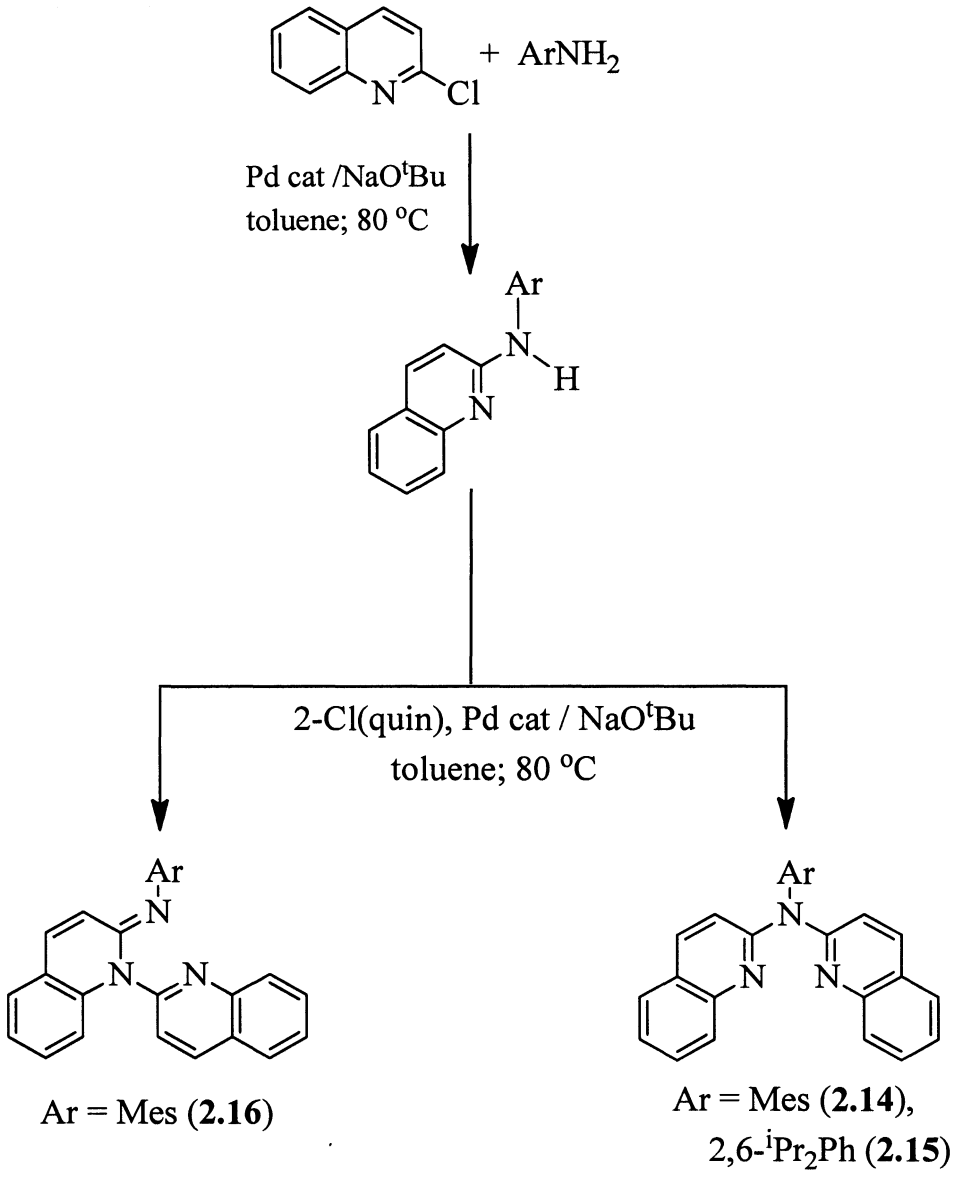

Scheme 2.2. Substituent dependence of the coupling reaction between a substituted aniline and 2-chloroquinoline. "Pd cat" = allyl[1,3-*bis*(2,6-diisopropylphenyl)imidazol-2-ylidene]palladium chloride.

The structure of compound **2.16** is shown in Figure 2.28. Bonding to the imine nitrogen [C(1)-N(1) = 1.293(3) Å and C(19)-N(1) = 1.414(3) Å] is similar to that previously reported for the related α-diimine 1,4-dicyclohexyl-1,4-diaza-1,3-butadiene

[1.258(3) Å and 1.456(3) Å, respectively].[26] The mesityl ring is oriented almost perpendicular (85.4°) to the imine-bound quinoline ring. The second quinoline is bonded through the cyclic nitrogen [N(2)-C(10) = 1.439 Å] and is oriented 72.4° out of plane with the imine bound quinoline.

Table 2.6. Selected bond lengths (Å) and bond angles (°) for compound **2.16**.

N(1)-C(1)	1.287(4)	N(2)-C(1)	1.404(4)
N(1)-C(19)	1.415(4)	N(2)-C(9)	1.413(4)
N(3)-C(10)	1.306(4)	N(2)-C(10)	1.445(4)
N(3)-C(18)	1.354(4)	C(3)-C(4)	1.421(4)
C(1)-C(2)	1.459(4)	C(4)-C(9)	1.411(4)
C(2)-C(3)	1.335(4)		
C(1)-N(1)-C(19)	119.7(3)	C(1)-N(2)-C(10)	116.7(3)
C(1)-N(2)-C(9)	122.6(3)		

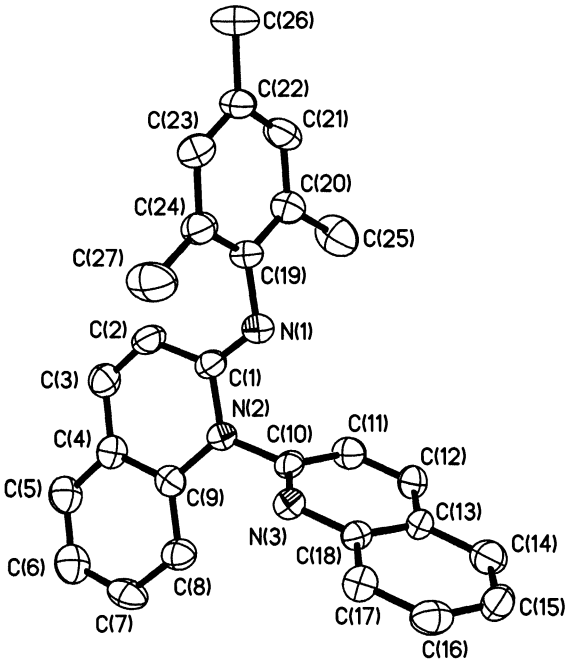

Figure 2.28. Structure of quinolin-1-(2-quinolyl)-2-one mesitylimine (**2.16**). Thermal ellipsoids are shown at the 30% level, and all hydrogen atoms are omitted for clarity.

The dearomatization of the imine-bound quinoline ring is apparent comparing cyclic bond lengths C(1)-C(2) = 1.443(4) Å, C(2)-C(3) = 1.329(4) Å, and C(3)-C(4) = 1.429(4) Å. These are more consistent with alternating single and double bonds than in the corresponding bond lengths in the second quinoline, which retains its aromaticity [C(10)-C(11) = 1.395(4) Å, C(11)-C(12) = 1.352(4) Å, C(12)-C(13) = 1.400(4) Å]. Moreover, the de-aromatized ring exhibits a higher degree of bending [N(2)-C(1)-C(2)-C(3) = 5.2°] than present for the more aromatic system [N(3)-C(10)-C(11)-C(12) = 1.1°].

Based upon the proposed mechanism for the palladium catalyzed coupling reaction[1] the reaction step that will differentiate between the formation of compound **2.16** and the expected tertiary amine (i.e., Scheme 2.2, Ar = Ph or 2,6-^{i}Pr$_2$Ph) would be the formation of the C-N bond via reductive elimination with either a three-membered or five-membered transition state. In order to understand the partition between these reactions we have undertaken *ab initio* calculations of the intermediate (see Experimental).

From *ab initio* calculations the palladium intermediate Pd(L)[N(Ar)quin](quin) (L = 1,3-*bis*(2,6-diisopropylphenyl)imidazol-2-ylidene) for Ar = Ph, Mes, and 2,6-^{i}Pr$_2$Ph shows the structure of the global minimum to be the *anti* conformation (**III**), in which the two quinoline rings are positioned *anti* with respect the Pd-N bond. In the case of the Ph and Mes derivatives the less stable *syn* conformation (**IV**) exists as a local minimum, however, unreasonably close contact are observed for this conformation for the 2,6-^{i}Pr$_2$Ph derivative making it energetically unlikely.

The relative calculated energies of the *syn* and *anti* conformations are given in Table 2.7. Clearly, reductive elimination from the energetically favored *anti* conformation (**III**) must result in the formation of the expected tertiary amine. However, reductive elimination can potentially occur from the *syn* conformation to form either the tertiary amine (**2.14**) or the imine (**2.16**).

Table 2.7. Calculated N···C intramolecular distances and energies for *syn* and *anti* conformations.

R	N	N···C (Å)		Energy (Hartree)	
		anti	*syn*	*anti*	*syn*
Ph	amine	3.45883	3.45883	-7136.8113	-7136.6797
	quin	5.13111	3.14243		
Mes	amine	3.45883	3.45883	-7252.9758	-7252.9203
	quin	5.11683	3.14243		
$^{i}Pr_2C_6H_2$	amine	3.45883	3.45883	-7369.2418	-7368.9722 [a]
	quin	5.10411	3.11828		

[a] Unreasonably close contacts observed.

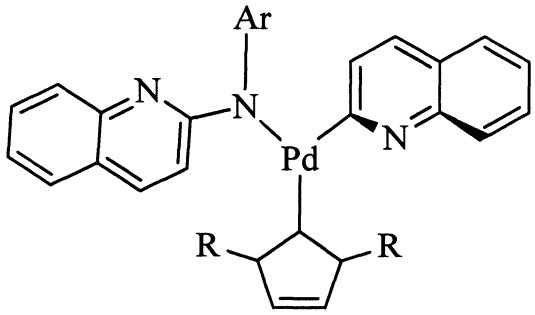

(III)

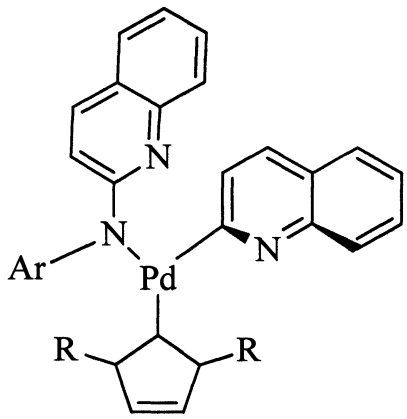

(IV)

A consideration of the $C_{(quin)}$···N distances in the *syn* conformation suggests that formation of the imine would be favored. Furthermore, as may be seen from the calculated structures of *syn*-Pd(L)[N(Mes)quin](quin) (Figure 2.29), the two quinoline rings are oriented for reductive elimination via $C_{(quin)}$-$N_{(quin)}$ bond formation yielding the imine.

rings are oriented for reductive elimination via $C_{(quin)}$-$N_{(quin)}$ bond formation yielding the imine.

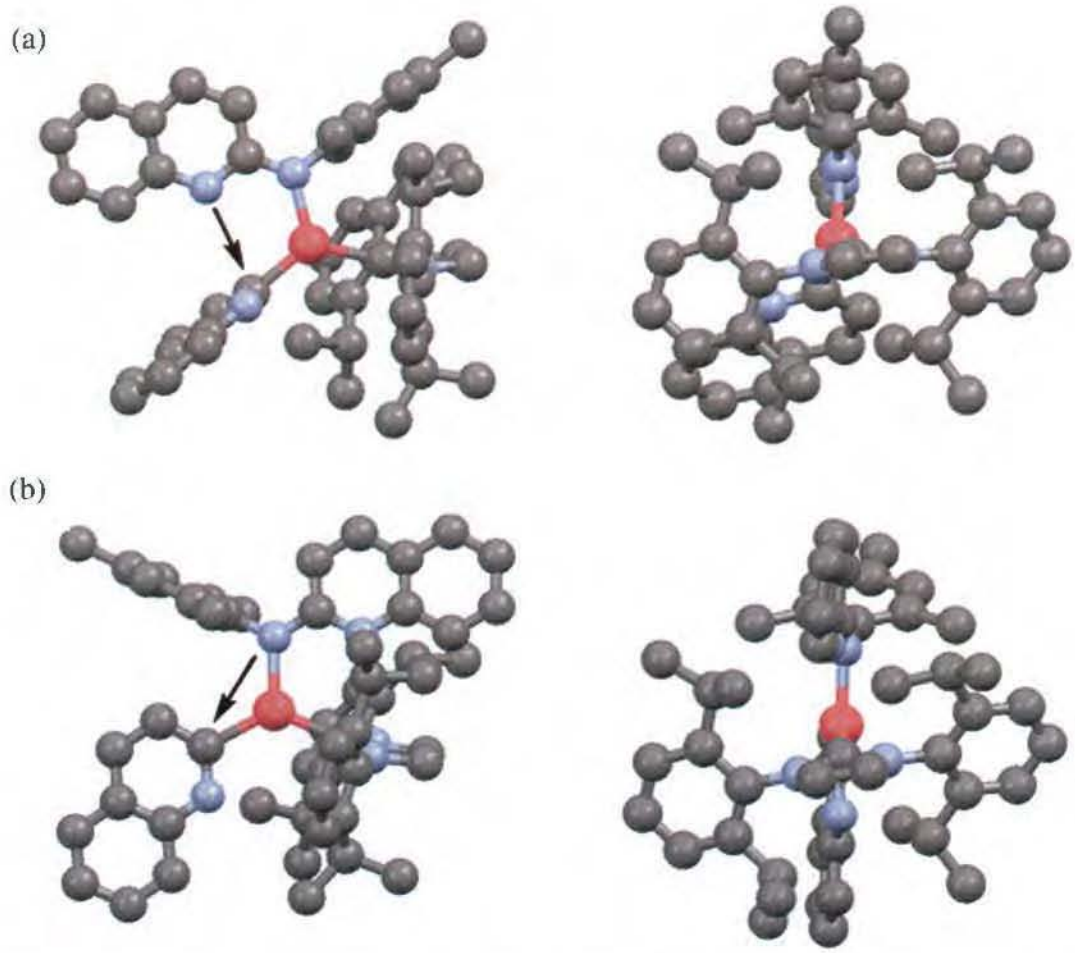

Figure 2.29. Calculated structures of Pd(L)[N(Mes)quin](quin) (L = 1,3-*bis*(2,6-diisopropylphenyl)imidazol-2-ylidene) with the quin rings oriented (a) *syn* and (b) *anti*. Hydrogen atoms are omitted for clarity.

It can be seen from the two orientations (rotated 90° from each other) shown for the *syn*-conformation in Figure 2.29(a) that no steric effects would prevent this particular coordination. Thereby, it would be expected that the reaction yields at least some degree of the imine product.

Figure 2.29(b) shows a similar lack of steric hindrance in the *anti*-conformation, which indicates that the formation of both imine and diquinolylamine should to be reasonable for the mesityl substituted derivatives. Regarding the 2,6-$^{i}Pr_2Ph$ substituted derivative, the reason for the absence of the analogous imine formation can be most clearly seen in Figure 2.30, which illustrates two orientations (90° rotation from one another) of the *syn*-conformation. In this case, the structure is very unlikely to actually adopt this configuration, as can be seen by the unreasonably close contacts produced by overcrowding isopropyl groups. Thus, the *anti*-conformation dominates in the transition state, yielding exclusively the diquinolyl adduct.

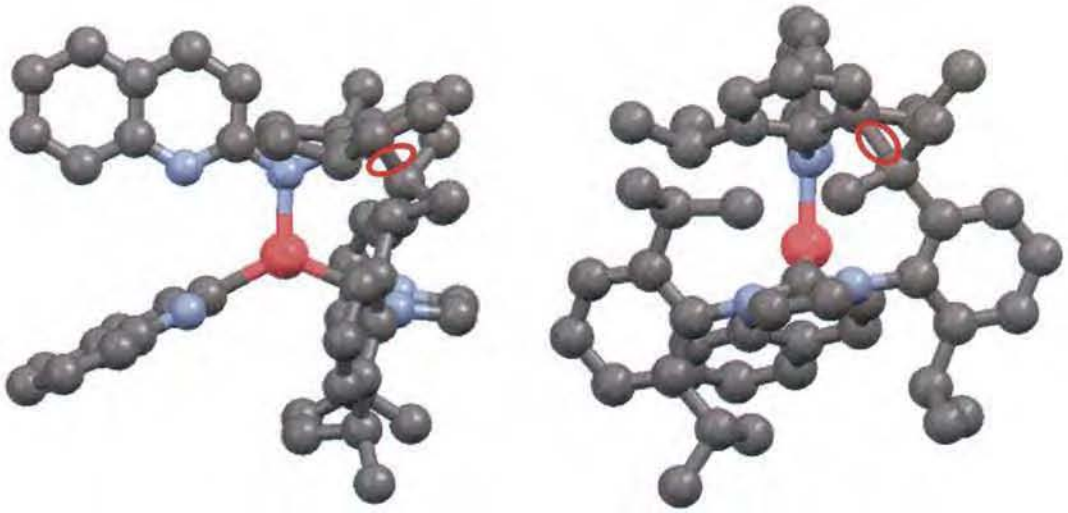

Figure 2.30. Calculated structure of Pd(L)[N(2,6-$^{i}Pr_2Ph$)quin](quin) (L = 1,3-*bis*(2,6-diisopropylphenyl)imidazol-2-ylidene) with the quin rings in *syn*-orientation; unreasonably close contacts indicated in red circles. Hydrogen atoms are omitted for clarity.

The isolation of compound **2.16** versus the tertiary amine (**2.14**) appears to be dependant on the identity of the substituents on the aniline's aryl ring. We can postulate, therefore, that as a consequence of steric interactions between the 1,3-*bis*(2,6-

diisopropylphenyl)imidazol-2-ylidene ligand and the Mes group, the *syn* conformation is energetically accessible, while the shorter N···C distance (Figure 2.31) and orientation (Table 2.7) favor reductive elimination via a five-membered transition state.

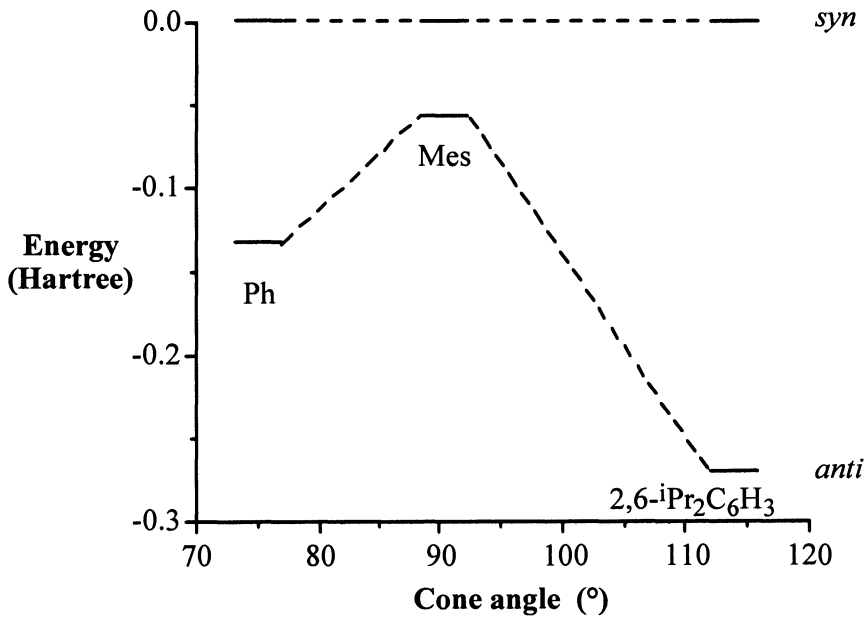

Figure 2.31. Plot of relative energy of *anti* and *syn* conformations of Pd(L)[N(Ar)quin](quin) (L = 1,3-*bis*(2,6-diisopropylphenyl)imidazol-2-ylidene) as a function of the steric bulk of the aryl's ortho substituent as measured by cone angle for Ar = Ph, Mes, and 2,6-$^{i}Pr_2Ph$.

It is interesting to note that while the Mes derivative allows for the isolation of the imine (**2.16**), both the sterically less and more demanding ligands result in the formation of the tertiary amine. As such the Mes derivative exists in a "sweet spot". As may be seen from Table 2.7, while the *anti* conformation is the more stable of the two conformers irrespective of the identity of the aryl substituent, the energy difference between *anti* and *syn* is smallest for the Mes-derivative, making its presence possible as a substantial fraction of the product.

Conclusions

We have shown that for a range of aryl-substituted *bis*(2-pyridyl)amine ligands, in addition to the structurally similar (2-pyridyl)(2-quinolyl)amine and *bis*(2-quinolyl)amine ligands, the presence of *ortho*-substitution in the uncomplexed Ar-dpa compounds results in a significant distortion of the coordination around the amine nitrogen (in the solid state) and twisting of the two pyridyl rings with respect top each other. Additionally, it was demonstrated that the steric bulk of the aryl substituents have a controlling influence on the orientation of the pyridyl rings.

Experimental

General experimental techniques were performed as laid out in Chapter 1. *Tris*(dibenzylideneacetone)-dipalladium(0) [$Pd_2(dba)_3$)] and 1,1'-*bis*(diphenylphosphino)-ferrocene (DPPF) were purchased from Aldrich. Free ligands were prepared according to previously established methods. N-(triphenylmethyl)-N-(2-pyridyl)amine was prepared according to the literature.[27] ArN(H)py (Ar = Ph, 2,6-^{i}Pr$_2$Ph, and 1-naphthyl) were prepared according to the literature methods.[15,16]

MesN(H)py (2.1). 2-Bromopyridine (9.5 g, 60 mmol) and 2,4,6-trimethylaniline (16.2 g, 120 mmol) were added to a round bottom flask topped with a reflux condenser. The reaction flask was heated under reflux for 2 h. The reaction mixture was then made alkaline with a saturated solution of Na_2CO_3 followed by steam distillation to remove excess reactants. The reaction mixture was extracted with Et_2O. After removal of solvent in vacuo the crude product was recrystallized twice from EtOH. Yield = 10 g (79 %). MS (EI, %): *m/z* 213.1 ($M+H^+$). FTIR (neat, ATR, cm^{-1}): 3189 (w, ν_{N-H}), 3151 (w), 3089 (w, aromatic ν_{C-H}), 2996 (w, alkyl ν_{C-H}), 2918 (w, alkyl ν_{C-H}), 2851 (w, alkyl ν_{C-H}), 1589 (s, δ_{N-H}), 1515 (s), 1450 - 1325 (s, aromatic $\delta_{C=C}$), 1225 (m), 1150 (m), 993 (m), 850 (s), 817 (s), 775 (s). ^{1}H NMR ($CDCl_3$): δ 8.11 [1H, d, *J*(H-H) = 5 Hz, pyridyl C*H*], 7.39 [1H, t,

J(H-H) = 7 Hz, pyridyl C*H*], 6.96 [2H, s, mesityl C*H*], 6.63 [1H, t, *J*(H-H) = 6 Hz, pyridyl C*H*], 6.42 [1H, br s, N*H*], 6.04 [1H, d, *J*(H-H) = 8 Hz, pyridyl C*H*], 2.31 [3H, s, *p*-CH_3, Mes], 2.19 [6H, s, mesityl *ortho*-CH_3]. ^{13}C NMR ($CDCl_3$): δ 157.9 (*C*N), 147.4 (*C*N), 138.6 (*C*N), 136.8 (*C*CH_3), 136.7 (*C*H), 133.6 (*C*CH_3), 129.5 (*m*-*C*H), 113.6 (*C*H), 106.3 (*C*H), 21.4 (*p*-*C*H_3), 18.8 (*o*-*C*H_3).

2,6-Et_2PhN(H)py (2.2). 2-Bromopyridine (20 g, 127 mmol) and 2,6-diethylaniline (37 g, 248 mmol) were added to a round bottom flask topped with a reflux condenser. The reaction flask was heated under reflux for 2 h. The reaction mixture was then made alkaline with a saturated solution of Na_2CO_3 followed by steam distillation to remove excess reactants. The reaction mixture was extracted with Et_2O. After removal of solvent *in vacuo* the crude product was recrystallized twice from absolute EtOH. Yield = 21 g (73 %). MS (EI, %): *m/z* 227.1 ($M+H^+$). FTIR (neat, ATR, cm^{-1}): 3200 (w, ν_{N-H}), 3084 (w, aromatic ν_{C-H}), 2960 (m, alkyl ν_{C-H}), 2934 (m, alkyl ν_{C-H}), 2876 (w, alkyl ν_{C-H}), 1599 (s, δ_{N-H}), 1586 (s), 1574 (s), 1518 - 1325 (s, aromatic $\delta_{C=C}$), 1288 (m), 1252 (w), 1148 (m), 990 (s), 867 (m), 805 (m), 767 (vs). ^{1}H NMR ($CDCl_3$): δ 8.13 [1H, d, *J*(H-H) = 5 Hz, pyridyl C*H*], 7.35 [1H, t, *J*(H-H) = 8 Hz, pyridyl C*H*], 7.25 [1H, d, *J*(H-H) = 7 Hz, arom. C*H*], 7.19 [2H, d, *J*(H-H) = 7 Hz, arom. C*H*], 6.62 [1H, t, *J*(H-H) = 6 Hz, pyridyl C*H*], 6.35 [1H, br s, N*H*], 6.00 [1H, d, *J*(H-H) = 8 Hz, pyridyl C*H*], 2.61 [4H, q, *J*(H-H) = 7 Hz, C$H_2$$CH_3$], 1.15 [6H, t, *J*(H-H) = 7 Hz, CH_2CH_3]. ^{13}C NMR ($CDCl_3$): δ 158.6 (*C*N), 148.3 (*C*N), 143.1 (*C*H), 138.0 (*C*N), 135.2 (*C*CH_2), 127.6 (*p*-*C*H), 127.0 (*m*-*C*H), 113.6 (*C*H), 105.9 (*C*H), 24.9 (*C*$H_2$$CH_3$), 14.7 ($CH_2CH_3$).

2-^{i}PrPhN(H)py (2.3). 2-isopropylaniline (49.86 g, 0.369 mol) and 2-bromopyridine (29.13 g, 0.184 mol) were refluxed under an argon atmosphere for 12 h. The reaction mixture was then made alkaline with a saturated solution of Na_2CO_3, followed by steam distillation to remove excess reactants. Extraction with Et_2O, followed

by removal of the solvent in vacuum gave an off-white powder. The crude product was recrystallized by the slow evaporation of methanol solution to afford colorless crystals. Yield: 32.24 g (82%). Mp (TGA; sublim.): 120 - 122 °C. MS (EI, %): *m/z* 212 (M^+, 8.7), 169 (M^+ - ^{i}Pr, 100). FTIR (neat, ATR, cm^{-1}): 3201 (w, ν_{N-H}), 3161 (w), 3091 (w, aromatic ν_{C-H}), 3008 (w, aromatic ν_{C-H}), 2954 (w, alkyl ν_{C-H}), 2859 (w, alkyl ν_{C-H}), 1584 (s), 1529 (s), 1450 - 1329 (s, aromatic $\delta_{C=C}$), 1150 (m), 1083 (m), 1033 (m), 993 (m). ^{1}H NMR ($CDCl_3$): δ 8.14 [1H, ddd, *J*(H-H) = 5.1 Hz, *J*(H-H) = 1.9 Hz, *J*(H-H) = 0.7 Hz, 6-C*H*, py], 7.44 [1H, ddd, *J*(H-H) = 8.5 Hz, *J*(H-H) = 7.2 Hz, *J*(H-H) = 1.9 Hz, 4-C*H*, py], 7.37-7.35 (2H, m, C*H*, Ph), 7.23-7.20 (2H, m, C*H*, Ph), 6.69 [1H, ddd, *J*(H-H) = 7.2 Hz, *J*(H-H) = 5.1 Hz, *J*(H-H) = 0.8 Hz, C*H*, 5-py], 6.67 (1H, br s, N*H*), 6.57 [1H, ddd, *J*(H-H) = 8.5 Hz, *J*(H-H) = 0.8 Hz, *J*(H-H) = 0.7 Hz, C*H*, 3-py], 3.23 [1H, sept, *J*(H-H) = 6.8 Hz, C*H*(CH_3)$_2$], 1.23 [6H, d, *J*(H-H) = 6.8 Hz, CH(C*H*$_3$)$_2$]. ^{13}C NMR ($CDCl_3$): δ 157.86, 147.94, 143.81, 138.29, 136.94, 126.81, 126.65, 126.10, 125.59, 114.40, 107.37, 28.12, 23.46.

Mes-dpa (2.5). N-(2,4,6-trimethyl)phenyl-N-(2-pyridyl)amine (21.23 g, 100 mmol), sodium *tert*-butoxide (11.53 g, 120 mmol), $Pd_2(dba)_3$ (2.289 g, 2.5 mmol),, and DPPF (2.772 g, 5.0 mmol) were added to a Schlenk flask in a drybox. The flask was capped with a septum, removed from the drybox, and toluene (ca. 15 mL) was added via cannula. The mixture was stirred, and 2-bromopyridine (19.02 g, 120 mmol) was injected via syringe into the reaction vessel. The reaction was stirred under nitrogen at 90 °C for 120 hours. After cooling, $CHCl_3$ (50 mL) was added, the mixture was filtered, and the solvent was removed under vacuum. The crude product was purified by column chromatography on silica gel (eluent: 5% ethyl acetate in hexanes). The purified product was recrystallized by cooling a saturated solution in hexanes to –12 °C for several days, giving colorless crystals. Yield: 20.58 g (71%). Mp (TGA; sublim.): 141 - 143 °C. MS (EI,%): *m/z* 289 (M^+, 13.2), 274 (M^+ - Me, 100). FTIR (neat, ATR, cm^{-1}): 3150 (w,

aromatic ν_{C-H}), 3068 (w, aromatic ν_{C-H}), 3048 (w, aromatic ν_{C-H}), 3004 (w, aromatic ν_{C-H}), 2972 (w, alkyl ν_{C-H}), 2916 (w, alkyl ν_{C-H}), 2854 (w, alkyl ν_{C-H}), 1584 (s), 1563 (m), 1463 - 1319 (s, aromatic $\delta_{C=C}$), 1257 (m, aromatic $\delta_{C=N}$), 1147 (s), 988 (s). ^{1}H NMR (CD_3OD): δ 8.17 [2H, ddd, J(H-H) = 5.0 Hz, J(H-H) = 1.9 Hz, J(H-H) = 0.7 Hz, C*H*, 6,6'-py], 7.65 [2H, ddd, J(H-H) = 8.6 Hz, J(H-H) = 7.2 Hz, J(H-H) = 1.9 Hz, C*H*, 4,4'-py], 7.01 (2H, s, C_6H_2), 6.98 [2H, ddd, J(H-H) = 7.2 Hz, J(H-H) = 5.0 Hz, J(H-H) = 0.9 Hz, C*H*, 5,5'-py], 6.88 [2H, ddd, J(H-H) = 8.6 Hz, J(H-H) = 0.9 Hz, J(H-H) = 0.7 Hz, C*H*, 3,3'-py], 2.33 (3H, s, *p*-CH_3), 1.96 (6H, s, *o*-CH_3). ^{13}C NMR (CD_3OD): δ 158.03, 148.74, 139.79, 139.74, 139.24, 138.49, 131.23, 119.01, 116.43, 21.28, 18.66.

2,6-Et$_2$Ph-dpa (2.6). Prepared in an analogous manner to that of compound **2.5**, using N-(2,6-diethyl)phenyl-N-(2-pyridyl)amine (2.26 g, 10 mmol), 2-bromopyridine (1.89 g, 12 mmol), sodium *tert*-butoxide (1.53 g, 16 mmol), $Pd_2(dba)_3$ (137 mg, 0.15 mmol), DPPF (166 mg, 0.30 mmol), and toluene (15 mL). The purified product was recrystallized by cooling a saturated solution in $CHCl_3$ to –12 °C for several days to give colorless crystals. Yield: 0.77 g (25%). Mp (TGA; sublim.): 86 - 88 °C. MS (EI, %): *m/z* 303 (M^+, 2.2), (M^+ - Et, 100). FTIR (neat, ATR, cm^{-1}): 3151 (w, aromatic ν_{C-H}), 3069 (w, aromatic ν_{C-H}), 3048 (w, aromatic ν_{C-H}), 3003 (w, aromatic ν_{C-H}), 2972 (w, alkyl ν_{C-H}), 2956 (w, alkyl ν_{C-H}), 2911 (w, alkyl ν_{C-H}), 2877 (w, alkyl ν_{C-H}), 1618 (m), 1584 (s), 1561 (m), 1465 - 1319 (s, aromatic $\delta_{C=C}$), 1279 (m, aromatic $\delta_{C=N}$), 1150 (m), 987 (m). ^{1}H NMR (298 K; $CDCl_3$): δ 8.28 [2H, ddd, J(H-H) = 5.0 Hz, J(H-H) = 2.0 Hz, J(H-H) = 0.8 Hz, C*H*, C*H*, 6,6'-py], 7.49 [2H, ddd, J(H-H) = 8.4 Hz, J(H-H) = 7.2 Hz, J(H-H) = 2.0 Hz, C*H*, 4,4'-py], 7.34 [1H, dd, J(H-H) = 7.7 Hz, J(H-H) = 7.7 Hz, p- C*H*, Ph], 7.23 [2H, d, J(H-H) = 7.7 Hz, m- C*H*, Ph], 6.94 [2H, ddd, J(H-H) = 8.4 Hz, J(H-H) = 0.9 Hz, J(H-H) = 0.8 Hz, C*H*, 3,3'-py], 6.83 [2H, ddd, J(H-H) = 7.2 Hz, J(H-H) = 5.0 Hz, J(H-H) = 0.9 Hz, C*H*, 5,5'-py], 2.44 [4H, q, J(H-H) = 7.6 Hz, CH_2CH_3], 0.96 [6H, t, J(H-H) = 7.6

Hz, CH_2CH_3]. ^{13}C NMR (298 K; $CDCl_3$): δ 157.11, 148.24, 143.28, 140.36, 137.35, 128.44, 127.21, 117.17, 114.76, 24.43, 13.90.

2-^{i}PrPh-dpa (2.7). Prepared in an analogous manner to that of compound **2.5**, using N-(2-isopropyl)phenyl-N-(2-pyridyl)amine (10.645 g, 50 mmol), 2-bromopyridine (9.980 g, 60 mmol), sodium *tert*-butoxide (5.765 g, 60 mmol), $Pd_2(dba)_3$ (1.373 g, 1.25 mmol), DPPF (1.663 g, 2.5 mmol), and toluene (200 mL). The crude product was purified by column chromatography on silica gel (eluent: 5% ethyl acetate in hexanes). The purified product was recrystallized by a slow evaporation of a 4:1 hexanes:CH_2Cl_2 solution to give colorless crystals. Yield 5.311 g (38%). Mp (TGA; sublim.): 101 - 103 °C. MS (EI,%): *m/z* 289 (M^+, 0.7), 246 (M^+ - ^{i}Pr, 100). FTIR (neat, ATR, cm^{-1}): 3054 (w, aromatic ν_{C-H}), 3005 (w, aromatic ν_{C-H}), 2959 (m, alkyl ν_{C-H}), 2922 (w, alkyl ν_{C-H}), 2866 (w, alkyl ν_{C-H}), 1583 (s), 1569 (s), 1463 - 1316 (s, aromatic $\delta_{C=C}$), 1277 (s, aromatic $\delta_{C=N}$), 1150(s), 1083 (m), 989 (m), 867 (w). ^1H NMR (CD_3OD): δ 8.18 [2H, ddd, *J*(H-H) = 5.0 Hz, *J*(H-H) = 2.0 Hz, *J*(H-H) = 0.8 Hz, C*H*, 6,6'-py], 7.65 [2H, ddd, *J*(H-H) = 8.4 Hz, *J*(H-H) = 7.3 Hz, *J*(H-H) = 2.0 Hz, C*H*, 4,4'-py], 7.47 [1H, dd, *J*(H-H) = 7.9 Hz, *J*(H-H) = 1.5 Hz, C*H*, Ph], 7.39 [1H, ddd, *J*(H-H) = 7.9 Hz, *J*(H-H) = 7.2 Hz, *J*(H-H) = 1.3 Hz, C*H*, Ph], 7.29 [1H, ddd, *J*(H-H) = 7.9 Hz, *J*(H-H) = 7.2 Hz, *J*(H-H) = 1.5 Hz, C*H*, Ph], 7.15 [1H, dd, *J*(H-H) = 7.9 Hz, *J*(H-H) = 1.3 Hz, C*H*, Ph], 6.99 [2H, ddd, *J*(H-H) = 7.3 Hz, *J*(H-H) = 5.0 Hz, *J*(H-H) = 1.0 Hz, C*H*, 5,5'-py], 6.88 [2H, ddd, *J*(H-H) = 8.4 Hz, *J*(H-H) = 1.0 Hz, *J*(H-H) = 0.8 Hz, C*H*, 3,3'-py], 3.05 [1H, sept, *J*(H-H) = 6.8 Hz, $CH(CH_3)_2$], 0.99 [6H, d, *J*(H-H) = 6.8 Hz, $CH(CH_3)_2$]. ^{13}C NMR (CD_3OD): δ 159.36, 148.83, 148.77, 142.76, 139.58, 131.43, 129.61, 129.00, 128.82, 119.32, 117.75, 29.28, 23.91.

2,6-^{i}Pr$_2$Ph-dpa (2.8). Prepared in an analogous manner to that of compound **3.5**, using 2,6-diisopropylaniline (0.355 g, 2.0 mmol), 2-bromopyridine (0.700 g, 4.4 mmol),

sodium *tert*-butoxide (0.550 g, 5.7 mmol), $Pd_2(dba)_3$ (0.055 g, 0.06 mmol), DPPF (0.083 g, 0.15 mmol), and toluene (10 mL). The crude product was purified by flash chromatography on silica gel (eluent: 2% MeOH in CH_2Cl_2) followed by recrystallization by vapor diffusion of pentane into a saturated $CHCl_3$ solution yielding colorless crystals Yield: yield 0.331 g (50%). Mp (TGA; sublim.): 95 - 97 °C. MS (EI, %): *m/z* 331 (M^+, 0.8), 288 (M^+ - ^{i}Pr, 100). FTIR (neat, ATR, cm^{-1}): 3178 (w, aromatic ν_{C-H}), 3057 (w, aromatic ν_{C-H}), 3008 (w, aromatic ν_{C-H}), 2959 (w, alkyl ν_{C-H}), 2926 (w, alkyl ν_{C-H}), 2867 (w, alkyl ν_{C-H}), 1595 (m), 1584 (s), 1527 (m), 1467 - 1328 (s, aromatic $\delta_{C=C}$), 1255 (m, aromatic $\delta_{C=N}$), 1147(m), 989 (m). ^{1}H NMR ($CDCl_3$): δ 8.27 [2H, ddd, *J*(H-H) = 5.0 Hz, *J*(H-H) = 1.9 Hz, *J*(H-H) = 0.8 Hz, C*H*, 6,6'-py], 7.50 [2H, ddd, *J*(H-H) = 8.4 Hz, *J*(H-H) = 7.2 Hz, *J*(H-H) = 1.9 Hz, C*H*, 4,4'-py], 7.42 [1H, dd, *J*(H-H) = 7.7 Hz, *J*(H-H) = 7.7 Hz, *p*- C*H*, Ph], 7.27 [2H, d, *J*(H-H) = 7.7 Hz, *m*- C*H*, Ph], 6.96 [2H, ddd, *J*(H-H) = 8.4 Hz, *J*(H-H) = 0.9 Hz, *J*(H-H) = 0.8 Hz, C*H*, 3,3'-py], 6.82 [2H, ddd, *J*(H-H) = 7.2 Hz, *J*(H-H) = 5.0 Hz, *J*(H-H) = 0.9 Hz, C*H*, 5,5'-py], 3.09 [2H, sept, *J*(H-H) = 6.9 Hz, C*H*$(CH_3)_2$], 0.95 [12H, d, *J*(H-H) = 6.9 Hz, CH(C*H*$_3)_2$]. ^{13}C NMR ($CDCl_3$): δ 157.45, 148.13, 148.00, 138.45, 137.23, 129.03, 124.92, 117.12, 114.99, 28.67, 23.94.

(1-naph)-dpa (2.9). Prepared in an analogous manner to that of compound **2.5**, using N-(1-naphthyl)-N-(2-pyridyl)amine (2.20 g, 10 mmol), 2-bromopyridine (1.89 g, 12 mmol), sodium *tert*-butoxide (1.53 g, 16 mmol), $Pd_2(dba)_3$ (137 mg, 0.15 mmol), DPPF (166 mg, 0.30 mmol), and toluene (15 mL). The purified product was recrystallized by a slow evaporation of a 1:1 hexanes:CH_2Cl_2 solution to yield 1.37 g (46%) colorless crystals. Mp (TGA; sublim.): 166 - 168 °C. MS (EI,%): *m/z* 297 (M^+, 41.9), 296 (M^+ - H, 100). FTIR (neat, ATR, cm^{-1}): 3129 (w, aromatic ν_{C-H}), 3074 (w, aromatic ν_{C-H}), 3044 (w, aromatic ν_{C-H}), 2992 (w, aromatic ν_{C-H}), 2975 (w, aromatic ν_{C-H}), 2910 (w), 1583 (s), 1559 (m), 1462 - 1314 (s, aromatic $\delta_{C=C}$), 1267 (m, aromatic $\delta_{C=N}$), 1151 (m), 990 (m). ^{1}H NMR ($CDCl_3$): δ 8.34 [2H, ddd, *J*(H-H) = 5.0 Hz, *J*(H-H) =

2.0 Hz, *J*(H-H) = 0.8 Hz, C*H*, *6,6'*-py], 7.91 [1H, d, *J*(H-H) = 8.2 Hz, C*H*, naph], 7.88 [1H, d, *J*(H-H) = 8.2 Hz, C*H*, naph], 7.84 [1H, ddd, *J*(H-H) = 8.5 Hz, *J*(H-H) = 1.8 Hz, *J*(H-H) = 0.9 Hz, C*H*, naph], 7.55 [1H, dd, *J*(H-H) = 8.2 Hz, *J*(H-H) = 7.2 Hz, C*H*, naph], 7.49 [2H, ddd, *J*(H-H) = 8.4 Hz, *J*(H-H) = 7.3 Hz, *J*(H-H) = 2.0 Hz, C*H*, 4,4'-py], 7.47 (2H, m, C*H*, naph), 7.37 [1H, ddd, *J*(H-H) = 8.3 Hz, *J*(H-H) = 6.9 Hz, *J*(H-H) = 1.2 Hz, C*H*, naph], 6.90 [2H, ddd, *J*(H-H) = 8.4 Hz, *J*(H-H) = 1.0 Hz, *J*(H-H) = 0.8 Hz, C*H*, 3,3'-py], 6.89 [2H, ddd, *J*(H-H) = 7.3 Hz, *J*(H-H) = 5.0 Hz, *J*(H-H) = 1.0 Hz, C*H*, 5,5'-py]. ^{13}C NMR ($CDCl_3$): δ 158.14, 148.30, 137.87, 135.45, 131.61, 128.76, 128.17, 127.87, 127.13, 126.62, 126.53, 123.78, 117.88, 115.98.

H-pqa (2.10). 2-chloroquinoline (2.140 g, 13.1 mmol), 2-aminopyridine (1.026 g, 10.9 mmol), sodium *tert*-butoxide (1.257 g, 13.1 mmol), $Pd_2(dba)_3$ (0.150 g, 0.16 mmol), and DPPF (0.181 g, 0.32 mmol) were placed in a Schlenk flask in a drybox. The flask was removed, and toluene (100 mL) was added via cannula. The reaction was stirred under an argon atmosphere at 80 °C for 60 hrs. After cooling to room temperature, hexane (100 mL) was added, and the mixture was extracted twice with brine solution. The solvent was removed from the organic phase under reduced pressure, and the resulting residue was purified by column chromatography on silica gel (eluent: 5% ethyl acetate in hexanes) followed by recrystallization from Et_2O gave translucent yellow plates. Yield: 2.057 g (85%). Mp (TGA; sublim.): 107 - 108 °C. MS (EI,%): *m/z* 221 (M^+, 5.5), 220 (M^+ - H·, 11.1). FTIR (neat, ATR, cm^{-1}): 3271 (m, ν_{N-H}), 3177 (w, aromatic ν_{C-H}), 3108 (w, aromatic ν_{C-H}), 3080 (w, aromatic ν_{C-H}), 3064 (w, aromatic ν_{C-H}), 3042 (w, aromatic ν_{C-H}), 3007 (w, aromatic ν_{C-H}), 1621 (w), 1584 (s), 1527 (s), 1474 - 1299 (s, aromatic $\delta_{C=C}$), 1228 (m, aromatic $\delta_{C=N}$), 1144 (m), 980 (m), 813 (s). ^{1}H NMR (CD_3OD): δ 8.37 [1H, dd, *J*(H-H) = 8.5 Hz, *J*(H-H) = 1.0 Hz, C*H*, 6-quin], 8.23 [1H, ddd, *J*(H-H) = 5.0 Hz, *J*(H-H) = 1.9, Hz, *J*(H-H) = 0.9 Hz, C*H*, 6-py], 8.06 [1H, d, *J*(H-H) = 8.9 Hz, C*H*, 4-quin], 7.77 [1H, ddd, *J*(H-H) = 8.5 Hz, *J*(H-H) = 1.0, Hz, *J*(H-H) =

0.9 Hz, C*H*, 3-py], 7.75 [1H, ddd, *J*(H-H) = 8.5 Hz, *J*(H-H) = 7.3 Hz, *J*(H-H) = 1.9 Hz, C*H*, 4-py], 7.72 [1H, dd, *J*(H-H) = 8.1 Hz, *J*(H-H) = 1.5 Hz, C*H*, 9-quin], 7.60 [1H, ddd, *J*(H-H) = 8.5 Hz, *J*(H-H) = 7.0 Hz, *J*(H-H) = 1.5 Hz, C*H*, 7-quin], 7.39 [1H, d, *J*(H-H) = 8.9 Hz, C*H*, 3-quin], 7.34 [1H, ddd, *J*(H-H) = 8.1 Hz, *J*(H-H) = 7.0 Hz, *J*(H-H) = 1.0 Hz, C*H*, 8-quin], 6.96 [1H, ddd, *J*(H-H) = 7.3 Hz, *J*(H-H) = 5.0, Hz, *J*(H-H) = 1.0 Hz, C*H*, 5-py]. ^{13}C NMR (CD_3OD): δ 155.47, 154.84, 148.73, 148.43, 139.40, 138.99, 130.88, 128.74, 127.83, 126.07, 124.93, 118.44, 115.24, 114.41.

Ph-pqa (2.11). This compound was prepared in an analogous manner to that of compound **2.10**, using N-phenyl-N-(2-pyridyl)amine (3.90 g, 22.9 mmol), 2-chloroquinoline (4.50 g, 27.5 mmol), sodium *tert*-butoxide (2.64 g, 27.5 mmol), $Pd_2(dba)_3$ (0.315 g, 0.34 mmol), DPPF (0.381 g, 0.68 mmol), and 200 mL toluene. Purification yielded 5.85 g (86%) of a viscous red/orange oil. The oil was exposed to the atmosphere for several weeks, which resulted in the formation of crystals suitable for X-ray diffraction. Mp (TGA): 97 - 98 °C. MS (EI,%): *m/z* 297 (M^+, 36), 296 (M^+ - H, 100). FTIR (neat, ATR, cm^{-1}): 3046 (w, aromatic ν_{C-H}), 3007 (w, aromatic ν_{C-H}), 2977 (w, aromatic ν_{C-H}), 1619 (w), 1589 (s), 1567 (m), 1495 - 1337 (s, aromatic $\delta_{C=C}$), 1287 (m, aromatic $\delta_{C=N}$), 1150 (m), 1120 (w), 821 (m). ^{1}H NMR (CD_3OD): δ 8.22 [1H, ddd, *J*(H-H) = 5.1 Hz, *J*(H-H) = 1.9, Hz, J(H-H) = 0.9 Hz, C*H*, 6-py], 8.00 [1H, dd, J(H-H) = 8.9 Hz, J(H-H) = 0.5 Hz, C*H*, 4-quin], 7.69 [1H, dd, J(H-H) = 8.1 Hz, J(H-H) = 1.4, Hz, C*H*, 9-quin], 7.67 [1H, ddd, J(H-H) = 8.4 Hz, J(H-H) = 1.3, J(H-H) = 0.5 Hz, C*H*, 6-quin], 7.63 [1H, ddd, J(H-H) = 8.4 Hz, J(H-H) = 7.3, Hz, J(H-H) = 1.9 Hz, C*H*, 4-py], 7.53 [1H, ddd, J(H-H) = 8.4 Hz, J(H-H) = 7.0, Hz, J(H-H) = 1.4 Hz, C*H*, 7-quin], 7.35 (2H, m, *o*-C*H*, Ph), 7.34 [1H, ddd, J(H-H) = 8.1 Hz, J(H-H) = 7.0, Hz, J(H-H) = 1.3 Hz, C*H*, 8-quin], 7.22 (1H, m, *p*-C*H*, Ph), 7.13 (2H, m, *m*-C*H*, Ph), 7.05 [1H, ddd, J(H-H) = 8.4 Hz, J(H-H) = 1.0, Hz, J(H-H) = 0.9 Hz, C*H*, 3-py], 7.04 [1H, ddd, J(H-H) = 7.3 Hz, J(H-H) = 5.1, Hz, J(H-H) = 1.0 Hz, 5-py], 6.97 [1H, d, J(H-H) = 8.9 Hz, C*H*, 3-quin]. ^{13}C NMR

(CD_3OD): δ 159.39, 158.47, 149.22, 148.43, 146.00, 139.96, 139.54, 131.17, 131.06, 128.83, 128.54, 128.01, 127.36, 127.12, 126.27, 120.75, 120.11, 118.49.

Mes-pqa (2.12). This compound was prepared in an analogous manner to that of compound **2.10**, using N-(mesityl)-N-(2-pyridyl)amine (10.61 g, 50 mmol), 2-chloroquinoline (9.816 g, 60 mmol), sodium *tert*-butoxide (5.766 g, 60 mmol), $Pd_2(dba)_3$ (0.550 g, 0.60 mmol), DPPF (0.668 g, 1.20 mmol), and toluene (350 mL). The reaction period was increased to 72 hours. The purified product was recrystallized from a slow evaporation of a saturated $CHCl_3$ solution. Yield: 11.93 g (70%). Mp (TGA; sublim.): 165 - 167 °C. MS (EI,%): *m/z* 339 (M^+, 26), 324 (M^+ - Me, 100). FTIR (neat, ATR, cm^{-1}): 3063 (w, aromatic ν_{C-H}), 3046 (w, aromatic ν_{C-H}), 2996 (w, aromatic ν_{C-H}), 2974 (w, alkyl ν_{C-H}), 2945 (w, alkyl ν_{C-H}), 2916 (w, alkyl ν_{C-H}), 2850 (w, alkyl ν_{C-H}), 1618 (m), 1584 (s), 1565 (m), 1462 - 1332 (s, aromatic $\delta_{C=C}$), 1286 (m, aromatic $\delta_{C=N}$), 1152 (m), 983 (m). ^1H NMR (CD_3OD): δ 8.21 [1H, ddd, *J*(H-H) = 5.0 Hz, *J*(H-H) = 1.9 Hz, *J*(H-H) = 0.8 Hz, C*H*, 6-py], 8.07 [1H, dd, *J*(H-H) = 9.0 Hz, *J*(H-H) = 0.5 Hz, C*H*, 4-quin], 7.76 [1H, dd, *J*(H-H) = 8.0 Hz, *J*(H-H) = 1.2 Hz, C*H*, 9-quin], 7.72 [1H, ddd, *J*(H-H) = 8.3 Hz, *J*(H-H) = 7.3 Hz, *J*(H-H) = 1.9 Hz, C*H*, 4-py], 7.71 [1H, ddd, *J*(H-H) = 8.6 Hz, *J*(H-H) = 1.1 Hz, *J*(H-H) = 0.5 Hz, C*H*, 6-quin], 7.60 [1H, ddd, *J*(H-H) = 8.6 Hz, *J*(H-H) = 7.0 Hz, *J*(H-H) = 1.2 Hz, C*H*, 7-quin], 7.40 [1H, ddd, *J*(H-H) = 8.0 Hz, *J*(H-H) = 7.0 Hz, *J*(H-H) = 1.1 Hz, C*H*, 8-quin], 7.19 [1H, ddd, *J*(H-H) = 8.3 Hz, *J*(H-H) = 1.0 Hz, *J*(H-H) = 0.8 Hz, C*H*, 3-py], 7.04 [1H, ddd, *J*(H-H) = 7.3 Hz, *J*(H-H) = 5.0 Hz, *J*(H-H) = 1.0 Hz, C*H*, 5-py], 7.03 (2H, s, C_6H_2), 6.93 [1H, d, *J*(H-H) = 9.0 Hz, C*H*, 3-quin], 2.35 (3H, s, *p*-CH_3), 1.99 (6H, s, *o*-CH_3). ^{13}C NMR (298 K; CD_3OD): δ 157.95, 157.14, 148.84, 148.48, 139.78, 139.60, 139.49, 139.36, 138.65, 131.22, 131.08, 128.75, 127.95, 126.70, 125.78, 119.57, 117.66, 116.44, 21.31, 18.79.

2,6-^{i}Pr$_2$Ph-pqa (2.13). 2-chloro-quinoline (1.00 g, 6.0 mmol), N-(2,6-diisopropyl)phenyl-N-(2-pyridyl)amine (1.27 g, 5.0 mmol), sodium *tert*-butoxide (0.75 g, 7.8 mmol), and allyl[1,3-*bis*(2,6-diisopropylphenyl)imidazol-2-ylidene]palladium(II) chloride (91 mg, 0.16 mmol) were placed in a Schlenk flask in a drybox. The flask was removed, and toluene (100 mL) was added via cannula. The reaction was stirred under an argon atmosphere at 80 °C for 5 days. After cooling to room temperature, CH_2Cl_2 (100 mL) was added, and the mixture was extracted twice with brine solution. The solvent was removed from the organic phase under reduced pressure, and the resulting residue was purified by column chromatography on silica gel (eluent: 2.5% ethyl acetate in hexanes). Recrystallization from a very slow (*ca.* 8 months) evaporation of a 1:1 mixture of Et_2O and EtOH gave translucent yellow plates suitable for diffraction. Yield: 0.75 g (39%), 97% pure by GC-MS. Mp (TGA; sublim.): 210 - 212 °C. MS (EI, %): *m/z* 381.2 (M^+, 1.0), 338.2 (M^+ - ^{i}Pr, 100). FTIR (neat, ATR, cm^{-1}): 3064 (w, aromatic ν_{C-H}), 3016 (w, aromatic ν_{C-H}), 2957 (w, alkyl ν_{C-H}), 2926 (m, alkyl ν_{C-H}), 2906 (w, alkyl ν_{C-H}), 2866 (w, alkyl ν_{C-H}), 1617 (m), 1602 (m), 1584 (s), 1570 - 1423 (s, aromatic $\delta_{C=C}$), 1384 (m), 1335 (s, 3° aromatic ν_{C-N}), 1310 (s), 1287 (s), 1260(s), 1150 (m), 1054 (m), 826 (m), 821 (s), 757 (s). ^{1}H NMR (CD_3OD): δ 8.21 [1H, ddd, *J*(H-H) = 5.0 Hz, *J*(H-H) = 2.0, Hz, *J*(H-H) = 0.8 Hz, C*H*, 6-py], 8.06 [1H, d, *J*(H-H) = 9.0 Hz, C*H*, 4-quin], 7.74 [1H, ddd, *J*(H-H) = 8.1 Hz, *J*(H-H) = 1.5 Hz, *J*(H-H) = 0.6 Hz, C*H*, 9-quin], 7.69 [1H, ddd, *J*(H-H) = 8.5 Hz, *J*(H-H) = 1.2 Hz, *J*(H-H) = 0.6 Hz, C*H*, 6-quin], 7.67 [1H, ddd, *J*(H-H) = 8.5 Hz, *J*(H-H) = 7.3, *J*(H-H) = 2.0 Hz, C*H*, 4-py], 7.58 [1H, ddd, *J*(H-H) = 8.5 Hz, *J*(H-H) = 6.9, Hz, *J*(H-H) = 1.5 Hz, C*H*, 7-quin], 7.45 [1H, t, *J*(H-H) = 7.8 Hz, *p*-C*H*, Ph], 7.38 [1H, ddd, *J*(H-H) = 8.1 Hz, *J*(H-H) = 6.9, Hz, *J*(H-H) = 1.2 Hz, C*H*, 8-quin], 7.32 [2H, d, *J*(H-H) = 7.8 Hz, *m*-C*H*, Ph], 7.11 [1H, ddd, *J*(H-H) = 8.5 Hz, *J*(H-H) = 0.9, Hz, *J*(H-H) = 0.8 Hz, C*H*, 3-py], 7.04 [1H, d, *J*(H-H) = 9.0 Hz, C*H*, 3-quin], 7.00 [1H, ddd, *J*(H-H) = 7.3 Hz, *J*(H-H) = 5.0, Hz, *J*(H-H) = 0.9 Hz, C*H*, 5-py], 3.15 [2H, sept, *J*(H-H) = 6.9 Hz, C*H*(CH_3)$_2$], 0.96 [6 H, d, *J*(H-H) = 6.9 Hz, CH(C*H*$_3$)$_2$], 0.94 [6 H, d, *J*(H-H) = 6.9 Hz,

$CH(CH_3)_2$]. ^{13}C NMR (CD_3OD): δ 158.80, 157.65, 149.44, 148.75, 148.50, 139.52, 139.28, 138.82, 130.94, 130.38, 128.69, 128.21, 126.66, 126.14, 125.75, 119.33, 117.51, 117.15, 29.89, 24.31, 24.19.

Mes-dqa (2.14). In a drybox, KO^{t}Bu (785 mg, 7.0 mmol), allyl[1,3-*bis*(2,6-diisopropylphenyl)-imidazol-2-ylidene]palladium(II)chloride (70 mg, 0.12 mmol), and 2-chloroquinoline (818 mg, 5.0 mmol) were added to a Schlenk flask. To this was added toluene (10 mL) followed by 2,4,6-trimethylaniline (338 mg, 2.5 mmol). The reaction was stirred under nitrogen at 70 °C for 120 h. After cooling, Et_2O (25 mL) was added to the reaction mixture and then washed twice with brine. The organic phase was dried over sodium sulfate before removing solvent in vacuo. The crude product was purified by flash chromatography on silica gel (eluent: 10% ethyl acetate in hexanes). The product was dissolved in hot hexanes and allowed to cool to room temperature. Subsequent cooling to –12 °C over several days resulted in the formation of crystals suitable for diffraction. Yield: 0.191 g (19%), 96% pure by GC-MS. Mp (TGA; sublim.): 254 - 256 °C. MS (EI,%): *m/z* 389 (M^+, 46), 374 (M^+ - Me, 100). FTIR (neat, ATR, cm^{-1}): 3133 (w, aromatic ν_{C-H}), 3052 (w, aromatic ν_{C-H}), 3015 (w, aromatic ν_{C-H}), 2988 (w, alkyl ν_{C-H}), 2946 (w, alkyl ν_{C-H}), 2913 (m, alkyl ν_{C-H}), 2853 (w, alkyl ν_{C-H}), 1617 (m), 1595 (s), 1562 (m), 1502 (s, aromatic $\delta_{C=C}$), 1466 - 1384 (s, aromatic $\delta_{C=C}$), 1344 (m), 1327 (s, 3° aromatic ν_{C-N}), 1293 (s), 1267 (m), 1154 (m), 1118 (m), 1009 (w), 950 (w), 825 (s). ^1H NMR (CD_2Cl_2) 8.00 [2H, d, *J*(H-H) = 8.9 Hz, C*H*, 4-quin], 7.74 [2H, ddd, *J*(H-H) = 8.1 Hz, *J*(H-H) = 1.5 Hz, *J*(H-H) = 0.7 Hz, C*H*, 9-quin], 7.69 [2H, ddd, *J*(H-H) = 8.5 Hz, *J*(H-H) = 1.3 Hz, *J*(H-H) = 0.7 Hz, C*H*, 6-quin], 7.58 [2H, ddd, *J*(H-H) = 8.5 Hz, *J*(H-H) = 6.9 Hz, *J*(H-H) = 1.5 Hz, C*H*, 7-quin], 7.39 [2H, ddd, *J*(H-H) = 8.1 Hz, *J*(H-H) = 6.9 Hz, *J*(H-H) = 1.3 Hz, C*H*, 8-quin], 7.30 [2H, d, *J*(H-H) = 8.9 Hz, C*H*, 3-quin], 7.04 (2H, s, *m*-C*H*), 2.39 (3H, s, *p*-CH_3), 2.05 (6H, s, *o*-CH_3). ^{13}C NMR (CD_2Cl_2): δ 155.91,

147.87, 139.23, 138.23, 138.18, 137.41, 130.13, 129.86, 128.15, 127.79, 125.87, 124.85, 116.68, 21.43, 18.75.

2,6-^{i}Pr$_2$Ph-dqa (2.15). 2,6-diisopropyl aniline (2.464 g, 13.9 mmol), sodium *tert*-butoxide (3.340 g, 34.7 mmol), $Pd_2(dba)_3$ (0.191 g, 0.21 mmol), and DPPF (0.231 g, 0.42 mmol) were added to a Schlenk flask in a drybox. The flask was capped with a septum, removed from the drybox, and toluene (200 mL) was added via cannula. The mixture was stirred, and 2-chloroquinoline (5.005 g, 30.5 mmol) was injected via syringe into the reaction vessel. The reaction was stirred under nitrogen at 90 °C for 96 hours. After cooling, $CHCl_3$ (50 mL) was added, the mixture was filtered, and the solvent was removed under vacuum. The crude product was purified by column chromatography on neutral alumina (eluent: 0.75% ethanol in chloroform), followed by recrystallization by a slow evaporation of a solution in Et_2O. Yield: 2.95 g (49%). Mp (TGA; sublim.): 143 - 144 °C. MS (EI,%): *m/z* 431 (M^+, 1.4), 388 (M^+ - ^{i}Pr, 100). FTIR (neat, ATR, cm^{-1}): 3061 (w, aromatic ν_{C-H}), 3041 (w, aromatic ν_{C-H}), 2961 (m, alkyl ν_{C-H}), 2924 (m, alkyl ν_{C-H}), 2866 (m, alkyl ν_{C-H}), 1707 (m), 1618 (m), 1598 (s), 1562 (m), 1502 (s), 1465 - 1321 (s, aromatic $\delta_{C=C}$), 1290 (vs, aromatic $\delta_{C=N}$), 1256 (m), 1182 (m), 1141 (m), 1055 (m), 968 (m), 814 (vs). ^{1}H NMR (d_6-acetone): δ 8.17 [2H, d, *J*(H-H) = 9.0 Hz, C*H*, 4-quin], 7.84 [2H, ddd, *J*(H-H) = 8.0 Hz, *J*(H-H) = 1.4 Hz, *J*(H-H) = 0.7 Hz, C*H*, 9-quin], 7.65 [2H, ddd, *J*(H-H) = 8.4 Hz, *J*(H-H) = 1.5 Hz, *J*(H-H) = 0.7 Hz, C*H*, 6-quin], 7.60 [2H, ddd, *J*(H-H) = 8.4 Hz, *J*(H-H) = 6.6 Hz, *J*(H-H) = 1.4 Hz, C*H*, 7-quin], 7.48 [1H, dd, *J*(H-H) = 8.0 Hz, *J*(H-H) = 8.0 Hz, *p*- C*H*, Ph], 7.42 [2H, d, *J*(H-H) = 9.0 Hz, C*H*, 3-quin], 7.41 [2H, ddd, *J*(H-H) = 8.0 Hz, *J*(H-H) = 6.6 Hz, *J*(H-H) = 1.5 Hz, C*H*, 8-quin], 7.37 [2H, d, *J*(H-H) = 8.0 Hz, *m*- C*H*, Ph], 3.24 [2H, sept, *J*(H-H) = 6.9 Hz, -C*H*$(CH_3)_2$], 0.97 [12H, d, *J*(H-H) = 6.9 Hz, -CH(C*H*$_3)_2$]. ^{13}C NMR (d_6-acetone): δ 159.6, 157.0, 149.0, 148.1, 137.7, 130.3, 129.9, 128.5, 128.4, 126.3, 125.4, 125.3, 117.4, 30.7, 24.1.

Quinolin-1-(2-quinolyl)-2-one mesitylimine (2.16). In a drybox, potassium *tert*-butoxide (785 mg, 7.0 mmol), allyl[1,3-*bis*(2,6-diisopropylphenyl)imidazol-2-ylidene]palladium(II) chloride (70 mg, 0.12 mmol), and 2-chloroquinoline (818 mg, 5.0 mmol) were added to a Schlenk flask. To this was added toluene (10 mL) followed by 2,4,6-trimethylaniline (338 mg, 2.5 mmol). The reaction was stirred under nitrogen at 70 °C for 120 h. After cooling, Et_2O (25 mL) was added to the reaction mixture and then washed twice with brine. The organic phase was dried over sodium sulfate before removing solvent in vacuo. The crude product was purified by flash chromatography on silica gel (eluent: 10% ethyl acetate in hexanes). The product was dissolved in hot hexanes and allowed to cool to room temperature. Subsequent cooling to –12 °C over several days resulted in the formation of crystals suitable for X-ray analysis. Yield 0.276 g (28% isolated). FTIR (ATR, cm^{-1}): 3058 (w, aromatic ν_{C-H}), 3003 (w, aromatic ν_{C-H}), 2971 (w, alkene ν_{C-H}), 2935 (w, alkene ν_{C-H}), 2912 (w, alkyl ν_{C-H}), 2851 (w, alkyl ν_{C-H}), 1631 (m, $\nu_{C=N}$), 1591 - 1425 (s, aromatic $\delta_{C=C}$ and $\delta_{C=N}$), 1327 (s, ν_{C-N}), 1214 (s), 1147 (s), 820 (s). ^1H NMR (298 K; CD_3OD): δ□ 8.68 [1H, d, J(H-H) = 8.5 Hz, CH], 8.10 [2H, d, J(H-H) = 8.5 Hz, CH], 7.86 [1H, dd, J(H-H) = 7.0 Hz, J(H-H) = 1.4 Hz, CH], 7.73 [1H, dd, J(H-H) = 7.0 Hz, J(H-H) = 1.4 Hz, CH], 7.66 [1H, d, J(H-H) = 8.5 Hz, CH], 7.52 [1H, d, J(H-H) = 8.5 Hz, CH], 7.48 [1H, d, J(H-H) = 9.8 Hz, CH], 7.24 [1H, t, J(H-H) = 7.6 Hz, CH], 7.10 [1H, t, J(H-H) = 7.6 Hz, CH], 6.80 (2H, s, m-CH), 6.28 [1H, d, J(H-H) = 8.4 Hz, CH], 6.19 [1H, d, J(H-H) = 9.8 Hz, CH], 2.20 (3H, s, p-CH_3), 2.02 (6H, s, o-CH_3). ^{13}C NMR (298 K; CD_3OD): δ 154.11, 150.71, 149.59, 142.86, 142.23, 137.98, 131.94, 131.75, 130.71, 130.61, 129.93, 129.87, 129.74, 129.46, 129.36, 129.12, 123.97, 123.12, 121.87, 116.98, 116.55, 115.43, 21.00 (1C, *p*-CH_3), 18.54 (2C, *o*-CH_3).

Computational Methods. Geometry optimization on Pd(L)[N(Ar)quin](quin) (Ar = Ph, Mes, 2,6-$^i Pr_2Ph$) was carried out at the Hartree-Fock level with the 3-21G basis set.[28] The calculated $N_{(amine)}\cdots C_{(quin)}$ and $N_{(quin)}\cdots C_{(quin)}$ intramolecular distances for anti

and syn conformations of Pd(L)[N(Ar)quin](quin) at the RHF/3-21G level are given in Table 2.7. All electron molecular orbital (MO) calculations were performed using the Gaussian 03, revision D.01 (Windows version), suite of programs.[42] Input files were prepared using MOPAC[29] semi-empirical energy minimizations.

Crystallographic Study. General details of X-ray data collection are given in chapter 1. All hydrogen atoms, with the exceptions noted for the amine H atoms in **2.3** and **2.10**, were placed in calculated positions [C-H (methine) = 0.98 Å, C-H (methylene) = 0.97 Å, C-H (methyl) = 0.96 Å, and C-H (aromatic) = 0.93 Å] and refined using a riding model with fixed isotropic displacement parameters. The amine hydrogen atoms in **2.3** and **2.10** were located through the difference map and refined freely. Selected bond lengths and angles are given in Tables 2.1 - 2.6. Refinement of noncentrosymmetric structures **2.5** ($P2_12_12_1$), **2.6** ($P2_1$), and **2.7** ($Pna2_1$) was performed according to previously established methods,[30,31] using TWIN/BASF instructions, and merging Friedel pairs (no atoms with Z > Si).

Compounds **2.6** - **2.8**, **2.11**, and **2.13** were each found to crystallize with two unique conformers in the asymmetric unit. Structure solution and refinement for compound **2.6** was performed in the asymmetric space group monoclinic $P2_1$, with TWIN/BASF instructions. Friedel pairs were merged (MERG 4) for refinement. Molecule 2 of the asymmetric unit is shown in Figure 2.10, and a comparison of the two comformers are shown in Figure 2.11.

One of the conformers in compound **2.7** refined with a site occupancy disorder of the isopropyl methyl groups. The disordered methyl carbon atoms were given different PART numbers, and use of the FVAR instruction refined the s.o.f. for each PART to be 50:50. Unless otherwise noted, for each compound having a disorder present, the site occupancies were determined using the free variable (FVAR) command for the different parts. Initial refinement cycles were performed with fixed-distance restraints (DFIX 1.53)

for all C(36)-C(methyl) bond lengths and (DANG 2.48) for corresponding C(methyl)-C(methyl) distances. Methyl hydrogen atoms were placed in idealized positions for a disordered methyl group (HFIX 123). Restraints were lifted for final refinement cycles. Structure solution and refinement was performed in the asymmetric space group orthorhombic $Pna2_1$, with TWIN/BASF instructions. Friedel pairs were merged (MERG 4) for refinement. The disorder in molecule 2 of the asymmetric unit is shown below in Figure 2.12, and a comparison of the two comformers is shown in Figure 2.13. Molecule 2 of the asymmetric unit of compound **2.8** is shown in Figure 2.14, and a comparison of the two comformers are shown in Figure 2.15.

The program PLATON was employed for structure validation,[32] which revealed solvent accessible voids in the crystal lattice of **2.4**. Use of the CALC SQUEEZE function to correct data of residual density in these voids did not result in better agreement amongst data. Consequently, refinement of the disordered toluene solvent molecule present in the asymmetric unit of compound **2.4** was performed in a consistent manner with established methods.[33] The free variable (FVAR) instruction led to refinement of 50:50 site occupancies of carbon atoms in each part (see Figure 2.32). Similar distance restraints (SADI) were placed on all aromatic C-C distances, *para*- C-C distances [i.e., C(1)-C(4)], as well as equivalent C(methyl)-C(aromatic) distances. In addition, similar ADP restraints (SIMU) and rigid bond restraints (DELU) were used for all C atoms.

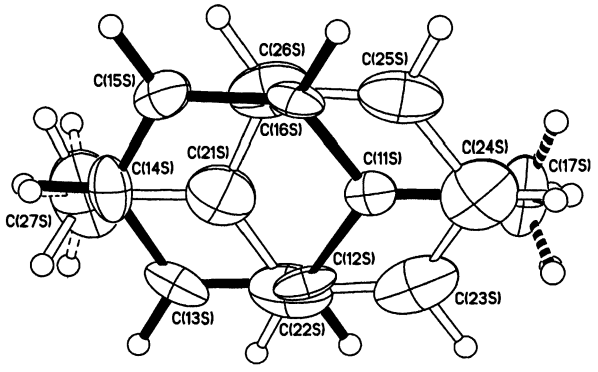

Figure 2.32. Disordered toluene solvent molecule present in unit cell of compound **2.4.**

Table 2.8. Summary of X-ray diffraction data.

Compound	**2.1**	**2.2**	**2.3**
empir. formula	$C_{14}H_{16}N_2$	$C_{15}H_{18}N_2$	$C_{14}H_{16}N_2$
M_W	212.29	226.31	212.29
cryst. system	monoclinic	monoclinic	monoclinic
space group	$P2_1/c$	$P2_1/n$	$P2_1/n$
a, Å	14.047(3)	13.035(3)	10.327(2)
b, Å	7.154(1)	8.120(1)	10.601(2)
c, Å	13.890(3)	13.562(3)	12.450(3)
α, deg.	-	-	-
β, deg.	116.45(3)	111.87(3)	112.81(3)
γ, deg.	-	-	-
V, $Å^3$	1249.7(4)	1345.2(5)	1256.5(5)
Z	4	4	4
D_{calc}, g/cm^3	1.128	1.117	1.122
μ, mm^{-1}	0.067	0.066	0.067
2θ range, deg.	3.24 – 56.64	5.48 - 56.66	4.38 – 56.58
No. collected	14657	15889	15089
No. ind. (R_{int})	3040 (0.0575)	3258 (0.0674)	3042 (0.0369)
No. obsd. ($\|F_o\| > 4.0\sigma \|F_o\|$)	1667	973	1876
R	0.0547	0.0669	0.0480
R_w	0.1397	0.1512	0.1180
$\Delta\rho_{max/min}$ ($eÅ^{-3}$)	0.297, -0.198	0.306, -0.163	0.134, -0.151
weights	0.0824, 0.1579	0.0444, 0.6430	0.0615, 0.2646
CCDC Dep. No.	697653	697654	720342

Table 2.8. contd.

Compound	**2.4**	**2.5**	**2.6**
empir. formula	$C_{55}H_{48}N_4$	$C_{19}H_{19}N_3$	$C_{20}H_{21}N_3$
M_W	764.97	289.37	303.40
cryst. system	monoclinic	orthorhombic	monoclinic
space group	$P2_1/c$	$P2_12_12_1$	$P2_1$
a, Å	26.729(5)	7.264(1)	8.546(1)
b, Å	17.008(3)	13.053(3)	17.299(4)
c, Å	18.903(4)	17.072(3)	11.402(2)
α, deg.	-	-	-
β, deg.	92.42(3)	-	92.17(3)
γ, deg.	-	-	-
V, $Å^3$	8586(3)	1618.7(6)	1684.4(6)
Z	8	4	4
D_{calc}, g/cm^3	1.184	1.187	1.196
μ, mm^{-1}	0.069	0.071	0.072
2θ range, deg.	2.84 - 56.62	3.92 - 56.82	3.58 - 56.62
No. collected	104767	19614	20430
No. ind. (R_{int})	20901 (0.2699)	2274 (0.0694)	4213 (0.0705)
No. obsd. ($\|F_o\| > 4.0\sigma \|F_o\|$)	4831	1323	1901
R	0.0911	0.0444	0.0491
R_w	0.163	0.1112	0.11181
$\Delta\rho_{max/min}$ ($eÅ^{-3}$)	0.209, -0.319	0.136, -0.141	0.246, -0.159
weights	0.0989, 0	0.0703, 0.0731	0.0827, 0
CCDC Dep. No.	697655	720335	720338

Table 2.8. contd.

Compound	**2.7**	**2.8**	**2.9**
empir. formula	$C_{19}H_{19}N_3$	$C_{22}H_{25}N_3$	$C_{20}H_{15}N_3$
M_W	289.37	331.45	297.35
cryst. system	orthorhombic	triclinic	monoclinic
space group	$Pna2_1$	$P\bar{1}$	$P2_1/c$
a, Å	14.616(3)	8.366(1)	7.825(1)
b, Å	8.891(1)	14.390(3)	11.121(2)
c, Å	24.367(5)	16.817(3)	17.574(4)
α, deg.	-	100.90(3)	-
β, deg.	-	100.91(3)	92.04(3)
γ, deg.	-	95.05(3)	-
V, $Å^3$	3166(1)	1935.8(7)	1528.4(5)
Z	8	4	4
D_{calc}, g/cm^3	1.214	1.137	1.292
μ, mm^{-1}	0.073	0.068	0.078
2θ range, deg.	3.34 - 56.60	2.52 - 57.00	4.34 - 56.62
No. collected	37351	22485	17948
No. ind. (R_{int})	3996 (0.0626)	9008 (0.0897)	3704 (0.0416)
No. obsd. ($\|F_o\| > 4.0\sigma \|F_o\|$)	2240	2967	2206
R	0.0517	0.0608	0.0417
R_w	0.1225	0.1460	0.0984
$\Delta\rho_{max/min}$ ($eÅ^{-3}$)	0.319, -0.198	0.267, -0.288	0.136, -0.139
weights	0.0868, 0.2396	0.0942, 0	0.0521, 0.2599
CCDC Dep. No.	720339	720340	720337

Table 2.8. contd.

Compound	**2.10**	**2.11**	**2.12**
empir. formula	$C_{14}H_{11}N_3$	$C_{20}H_{15}N_3$	$C_{23}H_{21}N_3$
M_W	221.26	297.35	339.43
cryst. system	monoclinic	monoclinic	monoclinic
space group	$P2_1/c$	$P2_1/n$	$P2_1/c$
a, Å	11.571(2)	8.081(1)	12.359(3)
b, Å	6.116(1)	13.920(3)	12.585(3)
c, Å	15.585(3)	27.697(6)	12.457(3)
α, deg.	-	-	-
β, deg.	90.00(3)	96.50(3)	104.09(3)
γ, deg.	-	-	-
V, $Å^3$	1103.0(4)	3095(1)	1879.4(7)
Z	4	8	4
D_{calc}, g/cm^3	1.332	1.276	1.200
μ, mm^{-1}	0.082	0.077	0.072
2θ range, deg.	3.52 - 56.68	2.96 - 56.66	3.40 - 56.70
No. collected	13045	25441	22633
No. ind. (R_{int})	2664 (0.0571)	7444 (0.0551)	4612 (0.0842)
No. obsd. ($\|F_o\| > 4.0\sigma \|F_o\|$)	1435	3006	1519
R	0.0439	0.0496	0.0709
R_w	0.1056	0.1174	0.1692
$\Delta\rho_{max/min}$ ($eÅ^{-3}$)	0.175, -0.136	0.157, -0.169	0.395, -0.187
weights	0.0615, 0.2129	0.0748, 0	0.0705, 1.1375
CCDC Dep. No.	720334	723245	720336

Table 2.8. contd.

Compound	**2.13**	**2.14**	**2.15**
empir. formula	$C_{26}H_{27}N_3$	$C_{27}H_{23}N_3$	$C_{30}H_{29}N_3$
M_W	381.51	389.48	431.56
cryst. system	monoclinic	monoclinic	monoclinic
space group	$P2_1/c$	$P2_1/c$	$P2_1/c$
a, Å	22.250(4)	14.058(3)	8.614(1)
b, Å	8.628(2)	12.202(2)	16.137(3)
c, Å	23.031(5)	12.831(3)	17.601(4)
α, deg.	-	-	-
β, deg.	98.74(3)	104.61(3)	93.32(3)
γ, deg.	-	-	-
V, $Å^3$	4370(2)	2129.8(8)	2442.5(9)
Z	8	4	4
D_{calc}, g/cm^3	1.16	1.215	1.174
μ, mm^{-1}	0.069	0.072	0.069
2θ range, deg.	1.86 - 58.08	3.00 - 58.14	3.42 - 56.64
No. collected	52928	25579	29249
No. ind. (R_{int})	10869 (0.0484)	5339 (0.0775)	5938 (0.0693)
No. obsd. ($\|F_o\| > 4.0\sigma \|F_o\|$)	6745	2705	2433
R	0.0514	0.0596	0.0544
R_w	0.1323	0.1453	0.1340
$\Delta\rho_{max/min}$ ($eÅ^{-3}$)	0.203, -0.195	0.218, -0.199	0.165, -0.147
weights	0.0771, 0	0.0779, 0.5859	0.0742, 0.3419
CCDC Dep. No.	779677	741964	720341

Table 2.8. contd.

Compound	**2.16**
empir. formula	$C_{27}H_{23}N_3$
M_W	389.48
cryst. system	monoclinic
space group	$P2_1/c$
a, Å	12.609(1)
b, Å	15.010(2)
c, Å	12.456(1)
α, deg.	-
β, deg.	112.679(2)
γ, deg.	-
V, $Å^3$	2175.3(5)
Z	4
D_{calc}, g/cm^3	1.189
μ, mm^{-1}	0.071
2θ range, deg.	3.50 - 54.32
No. collected	26422
No. ind. (R_{int})	5201 (0.1345)
No. obsd. ($\|F_o\| > 4.0\sigma \|F_o\|$)	1095
R	0.0526
R_w	0.1148
$\Delta\rho_{max/min}$ ($eÅ^{-3}$)	0.321, -0.337
weights	0.0887, 0
CCDC Dep. No.	683242

References

1 (a) National Research Council, "Separation and Purification: Critical Needs and Opportunities" National Academy Press, Washington, DC, 1987. (b) J. L. Humphrey, A. F. Seibert and R. A. Koort, *Separation Technologies: Advances and Priorities*, DOE/ID/12920-1, Washington, DC 1001.

2 (a) G. C. Blytas, *Concentrated Cuprous Nitrate/Propionitrile Solutions as Complexing Agents for Olefin Separations*, US Patent Office, Editor. 1974, Shell Oil Company: United States. (b) E. R. Brown and R. L. Hair, *Monoolefin/Paraffin Separation by Selective Absorption*, 1993, Phillips Petroleum Company: United States. (c) J. B. Cooper and K. Small, *Process for Recovering Olefins from Gaseous Mixtures*, 1997, BP Chemicals Limited: United States. (d) J. C. Davis and R. J. Valus, *Removal of Olefins from Fluids*, EP Office, Editor, 1998, BP Chemicals Limited: England. (e) T. W. Evans, B. O. Blackburn, and J. R. Scheibli, *Recovery of Olefins*, US Patent Office, Editor, 1945, Shell Development Company: United States. (f) H. S. Kim, Y. J. Kim, J. J. Kim, S. D. Lee, Y. S. Kang, and C. S. Chin, *Chem. Mater.*, 2001, **13**, 1720. (g) J. F. Knifton, *Process for Separating Liquid Olefin-Paraffin Mixtures*, Texaco Inc., United States, 1979. (h) C. L. Munson, L. C. Boudreau, M. S. Driver, and W. L. Schinski, *Separation of Olefins from Paraffins Using Ionic Liquid Solutions*, US Patent Office, Editor. Chevron U.S.A. Inc., 2002.

3 K. Wang and E. I. Stiefel, *Science*, 2001, **291**, 106.

4 W. A. Braunecker, T. Pintauer, N. V. Tsarevsky, G. Kickelbick, and K. Matyjaszewski, *J. Organomet. Chem.,* 2005, **690**, 916.

5 X. Dai and T. H. Warren, *Chem. Comm.,* 2001, 1998.

6 B. F. Straub, F. Eisentrager, and P. Hofmann, *Chem. Comm.,* 1999, 2507.

7 A. Boni, G. Pampaloni, R. Peloso, D. Belleti, C. Graiff, and A. Tiripicchio, *J. Organomet. Chem.,* 2006, **691**, 5602.

8 J. S. Thompson and J. F. Whitney, *Inorg. Chem.,* 1984, **23**, 2813.

9 J. S. Thompson, J. C. Calabrese, and J. F. Whitney, *Acta Cryst.,* 1985, **C41**, 890.

10 (a) J. Zhang, R.-G. Xiong, J.-L. Zuo, and X.-Z. You, *Chem. Commun.*, 2000, 1495; (b) J. Zhang, R.-G. Xiong, J.-L. Zuo, C.-M. Che and X.-Z. You, *J. Chem. Soc., Dalton Trans.*, 2000, 2898.

11 M. Munakata, S. Kitagawa, S. Kosome, and A. Asahara, *Inorg. Chem.,* 1986, **25**, 2622.

12 (a) A. E. Martelli, R. D. Hancock, and R. J. Motekaitis, *Coord. Chem. Rev.*, 1994, **133**, 39. (b) Z. Jin, L-L. Qiu, Y-Q. Li, H-B. Song, and J-X. Fang, *Organometallics*, 2010, **29**, 6578.

13 J. P. Wolfe, S. Wagaw, J.-F. Marcoux, and S. L. Buchwald, *Acc. Chem. Res.* 1998, **31**, 805.

14 J. F. Hartwig, *Angew. Chem., Int. Ed.* 1998, **37**, 2046.

15 (a) M. Polamo and M. Hamalainen, *Z. Kristallogr.-New Cryst. Struct.*, 2002, **217**, 563. (b) M. Polamo, M. Talja, and A. J. Piironen, *Z. Kristallogr.-New Cryst. Struct.*, 2005, **220**, 41. (c) M. Polamo and M. Talja, *Z. Kristallogr.-New Cryst. Struct.*, 2004, **219**, 67. (d) M. Polamo and M. Talja, *Z. Kristallogr.-New Cryst. Struct.*, 2004, **219**, 69. (e) M. Polamo, T. Repo, and M. Leskela, *Acta Chem. Scand.*, 1997, **51**, 325.

16 H. Schodel, C. Nather, H. Bock, and F. Butenschon, *Acta Cryst.*, 1996, **B52**, 842.

17 Y. Fang, C. Huang, Z. Zhu, X. Yu, and W. You, *Acta Cryst.* 2006, **E62**, m3347-m3348.

18 J.-S. Yang, Y.-D. Lin, Y.-H. Lin, and F.-L. Liao, *J. Org. Chem.*, 2004, **69**, 3517.

19 C. Sumby and P. Steel, *Inorg. Chim. Acta.*, 2007, **360**, 2100.

20 I. N. Polyakova, Z. A. Starikova, B. V. Parusnikov, and I. A. Krasavin, *Kristallografiya*. 1985, **30**, 1010.

21 I. N. Polyakova, Z. A. Starikova, V. K. Trunov, B. V. Parusnikov, and I. A. Krasavin, *Kristallografiya.*, 1980, **25**, 495.

22 J. F. Hartwig, *Angew. Chem., Int. Ed.*, 1998, **37**, 2046.

23 Polyakova, I. N.; Starikova, Z. A.; Trunov, V. K.; Parusnikov, B. V.; Krasavin, I. A. *Kristallografiya.* 1980, **25**, 501.

24 CRC Handbook of Chemistry and Physics. 60th Ed. CRC Press, Inc. Boca Raton, FL, (1980), D-194.

25 J. J. Allen, C. E. Hamilton, and A. R. Barron, *J. Chem. Cryst.*, 2008, **38**, 873.

26 J. Keijsper, H. Van Der Poel, L. H. Polm, G. Van Koten, K. Vrieze, P. Seignette, R. Varenhorst, and C. Stam, *Polyhedron* 1983, **2**, 1111.

27 P. A. Zunszain, M. M. Shah, Z. Miscony, M. Javadzadeh-Tabatabaie, D. G. Haylett, and C. R. Ganellin, *Arch. Pharm. Pharm. Med. Chem.* 2002, **4**, 159.

28 J. S. Binkley, J. A. Pople, and W. J. Hehre, *J. Am. Chem Soc.* 1980, **102**, 939.

29 *CS MOPAC Pro. v6.0*, 2000, CambridgeSoft Corporation: Cambridge, MA.

30 H. D. Flack and G. J. Bernardinelli, *Appl. Cryst.*, 2000, **33**, 1143.

31 W. Clegg, *Acta Cryst.*, 2003, **E59**, e2.

32 (a) A. L. Spek, *PLATON, Molecular Geometry Program*, 2008, Utrecht, The Netherlands. (b) A. L. Spek, *J. Appl. Cryst.*, 2003, **36**, 7-13.

33 (a) W. Clegg, *Crystal Structure Determination*, Oxford University Press, NY, 1998, 70-72. (b) G. Pampaloni, R. Peloso, C. Graiff, and A. Tripicchio, *Dalton Trans.* 2006, 3576. (c) G. Pampaloni, R. Peloso, C. Graiff, and A. Tripicchio, *Organometallics*, 2005, **24**, 4475. (d) P. Müller, *Crystal Structure Refinement, A Crystallographer's Guide to SHELXL*, Oxford University Press, UK, (2006).

Chapter 3

Structural Characterization of Complexes Incorporating New Ligands

Introduction

Based upon the structural trends of the Ar-dpa, Ar-pqa, and Ar-dqa compounds **2.5 – 2.15** from the previous chapter, it is clear that the steric bulk of the aryl substituents has a controlling influence on the orientation of the pyridyl rings. In the free compounds this influence results in the twisting of the pyridyl rings with regard to each other, and their splaying out [i.e., increased C(1)-N(1)-C(6) angle] to relieve the steric strain imposed by the aryl's *ortho*-substituents. However, in a coordination complex the pyridyl nitrogen atoms are held by the geometry of the complex, and thus a different distortion will be required to release the steric strain. Previous studies concerned with protonated H-dpa salts have demonstrated the confinement of the orientation of the pyridyl rings to be more or less coplanar. In order to ascertain the geometric effects of the aryl substituents in a simple complex we have structurally characterized the protonated derivatives.

While a number of complexes incorporating deprotonated N-(2-pyridyl)amines have been reported,[1] the scarcity of complexes having neutral N-pyridylamine ligands prompted the structural characterization of the copper(I) complex $[Cu\{MesN(H)py\}_2]BF_4$. There have been very few di-quinolyl amines reported or structurally characterized. Schareina, *et al.*, have reported the methyl substituted derivative, $(2,6\text{-}^{i}Pr_2Ph)N[2\text{-}(4\text{-}Me)quin]_2$ as well as its nickel dibromide complex,[2] while Polyakova, *et al.*, have reported the X-ray structure of the hydroxylated derivative, $MeN[2\text{-}(9\text{-}OH)quin]_2$.[3]

The presence of *ortho*-substitution in the complexed Ar-dpa compounds, in which the two pyridyl rings are constrained by a complexed atom, results in the bending-up of the aryl ring substituent out of the di-pyridyl plane with consequential folding of the two pyridyl into a "butterfly" conformation. In order to ascertain whether these distortions

translate to metal derivatives we have structurally characterized simple dimeric copper(II) complexes of Ar-dpa, and Ar-pqa, as well as two different solvates of $[Cu\{Ar\text{-}dqa\}_2]BF_4$.

Results and Discussion

Planar Ar-dpa Acid Salts. Protonation of $ArN(py)_2$ (and the quinolyl analogs) can be accomplished by the reaction KBF_4 dissolved in dilute HCl (Experimental).[17] The molecular structures of compounds $[H(Mes\text{-}dpa)]BF_4$ (**3.1**), $[H(2\text{-}^iPrC_6H_4\text{-}dpa)]BF_4$ (**3.2**), $[H(Ph\text{-}pqa)]BF_4$ (**3.3**), $[H(Mes\text{-}pqa)]BF_4$ (**3.4**), and $[H(2,6\text{-}^iPr_2C_6H_3\text{-}dqa)]BF_4$ (**3.5**), which are the HBF_4 salts of compounds **2.5**, **2.7**, **2.11**, **2.12**, and **2.15**, respectively, are shown in Figure 3.1 - 3.5. Selected bond lengths and angles are given in Table 3.1.

Table 3.1. Selected bond lengths (Å) and angles (°) for HBF_4 salts, **3.1** - **3.5**.

	3.1	**3.2**	**3.3**	**3.4**	**3.5**
N(1)-C(1)	1.394(3)	1.382(3)	1.419(3)	1.423(4)	1.413(4)
N(1)-C(6)	1.417(3)	1.403(3)	1.379(3)	1.377(3)	1.391(3)
N(1)-C(11)	1.453(3)	1.449(3)	1.452(3)	1.451(3)	1.452(3)
N(2)···H	1.04(3)	1.18(3)	1.77(3)	1.80(3)	1.70(4)
N(3)···H	1.61(3)	1.51(3)	0.96(3)	0.92(3)	1.01(4)
F···H	2.40(3)	2.28(3)	2.68(3)	2.58(3)	2.91(4)
C(1)-N(1)-C(6)	124.6(1)	125.4(2)	125.8(2)	125.8(2)	125.1(3)
C(1)-N(1)-C(11)	117.1(1)	116.9(2)	116.3(1)	115.7(2)	118.3(2)
C(6)-N(1)-C(11)	118.1(1)	117.7(2)	117.4(1)	118.6(2)	116.3(2)
$\Delta MPLN_{[py\text{-}py']}$	5.0(1)	1.7(1)	8.3(2)	4.0(1)	3.7(2)
$\Delta MPLN_{[py\text{-}Ar]}$	83.3(1)	89.5(1)	87.7(2)	88.0(1)	89.4(2)
$\Delta MPLN_{[py'\text{-}Ar]}$	81.3(1)	89.4(1)	87.3(2)	89.09(8)	86.4(2)

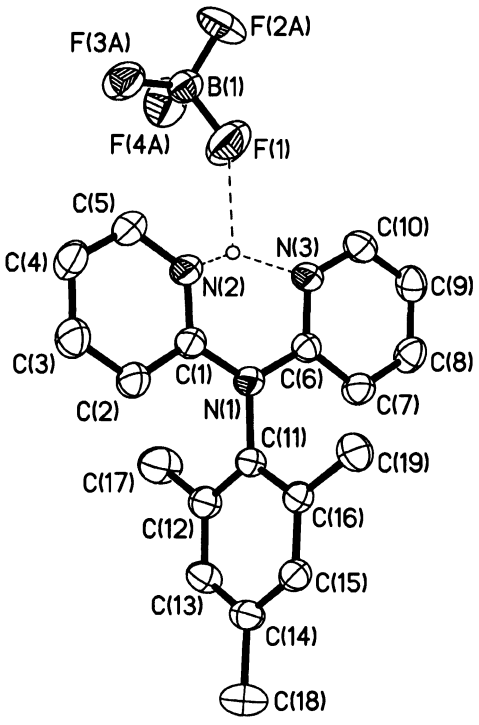

Figure 3.1. Molecular structure of [H(Mes-dpa)]BF_4 (**3.1**). Thermal ellipsoids are shown at the 30% level, and hydrogen atoms attached to carbon are omitted for clarity.

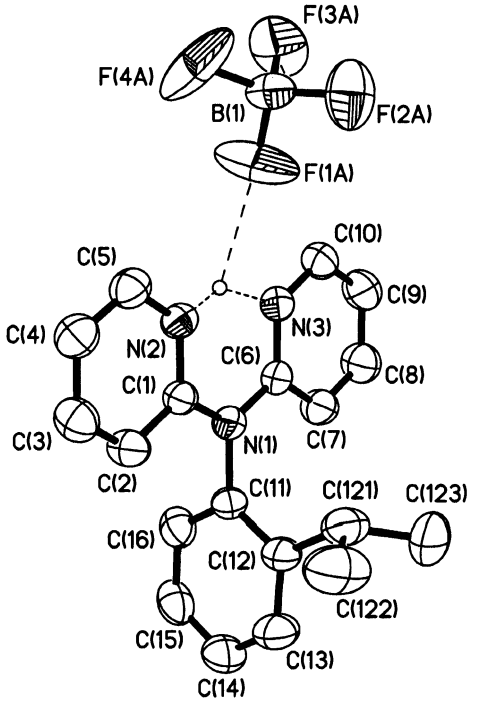

Figure 3.2. Molecular structure of [H(2-^{i}PrPh-dpa)]BF_4 (**3.2**). Thermal ellipsoids are shown at the 30% level, and hydrogen atoms attached to carbon are omitted for clarity.

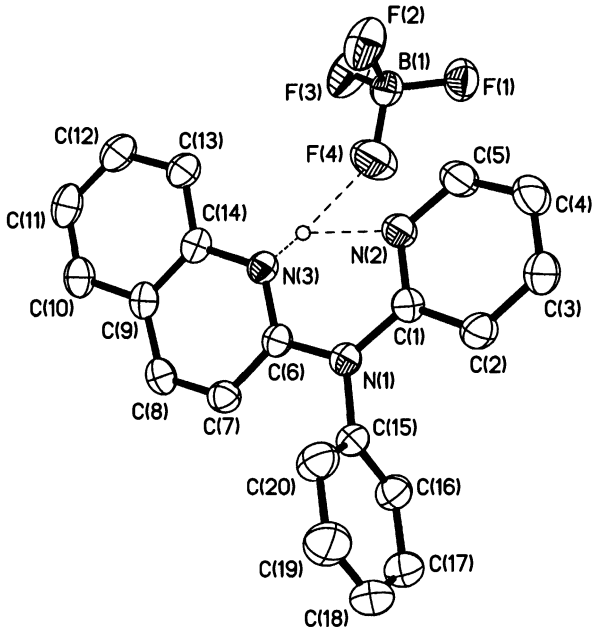

Figure 3.3. Molecular structure of [H(Ph-pqa)]BF_4 (**3.3**). Thermal ellipsoids are shown at the 30% level, and all hydrogen atoms attached to carbon are omitted for clarity.

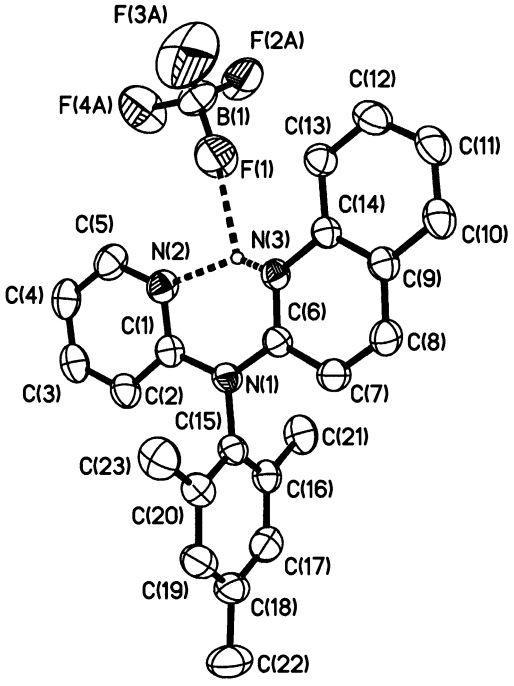

Figure 3.4. Molecular structure of [H(Mes-pqa)]BF_4 (**3.4**). Thermal ellipsoids are shown at the 30% level, and all hydrogen atoms attached to carbon are omitted for clarity.

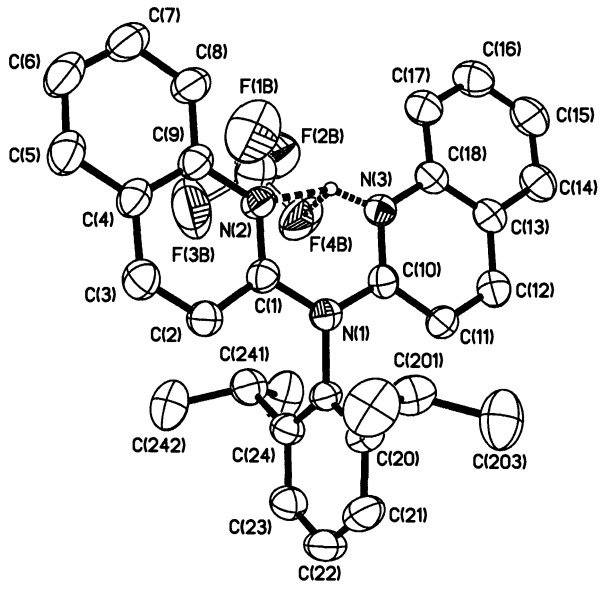

Figure 3.5. Molecular structure of [H(2,6-^{i}Pr$_2$Ph-dqa)}]BF_4 (**3.5**). Thermal ellipsoids are shown at the 30% level, and all hydrogen atoms attached to carbon are omitted for clarity.

The pyridyl nitrogen atoms in compounds **3.1** - **3.5** are found to coordinate their respective protons in an asymmetric fashion (Table 3.1). This degree of asymmetry is not observed in the structurally similar $HClO_4$ and HBr salts [1.362(6) and 1.362(6) Å; 1.33 and 1.40 Å],[4] or the [(H-dpa)H]$CoCl_4$ complex [1.33(3) and 1.36(3) Å].[5] The asymmetry is more pronounced for the mesityl derivative (**3.1**) than the 2-^{i}PrPh compound (**3.2**). The acid proton in compounds 3.3 and 3.4, not surprisingly, are chelated with an even higher degree of asymmetry between the pyridyl and quinolyl heterocycles, with a range of 0.92(3) - 1.18(3)° for the shorter interaction, and a range of 1.51(3) - 1.80(3)° for the longer interaction.

The N-C distances about the amine nitrogen in compounds **3.1** - **3.5** are reasonably similar to those observed in the free ligands, having slightly greater differences in magnitude than in the corresponding free ligands (see Table 3.1 and Chapter 2, Table 2.4), which feature nearly equal bond lengths to both heterocycles.

Consideration of the ΔMPLN between pyridyl rings [1.7(1) - 8.3(2)°], and the N-C_{py}···C_{py}-N torsion angle across the amine-bound carbons [1.3(2) - 5.2(2)°], reveals that, in contrast to the free ligands, the two heterocycles are nearly coplanar in these complexes. A consequence of this forced co-planarity of the two heterocycles is a bending-up of the aryl group out of the *bis*(heterocycle) plane. The observed bending of the aryl group is found to be slightly greater for the mesityl derivative [8.0(8)° versus 4.9(6)°]. Furthermore, the chelation of the proton in compound 3.5 is also seen to be asymmetric, with a magnitude intermediate between those in the dipyridyl complexes, and those in the pyridyl-quinolyl complexes. This is consistent with the protonation of one of the pyridyl or quinolyl heterocycles rather than a symmetric, equal sharing of the proton.

The protons also appear to be loosely associated with the BF_4^- anions [H···F = 2.88(4) and 2.58(3) Å]. The longer H···F distance and smaller N-H···F angle (from the shorter N-H interaction) in **3.5** [115(3)°] are indicative of a weaker H-bonding interaction than observed in **3.4** [N-H···F = 134(2)°]. This is to be expected, as the greater steric occupation of a second quinolyl group prevents the anion from approaching from the side, as seen in the case of **3.4**, where the anion occupies a pocket on the pyridyl side of the molecule.

As a result of the bidentate, albeit asymmetric, coordination, the two heterocycles are forced to adopt a nearly coplanar geometry [$\Delta MPLN_{[py/quin\text{-}quin]}$ = 3.7(2)° and 4.0(1)°$N_{py/quin}$-$C_{py/quin}$···C_{py}-N_{py} = 1.8(2) and 3.2(2)° respectively], which is clearly unfavorable sterically, considering the ΔMPLN values in the free ligands (see above). The N_a-$C_{quin/py}$ and N_a-C_{quin} distances in both compounds exhibit larger asymmetry [1.413(4) and 1.391(3) Å in **3.5**; 1.423(4) and 1.377(3) Å in **3.4**] compared to the analogous free ligands, each of which feature nearly identical bond lengths to both heterocyclic carbon atoms [1.400(2) and 1.410(2) Å in 2,6-^{i}Pr$_2$Ph-dqa; 1.400(4) and 1.406(4) Å in MesN(py)quin].

Crystal packing diagrams of compound **3.5** show π-π stacking between the quinolyl rings (Figure 3.6), with the distance and mean-plane-angle difference of 3.572(1) Å and 4.0(1)° between ring halves. The distance is within the sum of the van der Waals' half-thickness for an aromatic nucleus (3.70 Å).[30] Similarly, crystal packing in **3.3** shows a stacking interaction between quinolyl rings [3.638(2) Å; 0°].

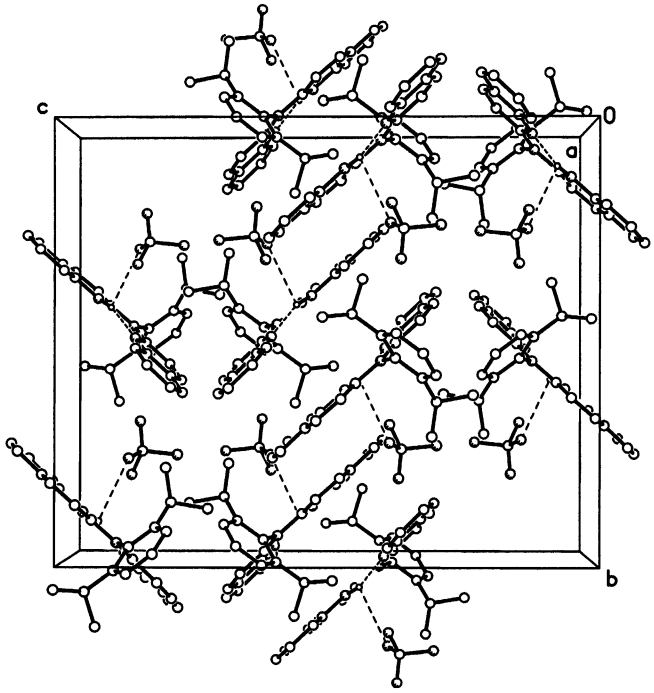

Figure 3.6. Crystal packing diagram of [H(2,6-^{i}Pr$_2$Ph)dqa}]BF_4 (**3.5**) (viewed along the *c*-axis), highlighting π···π stacking between heterocycles of adjacent molecules, in addition to the weak interaction between the pyridyl bound H atom and the BF_4^- anion.

Each of the acid salts was found to exhibit some degree of H-bonding with the anions. Not surprisingly, the H···F distance and N-H···F angle (from the shorter N-H interaction) in **3.5** [2.68(3) Å, 119(2)°] are consistent with a weaker interaction than observed in the less sterically hindered Ar-pqa analogs, which are weaker still with espect to their Ar-dpa counterparts. This is to be expected by the increased steric bulk of the quinolyl ring over that of the pyridyl group.

The N-Mesityl-N-(2-pyridyl)amine Copper(I) Complex. The structure of the cation **3.6** (Figure 3.7) is that of an electron deficient monomer with the copper adopting a two-coordinate geometry (c.f., $CuCl_2^-$), distorted from ideal linear [N(2)-Cu(1)-N(4) = 168.7(1)°]. This observed monodentate coordination through the pyridyl nitrogens is similar to that reported for the dichloro*bis*{2-[(triphenylmethyl)amino]pyridyl}cobalt(II) complex.[6] In contrast, the deprotonated aminopyridinato complexes have been shown to coordinate in a bidentate fashion.[1]

If long range interactions (i.e. not resulting in formal covalent bonds with the copper center) are taken into consideration, the geometry about the metal becomes trigonal bipyramidal. This results from the two pyridyl nitrogen atoms taking the two axial positions, with equatorial positions occupied by the ring center of gravity ($C_{g,i}$) for each mesityl ring [$Cu(1)\cdots C_{g,Mes1}$ = 3.081(5) Å; $Cu(1)\cdots C_{g,Mes2}$ = 3.259(5) Å], and finally, one of the fluorine atoms from the anion [Cu(1)···F(3)' = 3.662(5) Å]. The angles between equatorial positions are slightly distorted $Cg_{[Mes1]}\cdots Cu\cdots Cg_{[Mes2]}$ = 122.3°, $Cg_{[Mes1]}\cdots Cu\cdots F(3')$ = 135.7°, and $Cg_{[Mes2]}\cdots Cu\cdots F(3')$ = 101.7°, but are close enough to be consider the overall structure as pseudo-trigonal bipyramidal.

A consideration of the crystal packing diagram of compound **3.6** suggests that the orientation of the mesityl groups (and hence the N-Cu-N geometry) to be a function of the inter-cation packing. The cations stack in columns along the *a*-axis (Figure 3.9). Each cation is hydrogen bonded (N-H···F) to a BF_4^- anion, which is in turn positioned between two cations in an adjacent column.

This hydrogen bonding is evident comparing the FTIR spectra obtained for the complex and the dimeric MesN(H)py ligand. The N-H stretching and bending frequencies in the complex (3341 and 1620 cm^{-1}) are shifted to higher wavenumbers relative to those of the dimer (3190 and 1590 cm^{-1}), which is consistent with a weaker N-H···F hydrogen bond (in compound **3.6**) versus the N-H···N interactions seen in free compounds RN(H)py (**2.1** - **2.4**).

Table 3.2. Selected bond lengths (Å) and angles (°) for compound **3.6**.

Cu(1)-N(2)	1.909(3)	Cu(1)-N(4)	1.913(2)
N(1)-C(1)	1.342(4)	N(3)-C(15)	1.364(4)
N(1)-C(6)	1.423(4)	N(3)-C(20)	1.423(4)
N(2)-C(1)	1.346(4)	N(4)-C(15)	1.347(4)
C(1)-N(1)-C(6)	126.8(3)	C(15)-N(3)-C(20)	127.2(2)
N(1)-C(1)-N(2)	119.9(3)	N(3)-C(15)-N(4)	119.4(3)
N(2)-Cu(1)-N(4)	168.7(1)		
N(2)-C(1)-N(1)-C(6)	3.2(5)	N(4)-C(15)-N(3)-C(20)	10.4(5)
C(1)-N(1)-C(6)-C(11)	103.4(4)	C(15)-N(3)-C(20)-C(25)	122.6(4)

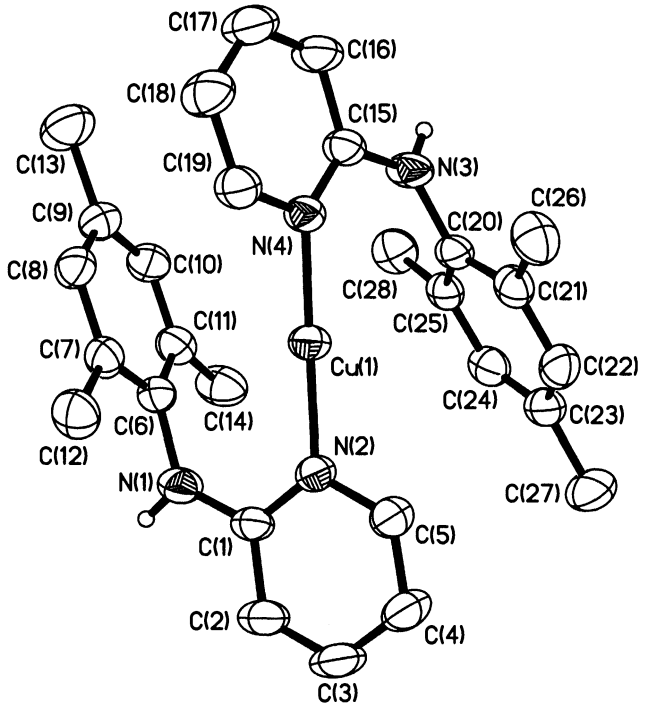

Figure 3.7. Structure of the $[Cu\{MesN(H)py\}_2]^+$ cation in (**3.6**). Thermal ellipsoids are shown at the 30% level, and hydrogen atoms attached to carbon are omitted for clarity.

The Cu-N distances [1.909(3) and 1.913(2) Å] and the N-Cu-N angle [168.7(1)°] are similar to those previously reported for the two-coordinate Cu(I) complexes of 2-(4'-aminophthalimidoethyl)pyridine [Cu-N = 1.891(4) Å, N-Cu-N = 176.8(1)°],[7] 1,3,5-trimethylpyrazole [Cu-N = 1.878(3) Å and 1.863(4) Å, N-Cu-N = 173.8(2)°] [8], and 1,2-dimethylimidazole [Cu-N = 1.865(8) Å, N-Cu-N = 179.2(7)°] [9]. The N-C distances within the $(MesC_6H_2)N(H)py$ ligand remain unchanged upon coordination. However, the C-N-C angle at the amine nitrogen is opened up upon coordination, presumably to relieve intra-complex steric strain.

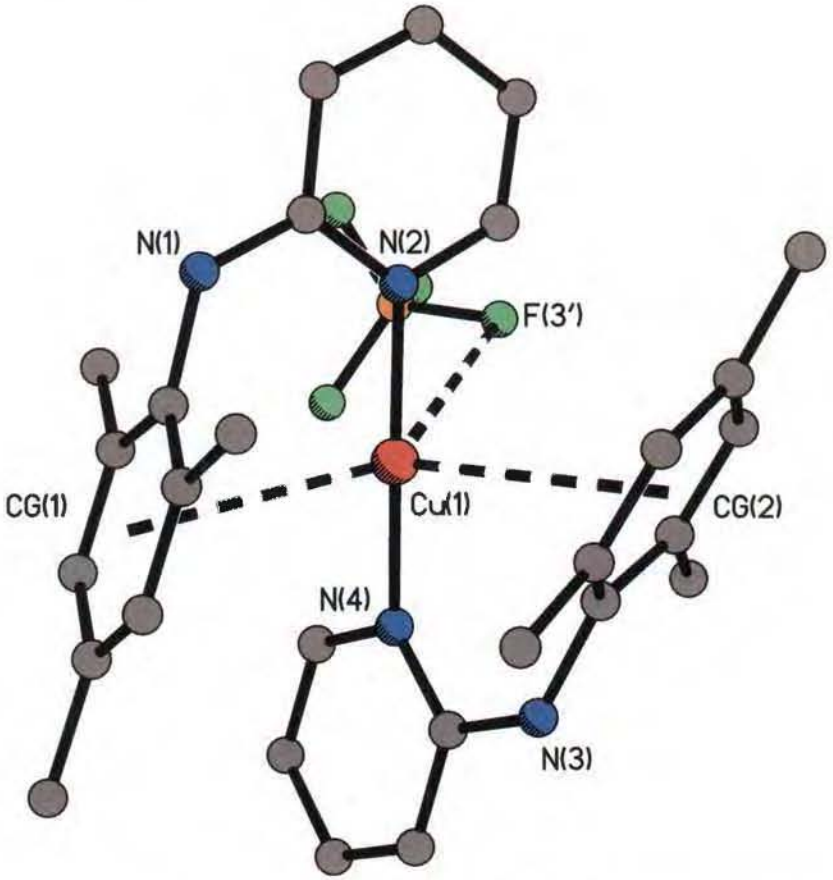

Figure 3.8. Geometry about the copper center in **3.6**, including contacts to the metal center outside of expected covalent bonding distances.

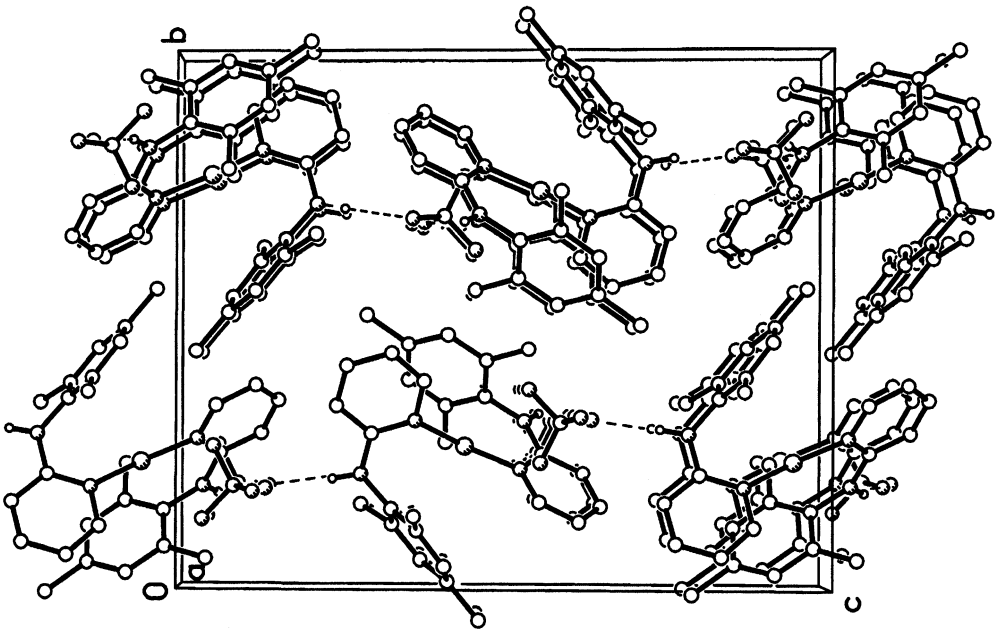

Figure 3.9. Molecular packing diagram of $[Cu\{MesN(H)py\}_2]BF_4$ (**3.6**) viewed along the *a*-axis. Hydrogen atoms attached to carbon are omitted for clarity.

Copper(II) complexes of Ar-dpa. The copper complexes $[Cu(Ph\text{-}dpa)(Cl)(\mu\text{-}Cl)]_2$ (**3.7**), $[Cu(2\text{-}iPrPh\text{-}dpa)(Cl)(\mu\text{-}Cl)]_2$ (**3.8**), $[Cu(Nap\text{-}dpa)(Cl)(\mu\text{-}Cl)]_2 \cdot (MeOH)_2$ (**3.9**), and $Cu[PhN(py)quin]Cl_2$ (**3.10**) are prepared by the reaction of $[Cu(MeCN)_4]BF_4$ with the appropriate Ar-dpa in tetraethylelene glycol in the presence of dilute HCl. If the reaction is carried out using Mes-dpa (compound **2.5**) in the presence of water, the structurally related hydroxy derivative, [Cu(Mes-dpa)(H2O)(μ-OH)]2[BF4]2·(MeOH)2, (**3.11**) is isolated. Despite the difference in ligation and charge, compound **3.11** is isolobal with compounds **3.7** – **3.10**. The molecular structures of compounds **3.7** – **3.11** are shown in Figure 3.10 – Figure 3.14; selected bond lengths and angles are given in Table 3.3.

The structure of the cation, $[Cu(Mes\text{-}dpa)(H_2O)(\mu\text{-}OH)]_2^+$, is shown in Figure 3.13, with selected bond lengths and angles given in Table 3.1. Compounds **3.7**, **3.8**, **3.10** and **3.11** all crystallize with only half of the molecule in the asymmetric unit. In each case, the second half of the molecule is symmetry related through an inversion center.

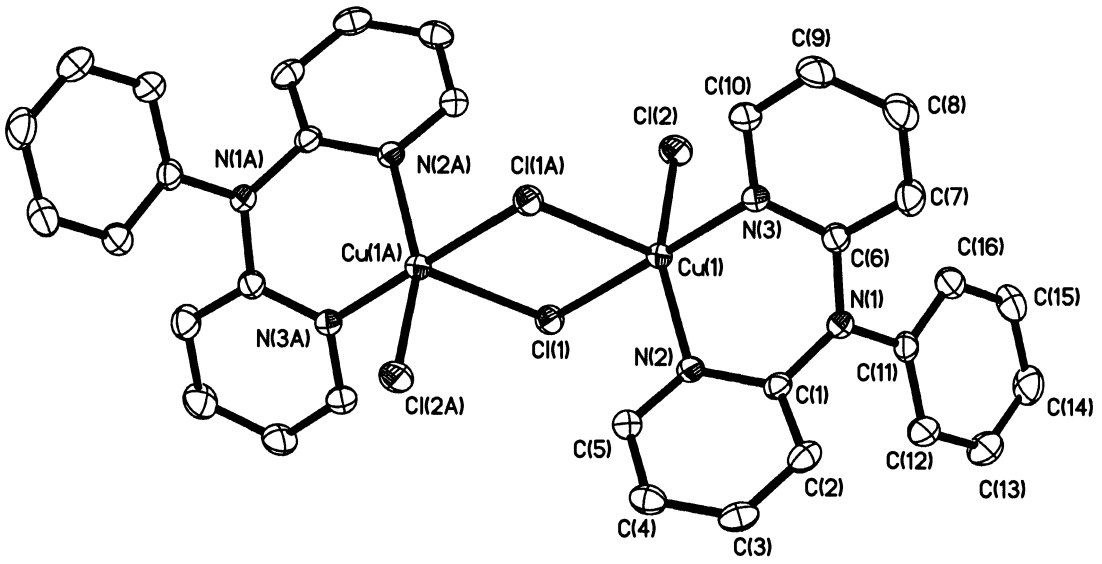

Figure 3.10. Molecular structure of the $[Cu(Ph\text{-}dpa)(Cl)(\mu\text{-}Cl)]_2$ (**3.7**) dimer. Thermal ellipsoids are shown at the 30% level, and all hydrogen atoms are omitted for clarity.

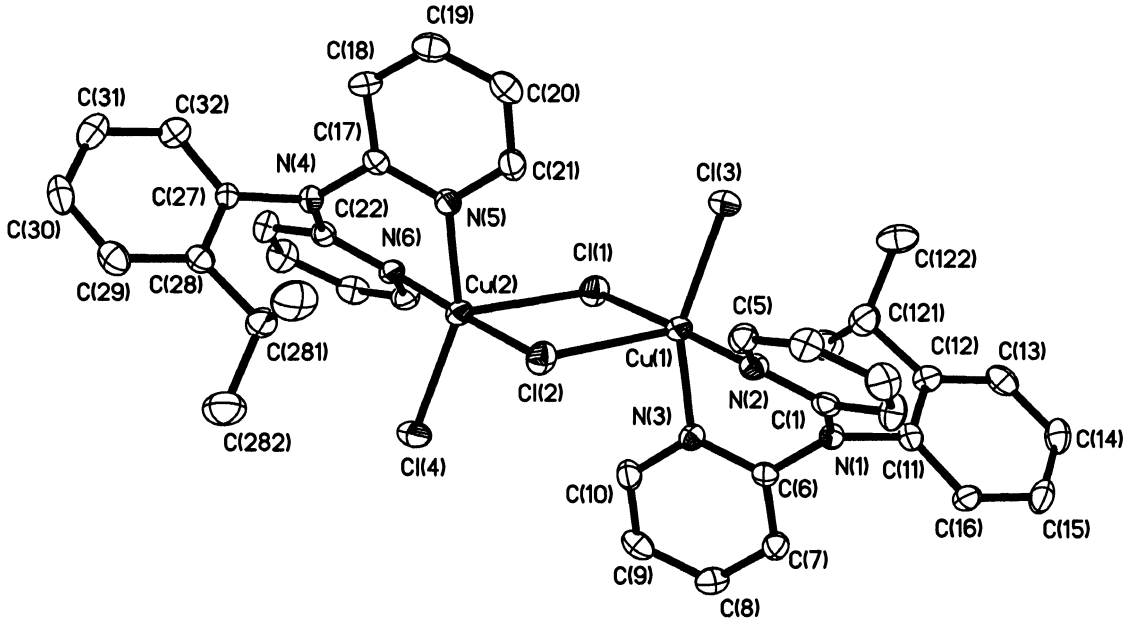

Figure 3.11. Molecular structure of the $[Cu(2\text{-}^{i}PrPh\text{-}dpa)(Cl)(\mu\text{-}Cl)]_2$ (**3.8**) complex. Thermal ellipsoids are shown at the 30% level, and all hydrogen atoms are omitted for clarity.

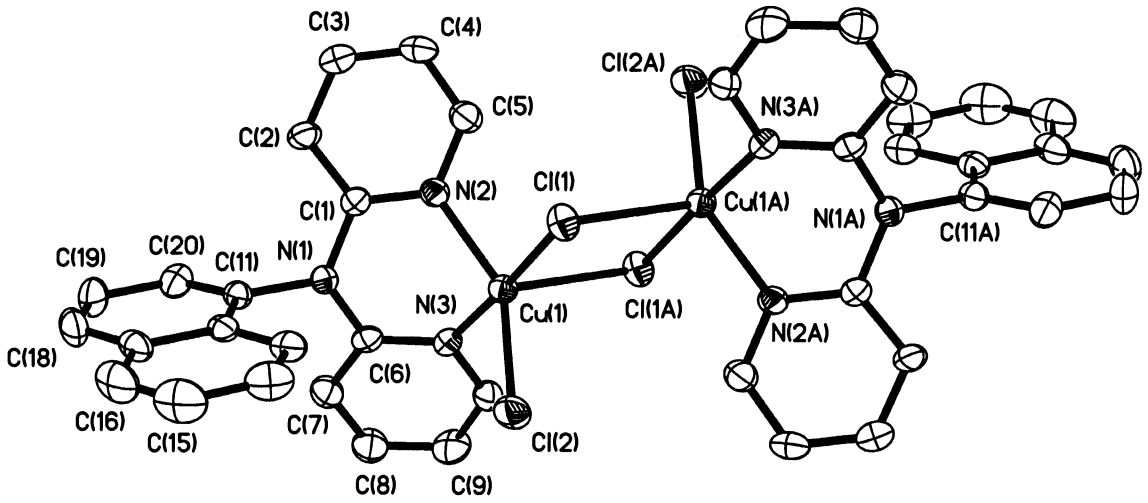

Figure 3.12. Molecular structure of the $[Cu(Naph\text{-}dpa)(Cl)(\mu\text{-}Cl)]_2$ (**3.9**) dimer. Thermal ellipsoids are shown at the 30% level, and all hydrogen atoms are omitted for clarity.

The coordination geometry about the copper centers in compounds **3.7** – **3.11** is distorted trigonal bipyramidal, with the axial positions occupied by one the two pyridyl nitrogens and one of the bridging ligands (i.e., Cl or OH), with the *trans*-angle ranging from 171.8(1) – 178.2(1)° (). The trigonal bipyramidal coordination spheres observed in these bridged dimers is common in other structurally related compounds, such as $[Cu\{CH_2(py)_2\}(Cl)(\mu\text{-}Cl)]_2$, [10] $[Cu(o\text{-}phen)(Cl)(\mu\text{-}Cl)]_2$, [11] $[Cu(bipy)(Cl)(\mu\text{-}Cl)]_2$, [12] and $[Cu(o\text{-}phen)(H_2O)(\mu\text{-}OH)]_2NO_3$.[13]

The solid state structure of compound **3.10** was found to exhibit two crystallographically unique conformers in the asymmetric unit. The molecular structures of the two independent molecules in the asymmetric unit are shown in Figure 3.14; selected bond lengths and angles are given in Table 3.3.

The Cu-Cl distances between bridging and non-bridging chlorine atoms in **3.7** – **3.10** are with the ranges [2.255(3) – 2.722(3) Å and 2.256(1) – 2.272(3) Å] previously reported for similar compounds.[31-33] The Cu-O distances for the bridging hydroxo ligands [1.960(2) and 1.953(2) Å] are similar to those reported for the aforementioned *ortho*-phen complex [1.944(3) Å], the neutral β-diketiminato complex [1.914(1) and 1.923(1) Å],[14]

the bipy/PhNHpy complex [1.94(1) and 1.96(1) Å],[15] and the *bis*(imidazolin-2-imine) complex [1.932(2) and 1.930(2) Å].[16]

The Cu-O distance for the aquo ligand [2.223(3) Å] is also similar to those previously reported [2.035(4) – 2.518(1) Å].[17,18] The observed Cu-(μ-O)-Cu(1A) angle in **3.11** is slightly larger than the corresponding angles in the chloride analogs, but much longer distances between bridging atoms in the latter result in significantly longer [3.513(1) – 3.6728(8) Å] Cu···Cu distances than in **3.11** [2.9666(9) Å].

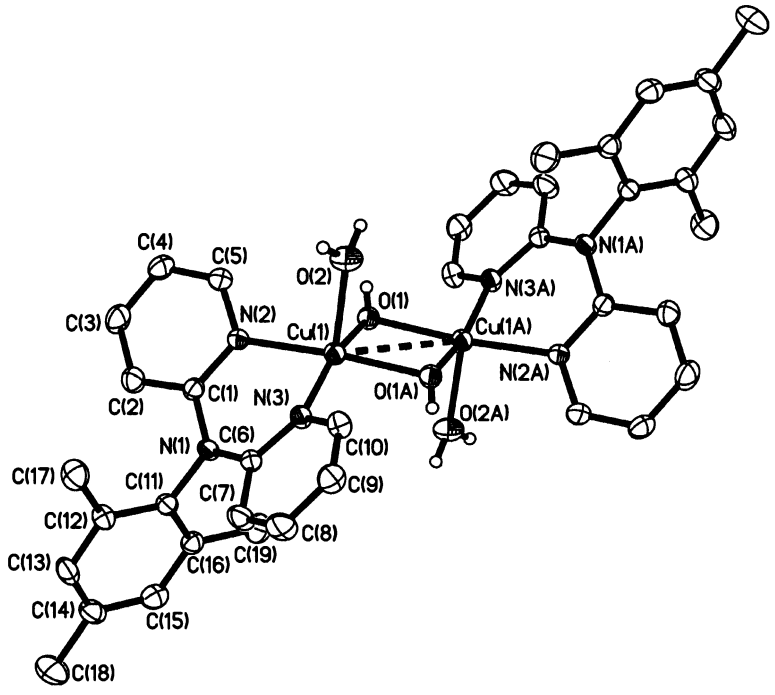

Figure 3.13. Molecular structure of the $[Cu(Mes\text{-}dpa)(H_2O)(\mu\text{-}OH)]_2^{2+}$ cation (**3.11**). Thermal ellipsoids are shown at the 30% level, and hydrogen atoms attached to carbon are omitted for clarity.

Overall, the $[Cu(X)(\mu\text{-}X)_2Cu(X)]$ core in compounds **3.7** – **3.11** is rigid and appears to be unaffected by the nature of the Ar-dpa ligand. It is therefore useful to look at the distortions in the Ar-dpa ligands as a function of the steric bulk of the aryl substituents.

Table 3.3. Selected bond lengths (Å) and angles (°) in compounds $[Cu(Ar\text{-}dpa)(\mu\text{-}X)X]_2$

	3.7	**3.8**	**3.9**	**3.10**(dimer)	**3.10**(mono.)	**3.11**[a]
Cu-N	2.025(1)	2.013(4), 2.016(4)	2.020(6)	1.985(3)	1.978(4)	1.977(2)
Cu-N'	2.030(1)	2.018(4), 2.028(4)	1.998(6)	2.030(3)	1.997(4)	1.987(2)
Cu-(μ-Cl)	2.2755(6)	2.261(1), 2.264(1)	2.296(2)	2.275(1)	2.218(1)	1.960(2)
Cu-(μ-Cl)'	2.7299(7)	2.698(1), 2.683(1)	2.596(2)	2.560(1)	3.803(1)	1.953(2)
Cu-Cl	2.2547(9)	2.286(1), 2.285(1)	2.285(2)	2.307(1)	2.236(1)	2.223(3)
Cu···Cu'	3.6728(8)	3.594(1)	3.513(1)	3.613(1)	4.740(1)	2.9666(9)
N_a-C_{py}	1.421(2)	1.399(6), 1.417(6)	1.415(9)	1.411(5)	1.413(6)	1.404(3)
N_a-$C_{py'}$	1.421(3)	1.412(7), 1.403(6)	1.404(8)	1.401(5)	1.397(5)	1.407(3)
N_a-C_{Ar}	1.416(3)	1.450(7), 1.454(6)	1.466(8)	1.454(5)	1.449(5)	1.453(4)
Cl-Cu(1)-N	156.14(5)	90.5(1), 92.9(1)	148.7(1)	99.4(1)	101.5(1)	95.6(1)
Cl-Cu(1)-N'	89.30(5)	97.5(1), 91.32(1)	88.6(1)	97.06(6)	133.3(1)	101.3(1)
Cu-(μ-Cl)-Cu'	93.97(2)	92.30(5), 91.95(5)	91.59(7)	96.53(5)	100.51(5)	98.61(9)
N-Cu-N'	86.52(6)	86.7(1), 85.6(1)	85.7(2)	85.2(1)	88.0(1)	86.6(1)
C_{py}-N-$C_{py'}$	115.6(1)	122.4(4), 122.1(4)	123.1(6)	124.9(4)	125.6(4)	125.4(2)
(μ-Cl)-Cu-(μ-Cl)'	86.03(2)	87.64(5), 88.03(5)	88.41(7)	83.47(5)	79.49(5)	81.39(9)
(μ-Cl)-Cu-Cl	93.45(3)	92.85(6), 93.39(6)	91.92(9)	97.06(6)	103.13(6)	96.0(1)
(μ-Cl)-Cu-N	92.01(5)	177.8(1), 178.2(1)	92.4(1)	161.2(1)	141.8(1)	171.8(1)
(μ-Cl)-Cu-N'	176.18(5)	93.4(1), 99.0(1)	177.2(1)	93.3(1)	95.8(1)	94.9(1)
Cu···N_a-C_{Ar}	125.4(1)	138.2(3), 137.5(3)	143.1(4)	145.6(3)	144.2(3)	157.8(2)
$\Delta MPLN_{[py\text{-}py']}$	59.2(1)	43.2(2) ,43.6(2)	39.8(4)	33.3(1)	28.3(2)	31.5(2)

[a] atoms μ-O and O substitute for atoms μ-Cl and Cl, respectively.

(a)

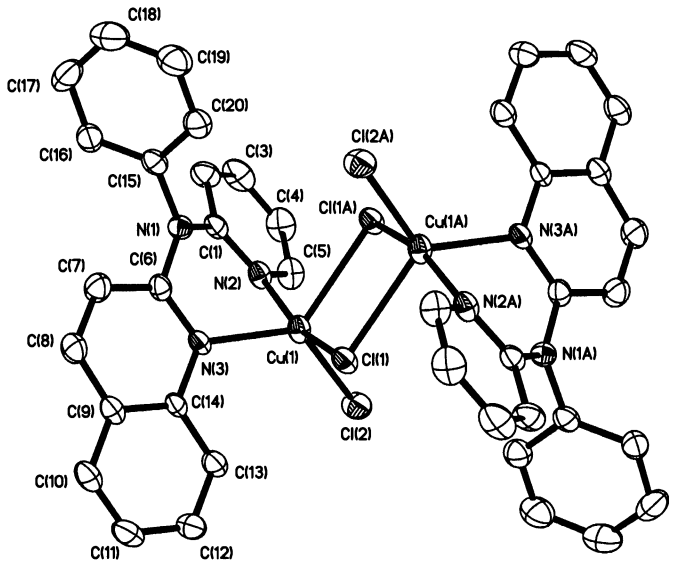

(b)

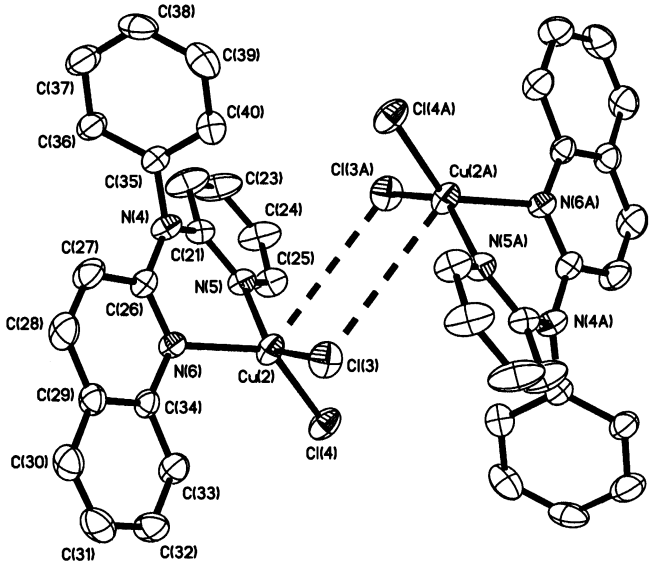

Figure 3.14. Molecular structures of (a) the dimeric and (b) monomeric forms of Cu[PhN(py)quin]Cl_2 (**3.10**). Thermal ellipsoids are shown at the 30% level, and all hydrogen atoms are omitted for clarity.

As may be seen from Figure 3.15, the bend of the N-C_{Ar} out of the plane of the two pyridyl rings is proportional to the folding along the Cu···N vector (i.e., formation of a butterfly conformation).

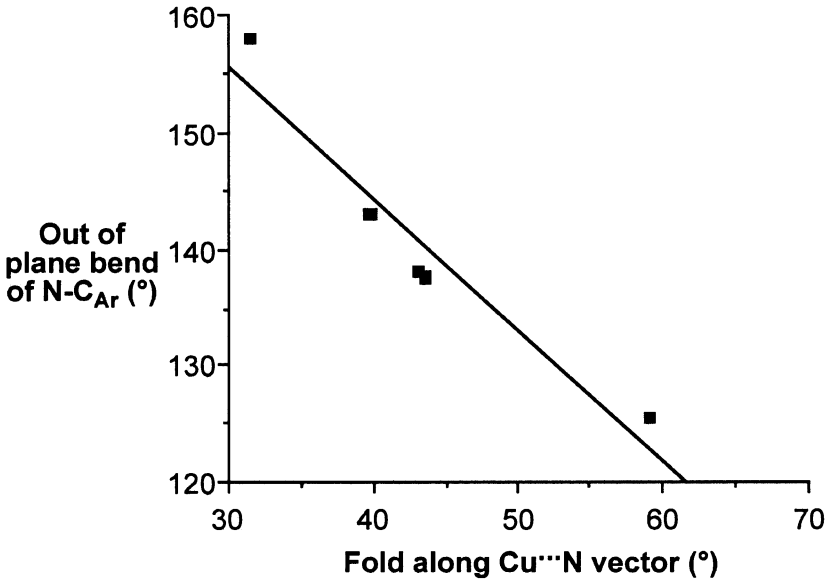

Figure 3.15. Plot of the bend of the N-C_{Ar} out of the plane of the two pyridyl rings versus folding along the Cu···N vector for compounds **3.7** – **3.11** ($R^2 = 0.928$).

It is interesting to note that of the ligands studied, it is the phenyl derivative (compound **3.7**) that appears to have the greatest steric differentiation about the copper due to the remotely substituted aryl group. A comparison of the structure of **3.7** in Figure 3.10 with the other dimers (Figure 3.11 - Figure 3.13), suggests that this is due to the nearly eclipsed orientation of the phenyl group with respect to the two pyridyl rings. Clearly, in solution this will be averaged due to free rotation about the N(1)-C(11) bond.

Based upon the forgoing, the presence of *ortho*-substitution in the uncomplexed Ar-dpa compounds results in a significant distortion of the coordination around the amine nitrogen and twisting of the two pyridyl rings with respect to each other. What this result does show is that the steric bulk of the substituents on the aryl ring in Ar-dpa does have a significant effect on the orientation and configuration of the two pyridyl rings, even when the pyridyl nitrogens are rigidly coordinated to a copper center.

Although it is not unusual to observe two independent molecules within a given asymmetric unit, it is rather surprising to see the degree to which the geometries differ about the copper atoms for each conformer in **3.10**. Specifically, Cu(1) exists in the dimeric form (**I**) as is observed for the $PhN(py)_2$ analog (**3.7**). The proximity of a symmetry related Cu(2)-unit gives the initial appearance that Cu(2) also exists as a dimer [as seen in Cu(1)]; however, a consideration of the intramolecular distances and the geometry about Cu(2) are more consistent with a monomeric form (**II**).

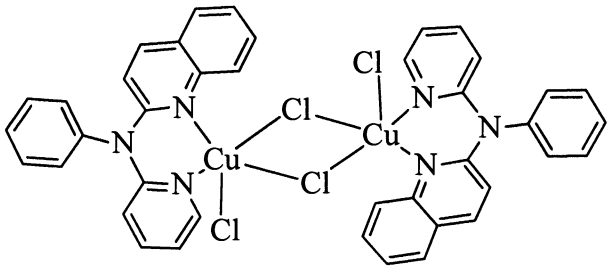

(I)

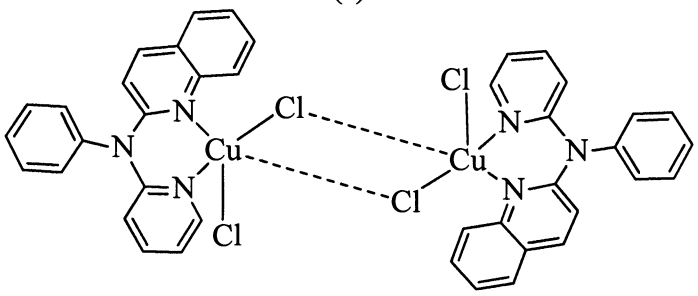

(II)

The coordination geometry about Cu(1) in compound **3.10** is that of a distorted trigonal bipyramid, with the axial positions occupied by the pyridyl nitrogen and one of the bridging chlorides. The *trans*-angle [161.2(1)°] is slightly smaller than the range seen for the related $RN(py)_2$ derivatives [176.18(5) – 178.2(1)°].[1] The trigonal bipyramidal coordination spheres observed in these bridged dimers is also observed in the structurally related compounds $\{Cu[CH_2(py)_2]Cl_2\}_2$,[19] $[Cu(o\text{-}phen)Cl_2]_2$,[20] and $[Cu(bipy)Cl_2]_2$.[21] In contrast, the geometry about Cu(2) is much closer to that expected for a square planar

monomer typical for Cu(II) compounds, with the *trans*-angles being 141.8(1)°. A comparison of the inner coordination sphere of the copper atoms is shown in Figure 3.16.

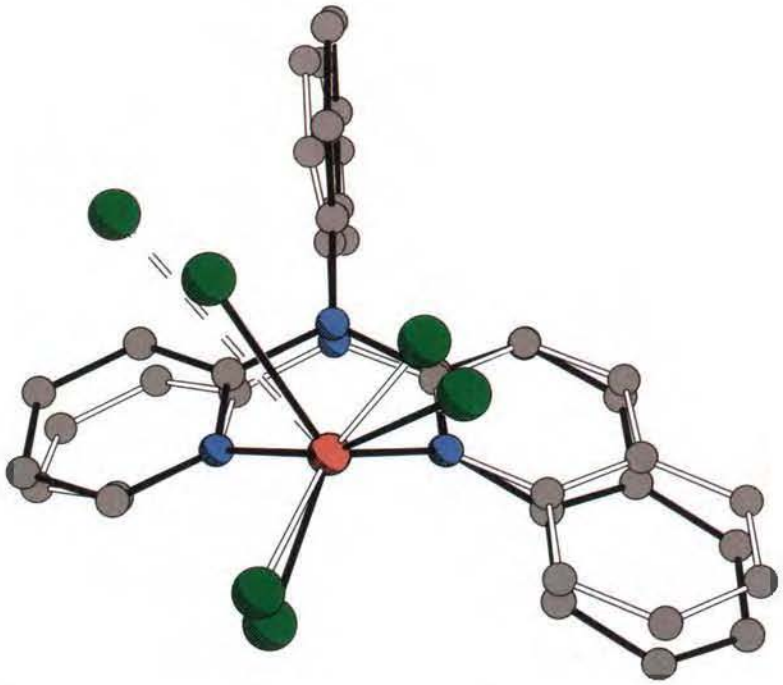

Figure 3.16. Partial inner coordination spheres of monomer (open bonds) and dimer (solid bonds) in Cu[PhN(py)quin]Cl_2 (**3.10**), which have been superimposed to highlight geometrical differences.

The bridging Cu-Cl distances associated with Cu(1), 2.270(1) and 2.554(1) Å, are similar to those observed for [Cu{RN(py)$_2$}Cl_2]$_2$ [2.261(1) - 2.296(2) Å and 2.596(2) - 2.7299(7) Å, respectively], where R = Ph, 2-^{i}PrPh, and 1-naph. Furthermore, they are consistent with the hybridization associated with the trigonal bipyramidal structure (i.e., the axial = *p* and equatorial = sp^2), as well as the relative *trans*-influences of the chloride and pyridyl ligand. A comparison of the distances for Cu(2) shows that while one of the distances to the "bridging" chloride atoms is reasonable [2.232(1) Å] the other is significantly longer than expected for a covalent Cu-Cl bond [3.795(1) Å]. Both Cu(2)-Cl(3) and Cu(2)-Cl(4) distances are within the range expected for terminal interactions.

A measure of the relative asymmetry of the bridging unit can be defined as the ΔCu-Cl. For Cu(1) in **3.10** this is 0.284 Å, while for $[Cu\{RN(py)_2\}Cl_2]_2$ the values are as follows: 0.4544 Å (R = Ph); 0.3 Å (R = ^{i}PrPh), and 0.437 and 0.419 Å (R = 1-naph). Thus, the dimeric form of compound **3.10** is actually more symmetrical than the $RN(py)_2$ derivatives. In contrast, the difference between chloro-distances associated with Cu(2) is 1.563 Å, over three times that of the dimeric compounds.

The crystal packing diagram for compound **3.7** (Figure 3.17) as compared to that in compound **3.10** (Figure 3.18) clearly shows the difference in Cu···Cu distances between the two forms. Packing in compound **3.7** also demonstrates the π···π packing interaction present between stacked pyridyl rings. We propose that the presence of both monomeric and dimeric forms in **3.10** suggests that the energetic difference between each form is comparable to the crystal packing forces observed in the solid state. We have previously observed monomer/dimer disorder where crystal packing forces dominate, allowing for either conformation.[22]

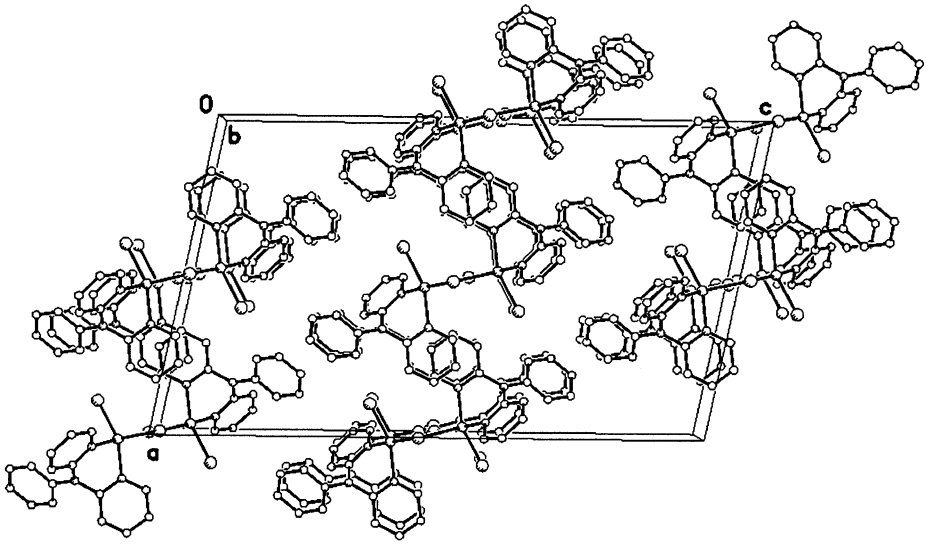

Figure 3.17. Molecular packing diagram of **3.7** viewed along the *b*-axis, showing π···π stacking interaction between pyridyl rings of adjacent molecules. All hydrogen atoms are omitted for clarity.

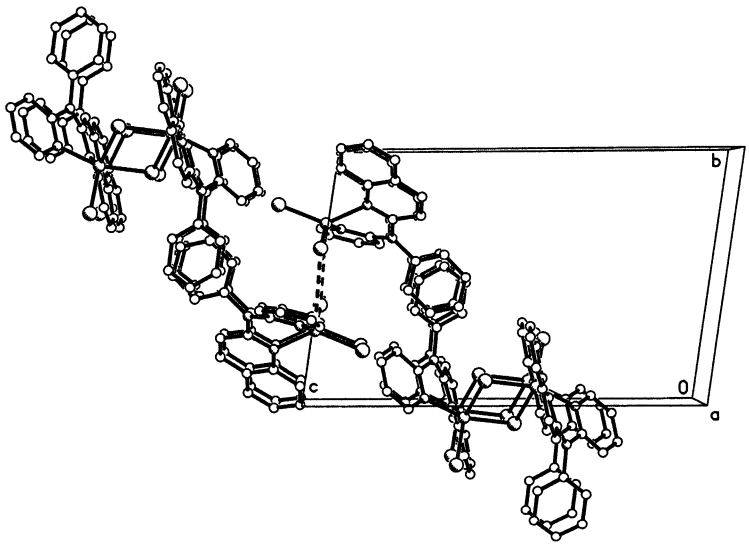

Figure 3.18. Crystal packing of Cu[PhN(py)quin]Cl_2 (**3.10**), viewed along the *c*-axis, highlighting packing differences between different forms.

Copper(I) Complexes of Ar-dqa. Reaction of (^{i}Pr$_2$Ph)-N(quin)$_2$ with [Cu(MeCN)$_4$]BF_4 in MeOH/CH_2Cl_2 yielded the complex [Cu{(2,6-^{i}Pr$_2$Ph)N(quin)$_2$}$_2$]BF_4 (**3.12**) as its methanol solvate (**3.12**·MeOH). Recrystallization of a methanol/toluene solution yields the toluene solvate [**3.12**·2(tol)]. The crystal structures of both solvates have been determined. Selected bond lengths and angles of the [Cu{(2,6-^{i}Pr$_2$Ph)N(quin)$_2$}$_2$]$^+$ cation in each solvate are given in Table 3.4.

The complex [Cu{(2,6-^{i}Pr$_2$)PhN(quin)$_2$}$_2$]BF_4·MeOH (**3.12**·MeOH) crystallizes with only half of the molecule in the asymmetric unit in the unit cell. The second half of the complex is symmetry related through a C_2-rotation axis (Figure 3.19). In contrast, the cation in **3.12**·(tol) is crystallographically independent (Figure 3.20). This difference appears to be a result of interactions in the crystal packing, which results in significant changes within the coordination geometry about the copper centers.

The geometry about the copper center in **3.12**·MeOH is distorted from tetrahedral [94.23(8) and 126.07(8)°] as expected from a *bis*-five-membered chelate complex. In

comparison, the geometry about copper in **3.12**·(tol) exhibits much greater distortion from tetrahedral [91.33(8) - 144.43(9)°]. This difference in the distorted geometries can also be seen clearly upon examination of the Cu-N distances. Specifically, the Cu-N distances in **3.12**·MeOH are very similar to one another [2.013(1) and 2.042(2) Å], while those in **3.12**·(tol) span a much larger range [1.982(2) - 2.132(2) Å]. Both of these parameters suggest that the coordination around the copper center is supple.

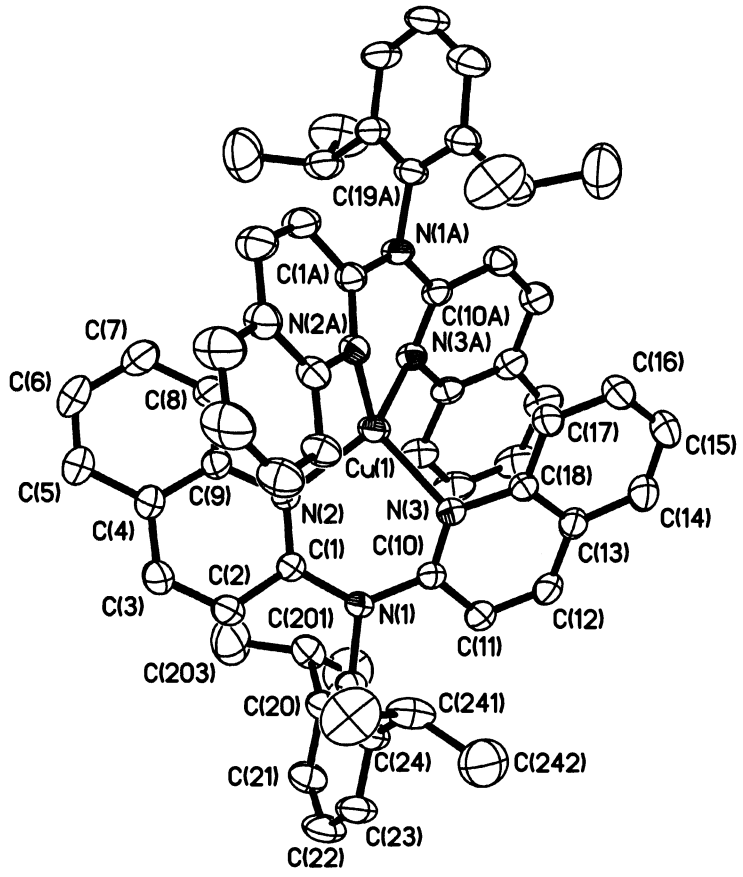

Figure 3.19. Structure of the cation $[Cu\{(2,6\text{-}^{i}Pr_2Ph)\text{-}dqa\}_2]^+$ in **3.12**·MeOH. Thermal ellipsoids are shown at the 30% level, and all hydrogen atoms have been omitted for clarity.

The distances between the amine nitrogen and both the quinolyl carbons and aryl carbon in **3.12**·MeOH are within experimental error of those of the free ligand **2.15**. In

contrast, while one ligand in **3.12**·(tol) has the distances associated with the amine nitrogen within error of those of the free ligand, the other ligand appears distorted with the two bond lengths between the amine nitrogen and the pyridyl carbons being more asymmetric [1.395(3) and 1.424(3) Å]. Another significant difference regarding complex geometry observed between the two ligands in **3.12**·(tol) is the Cu···N-C_{Ar} bend angle. This angle is far smaller [160.1(1)°] in the N(1)-ligand than in the N(4)-ligand [174.8(1)°], the latter of which is similar to that found in **3.12**·MeOH [177.0(1)°].

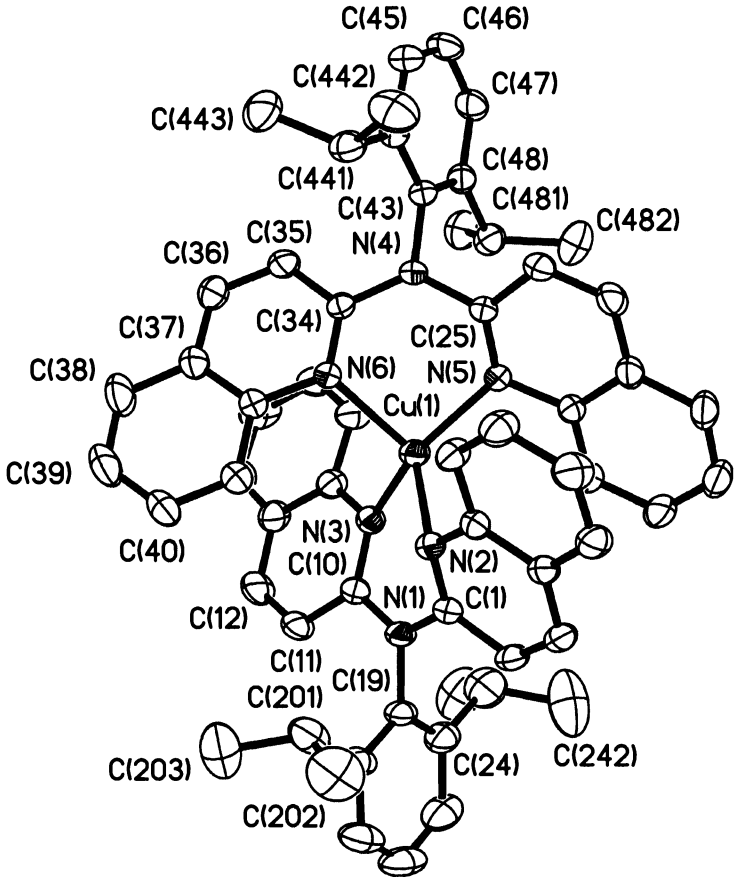

Figure 3.20. Structure of the cation $[Cu\{(2,6\text{-}^{i}Pr_2Ph)\text{-}dqa\}_2]^+$ in **3.12**·(tol). Thermal ellipsoids are shown at the 30% level, and all hydrogen atoms have been omitted for clarity.

An examination of the mean-plane-angle differences between adjacent quinolyl rings reveals that intramolecular π···π stacking between the rings is present in both solvates of compound **3.12**. Specifically, distances and mean-plane-differences between stacking ring pairs in **3.12**·MeOH [3.611(1) and 4.354(2) Å; 0.0(1) and 45.3(1)°] indicate that only one of the pairs of quinolyl rings forms a π···π interaction. The analogous stacking in **3.12**·(tol) [3.665(1) and 3.986(2) Å; 13.2(1) and 26.8(1)°] shows a much closer distance between the second pair. The presence of a possible second, albeit weak, π···π stacking interaction between ring pairs could be responsible for the distortions observed around the copper center, as well as in the ligand.

Table 3.4. Selected bond lengths (Å) and angles (°) for the solvates of compound **3.12**.

	3.12·MeOH		**3.12**·2(tol)
Cu(1)-N(2)	2.013(1)	2.132(2)	1.984(2)
Cu(1)-N(3)	2.042(2)	1.982(2)	2.123(2)
N(1)-C(1)	1.411(3)	1.409(3)	1.424(3)
N(1)-C(10)	1.405(3)	1.408(3)	1.395(3)
N(1)-C(19)	1.458(3)	1.453(3)	1.459(3)
N(2)-Cu(1)-N(3)	94.23(8)	92.37(9)	91.33(8)
N(2)-Cu(1)-N(2A)	111.7(1)	107.33(9)	
N(3)-Cu(1)-N(2A)	126.07(8)	144.43(9)	
N(3)-Cu(1)-N(3A)	107.6(1)	108.44(9)	
C(1)-N(1)-C(10)	129.4(2)	127.6(2)	126.9(2)
C(1)-N(1)-C(19)	114.4(2)	115.5(2)	114.3(1)
C(10)-N(1)-C(19)	115.9(2)	116.8(2)	118.6(1)

Experimental

General experimental techniques were performed as laid out in Chapter 1. N-(triphenylmethyl)-N-(2-pyridyl)amine was prepared according to the literature.[23]

[(Mes-dpa)H]BF_4 (3.1). In a 25 mL round bottom flask, Mes-dpa (0.289 g, 1.0 mmol) was dissolved in MeOH (5 mL). With stirring, KBF_4 (0.130 g, 1.0 mmol) dissolved in dilute HCl (5 mL). The mixture was allowed to stir for 30 minutes, followed by extraction with CH_2Cl_2 (2 x 5 mL) The solvent was removed under vacuum, and the solid was dissolved in methanol, followed by filtration through a medium porosity sintered-glass frit. Slow evaporation of the filtrate yielded 0.156 g (41%) colorless crystals. Mp (TGA; decomp.): 228-229 °C. FTIR (neat, ATR, cm^{-1}): 3104 (w, aromatic ν_{C-H}), 3063 (w, aromatic ν_{C-H}), 2941 (w, alkyl ν_{C-H}), 2921 (w, alkyl ν_{C-H}), 2859 (w, alkyl ν_{C-H}), 2736 (w, vb), 1634 (w), 1593 (s), 1527 (m), 1458-1367 (s, aromatic $\delta_{C=C}$), 1292 (m), 1253 (m, aromatic $\delta_{C=N}$), 1164 (m), 1032 (vs), 769 (vs). ^{1}H NMR (CD_3OD): δ 8.60 [2H, ddd, *J*(H-H) = 5.7 Hz, *J*(H-H) = 1.9 Hz, *J*(H-H) = 0.7 Hz, C*H*, 6,6'-py], 8.05 [2H, ddd, *J*(H-H) = 8.9 Hz, *J*(H-H) = 7.3 Hz, *J*(H-H) = 1.9 Hz, C*H*, 4,4'-py], 7.42 [2H, ddd, *J*(H-H) = 7.3 Hz, *J*(H-H) = 5.7 Hz, *J*(H-H) = 0.8 Hz, C*H*, 5,5'-py], 7.28 (2H, s, C_6H_2), 6.63 [2H, ddd, *J*(H-H) = 8.9 Hz, *J*(H-H) = 0.8 Hz, *J*(H-H) = 0.7 Hz, C*H*, 3,3'-py], 2.45 (3H, s, *p*-CH_3), 2.02 (6H, s, *o*-CH_3). ^{13}C NMR (CD_3OD): δ 154.51, 144.89, 143.25, 142.88, 138.10, 133.36, 132.55, 120.40, 114.93, 21.38, 17.32.

[(2-^{i}PrPh-dpa)H]BF_4 (3.2). This compound was prepared in an analogous manner to that of compound (**3.1**), using 0.289 g (1.0 mmol) of 2-^{i}PrPh-dpa. Crystals suitable for X-ray diffraction were obtained cooling a saturated solution in ^{i}PrOH to -12 °C for several days. Yield = (78%). Mp (TGA; decomp.): 222-224 °C. FTIR (neat, ATR, cm^{-1}): 3106 (w, aromatic ν_{C-H}), 3061 (w, aromatic ν_{C-H}), 2965 (w, alkyl ν_{C-H}), 2928 (w, alkyl ν_{C-H}), 2870 (w, alkyl ν_{C-H}), 2600 (vw, vb), 1639 (w), 1594 (s), 1527 (s), 1491-1370

(s, aromatic $\delta_{C=C}$), 1296 (m), 1257 (m, aromatic $\delta_{C=N}$), 1169 (m), 1032 (vs), 768 (vs). ^{1}H NMR (CD_3OD): δ 8.58 [2H, ddd, *J*(H-H) = 5.7 Hz, *J*(H-H) = 1.9 Hz, *J*(H-H) = 0.7 Hz, C*H*, 6,6'-py], 8.02 [2H, ddd, *J*(H-H) = 8.9 Hz, *J*(H-H) = 7.3 Hz, *J*(H-H) = 1.9 Hz, C*H*, 4,4'-py], 7.78 (1H, C*H*), 7.75 (1H, C*H*), 7.60 (1H, C*H*),7.45 (1H, C*H*), 7.41 [2H, ddd, *J*(H-H) = 7.3 Hz, *J*(H-H) = 5.7 Hz, *J*(H-H) = 0.8 Hz, C*H*, 5,5'-py], 6.65 [2H, ddd, *J*(H-H) = 8.9 Hz, *J*(H-H) = 0.8 Hz, *J*(H-H) = 0.7 Hz, C*H*, 3,3'-py], 2.80 [1H, sept, *J*(H-H) = 8.9 Hz, C*H*$(CH_3)_2$], 1.08 [6H, d, *J*(H-H) = 8.9 Hz, CH(C*H*$_3)_2$]. ^{13}C NMR (CD_3OD): δ 155.60, 148.89, 144.12, 142.92, 136.03, 133.05, 130.87, 130.76, 130.66, 120.30, 116.27, 29.21, 24.03.

[(Ph-pqa)H]BF_4 (3.3). In a 25 mL round bottom flask, compound **3.1** (0.297 g, 1.0 mmol) was dissolved in MeOH (5 mL). With stirring, KBF_4 (0.130 g, 1.0 mmol) was dissolved in dilute HCl (5 mL). The mixture was allowed to stir for 30 minutes, followed by extraction with CH_2Cl_2 (2 x 5 mL). The solvent was removed under vacuum, and the solid was dissolved in MeOH, followed by filtration through a medium porosity sintered-glass frit. Slow evaporation of the filtrate yielded colorless crystals. Yield: 54%. Mp (TGA; decomp.): 230-232 °C. FTIR (neat, ATR, cm^{-1}): 3106 (w, aromatic ν_{C-H}), 3076 (w, aromatic ν_{C-H}), 3060 (w, aromatic ν_{C-H}), 2734 (w, vb) 1627 (m), 1591 (s), 1536 (s), 1479-1366 (s, aromatic $\delta_{C=C}$), 1282 (m, aromatic $\delta_{C=N}$), 1254 (m), 1228 (m), 1156 (m), 1038 (vs), 907 (m), 772 (vs). ^{1}H NMR (CD_3OD): δ 8.71 [1H, ddd, *J*(H-H) = 5.4 Hz, *J*(H-H) = 1.8, Hz, *J*(H-H) = 0.7 Hz, C*H*, 6-py], 8.49 [1H, dd, *J*(H-H) = 9.3 Hz, *J*(H-H) = 0.5 Hz, C*H*, 4-quin], 8.21 [1H, ddd, *J*(H-H) = 8.5 Hz, *J*(H-H) = 1.2, Hz, *J*(H-H) = 0.5 Hz, C*H*, 6-quin], 8.02 [1H, dd, *J*(H-H) = 8.2 Hz, *J*(H-H) = 1.1, Hz, C*H*, 9-quin], 8.01 [1H, ddd, *J*(H-H) = 8.6 Hz, *J*(H-H) = 7.3, Hz, *J*(H-H) = 1.8 Hz, C*H*, 4-py], 7.98 [1H, ddd, *J*(H-H) = 8.5 Hz, *J*(H-H) = 7.2, Hz, *J*(H-H) = 1.1 Hz, C*H*, 7-quin], 7.82-7.75 (3H, m, C*H*, Ph), 7.71 [1H, ddd, *J*(H-H) = 8.2 Hz, *J*(H-H) = 7.2, Hz, *J*(H-H) = 1.2 Hz, C*H*, 8-quin], 7.60 (2H, m, C*H*, Ph), 7.47 [1H, ddd, *J*(H-H) = 7.3 Hz, *J*(H-H) = 5.4, Hz, *J*(H-H) = 0.8

Hz, C*H*, 5-py], 6.84 [1H, d, *J*(H-H) = 9.3 Hz, C*H*, 3-quin], 6.82 [1H, ddd, *J*(H-H) = 8.6 Hz, *J*(H-H) = 0.8, Hz, *J*(H-H) = 0.7 Hz, C*H*, 3-py]. ^{13}C NMR (CD_3OD): δ 156.79, 155.07, 145.02, 144.58, 143.07, 139.64, 136.32, 134.54, 133.20, 132.11, 130.64, 129.83, 128.59, 125.52, 123.26, 121.81, 117.63, 115.56.

[(Mes-pqa)H]BF_4 (3.4). This compound was prepared in an analogous manner to that of **3.1**, using MesN(py)quin (0.339 g, 1.0 mmol) as ligand. Yield: 0.191 g (45%) colorless crystals. Mp (TGA; decomp.): 197-199 °C. FTIR (neat, ATR, cm-1): 3120 (m, aromatic ν_{C-H}), 3061 (w, aromatic ν_{C-H}), 2983 (w, alkyl ν_{C-H}), 2926 (m, alkyl ν_{C-H}), 2858 (w, alkyl ν_{C-H}), 2736 (w), 2645 (w, vbr), 1624 (s), 1597 (s), 1506 - 1437 (s, aromatic $\delta_{C=C}$), 1364 (3° aromatic ν_{C-N}), 1321 (m), 1267 (m), 1149 (m), 1031 (s, ν_{B-F}), 831 (s), 762 (s).. ^{1}H NMR (CD_3OD): δ 8.81 [1H, ddd, *J*(H-H) = 5.4 Hz, *J*(H-H) = 1.9 Hz, *J*(H-H) = 0.9 Hz, C*H*, 6-py], 8.57 [1H, dd, *J*(H-H) = 9.4 Hz, *J*(H-H) = 0.7 Hz, C*H*, 4-quin], 8.32 [1H, ddd, *J*(H-H) = 8.5 Hz, *J*(H-H) = 1.5 Hz, *J*(H-H) = 0.8 Hz, C*H*, 9-quin], 8.07 [1H, ddd, *J*(H-H) = 8.4 Hz, *J*(H-H) = 7.3 Hz, *J*(H-H) = 1.9 Hz, C*H*, 4-py], 8.05 [1H, dd, *J*(H-H) = 8.5 Hz, *J*(H-H) = 1.0 Hz, C*H*, 6-quin], 8.01 [1H, ddd, *J*(H-H) = 8.5 Hz, *J*(H-H) = 7.2 Hz, *J*(H-H) = 1.3 Hz, C*H*, 7-quin], 7.74 [1H, ddd, *J*(H-H) = 8.1 Hz, *J*(H-H) = 7.0 Hz, *J*(H-H) = 1.0 Hz, C*H*, 8-quin], 7.51 [1H, ddd, *J*(H-H) = 7.3 Hz, *J*(H-H) = 5.4 Hz, *J*(H-H) = 1.0 Hz, C*H*, 5-py], 7.32 (2H, s, *m*-C_6H_2), 6.75 [1H, d, *J*(H-H) = 9.4 Hz, C*H*, 3-quin], 6.71 [1H, ddd, *J*(H-H) = 8.4 Hz, *J*(H-H) = 1.0 Hz, *J*(H-H) = 0.9 Hz, C*H*, 3-py], 2.47 (3H, s, *p*-CH_3), 2.07 (6H, s, *o*-CH_3). ^{13}C NMR (CD_3OD): δ 155.27, 153.96, 146.01, 144.97, 144.17, 143.17, 139.68, 138.21, 134.77, 133.42, 132.57, 129.84, 128.75, 125.59, 123.43, 121.78, 115.40, 113.67, 21.42, 17.44.

[(2,6-^{i}Pr_2Ph-dqa)H]BF_4 (3.5). In a 25 mL round bottom flask, (2,6-^{i}Pr_2Ph)N(quin)$_2$ (0.431 g, 1.0 mmol) was dissolved in MeOH (15 mL). With stirring, KBF_4 (0.130 g, 1.0 mmol) dissolved in dilute HCl (5 mL) was slowly added. The mixture

was allowed to stir for 30 minutes, followed by extraction with CH_2Cl_2 (ca. 15 mL) The solvent was removed under vacuum, and the solid was dissolved in methanol, followed by filtration through a medium porosity sintered-glass frit. Slow evaporation of the filtrate yielded 0.186 g (36%) colorless crystals. Mp (TGA; decomp.): 220-222 °C. FTIR (neat, ATR, cm-1): 3058 (w, aromatic ν_{C-H}), 2969 (s, alkyl ν_{C-H}), 2931 (w, alkyl ν_{C-H}), 2912 (w, alkyl ν_{C-H}), 2877 (m, alkyl ν_{C-H}), 2649 (w, vbr), 1637 (w), 1598 - 1433 (s, aromatic $\delta_{C=C}$), 1366 (m), 1331 (s, 3° aromatic ν_{C-N}), 1299 (w), 1229 (m), 1157 (m), 1045 (s, ν_{B-F}), 823 (s), 759 (s). ^{1}H NMR (CD_3OD): δ 8.58 [2H, d, *J*(H-H) = 9.3 Hz, C*H*, 4-quin], 8.39 [2H, dd, *J*(H-H) = 8.3 Hz, *J*(H-H) = 0.8 Hz, C*H*, 6-quin], 8.08 [2H, dd, *J*(H-H) = 8.0 Hz, *J*(H-H) = 1.3 Hz, C*H*, 9-quin], 8.08 [2H, ddd, *J*(H-H) = 8.3 Hz, *J*(H-H) = 7.1 Hz, *J*(H-H) = 1.3 Hz, C*H*, 7-quin], 7.80 [1H, t, *J*(H-H) = 8.2 Hz, *p*-C*H*, Ph], 7.78 [2H, ddd, *J*(H-H) = 8.0 Hz, *J*(H-H) = 7.1 Hz, *J*(H-H) = 0.8 Hz, C*H*, 8-quin], 7.66 [2H, d, *J*(H-H) = 8.2 Hz, *m*-C*H*, Ph], 6.87 [2H, d, *J*(H-H) = 9.3 Hz, C*H*, 3-quin], 2.90 [2H, sept, *J*(H-H) = 6.8 Hz, C*H*$(CH_3)_2$], 1.09 [12 H, d, *J*(H-H) = 6.8 Hz, CH(C*H*$_3)_2$]. ^{13}C NMR (CD_3OD): δ 155.23, 148.72, 144.45, 141.43, 134.57, 133.55, 133.42, 129.78, 128.99, 128.12, 126.35, 125.03, 115.06, 29.85, 24.41.

$[Cu(Mes\text{-}dpa)_2]BF_4$ (3.6). $[Cu(MeCN)_4]BF_4$ (0.314 g, 1.0 mmol) and MesN(H)py (0.420 g, 2.0 mmol) were charged to a 100 mL schlenk flask in a dry box. MeOH (20 mL) was added, and the mixture was allowed to stir for three hours at room temperature. The solution volume was then reduced by approximately half under vacuum, followed by gentle warming with a water bath to redissolve product. The solution was then filtered through a medium porosity glass frit to remove insoluble impurities. Upon standing for several days at room temperature under an argon atmosphere, the solution yielded 0.439 g (77%) colorless crystals of $[Cu\{MesN(H)py\}_2]BF_4$. IR (neat, ATR, cm^{-1}): 3341 (m, ν_{N-H}), 3079 (w, aromatic ν_{C-H}), 2979 (w, alkyl ν_{C-H}), 2917 (w, alkyl ν_{C-H}), 2859 (w, alkyl ν_{C-H}), 1659 (w), 1621 (s, δ_{N-H}),

1577 (w), 1508-1367 (s, aromatic $\delta_{C=C}$), 1287 (s, aromatic $\delta_{C=N}$), 1225 (w), 1057-998 (br vs). ^{1}H NMR (298 K; CD_3OD): δ 7.64 (2H, br t, C*H*), 7.57 (2H, br s, C*H*), 6.94 (4H, s, *m*-C*H*), 6.74 (2H, br s, C*H*), 6.66 (2H, br t, C*H*), 2.17 (12H, s, *o*-CH_3), 2.05 (6H, s, *p*-CH_3).

[Cu(Ph-dpa)(Cl)(μ-Cl)]$_2$ (3.7). [Cu(MeCN)$_4$]BF$_4$ (0.157 g, 0.5 mmol) and Ph-dpa (0.124 g, 0.5 mmol) were stirred together in tetraethylelene glycol (2 mL) in a conical vial open to the atmosphere, until all solids had dissolved. Dilute HCl (2 mL) was then added to the mixture, turning the dark blue/green solution milky white. The mixture was then extracted with CH_2Cl_2 (2 x 5 mL), and the combined organic layers were allowed to evaporate. The resulting brown residue was taken up in MeOH (5 mL), which was filtered and cooled to –12 °C for several days, yielding dark green plates. Yield: 0.114 g (60%). Mp (TGA; decomp.) 265-267 °C. FTIR (neat, ATR, cm^{-1}): 3106 (w, aromatic ν_{C-H}), 3075 (w, aromatic ν_{C-H}), 3061 (w, aromatic ν_{C-H}), 3039 (w, aromatic ν_{C-H}), 3021 (w, aromatic ν_{C-H}), 1600 (s), 1589 (s), 1566-1317 (s, aromatic $\delta_{C=C}$), 1274 (s, aromatic $\delta_{C=N}$), 1160 (m), 1053 (m), 1029 (m), 936 (m), 787 (s).

[Cu(2-^{i}PrPh-dpa)(Cl)(μ-Cl)]$_2$ (3.8). This compound was prepared in an analogous manner to that of compound **3.7**, using 2-^{i}PrPh-dpa (0.149 g, 0.5 mmol) for the ligand. Recrystallization by slow evaporation of MeOH solution. Yield: 48%. Mp (TGA; decomp.) 231-233 °C. FTIR (neat, ATR, cm^{-1}): 3582 (w, ν_{O-H}), 3487 (w, ν_{O-H}), 3114 (w, aromatic ν_{C-H}), 3081 (w, aromatic ν_{C-H}), 3059 (w, aromatic ν_{C-H}), 3045 (w, aromatic ν_{C-H}), 3014 (w, aromatic ν_{C-H}), 1595 (s), 1578 (s), 1485-1321 (s, aromatic $\delta_{C=C}$), 1261 (m, aromatic $\delta_{C=N}$), 1248 (m), 1164 (m), 1060 (m), 1024 (m), 922 (m), 803 (m), 768 (vs).

[Cu(1-naph-dpa)(Cl)(μ-Cl)]$_2$ (3.9). This compound was prepared in an analogous manner to that of compound **3.7**, using naph-dpa (0.149 g, 0.5 mmol) for the

ligand. Recrystallized by a slow evaporation of MeOH solution. Yield: 48%. Mp (TGA; decomp.) 230-232 °C. FTIR (neat, ATR, cm^{-1}): 3582 (w, ν_{O-H}), 3487 (w, ν_{O-H}), 3114 (w, aromatic ν_{C-H}), 3081 (w, aromatic ν_{C-H}), 3059 (w, aromatic ν_{C-H}), 3045 (w, aromatic ν_{C-H}), 3014 (w, aromatic ν_{C-H}), 1595 (s), 1578 (s), 1485-1321 (s, aromatic $\delta_{C=C}$), 1261 (m, aromatic $\delta_{C=N}$), 1248 (m), 1164 (m), 1060 (m), 1024 (m), 922 (m), 803 (m), 768 (vs).

[Cu(Ph-pqa)Cl_2] (3.10). This compound was prepared in an analogous manner to that of compound **3.7**, using Ph-pqa (0.149 g, 0.5 mmol) for the ligand. The resulting brown residue was taken up in MeOH (5 mL), and then filtered. Recrystallization by a very slow evaporation of MeOH solution yielded dark red plates suitable for diffraction. Yield: 48%. Mp (TGA; decomp.) 89 - 91 °C. FTIR (neat, ATR, cm^{-1}): 3555 (w, br), 3433 (m, v br), 3111 (w, aromatic ν_{C-H}), 3088 (w, aromatic ν_{C-H}), 3061 (w, aromatic ν_{C-H}), 3048 (w, aromatic ν_{C-H}), 3023 (w, aromatic ν_{C-H}), 2919 (w, br), 1688 (m), 1604 (s), 1507 - 1428 (s, aromatic $\delta_{C=C}$), 1343 (s, 3° aromatic ν_{C-N}), 1317 (m), 1255 (m), 1148 (m), 1077 (m), 822 (m), 764 (s).

[Cu(Mes-dpa)(H_2O)(μ-OH)]$_2$[BF_4]$_2$ (3.11). [Cu(MeCN)$_4$]BF_4 (0.314 g, 1.0 mmol) and **2.5** (0.289 g, 1.0 mmol) were stirred together in MeOH (5 mL) and H_2O (1 mL) in a vial open to the atmosphere. After the solution had taken on a dark blue color (ca. 1 hr), the solvent was removed under vacuum, and the resulting powder was dissolved in 5:1 MeOH:acetone, filtered, and cooled to –12 °C for several days, yielding dark blue crystals of the methanol solvate. Yield: 0.569 g (56%). Mp (TGA; decomp.) 198-202 °C. FTIR (neat, ATR, cm^{-1}): 3532 (w, ν_{O-H}), 3197 (br, w), 3124 (w, aromatic ν_{C-H}), 3091 (w, aromatic ν_{C-H}), 3041 (w, aromatic ν_{C-H}), 2975 (w, alkyl ν_{C-H}), 2939 (w, alkyl ν_{C-H}), 2858 (w, alkyl ν_{C-H}), 2828 (w, alkyl ν_{C-H}), 1597 (s), 1580 (m), 1487-1327 (s, aromatic $\delta_{C=C}$), 1238 (m, aromatic $\delta_{C=N}$), 1027 (br, vs), 931 (w), 856 (w).

[Cu{2,6-^{i}Pr$_2$PhN(quin)$_2$}$_2$]BF$_4$ (3.12). In a drybox, [Cu(MeCN)$_4$]BF$_4$ (0.314 g, 1.0 mmol) and compound **2.15** (0.860 g, 2.0 mmol) were charged to a Schlenk flask. After the flask was removed from the drybox, MeOH (20 mL) and CH_2Cl_2 (10 mL) were added via cannula. The mixture was stirred under an argon atmosphere for 90 minutes, and the solvent was reduced to ca. 10 mL under vacuum. The solution was filtered and allowed to crystallize at –12 °C for several days, yielding bright red crystals (**3.12**·MeOH). Yield: 0.852 g (84.1%). A portion of the final product was recrystallized cooling a 2:1 MeOH:toluene solution to –12 °C for several days yielded a small quantity of the toluene solvate (**3.12**·tol). Mp (TGA; decomp.) 224-225 °C. FTIR (neat, ATR, cm^{-1}): 3121 (w), 3062 (w, aromatic ν_{C-H}), 3024 (w, aromatic ν_{C-H}), 2964 (m, alkyl ν_{C-H}), 2928 (w, alkyl ν_{C-H}), 2869 (w, alkyl ν_{C-H}), 1658 (w), 1616 (m), 1594 (s), 1568 (m), 1498-1343 (s, aromatic $\delta_{C=C}$), 1316 (vs, aromatic $\delta_{C=N}$), 1263 (m), 1248 (m), 1215 (m), 1146 (m), 1049 (br, vs), 934 (w), 816 (s), 756 (s). ^{1}H NMR (CD_3OD): δ 8.48 [4H, dd, *J*(H-H) = 8.4 Hz, *J*(H-H) = 1.1 Hz, C*H*, 6-quin], 7.88 [4H, d, *J*(H-H) = 9.1 Hz, C*H*, 4-quin], 7.70 [2H, dd, J(H-H) = 7.8 Hz, *J*(H-H) = 7.8 Hz, p-C*H*, Ph], 7.57 [4H, d, *J*(H-H) = 7.8 Hz, m-C*H*, Ph], 7.34 [4H, dd, *J*(H-H) = 8.0 Hz, *J*(H-H) = 1.4 Hz, C*H*, 9-quin], 7.17 [4H, ddd, J(H-H) = 8.4, *J*(H-H) = 7.0 Hz, *J*(H-H) = 1.4 Hz, C*H*, 7-quin], 7.12 [4H, ddd, *J*(H-H) = 8.0 Hz, *J*(H-H) = 7.0 Hz, *J*(H-H) = 1.1 Hz, C*H*, 8-quin], 6.57 [4H, d, *J*(H-H) = 9.1 Hz, C*H*, 3-quin], 3.38 [4H, sept, *J*(H-H) = 6.9 Hz, C*H*(CH$_3$)$_2$], 1.15 [24H, d, *J*(H-H) = 6.9 Hz, CH(C*H*$_3$)$_2$]. ^{13}C NMR (CD_3OD): δ 157.63, 149.01, 146.51, 141.07, 138.63, 132.50, 131.45, 130.08, 128.60, 128.00, 126.70, 126.59, 117.52, 30.20, 24.39.

Crystallographic Study. General aspects of X-ray data collection are given in Chapter 1. Pertinent details are given in Table 3.5. Heavy atom sites were located by Patterson methods for **3.12**·MeOH, while all others were solved by direct methods. The pyridyl-bound hydrogen atoms in compounds **3.1** - **3.5**, and the oxygen-bound H atoms in **3.11** were located in the difference map and refined freely.

Refinement of noncentrosymmetric structures **3.8** ($Pna2_1$) and **3.12**·MeOH ($P3_221$) were performed according to previously established methods,[24, 25] using TWIN/BASF instructions. In the case of compound **3.8**, the Flack x parameter (i.e., the fractional presence of the present absolute configuration versus that of its inversion twin) refined to 0.44(2), with 4361 (97.1 %) of Friedel pairs being measured. In the latter case, the compound crystallized in the chiral space group $P3_221$, and its absolute configuration was confirmed as pure chiral compound, with the Flack x parameter refining to a value essentially equal to zero.

The program PLATON was employed for structure validation, and the squeeze function therein was utilized to identify residual electron density in solvent accessible voids found present in compounds **3.2** and **3.12**·(tol).[26] The corrected data set was only used for the case of **3.2**, as its application in **3.12**·(tol) did not result in better agreement amongst data. Consequently, refinement of the disordered toluene solvent molecules present in the asymmetric unit of compound **3.12**·(tol) (Figure 3.21) was performed in a similar manner to that of compound **2.4** in Chapter 2.

Two different disordered toluene solvent molecules were found to be present in the asymmetric unit of **3.12**·2(tol). The FVAR instruction led to refinement of the disordered toluene solvent molecules as having site occupancies of 70:30 (molecule 1) and 50:50 (molecule 2) for carbon atoms in each part.

For initial refinement cycles, fixed-distance restraints (DFIX 1.35) were placed on all aromatic C-C distances, and similar distance restraints (SADI) were placed on all *para*-C-C distances [i.e., C(1)-C(4)], as well as equivalent C(methyl)-C(aromatic) distances. In addition, similar ADP restraints (SIMU) and rigid bond restraints (DELU) were used for all C atoms. DFIX, SIMU, and DELU restraints were kept throughout final refinement cycles. See chapter 7 for refinement details concerning the disordered tetrafluoroborate anions present in compounds **3.1**, **3.2**, **3.4**, **3.5**, **3.11**, and **3.12**·MeOH.

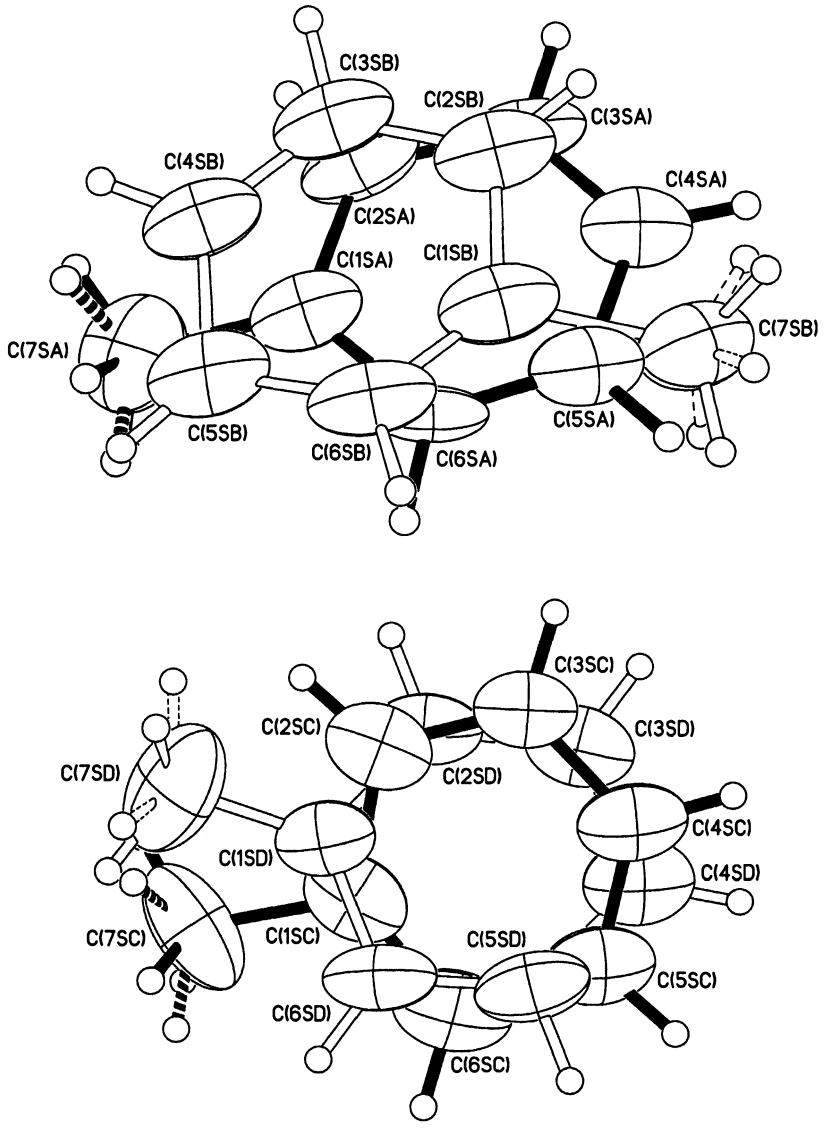

Figure 3.21. Disordered toluene solvent molecule 1 (top) and molecule 2 (bottom) present in the asymmetric unit of **3.12**·(tol), with both parts of the disorder present. For clarity, thermal ellipsoids are shown at the 15% level.

Table 3.5. Summary of X-ray diffraction data for acid salts and copper complexes of selected new ligands.

Compound	**3.1**	**3.2**	**3.3**
empir. formula	$C_{19}H_{20}N_3BF_4$	$C_{19}H_{20}N_3BF_4$	$C_{20}H_{16}N_3BF_4$
M_W	377.19	377.19	385.17
cryst. system	monoclinic	monoclinic	monoclinic
space group	$P2_1/c$	$P2_1/n$	$P2_1/c$
a, Å	8.730(1)	8.841(1)	15.308(3)
b, Å	10.151(2)	19.190(4)	7.585(1)
c, Å	21.326(4)	11.776(2)	17.227(3)
α, deg.	-	-	-
β, deg.	93.43(3)	94.00(3)	113.43(3)
γ, deg.	-	-	-
V, $Å^3$	1886.5(6)	1993.0(7)	1835.5(6)
Z	4	4	4
D_{calc}, g/cm^3	1.328	1.257	1.394
μ, mm^{-1}	0.107	0.101	0.111
2θ range, deg.	3.82 - 56.70	4.06 - 58.30	4.80 - 56.58
No. collected	22802	24786	21994
No. ind. (R_{int})	4646 (0.0615)	5040 (0.0876)	4390 (0.0678)
No. obsd. ($\|F_o\| > 4.0\sigma \|F_o\|$)	1996	1540	1861
R	0.059	0.0645	0.0536
R_w	0.1503	0.1694	0.1341
$\Delta\rho_{max/min}$ ($eÅ^{-3}$)	0.352, -0.183	0.189, -0.196	0.242, -0.236
weights	0.0815, 0.1418	0.0932, 0	0.0828, 0
CCDC Dep. No.	720347	735399	720348

Table 3.7. contd.

Compound	**3.4**	**3.5**	**3.6**
empir. formula	$C_{23}H_{22}N_3BF_4$	$C_{30}H_{30}N_3BF_4$	$CuC_{28}H_{32}N_4BF_4$
M_W	427.25	519.38	574.93
cryst. system	monoclinic	orthorhombic	monoclinic
space group	$P2_1/c$	Pbca	$P2_1/c$
a, Å	10.629(2)	13.886(3)	9.149(1)
b, Å	18.489(4)	18.016(4)	15.901(3)
c, Å	10.907(2)	21.347(4)	19.703(4)
α, deg.	-	-	-
β, deg.	92.88(3)	-	102.89(3)
γ, deg.	-	-	-
V, $Å^3$	2140.6(7)	5340(2)	2794(1)
Z	4	8	4
D_{calc}, g/cm^3	1.326	1.292	1.367
μ, mm^{-1}	0.103	0.095	0.832
2θ range, deg.	3.84 - 55.12	3.82 - 56.64	3.32 - 56.72
No. collected	25553	63544	33693
No. ind. (R_{int})	4934 (0.1101)	6620 (0.1919)	6797 (0.0537)
No. obsd. ($\|F_o\| > 4.0\sigma \|F_o\|$)	1728	2009	3489
R	0.0551	0.0722	0.0504
R_w	0.1531	0.1635	0.1291
$\Delta\rho_{max/min}$ ($eÅ^{-3}$)	0.249, -0.221	0.171, -0.222	0.572, -0.346
weights	0.0963, 0	0.0945, 0	0.0819, 0.1389
CCDC Dep. No.	779678	779679	697652

Table 3.7. contd.

Compound	**3.7**	**3.8**	**3.9**
empir. formula	$Cu_2C_{32}H_{26}N_6Cl_4$	$Cu_2C_{38}H_{38}N_6Cl_4$	$Cu_2C_{42}H_{38}N_6Cl_4O_2$
M_W	763.47	847.62	927.66
cryst. system	monoclinic	orthorhombic	monoclinic
space group	C2/c	$Pna2_1$	$P2_1/n$
a, Å	16.282(3)	15.295(3)	8.996(1)
b, Å	7.367(1)	9.059(1)	8.060(1)
c, Å	27.085(5)	26.601(5)	28.486(6)
α, deg.	-	-	-
β, deg.	101.28(3)	-	98.00(3)
γ, deg.	-	-	-
V, $Å^3$	3186(1)	3686(1)	2045.7(7)
Z	4	4	2
D_{calc}, g/cm^3	1.592	1.527	1.506
μ, mm^{-1}	1.704	1.481	1.345
2θ range, deg.	3.06 - 56.60	3.06 - 56.62	2.88 - 56.72
No. collected	19084	43741	24044
No. ind. (R_{int})	3900 (0.0331)	9011 (0.0924)	4985 (0.0591)
No. obsd. ($\|F_o\| > 4.0\sigma \|F_o\|$)	3135	5711	3528
R	0.0286	0.0476	0.0870
R_w	0.0695	0.1002	0.2496
$\Delta\rho_{max/min}$ ($eÅ^{-3}$)	0.285, -0.439	0.481, -0.450	1.697, -0.553
weights	0.0356, 2.4183	0.0515, 0	0.0886, 13.2506
CCDC Dep. No.	720344	733833	720343

Table 3.7. contd.

Compound	**3.10**	**3.11**	**3.12**·MeOH
empir. formula	$Cu_4C_{80}H_{60}N_{12}Cl_8$	$Cu_2C_{40}H_{52}N_6O_6B_2F_8$	$CuC_{61}H_{62}N_6OBF_4$
M_W	1727.2	1013.58	1045.52
cryst. system	triclinic	monoclinic	trigonal
space group	$P\bar{1}$	$P2_1/n$	$P3_221$
a, Å	9.706(2)	12.762(3)	13.254(1)
b, Å	11.325(2)	7.775(1)	13.254(1)
c, Å	17.322(4)	23.501(5)	27.214(5)
α, deg.	98.28(3)	-	-
β, deg.	94.85(3)	100.72(3)	-
γ, deg.	91.83(3)	-	-
V, $Å^3$	1875.6(7)	2291.4(8)	4140(1)
Z	1	2	3
D_{calc}, g/cm^3	1.529	1.469	1.258
μ, mm^{-1}	1.458	1.012	0.455
2θ range, deg.	2.38 - 58.14	3.52 - 56.62	3.00 - 56.60
No. collected	22968	27141	50470
No. ind. (R_{int})	9003 (0.0880)	5577 (0.0686)	6768 (0.0508)
No. obsd. ($\|F_o\| > 4.0\sigma \|F_o\|$)	3802	3355	4212
R	0.0481	0.052	0.0392
R_w	0.0946	0.1118	0.0917
$\Delta\rho_{max/min}$ ($eÅ^{-3}$)	0.548, -0.417	0.690, -0.569	0.349, -0.232
weights	0.0398, 0	0.0557, 2.1475	0.0501, 0.8649
CCDC Dep. No.	732508	720346	720345

Table 3.7. contd.

Compound	**3.12**·tol
empir. formula	$CuC_{74}H_{74}N_6BF_4$
M_W	1197.74
cryst. system	triclinic
space group	$P\bar{1}$
a, Å	11.677(2)
b, Å	16.261(3)
c, Å	17.077(3)
α, deg.	93.63(3)
β, deg.	97.30(3)
γ, deg.	96.26(3)
V, $Å^3$	3187(1)
Z	2
D_{calc}, g/cm^3	1.248
μ, mm^{-1}	0.402
2θ range, deg.	2.42 - 56.70
No. collected	40080
No. ind. (R_{int})	15294 (0.0596)
No. obsd. ($\|F_o\| > 4.0\sigma \|F_o\|$)	7089
R	0.0526
R_w	0.1221
$\Delta\rho_{max/min}$ ($eÅ^{-3}$)	0.300, -0.295
weights	0.0790, 0
CCDC Dep. No.	721175

References.

1 (a) E. J. Crust, I. J. Munslow, C. Morton, and P. Scott, *Dalton Trans.* 2004, **15**, 2257. (b) N. M. Scott, T. Schareina, O. Tok, and R. Kempe, *Eur. J. Inorg. Chem.* 2004, 3297-3304. (c) C. Morton, P. O'Shaughnessy, and P. Scott, *Chem. Comm.* 2000, 2099-2100.

2 T. Schareina, G. Hillebrand, H. Fuhrmann, and R. Kempe, *Eur. J. Inorg. Chem.* 2001, **9**, 2421.

3 I. N. Polyakova, Z. A. Starikova, V. K. Trunov, B. V. Parusnikov, and I. A. Krasavin, *Kristallografiya.*, 1980, **25**, 495.

4 P. C. Junk, W. Lu, L. I. Semenova, B. W. Skelton, and A. H. White, *Z. Anorg. Allg. Chem.*, 2006, **632**, 1303.

5 F. A. Cotton, L. M. Daniels, G. T. Jordan, and C. A. Murillo, *Polyhedron.* 1998, **17**, 589.

6 Y. Fang, C. Huang, Z. Zhu, X. Yu, and W. You,. *Acta Cryst.* 2006, **E62**, m3347-m3348.

7 S. Banthia ane A. Samanta, *Polyhedron.* 2006, **25**, 2269.

8 Sorrell, T. N.; Jameson, D. L. *J. Am. Chem. Soc.* 1983, **105**, 6013.

9 I. Sanyal, K. D. Karlin, R. W. Strange,and N. J. Blackburn, *J. Am. Chem. Soc.* 1993, **115**, 11259.

10 E. Spodine, J. Manzur, M. T. Garland, J. P. Fackler, R. J. Staples, and B. Trzcinska-Bancroft, *Inorg. Chim. Acta.*, 1993, **203**, 73.

11 B. Viossat, J. F. Gaucher, A. Mazurier, M. Selkti, and A. Tomas, *Z. Kristallogr.-New Cryst. Struct.*, 1998, **213**, 329.

12 G. E. Kostakis, E. Norlander, M. Haukka, and J. C. Plakatouras, *Acta Cryst.*, 2006, **E62**, m77.

13 L. Lu, S. Qin, P. Yang, and M. Zhu, *Acta Cryst.*, 2004, **E60**, m950.

14 X. Dai and T. H. Warren, *Chem. Commun.*, 2001, 1998.

15 J. M. Seco, U. Amador, and M. J. Gonzalez Garmendia, *Polyhedron*, 1999, **18**, 3605-3610.

16 D. Petrovic, L. M. R. Hill, P. G. Jones, W. B. Tolman, and M. Tamm, *Dalton Trans.*, 2008, 887.

17 M.-M. Yu, Y.-N. Zhang, and L.-H. Wei, *Acta Cryst.*, 2007, **E63**, m2380.

18 S. Youngme, J. Phatchimkun, U. Suksangpanya, C. Pakawatchai, G. A. van Albada, M. Quesada, and J. Reedijk, *Inorg. Chem. Commun.*, 2006, **9**, 242.

19 Spodine, E.; Manzur, J.; Garland, M.T.; Fackler, J.P.; Staples, R.J.; Trzcinska-Bancroft, B. (1993) *Inorg Chim Acta*, 203: 73.

20 Viossat, B.; Gaucher, J.F.; Mazurier, A.; Selkti, M.; Tomas, A. (1998) *Z. Kristallogr.- New Cryst. Struct*, 213:329.

21 Kostakis, G.E.; Norlander, E.; Haukka, M.; Plakatouras, J.C. (2006) *Acta Cryst*, E62:m77.

22 Healy MD, Gravelle PW, Mason MR, Bott SG, Barron AR (1993) *J Chem Soc Dalton Trans.*, 441-454.

23 Zunszain, P. A.; Shah, M. M.; Miscony, Z.; Javadzadeh-Tabatabaie, M.; Haylett, D. G.; Ganellin, C. R. *Arch. Pharm. Pharm. Med. Chem.* **2002**, *4*, 159.

24 Flack, H. D.; Bernardinelli, G. *J. Appl. Cryst.* 2000, **33**, 1143.

25 Clegg, W. *Acta Cryst.* 2003, **E59**, e2.

26 (a) A. L. Spek, *PLATON, A multipurpose Crystallographic Tool.* Utrecht University, Ulrecht. 2000. (b) A. L. Spek, *J. Appl. Cryst.*, 2003, **36**, 7.

Chapter 4

Effects of Remote Substitution of Ligand on Olefin Complexation

Introduction

The preceding chapter noted that the presence of a sterically imposing aryl group on the amine nitrogen (N_a) results in complexes having greater distortion about that nitrogen atom, and consequently, about the complexed atom (i.e., a metal center) as well. This chapter examines the copper(I)-olefin complexes of aryl-substituted dipyridylamines (Ar-dpa) and the concomitant structural changes associated with additional steric bulk on the amine nitrogen, specifically with regard to olefin binding.

Considering **I** and **II** below, there should be a clear steric consequence of the Ar-dpa ligand's butterfly conformation on the coordination of an olefin ligand. Based upon this observation, the complexation of a mono-substituted or *cis*-substituted olefin should be favored over complexation of a *trans*-substituted olefin in complexes having a higher degree of substituent bulk on the amine nitrogen. In other words, Ar-dpa ligands with sterically larger aryl substituents should yield complexes with greater distortion about the amine nitrogen, and therefore, greater propensity for isomeric differentiation of olefins. For example, for the *trans*-olefin complex (**I**), there should be inter-ligand interaction regardless of the olefin's approach to the metal center. In contrast, for the *cis*-olefin complex (**II**), steric interaction would be minimized (or avoided altogether), depending on the approach taken by the olefin to the metal center.

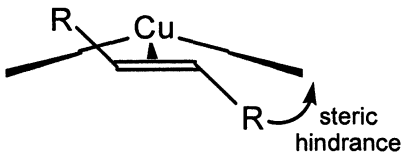

(I)

(II)

In Chapter 1, it was shown that the ^{1}H and ^{13}C NMR spectra of [Cu(H-dpa)(olefin)]BF_4 exhibit an upfield shift in the olefin signal as compared to free olefin. A comparison of the olefinic $\Delta\delta(^{13}C)$ values with olefin dissociation temperatures (determined by TG/DTA) in these complexes confirmed the shift of the olefin NMR resonances to be correlated to the strength of olefin binding in the complex. Thus, the ^{1}H and ^{13}C NMR spectral data can be a convenient means of comparing binding strength between complexes. Several complexes of the type [Cu(Ar-dpa)(η^2-olefin)]BF_4 have been prepared and characterized by ^{1}H and ^{13}C NMR, FTIR, and TG/DTA using the olefins styrene and norbornylene (Ar = Ph, Mes, 2-^{i}PrPh, and 1-naph), in addition to a number of internal *cis*- and *trans*-octene isomers (Ar = Mes, 2-^{i}PrPh).

Results and Discussion

The reaction of [Cu(MeCN)$_4$]BF_4 with styrene in the presence of the appropriate Ar-dpa results in the formation of the olefin complex, [Cu(Ar-dpa)(η^2-styrene)]BF_4 (Eq. 4.1) where Ar = Ph (**4.1**), Mes (**4.2**), (2-^{i}Pr)Ph (**4.3**), and naph (**4.4**). The analogous norbornylene derivatives, [Cu(Ar-dpa)(η^2-norbornylene)]X, where Ar = Mes with X = PF_6 (**4.5**) and (2-^{i}Pr)Ph with X = BF_4 (**4.6**), were also prepared using Mes-dpa (**2.5**) and ^{i}PrPh-dpa (**2.7**) as ligands, respectively.

The reaction of [Cu(MeCN)$_4$]BF_4 with either *cis* or *trans* 3-octene in the presence of the appropriate Ar-dpa results in the formation of the olefin complex, [Cu(Ar-dpa)(η^2-olefin)]BF_4, where Ar = H for *cis*-3-octene (**1.8**) and *trans*-3-octene (**1.9**);[35] Ar = Mes for *cis*-3-octene (**4.7**) and *trans*-3-octene (**4.8**); and Ar = 2-^{i}PrPh for *cis*-3-octene (**4.9**) and *trans*-3-octene (**4.10**). In addition the 4-octene derivatives were prepared, where Ar = 2-^{i}PrPh for *cis*-4-octene (**4.11**) and *trans*-4-octene (**4.12**).

$$[Cu(MeCN)_4]BF_4 + \text{Ar-dpa} + \text{styrene} \rightarrow [Cu(\text{Ar-dpa})(\eta^2\text{-styrene})]BF_4 + 4\ MeCN \quad (4.1)$$

Similar to their H-dpa analogs (see Chapter 1), compounds **4.1** - **4.12** are readily soluble in alcohols and other polar organic solvents, i.e. acetone and acetonitrile, although solutions of the latter have proven more difficult to re-isolate the olefin product. The complexes show fair solubility in solutions of dichloromethane and chloroform, while almost no solubility is seen in non-polar organic solvents. Moreover, each compound shows moderate instability, in the solid state, under atmospheric conditions (with regard to oxidation). In solution, the oxidation process is essentially instantaneous. Compounds **4.1** - **4.12** and have been characterized by ^{1}H and ^{13}C NMR, FT-IR, and TG/DTA. The structures of compounds **4.1** – **4.5** and **4.8** have been determined via X-ray crystallography.

The structures of the complex cations, $[Cu(Ar\text{-}dpa)(\eta^2\text{-styrene})]^+$, in compounds **4.1** - **4.4** are shown in Figure 4.1, Figure 4.2, Figure 4.4, and Figure 4.5, respectively. Selected bond lengths and angles are given in Table 4.1. Two independent molecules of the complex cation in compounds **4.2** and **4.4** are present in their respective asymmetric units (see Figure 4.3 and Figure 4.6). The fluoro-anions in **4.1** - **4.3** and **4.5** were observed to be disordered (Chapter 7). The structure of the complex cation, $[Cu(Ar\text{-}dpa)(\eta^2\text{-norbornylene})]^+$, in compound **4.5** is shown in Figure 4.7. Selected bond lengths and angles are compared with those of $[Cu(H\text{-}dpa)(nbn)]^+$ (**1.10**) in Table 4.2.

The copper atoms in compounds **4.1** - **4.5** are each coordinated to two pyridine nitrogen atoms and the appropriate olefin; consistent with three-coordinate Cu(I) cation. The Cu-N distances [1.949(3) - 1.973(3) Å] are within experimental error of the analogous ethylene and cyclohexene complexes [1.963(2) - 1.973(3) Å]. In a similar manner the Cu-C distances [1.972(5) - 2.064(2) Å] overlap the range for the previously reported derivatives [2.019(3) - 2.032(4) Å].

The styrene C=C bond lengths found in compounds **4.1** - **4.4** [1.371(6) - 1.395(6) Å] match well with the H-dpa (**1.12**) analog [1.387(8) Å], and appear longer than seen in free styrene [1.325(2) Å],[1] the Ag(I) H-dpa (**5.1**) complex [1.366(6) Å], as well as

compared to the cuprous PMDETA, bipy, and neutral β-diketiminato complexes [1.35(1) - 1.373(6) Å].[2] The C=C bond determined for compound **4.5** [1.361(5) Å] is somewhat lengthened compared to free norbornylene [1.334(1) Å],[3] and is slightly shorter than those observed in the neutral iminophosphanamide-norbornylene and diethylenetriamine (detn) complexes [1.37(2) and 1.38(2) Å, respectively],[14,4] as well as the H-dpa complex (**1.10**) $[Cu(H\text{-}dpa)(\eta^2\text{-norbornylene})]^+$ [1.388(7) Å].[15]

Distortion about the amine nitrogen can be seen in the N_a-C_{Ar} bond lengths comparing the free ligands Mes-dpa (**2.5**), 2-^{i}PrPh-dpa (**2.7**), and (1-naph)-dpa (**2.9**) with their corresponding olefin complexes, which exhibit a slight lengthening of the bond. Not surprisingly, the C_{py}-N_a-$C_{py'}$ bond angle is greater in complexes than in the free ligands, which is a result of the widening between pyridyl rings to accomodate the geometry necessary to chelate the metal center.

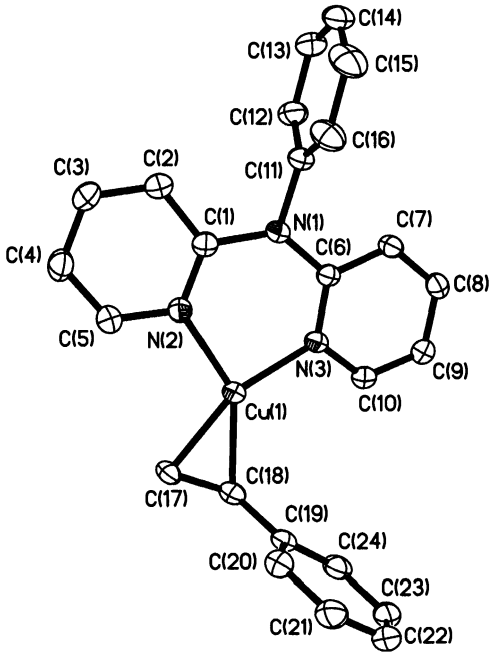

Figure 4.1. Structure of the $[Cu(Ph\text{-}dpa)(\eta^2\text{-styrene})]^+$ cation in compound **4.1**. Thermal ellipsoids are shown at the 30% level, and hydrogen atoms attached to carbon are omitted for clarity.

(a)

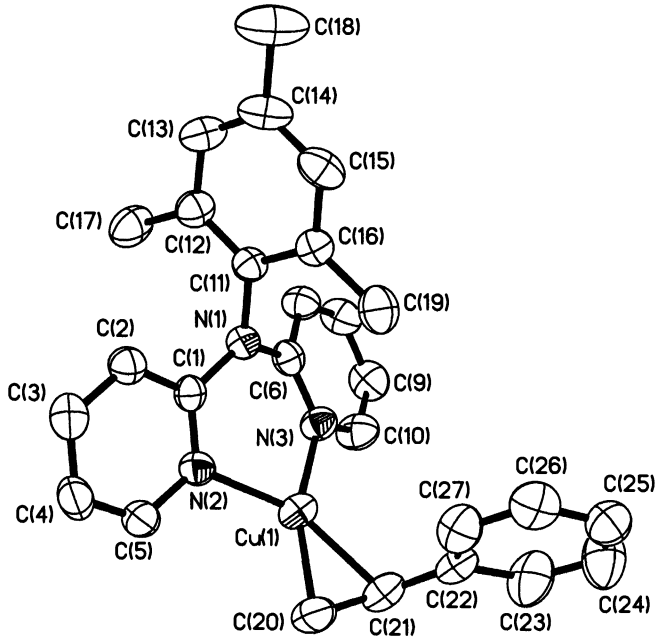

(b)

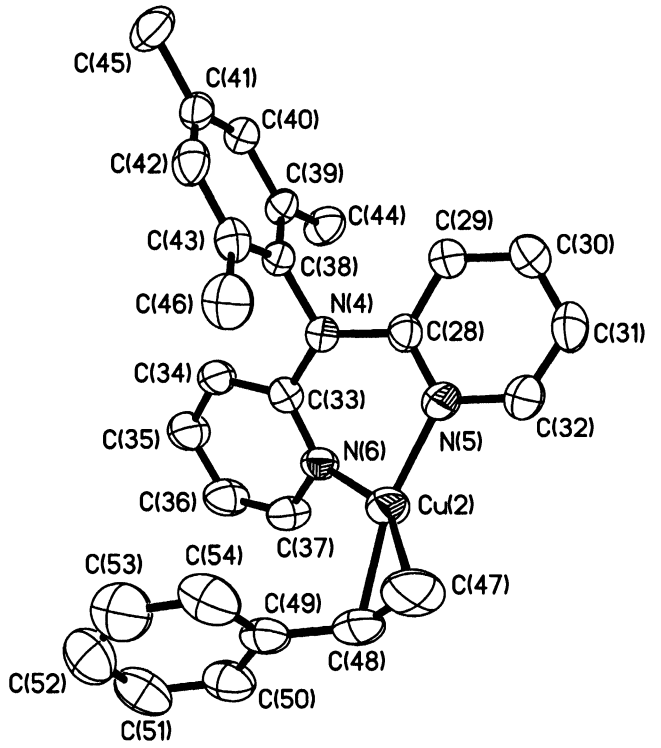

Figure 4.2. Molecular structure of the two unique conformers present in the asymmetric unit of compound **4.2**. Thermal ellipsoids are shown at the 30% level, and all hydrogen atoms are omitted for clarity.

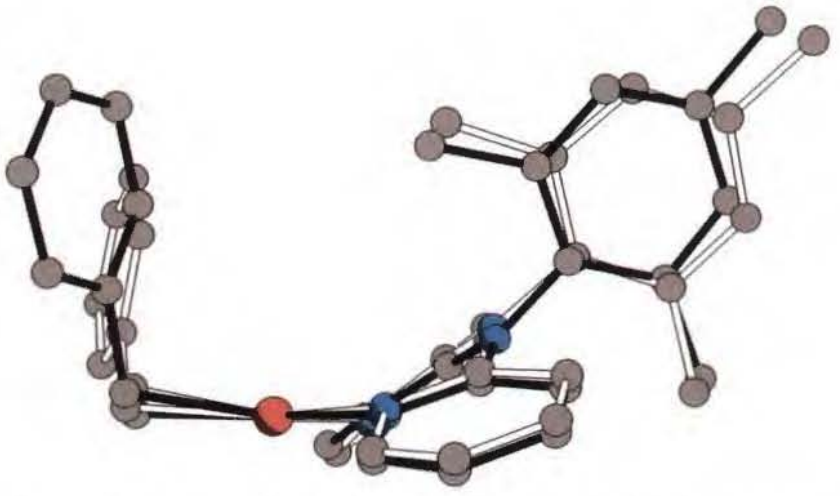

Figure 4.3. Comparison of unique conformers present in the asymmetric unit of compound **4.2**.

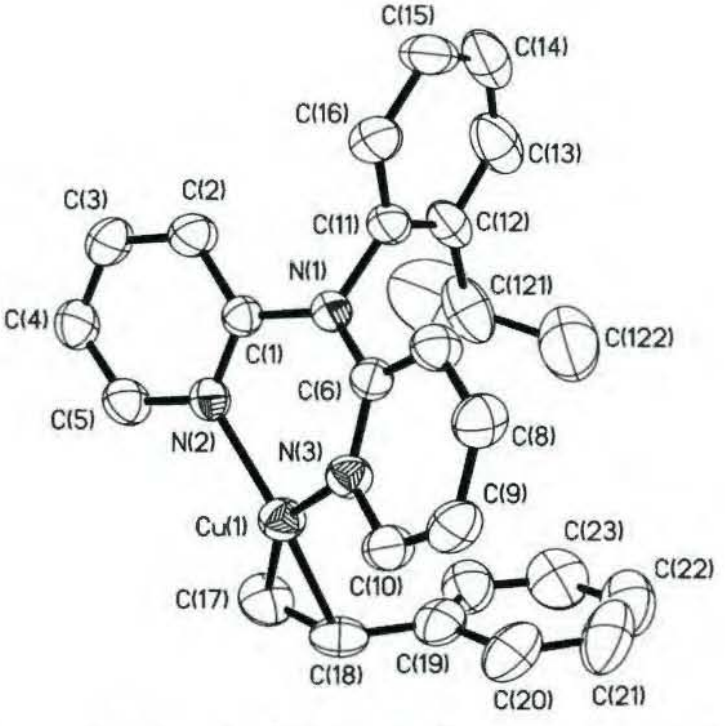

Figure 4.4. Structure of the [Cu(2-^{i}PrPh-dpa)(η^2-styrene)]$^{+}$ cation in compound **4.3**. Thermal ellipsoids are shown at the 30% level, and hydrogen atoms attached to carbon are omitted for clarity.

(a)

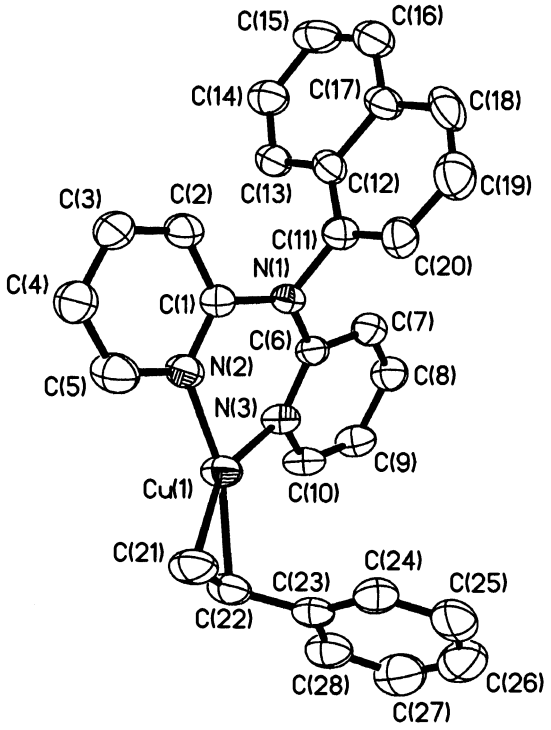

(b)

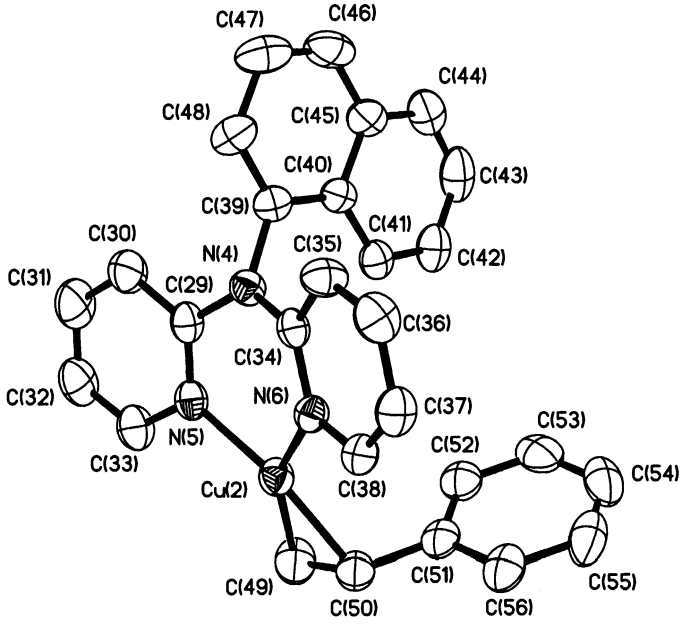

Figure 4.5. Molecular structure of the two unique molecules present in the asymmetric unit of compound **4.4**. Thermal ellipsoids are shown at the 30% level, and all hydrogen atoms are omitted for clarity.

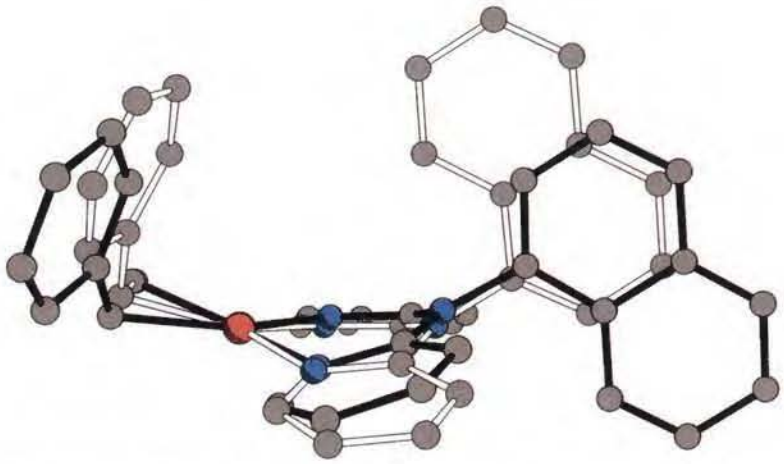

Figure 4.6. Comparison of the two crystallographically unique conformers of the [Cu(1-naph-dpa)(η^2-styrene)]$^+$ cation present in compound **4.4**.

Table 4.1. Selected bond lengths (Å) and angles (°) for [Cu(Ar-dpa)(η^2-styrene)]BF_4.

Compound	**4.1**	**4.2**[a]	**4.3**	**4.4**[a]
Ar =	Ph	Mes	(2-^{i}Pr)Ph	1-naph
Cu-C	1.984(2)	1.972(5), 1.981(6)	1.992(5)	1.978(4), 1.997(4)
Cu-C'	2.064(2)	2.042(5), 2.032(6)	2.022(5)	2.021(4), 2.027(4)
Cu-N	1.965(2)	1.968(4), 1.951(4)	1.958(3)	1.949(3), 1.956(3)
Cu-N'	1.956(2)	1.951(4), 1.965(4)	1.973(3)	1.968(3), 1.959(3)
C=C'	1.381(3)	1.372(7), 1.381(8)	1.395(6)	1.371(6), 1.393(6)
N_a-C_{Ar}	1.462(2)	1.455(5), 1.449(5)	1.461(5)	1.463(5), 1.437(4)
N-Cu-N'	95.20(7)	91.9(2), 92.3(2)	92.3(2)	94.0(1), 95.8(1)
C-Cu-C'	39.82(9)	39.9(2), 40.2(2)	40.7(2)	40.1(2), 40.5(2)
C_{py}-N-$C_{py'}$	130.5(2)	126.7(4), 126.5(4)	127.6(3)	129.0(3), 128.4(3)
Cu$^{\cdots}$N$_a$-C_{Ar}	171.5(1)	151.2(3), 159.7(3)	149.5(3)	155.8(2), 147.9(2)
N'$^{\cdots}$N$^{\cdots}$C=C'	1.8(2)	11.1(4), 7.3(5)	5.4(4)	9.7(3), 2.1(3)
$\Delta MPLN_{[py...py']}$	15.9(1)	28.9(2), 33.3(2)	28.9(2)	22.7(2), 23.1(2)

[a] Two unique conformers in the asymmetric unit.

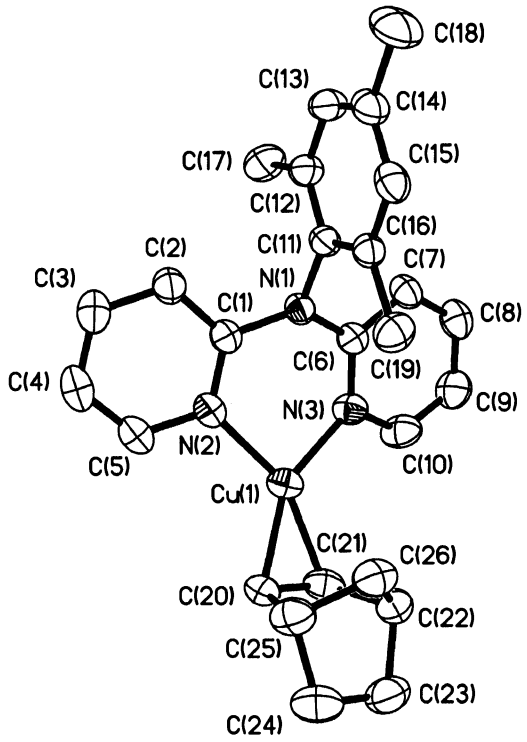

Figure 4.7. Structure of the cation in compound **4.5**. Thermal ellipsoids are shown at the 30% level, and hydrogen atoms attached to carbon are omitted for clarity.

Table 4.2. Selected bond lengths (Å) and angles (°) for [Cu(Ar-dpa)(η^2-norbornylene)]$^+$.

R	H (**1.10**)	Mes (**4.5**)
Cu-C	2.026(6)	2.027(3)
Cu-C'	2.030(6)	2.007(4)
Cu-N	1.957(5)	1.957(3)
Cu-N'	1.962(5)	1.961(3)
C=C'	1.388(7)	1.361(5)
N_a-C_{Ar}	-	1.466(4)
Cu···H	2.46	2.46(4)
N(2)-Cu(1)-N(3)	97.7(2)	94.0(1)
C-Cu(1)-C'	40.0(2)	39.5(2)

For a *trans*-olefin (**I**) there will be inter-ligand interactions irrespective of the olefin conformation, while for a *cis*-olefin (**II**) the substituents could adopt a conformation that would limit steric interactions. The alternative view of the norbornylene complex cation $[Cu(Ar\text{-}dpa)(\eta^2\text{-norbornylene})]^+$ in compound **4.5** (Figure 4.8) shows the preferred orientation of a *cis*-substituted olefin with its substituents away from the Ar-dpa ligand.

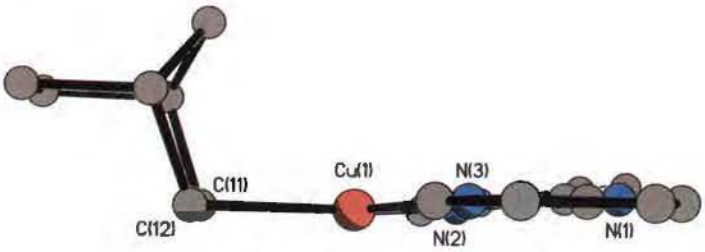

(1.10)

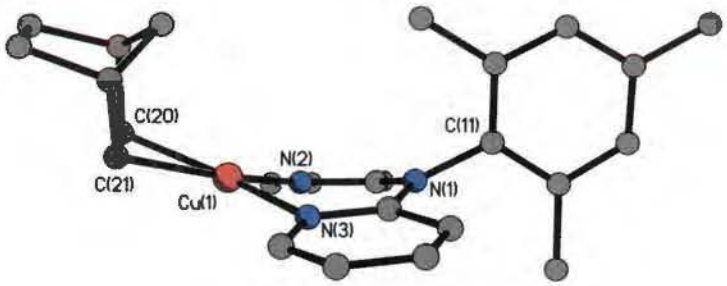

(4.5)

Figure 4.8. Comparison of the $[Cu(R\text{-}dpa)(\eta^2\text{-norbornylene})]^+$ cations in **1.10** and **4.5** showing the preferred orientation of the *cis*-substituted olefin and the Mes-dpa ligand.

As was observed in compound **1.10**, the crystal structure of **4.5** also exhibits an agostic C-H···M close contact[5] interaction [2.46(2) Å] between the copper center and the norbornyl hydrogen-atom located on the double-bond side of the five-membered ring. This distance is consistent with previously reported ranges of 2.32 - 2.88 Å within a cuprous *bis*(imidazolin-2-imine) compound.[6]

The aforementioned presence of *ortho*-substitution in the uncomplexed Ar-dpa compounds results in a significant distortion of the coordination around the amine nitrogen, N_a. Additional distortions, resulting in the ligand to fold along the Cu···N vector, occur when the ligand is bound to a copper center. In the olefin complexes (**4.1** - **4.4**), both of these deformations are observed.

More significantly, however, the folding along the Cu···N vector (i.e., formation of a butterfly conformation) is related to the size of the ligand's aryl group (Figure 4.9). This is also amply demonstrated by a comparison of the ligand dpa and styrene conformations for the two crystallographically unique conformers of the [Cu(1-naph-dpa)(η^2-styrene)]$^+$ cation present in compound **4.4**, Figure 4.6.

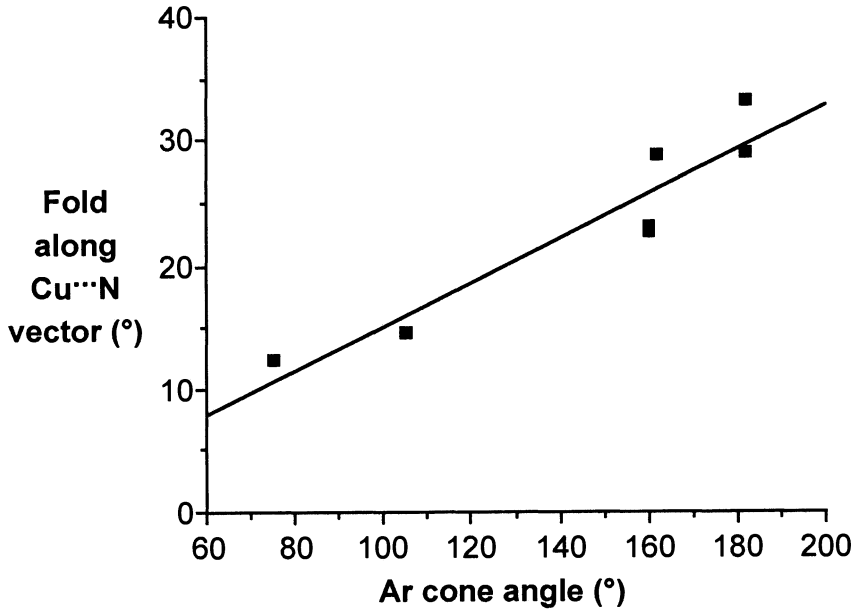

Figure 4.9. Plot of the folding of the Ar-dpa ligand as a function of the substituent's cone angle (°) for [Cu(Ar-dpa)(η^2-styrene)]$^+$.

The increased folding of the Ar-dpa ligand can be seen from the [Cu(Ar-dpa)(η^2-styrene)]$^+$ cations viewed down the Cu···N vector (Figure 4.10). Furthermore, this demonstrates there exists a clear steric consequence of the butterfly conformation of the

Ar-dpa ligand on the olefin ligand. Based upon this observation we propose that the complexation of a mono-substituted or *cis*-substituted olefin should be favored over complexation of a *trans*-substituted olefin in complexes where the Ar-dpa ligand has the most distortion due to a sterically large aryl substituent (Ar).

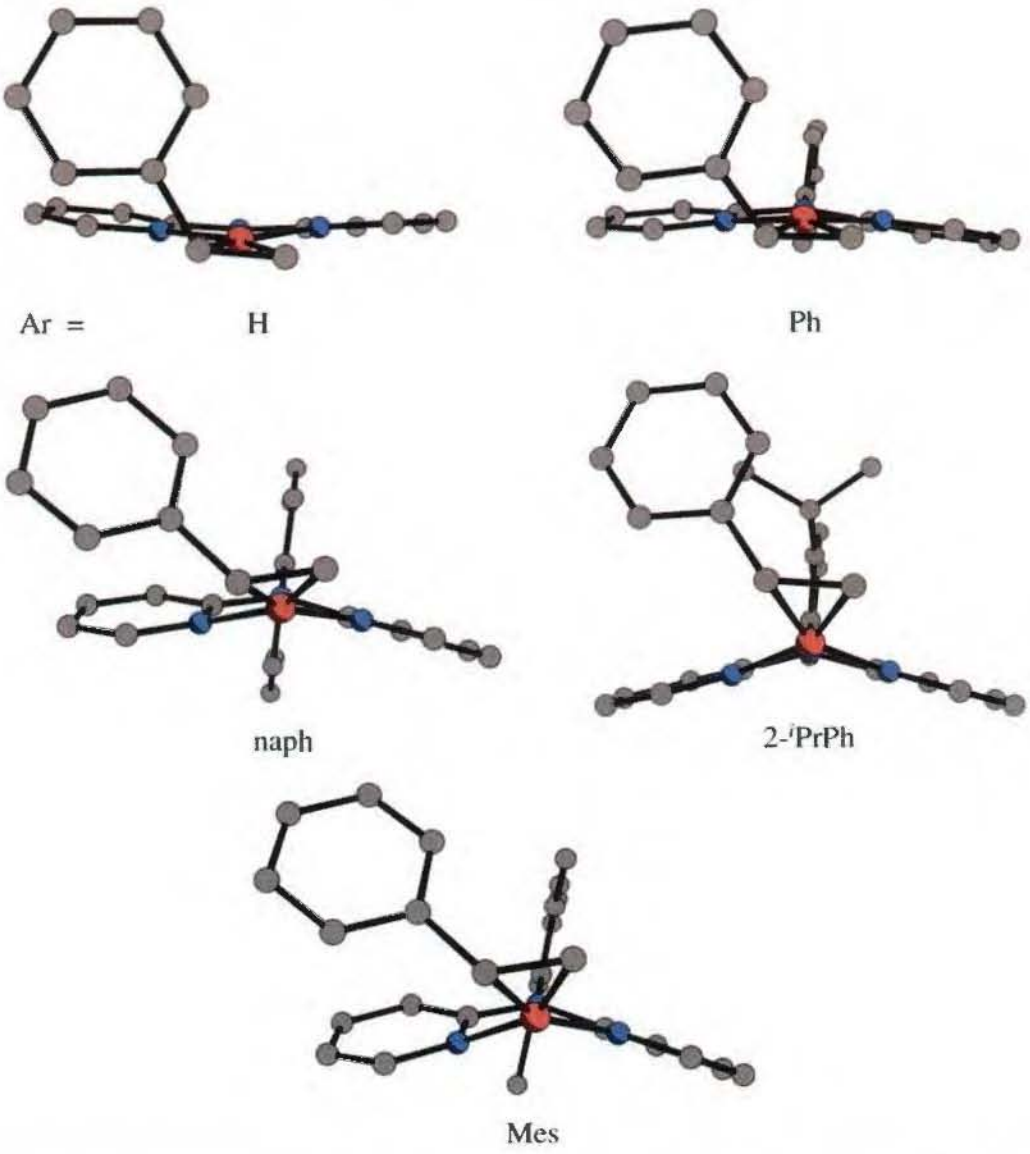

Figure 4.10. The folding of the Ar-dpa ligand in the $[Cu(Ar\text{-}dpa)(\eta^2\text{-styrene})]^+$ cations as viewed along the Cu···N vector, for Ar = H (**1.12**), Ph (**4.1**), 1-naph (**4.4**), (2-^{i}Pr)Ph (**4.3**) , and Mes (**4.2**).

Crystal packing in compound **4.1** (Figure 4.11) shows a number of intermolecular interactions, including Cu···Ph_{sty} π-interaction, py···py' π-stacking in adjacent molecules. Moreover, Cu···O and hydrogen-bonding interactions with the BF_4^- anion are observed with the ethanol solvent of crystallization molecule.

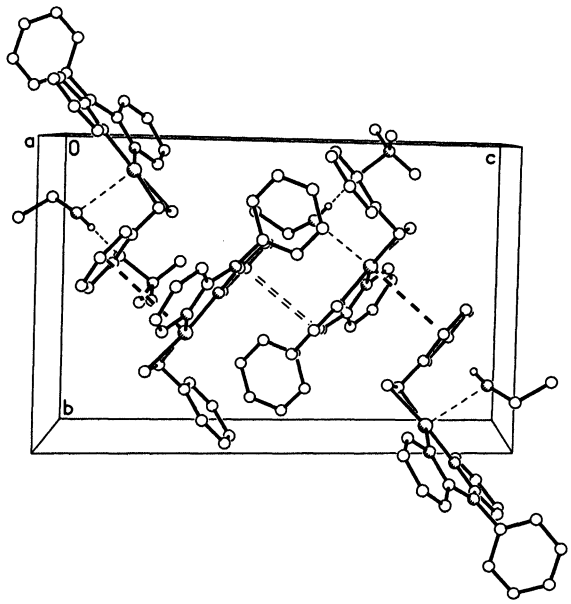

Figure 4.11. Molecular packing diagram of compound **4.1** viewed along the *a*-axis; Cu···Ph_{sty} π-interactions shown as bold dashed lines, π-π stacking between pyridyl rings shown as double-dashed lines, Cu···O interactions and H-bonding between ethanol solvent molecule and BF_4^- anion shown as single thin dashed lines.

In Chapter 1, it was demonstrated that the bond distances around copper in [Cu(H-dpa)(η^2-olefin)]$^+$ do not correlate well with changes in binding constant. Instead it was shown that the difference in the ^{1}H and ^{13}C NMR shift values between free and complexed olefins can be used to compare binding interactions. Additionally, they compare well with the temperature of dissociation of the olefin in the solid state as determined by TGA. Figure 4.12 shows that the change in the ^{1}H and ^{13}C chemical shifts for the styrene ligand in [Cu(Ar-dpa)(η^2-styrene)]$^+$ as compared to uncomplexed styrene

(i.e., Δδ) is indeed related to the stability of the Cu···styrene interaction as determined by the compound's decomposition temperature.

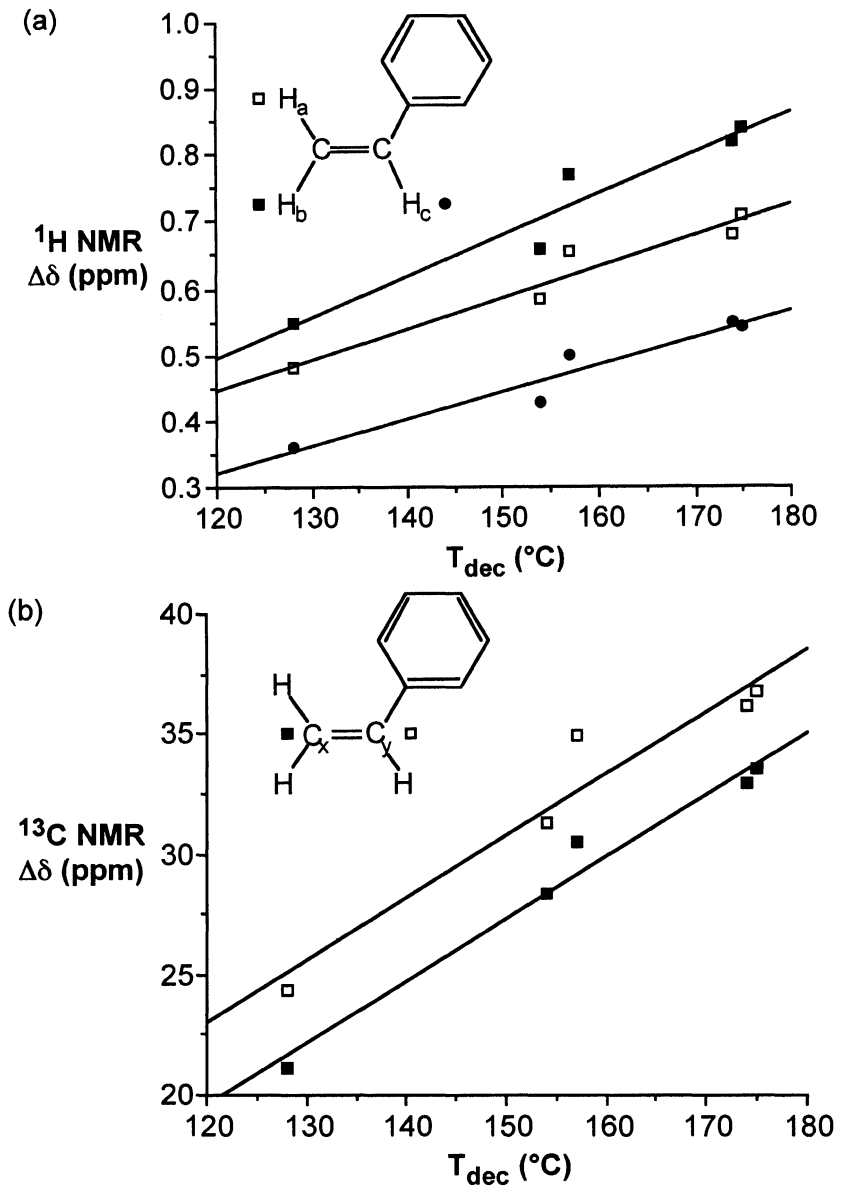

Figure 4.12. Plots of the difference in chemical shift (Δδ) for styrene (a) ^{1}H and (b) ^{13}C NMR spectra between free styrene and [Cu(Ar-dpa)(η^2-styrene)]BF_4 versus the temperature for dissociation of the styrene. R^2 values are as follows: (a) □ = 0.922, ■ = 0.897, ● = 0.906 (b) ■ = 0.967, □ = 0.932.

Thus, the binding efficiency of an olefin to the copper is affected by the identity of the remote aryl substituent. In the case of the aryl substituted ligands (i.e., Ar-dpa), the binding efficiency follows the order: Ph << 1-naph < 2-^{i}PrPh < Mes. In fact, the complex stability is directly related to the steric bulk (cone angle) of the aryl, see Figure 4.13.

It is interesting, however, that the complex of the parent ligand (H-dpa) shows a complex stability almost equal to that of the Mes-dpa complex, despite the difference in steric bulk, and hence folding of the ligand. This result reinforces the idea that the stability of the Cu···olefin interaction is controlled by both electronic and remote steric effects.

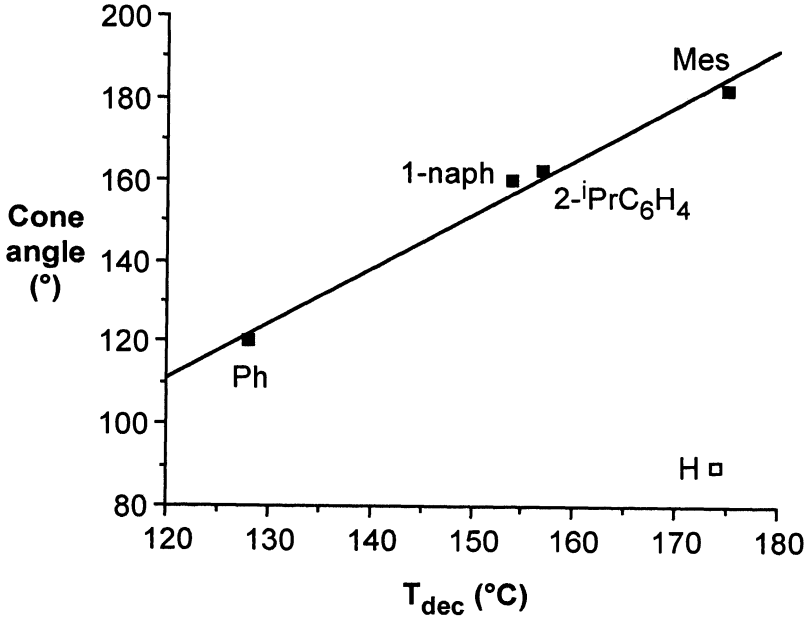

Figure 4.13. Plot of relationship between the temperature for dissociation of the styrene in [Cu(Ar-dpa)(η^2-styrene)]BF_4 as a function (R^2 = 0.988) of the aryl substituent Tolman cone angle (°). The value for the parent [Cu(Ar-dpa)(η^2-styrene)]BF_4 is shown for comparison (□).

A strong Cu···olefin interaction is enabled by either an electron donating substituent at the central nitrogen of the dpa ligand or a sterically large substituent at the central nitrogen of the dpa ligand. The first effect is presumably due to the increased electron density on copper and thence increased π back-donation to the olefin. We propose that the second effect is due to the increased folding of the dpa ligand, resulting in a decrease in intra-complex inter-ligand steric hindrance, which allows for a tighter binding of the olefin to the copper.

The structures of the two unique conformations of the complex cation, [Cu(Mes-dpa)(η^2-*trans*-3-octene)]$^+$, in compound **4.8** are shown in Figure 4.14. The two conformations are related by some non-crystallographic symmetry element, but are shown to be unique in other structural aspects. Selected bond lengths and angles are given in Table 4.3.

Both conformers of **4.8** exhibit a pseudo-trigonal planar geometry about the copper centers, with coordination sites occupied by the two pyridine nitrogen atoms and the approximate midpoint of the olefin C=C bond. The Cu-N distances for each are within experimental error of one another, and are consistent with the [Cu(Ar-dpa)(η^2-styrene)]BF_4 complexes (**4.1** - **4.4**) where Ar = Ph, Mes, 2-^{i}PrPh, and 1-naph [1.949(3) - 1.973(3) Å], as well as [Cu(H-dpa)(η^2-olefin)]X, where olefin = 1-octene (**1.5**), *cis*-2-octene (**1.6**), *cis*-3-octene (**1.8**), norbornylene (**1.10**), 1,5-cyclooctadiene (**1.11**), styrene (**1.12**), *cis*-stilbene (**1.13**), ethylene, and cyclohexene [1.957(3) - 1.979(4) Å].[35]

In a similar manner, the Cu-C distances overlap the range found for similar derivatives [1.972(5) - 2.087(4) Å]. Regarding the geometry about the amine nitrogen, the N_a-C_{py} and N_a-C_{Ar} bond lengths and the C-N_a-C angles observed in the complexed Mes-dpa ligand are within error of those seen in the free ligand (**2.5**) [N_a-C_{py} = 1.398(3), 1.411(3), and N_a-C_{Ar} = 1.439(3) Å; C_{py}-N_a-C_{Ar} = 118.3(2), 117.6(1) and C_{py}-N_a-$C_{py'}$ = 124.0(2)°].

(a)

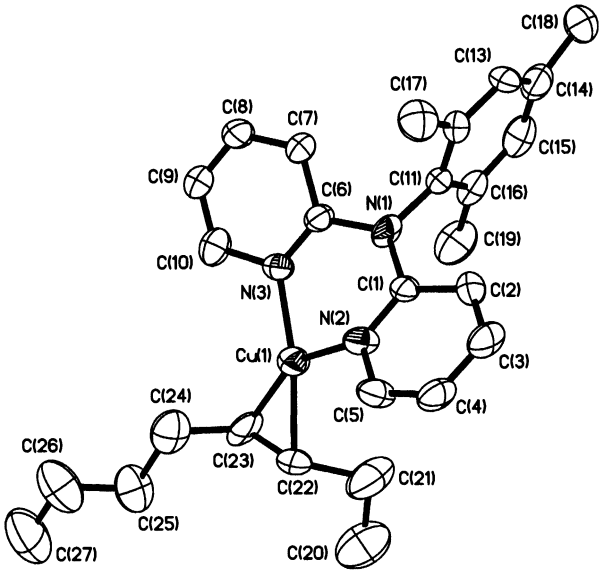

(b)

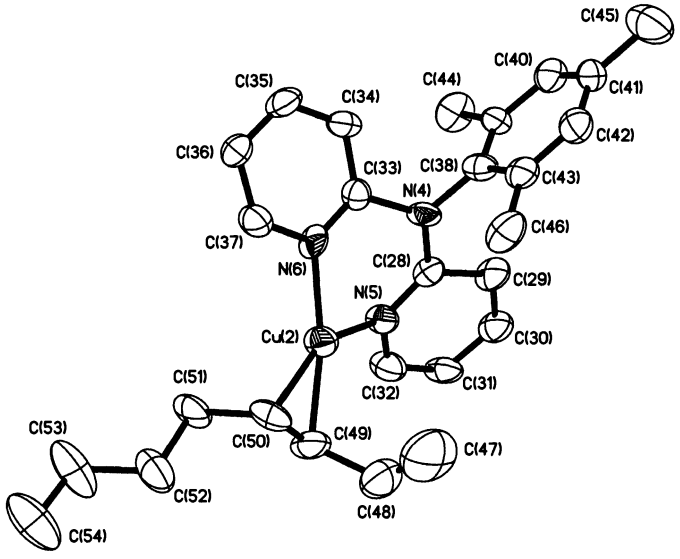

Figure 4.14. Molecular structures of the two unique cation conformers in **4.8**. Thermal ellipsoids are shown at the 30% level, and hydrogen atoms are omitted for clarity.

Table 4.3. Selected bond lengths (Å) and angles (°) in the conformers of **4.8**.

	conf. a	conf. b
Cu-C	2.038(7)	2.016(8)
Cu-C'	2.014(7)	2.059(6)
Cu-N	1.967(5)	1.980(5)
Cu-N'	1.936(5)	1.991(6)
C=C'	1.36(1)	1.39(1)
N_a-C_{Ar}	1.435(9)	1.416(9)
N-Cu-N'	92.9(2)	92.5(2)
C-Cu-C'	39.3(3)	40.0(3)
C_{py}-N-$C_{py'}$	125.2(6)	122.5(6)
C_{py}-N-C_{Ar}	119.3(5)	121.8(5)
$C_{py'}$-N-C_{Ar}	115.5(5)	115.1(6)
Cu···N_a-C_{Ar}	156.0(5)	159.0(5)
TWIST	11.2(6)	2.5(7)
$\Delta MPLN_{[py-py']}$	32.2(4)	34.5(4)

Several aspects of the geometries in determined structures of both conformers in **4.8** are consistent with trends observed in the other copper complexes incorporating aryl-functionalized *bis*(2-pyridyl)amines (**4.1** - **4.5**). As may be seen from Figure 4.15, a correlation exists between the C_{py}-N-$C_{py'}$ bond angle and the fold of the Ar-dpa ligand (i.e. the mean-plane angle difference between pyridyl rings), as well as the out of plane bend of the aryl substituent (i.e. the angle resulting from Cu···N_a-C_{Ar}).

Munakata *et al.* have previously demonstrated that ^{1}H NMR can be used to assess the binding efficacy of various ligand/olefin combinations in Cu(I) olefin complexes,[34] while we have used similar methods for Lewis acid-base complexes.[7]

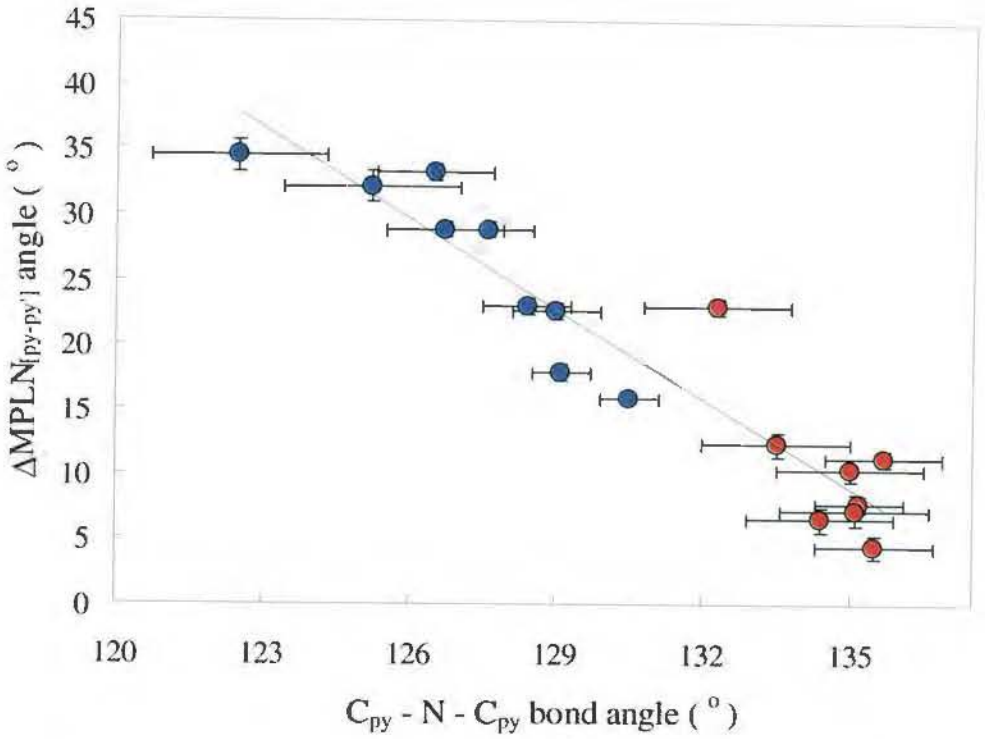

Figure 4.15. Relation between the fold angle [$\Delta MPLN_{(py\text{-}py')}$] and the C_{py}-N_a-$C_{py'}$ bond angle in [Cu(Ar-dpa)(olefin)]$^+$ cations for Ar = H (●) and Ar = Ph, Mes, 2-^{i}PrPh, and 1-naph (●); $R^2 = 0.89$.

As mentioned above, the change in NMR shift ($\Delta\delta$) correlates with the decomposition temperature (T_{dec}) of the complex, which is essentially the dissociation temperature of the olefin from the complex (determined by change in mass fraction in TG/DTA measurements). Thus, the change in chemical shift for Ar-dpa type complexes is a direct measure of the relative stabilities of complexes as a whole, and thus a measure of the strength of the metal-olefin bond in the respective copper complex. In the class of compound at hand (i.e. internal olefins), the $\Delta\delta(^{13}C)$ from NMR data results in a reasonably linear trend with dissociation temperatures (Figure 4.16). This also shows *trans*- complexes to have generally lower values for their dissociation temperatures than do their *cis*- analogs.

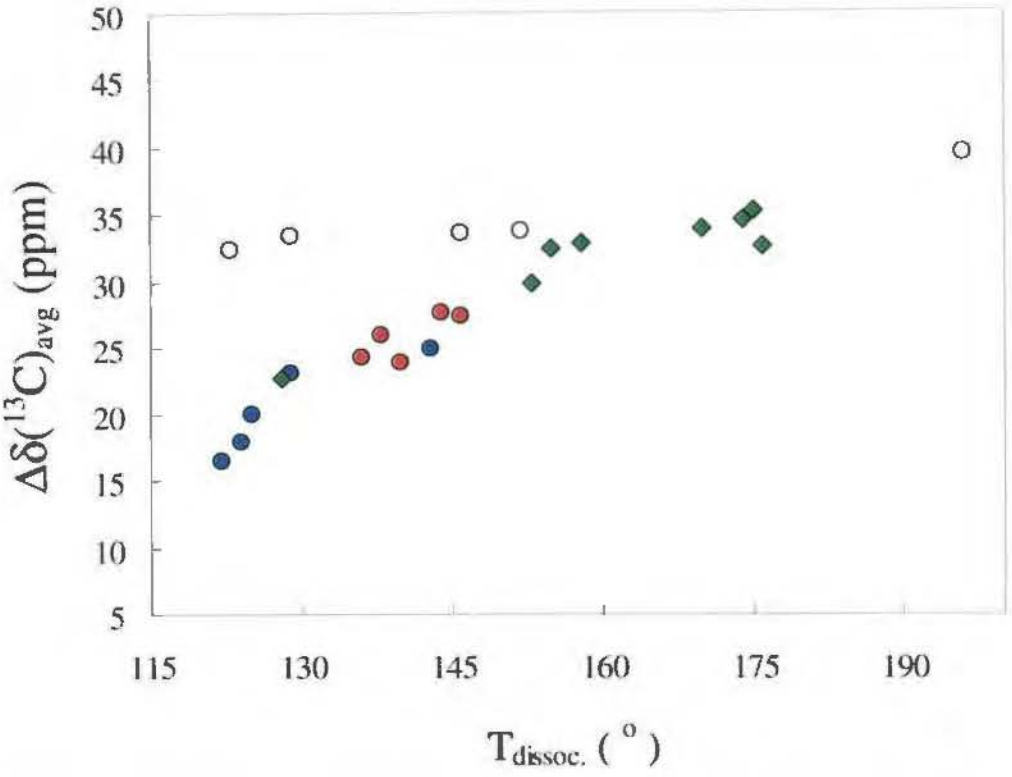

Figure 4.16. Overall trend observed between $\Delta\delta(^{13}C)$ and dissociation temperature for R-dpa (R = H, Ph, Mes, 2-^{i}PrPh, and naph) complexes of various olefin types (O = terminal alkyl, ● = *cis*-octenes, ● = *trans*-octenes, ◆ = sty/nbn).

The ^{13}C NMR spectra of [Cu(Ar-dpa)(olefin)]BF_4 exhibit an upfield shift in the olefin signal as compared to free olefin (consistent with the difference between complexed and free olefin). In simple terms, the further upfield (lower δ) peaks are, the more complexed the olefin. A consideration of the data in Table 4.4 shows that the change in the ^{13}C NMR shifts upon coordination is greater for *cis* isomers than corresponding *trans* isomers.

The binding of the *cis* isomers of both 3-octene and 4-octene to the copper center is observed to be stronger than the that for *trans* isomers, as evident from the NMR spectral data. This trend is consistent with the concept that the folded Ar-dpa ligand

provides a steric differentiation between *trans* and *cis* olefins (i.e., **I** versus **II**). Using the alteration in the ^{13}C NMR shift of the C=C unit upon coordination (i.e. $\Delta\delta$ values), it is possible to compare the differentiation in binding efficiency as a function of the Ar group.

Table 4.4. Olefin dissociation temperatures (°C) and the upfield shift, $\Delta\delta(^{13}C)$ in ppm, for olefin resonances in ^{13}C NMR spectra upon coordination in complexes [Cu(Ar-dpa)(η^2-olefin)]BF_4.

Ar	olefin	$\Delta\delta(C_x)$	$\Delta\delta(C_y)$	$T_{dis.}$
H	*cis*-3-octene	27.80	27.40	143-146
H	*trans*-3-octene	24.80	25.00	144-146
Mes	*cis*-3-octene	24.01	23.68	135-137
Mes	*trans*-3-octene	20.06	19.95	123-125
2-^{i}PrPh	*cis*-3-octene	26.07	25.78	134-136
2-^{i}PrPh	*trans*-3-octene	16.46	16.35	122-124
2-^{i}PrPh	*cis*-4-octene	24.20	-	136-138
2-^{i}PrPh	*trans*-4-octene	17.85	-	121-123

Consideration of Figure 4.17 shows that while there is a small difference between $\Delta\delta$ values for *cis*-3-octene versus *trans*-3-octene in the parent H-dpa complex,[35] the difference in $\Delta\delta$ increases with increased steric bulk: H < Mes << 2-^{i}PrC$_6$H$_4$. Again this result is consistent with the proposed concept of steric differentiation as a consequence of the folding of the Ar-dpa ligand. We have previously shown that ligand folding increases as the degree of substituent bulk is increased. Perhaps more importantly, the steric asymmetry (2-^{i}PrPh versus 2,6-^{i}Pr$_2$Ph) of the substituent has also proven to increase

ligand folding. This suggests that the preferential complexation of *cis* versus *trans* isomers should be most apparent in the 2-^{i}PrPh-dpa complex, which is indeed observed.

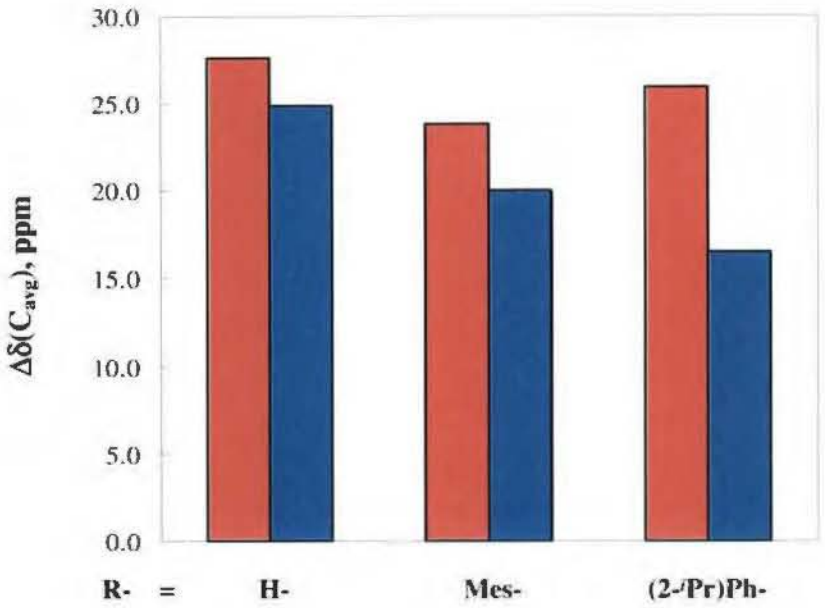

Figure 4.17. Comparison of averaged $\Delta\delta(^{13}C)$ values for olefin resonances in *cis*- (■) and *trans*- (■) 3-octene complexes [Cu(Ar-dpa)(3-octene)]BF_4 as the substituent Ar is varied.

The IR spectra for the complexes generally feature moderate alkyl $\nu_{C\text{-}H}$ stretching bands, while the aromatic and olefinic $\nu_{C\text{-}H}$ bands, if present, are very weak with respect to those in the free ligand/olefin. Several strong signals from aromatic ring stretching are present in the 1600 - 1400 cm^{-1} region, which unfortunately cause some ambiguity in the assignment of the alkene $\nu_{C=C}$ stretching band. As a result, no assessment of the olefin C=C double bond could be made from the IR spectral data. The most apparent feature in the IR spectral data is the $\nu_{B\text{-}F}$ band,[8] which is very broad (1060 - 1020 cm^{-1}) and usually the most intense signal in the spectrum. The 3° aromatic amine $\nu_{C\text{-}N}$ stretching also

exhibits intense bands, and are observed at slightly higher wavenumber (1324 - 1328 cm^{-1}) than seen in the corresponding free ligands (1317 and 1319 cm^{-1}).

Conclusions

We have shown that for a range of aryl-substituted *bis*(2-pyridyl)amine ligands the presence of *ortho*-substitution in the uncomplexed Ar-dpa compounds results in a significant distortion of the coordination around the amine nitrogen (in the solid state) and twisting of the two pyridyl rings with respect to each other. Thus, the steric bulk of the aryl substituents have a controlling influence on the orientation of the pyridyl rings.

The stability of the Cu···olefin interaction is controlled by both electronic and remote steric effects. Interestingly, the complex of the parent ligand (H-dpa) shows a complex stability almost equal to that of the Mes-dpa complex, despite the difference in steric bulk, and hence folding of the ligand. A strong Cu···olefin interaction is enabled by either an electron donating substituent at the central nitrogen of the dpa ligand or a sterically large substituent at the central nitrogen of the dpa ligand. The first effect is presumably due to the increased electron density on copper and thence increased π back-donation to the olefin. We propose that the second effect is due to the increased folding of the dpa ligand, resulting in a decrease in intra-complex inter-ligand steric hindrance, and thus allowing for a tighter binding of the olefin to the copper.

The presence of *ortho*-substitution in the complexed Ar-dpa compounds, in which the two pyridyl rings are constrained by a complexed atom, results in the bending-up of the aryl ring substituent out of the pyridyl plane. Associated with this is a consequential folding of the two pyridyl into a "butterfly" conformation. For olefin complexes of the type [Cu(Ar-dpa)(η^2-styrene)]BF_4, the increased steric bulk of the aryl group results in the folding of the dpa ligand and the subsequent facial differentiation of the complex so as to favor *cis*- or mono-substituted olefins. In addition, binding interaction of the olefin with the copper is controlled by the steric bulk of the remote aryl group.

The ^{1}H and ^{13}C NMR spectra of [Cu(Ar-dpa)(η^2-olefin)]BF_4 exhibit olefin resonances shifted upfield with respect to the corresponding free olefin. The difference in relative magnitudes of $\Delta\delta(^{13}C)$ between *cis*- and *trans*- complexes, i.e., the degree of π^* back-donation in *cis*- versus *trans*- complexes, correlates with the degree of substitution at the amine nitrogen. The identity of the remote ligand substituent (Ar) controls the differentiation of binding between *cis*- and *trans*- isomers as a consequence of increased folding of the Ar-dpa ligand along the Cu···N axis.

Experimental

[Cu(Ph-dpa)(η^2-styrene)]BF_4 (4.1) In a drybox, [$Cu(MeCN)_4$]BF_4 (0.314 g, 1.0 mmol) and Ph-dpa (0.247 g, 1.0 mmol) were charged to separate schlenk flasks. After removal from the drybox, EtOH (15 mL) was added via cannula to the flask containing the ligand, which was stirred to dissolve the solid. Styrene (ca. 3 mL) in EtOH (12 mL) was added via cannula to the flask containing the copper precursor. After stirring for one hour, the ligand solution was added to the copper-olefin mixture, and the combined solutions were stirred under an argon atmosphere for 6 hours. The solution volume was then reduced under vacuum by approximately half, warmed gently with a water bath to redissolve the product, and then filtered through a medium porosity glass frit to remove insoluble impurities. Argon was vigorously bubbled through the resulting pale green solution to further reduce its volume to ca. 5 - 10 mL. The solution was gently warmed to dissolve any precipitate, and upon cooling to –12 °C for several days, yielded colorless crystals of the ethanol solvate. Yield: 0.203 g (37%). Mp (TGA; decomp.) 128 °C. FTIR (neat, ATR, cm^{-1}): 3136 (w, aromatic $\nu_{C\text{-}H}$), 3102 (w, aromatic $\nu_{C\text{-}H}$), 3079 (w, alkene $\nu_{C\text{-}H}$), 3056 (w, alkene $\nu_{C\text{-}H}$), 3037 (w, alkene $\nu_{C\text{-}H}$), 1596 (s), 1572 - 1430 (s, aromatic $\delta_{C=C}$), 1328 (s), 1237 (m, aromatic $\delta_{C=N}$), 1063-1021 (br vs). ^{1}H NMR (298 K; CD_3OD): δ 8.06 (2H, br s, C*H*, *6,6'*-py), 7.83 (2H, br t, C*H*, *4,4'*-py), 7.51 (2H, br t, *m*-C*H*, Ph), 7.46 (1H, br s, *p*-C*H*, Ph), 7.43 (2H, mult., *o*-C*H*, styrene), 7.26 (2H, mult., *m*-C*H*, styrene), 7.22

(2H, br s, C*H*, Ph), 7.19 (1H, mult., *p*-C*H*, styrene), 7.17 (2H, br t, C*H*, *5,5'*-py), 6.93 (2H, br d, C*H*, *3,3'*-py), 6.29 [1H, dd, *J*(H-H) = 16.4 Hz, *J*(H-H) = 10.0 Hz, C*H*Ph], 5.13 [1H, d, *J*(H-H) = 16.4 Hz, *cis*-C*H*, Ph], 4.67 [1H, d, *J*(H-H) = 10.0 Hz, *trans*-C*H*, Ph], 3.60 [2H, q, *J*(H-H) = 6.9 Hz, OCH_2CH$_3$], 1.17 [3H, t, *J*(H-H) = 6.9 Hz, OCH$_2$CH_3]. ^{13}C NMR (298 K; CD_3OD): δ 157.10, 150.21, 143.48, 142.14, 138.70, 132.15, 129.94, 129.52, 129.11, 128.61, 127.18, 121.44, 120.35, 116.06 (H_2C=*C*H), 89.69 (H_2*C*=CH), 58.42 (O*C*H$_2$CH$_3$), 18.50 (OCH$_2$*C*H$_3$).

[Cu(Mes-dpa)(η^2-styrene)]BF$_4$ (4.2). This compound was prepared in an analogous manner to that of compound **4.1**, using 2-butanol as solvent and compound Mes-dpa as ligand. Yield: 61%. Mp (TGA; decomp.) 174 °C. FTIR (neat, ATR, cm^{-1}): 3100 (w, aromatic $\nu_{C\text{-}H}$), 3077 (w, alkene $\nu_{C\text{-}H}$), 3026 (w, alkene $\nu_{C\text{-}H}$), 2982 (w, alkyl $\nu_{C\text{-}H}$), 2918 (w, alkyl $\nu_{C\text{-}H}$), 2858 (w, alkyl $\nu_{C\text{-}H}$), 1598 (s), 1580 - 1426 (s, aromatic $\delta_{C=C}$), 1329 (s), 1233 (m, aromatic $\delta_{C=N}$), 1164 (m), 1046 (br vs). ^{1}H NMR (298 K; CD_3OD): δ 8.33 (2H, br d, C*H*, *6,6'*-py), 7.73 [2H, ddd, *J*(H-H) = 8.9 Hz, *J*(H-H) = 7.3 Hz, *J*(H-H) = 2.0 Hz, *m*-sty], 7.46 (2H, m, C*H*, *4,4'*-py), 7.24-7.18 (3H, m, C*H*, *3,3'*-py and *p*- C*H*, styrene), 7.18 (2H, s, *m*-C*H*, Mes), 7.13 [2H, ddd, *J*(H-H) = 6.3 Hz, *J*(H-H) = 5.5 Hz, *J*(H-H) = 0.9 Hz, C*H*, *5,5'*-py], 6.45 [2H, d, *J*(H-H) = 8.9 Hz, C*H*, *o*-C*H*, styrene], 6.11 [1H, dd, *J*(H-H) = 15.8 Hz, *J*(H-H) = 9.6 Hz, C*H*Ph], 4.84 [1H, d, *J*(H-H) = 15.8 Hz, *cis*-C*H*, styrene], 4.44 [1H, d, *J*(H-H) = 9.6 Hz, *trans*-C*H*, styrene], 2.38 (3H, s, *p*-CH_3), 1.89 (6H, s, *o*-CH_3). ^{13}C NMR (298 K; CD_3OD): δ 155.49, 150.62, 142.23, 141.80, 138.64, 138.07, 137.54, 132.40, 130.12, 129.29, 127.11, 119.80, 116.26, 104.60 (H_2C=*C*H), 77.28 (H_2*C*=CH), 21.31 (*p*-*C*H$_3$), 17.78 (*o*-*C*H$_3$).

[Cu(2-^{i}PrPh-dpa)(η^2-styrene)]BF$_4$ (4.3). This compound was prepared in an analogous manner to that of compound (**4.1**), using ^{i}PrOH as solvent and 2-^{i}PrPh-dpa as ligand. Yield: 66%. Mp (TGA; decomp.) 156 - 158 °C. FTIR (neat, ATR, cm^{-1}): 3126 (w,

aromatic ν_{C-H}), 3079 (w, alkene ν_{C-H}), 3060 (w, alkene ν_{C-H}), 3033 (w, alkene ν_{C-H}), 2967 (m, alkyl ν_{C-H}), 2927 (w, alkyl ν_{C-H}), 2871 (w, alkyl ν_{C-H}), 1600 (s), 1580 - 1430 (s, aromatic $\delta_{C=C}$), 1335 (s), 1233 (m, aromatic $\delta_{C=N}$), 1245 (s), 1055 (br vs), 1020 (br vs). ^{1}H NMR (298 K; CD_3OD): δ 8.31 (2H, br d, C*H*, *6,6'*-py), 7.73 (2H, br t, C*H*, *4,4'*-py), 7.62 (1H, br d, C*H*, Ph), 7.61 (1H, br t, C*H*, Ph), 7.52 (1H, br t, C*H*, Ph), 7.48 (2H, mult., C*H*, sty), 7.44 (1H, br d, C*H*, Ph), 7.27 (2H, mult., C*H*, sty), 7.23 (1H, mult., *p*-C*H*, sty), 7.14 (2H, br t, C*H*, *5,5'*-py), 6.67 (2H, br d, C*H*, *3,3'*-py), 6.15 [1H, dd, *J*(H-H) = 15.7 Hz, *J*(H-H) = 9.6 Hz, C*H*Ph], 4.90 [1H, d, *J*(H-H) = 15.7 Hz, *cis*-C*H*, styrene], 4.49 [1H, d, *J*(H-H) = 9.6 Hz, *trans*-C*H*, styrene], 2.71 [1H, sept, *J*(H-H) = 6.8 Hz, C*H*$(CH_3)_2$], 0.87 [6H, d, *J*(H-H) = 6.8 Hz, CH(C*H*$_3)_2$]. ^{13}C NMR (298 K; CD_3OD): δ 156.76, 150.32, 148.45, 141.62, 139.81, 138.66, 132.58, 131.99, 130.62, 130.17, 129.74, 129.31, 127.12, 120.06, 118.05, 106.32 (H_2C=*C*H), 79.07 (H_2*C*=CH), 29.17, 23.73.

[Cu(1-naph-dpa)(η^2-styrene)]BF_4 (4.4). This compound was prepared in an analogous manner to that of compound (**4.1**), using ^{i}PrOH as solvent and compound naph-dpa as ligand. Yield: 58%. Mp (TGA; decomp.) 153 - 155 °C. FTIR (neat, ATR, cm^{-1}): 3563 (m), 3167 (vw, aromatic ν_{C-H}), 3096 (w, aromatic ν_{C-H}), 3058 (w, alkene ν_{C-H}), 3028 (w, alkene ν_{C-H}), 2976 (w, alkyl ν_{C-H}), 2884 (w, alkyl ν_{C-H}), 1598 (s), 1578 - 1390 (s, aromatic $\delta_{C=C}$), 1330 (s), 1245 (m, aromatic $\delta_{C=N}$), 1165 (s), 1043 (br vs). ^{1}H NMR (298 K; CD_3OD): δ 8.24 (2H, br s, *6*-C*H*, py), 8.14 (1H, br d, C-*H*, naph), 8.07 (1H, br d, C-*H*, naph), 7.70 (1H, br t, C-*H*, naph), 7.63 (2H, br t, *4*-C*H*, py), 7.61 (1H, br d, C-*H*, naph), 7.60 (1H, br d, C-*H*, naph), 7.58 (1H, br s, C-*H*, naph), 7.52 (2H, m, C-*H*, sty), 7.48 (1H, br t, C-*H*, naph), 7.30 (2H, m, C-*H*, sty), 7.24 (1H, m, C-*H*, sty),7.12 (2H, br t, *5*-C*H*, py), 6.58 (2H, br d, *3*-C*H*, py), 6.23 [1H, dd, *J*(H-H) = 15.9 Hz, *J*(H-H) = 9.8 Hz, C*H*Ph], 5.03 [1H, d, *J*(H-H) = 15.9 Hz, *cis*-C*H*, styrene], 4.57 [1H, d, *J*(H-H) = 9.8 Hz, *trans*-C*H*, styrene]. ^{13}C NMR (298 K; CD_3OD): δ 157.13, 150.03, 141.70, 138.83,

138.73, 137.13, 131.88, 131.72, 130.56, 130.15, 129.75, 129.60, 129.36, 128.69, 128.04, 127.27, 123.22, 120.31, 118.30, 109.85 (H_2C=*C*H), 82.77 (H_2*C*=CH).

[Cu(Mes-dpa)(η^2-norbornylene)]PF_6 (4.5) This compound was prepared in an analogous manner to that of **4.1**, using 2-butanol as solvent, Mes-dpa as ligand, and norbornylene as olefin Yield: 76%. Mp (TGA; decomp.) 176 - 178 °C. FTIR (neat, ATR, cm^{-1}): 3678 (m), 3595 (m), 3128 (w, aromatic ν_{C-H}), 3105 (w, aromatic ν_{C-H}), 3015 (w, alkene ν_{C-H}), 2978 (w, alkene ν_{C-H}), 2933 (w, alkyl ν_{C-H}), 2872 (w, alkyl ν_{C-H}), 2860 (w, alkyl ν_{C-H}), 1600 (m), 1579 - 1429 (s, aromatic $\delta_{C=C}$), 1337 (s), 1244 (m), 1226 (m), 1170 (m), 1024 (w), 822 (br vs), 772 (s). ^{1}H NMR (298 K; CD_3OD): δ 8.56 (2H, br d, *6*-C*H*, py), 7.82 (2H, br t, *4*-C*H*, py), 7.25 (2H, br t, *5*-C*H*, py), 7.23 (2H, s, C*H*), 6.52 (2H, br d, *3*-C*H*, py), 5.10 (2H, br s, *H*C=C*H*), 3.13 (2H, br s, C*H*CH_2C*H*), 2.42 (3H, s, *p*-CH_3), 1.97 (6H, s, *o*-CH_3), 1.66 (2H, m, CH_2), 1.29 (1H, m, CHC*H*$_2$CH), 1.12 (2H, m, CH_2), 0.99 (1H, m, CHC*H*$_2$CH). ^{13}C NMR (298 K; CD_3OD): δ 155.48, 153.60, 142.82, 142.01, 141.22, 138.06, 132.75, 119.95, 116.54, 103.75 (*C*H=*C*H), 44.32, 44.07, 25.61, 21.35, 17.59.

[Cu(2-^{i}PrPh-dpa)(η^2-norbornylene)]BF_4 (4.6). This compound was prepared in an analogous manner to that of compound **4.5**, using ^{i}PrOH as solvent and 2-^{i}PrPh-dpa as ligand. Yield: 66%. Mp (TGA; decomp.) 152 - 155 °C. FTIR (neat, ATR, cm^{-1}): 3635 (m), 3547 (m), 3127 (w, aromatic ν_{C-H}), 3080 (w, aromatic ν_{C-H}), 3058 (w, alkene ν_{C-H}), 3031 (w, alkene ν_{C-H}), 2967 (w, alkyl ν_{C-H}), 2927 (w, alkyl ν_{C-H}), 2871 (w, alkyl ν_{C-H}), 1600 (s), 1582 - 1430 (s, aromatic $\delta_{C=C}$), 1334 (s), 1245 (m), 1055 (br vs), 1023 (br, vs), 780 (s). ^{1}H NMR (298 K; CD_3OD): δ 8.54, 7.80, 7.69 (1H, br d, C*H*, Ph), 7.66 (1H, br t, C*H*, Ph), 7.56 (1H, br t, C*H*, Ph), 7.45 (1H, br d, C*H*, Ph), 7.25 (2H, br t, C*H*, 5-py), 6.68 (2H, br d, C*H*, 3-py), 5.11 (2H, br s, *H*C=C*H*), 3.12 (2H, br s, C*H*CH_2C*H*), 2.87 [1H, sept, *J*(H-H) = 7.0 Hz, C*H*$(CH_3)_2$], 1.67 (2H, m, CH_2), 1.30 (1H, m, CHC*H*$_2$CH), 1.12

(2H, m, CH_2), 1.01 (1H, m, CHCH_2CH), 0.97 [6H, d, J(H-H) = 7.0 Hz, CH(CH_3)$_2$]. ^{13}C NMR (298 K; CD_3OD): δ 156.63, 150.71, 141.85, 138.07, 132.31, 132.17, 130.78, 130.73, 130.15, 119.92, 118.18, 103.87 (*C*H=*C*H), 44.31, 44.07, 29.11, 25.60, 23.82.

[Cu(Mes-dpa)(η^2-*cis*-3-octene)]BF_4 (4.7) In a drybox, [Cu(MeCN)$_4$]BF_4 (0.314 g, 1.0 mmol) and Mes-dpa (0.291 g, 1.0 mmol) were charged to separate schlenk flasks. After removal from the drybox, EtOH (20 mL) was added via cannula to the flask containing the ligand, which was stirred to dissolve the solid. *Cis*-3-octene (ca. 4 mL) in ^{i}PrOH (25 mL) was added via cannula to the flask containing the copper precursor. After stirring for one hour, the ligand solution was added to the copper-olefin mixture, and the combined solutions were stirred under an argon atmosphere overnight. The solution volume was then reduced by approximately half under vacuum, warmed gently with a water bath to redissolve the product, and then filtered through a medium porosity glass frit to remove insoluble impurities. Argon was vigorously bubbled through the resulting pale green solution to further reduce its volume to ca. 15 mL. The solution was gently warmed to dissolve any precipitate, and upon cooling to –12 °C for several days, afforded 0.292 g colorless semi-crystalline powder. Yield: 53 %. MP (TGA; decomp.) 137 - 139 °C. FTIR (neat, ATR, cm^{-1}): 3100 (w, aromatic $\nu_{C\text{-}H}$), 3039 (w, alkene $\nu_{C\text{-}H}$), 2964 (m, alkyl $\nu_{C\text{-}H}$), 2929 (m, alkyl $\nu_{C\text{-}H}$), 2872 (w, alkyl $\nu_{C\text{-}H}$), 2859 (w, alkyl $\nu_{C\text{-}H}$), 1600 (s), 1581 - 1429 (s, aromatic $\delta_{C=C}$), 1327 (s, 3° aromatic $\nu_{C\text{-}N}$), 1233 (m), 1168 (m), 1025 (br vs, $\nu_{B\text{-}F}$), 930 (w), 909 (w), 856 (w), 777 (s). ^{1}H NMR (298 K; CD_3OD): δ 8.32 (2H, br s, *6*-py), 7.78 (2H, br t, *4*-py), 7.20 (2H, s, C*H*, *m*-Mes), 7.19 (2H, br s, *5*-py), 6.57 (2H, br d, *3*-py), 5.04 (2H, m, *H*C=C*H*), 2.38 (3H, s, *p*-CH_3), 2.02 (6H, s, *o*-CH_3), 1.96 (4H, m, CHCH_2), 1.36 (4H, m, CH_2CH_2CH$_3$), 1.01 [3H, t, J(H-H) = 7.5 Hz, CHCH$_2$CH_3], 0.89 [3H, t, J(H-H) = 7.1 Hz, CH$_2$CH$_2$CH_3]. ^{13}C NMR (298 K; CD_3OD): δ 156.19, 149.93, 141.98, 141.66, 138.12, 137.59, 132.40, 119.88, 116.48, 108.54 (*C*HEt), 106.57 (*C*HCH$_2$), 33.80, 28.84, 23.59, 22.46, 21.32, 17.99, 15.18, 14.36.

[Cu(Mes-dpa)(η^2-*trans*-3-octene)]BF_4 (4.8) This compound was prepared in an analogous manner to that of (**4.7**), using the olefin *trans*-3-octene. Yield: 45 %. MP (TGA; decomp.) 123 - 125 °C. FTIR (neat, ATR, cm^{-1}): 3123 (w, aromatic ν_{C-H}), 3097 (w, aromatic ν_{C-H}), 3043 (w, alkene ν_{C-H}), 2960 (w, alkyl ν_{C-H}), 2930 (w, alkyl ν_{C-H}), 2871 (w, alkyl ν_{C-H}), 1599 (s), 1581 - 1426 (s, aromatic $\delta_{C=C}$), 1383 (w), 1327 (s, 3° aromatic ν_{C-N}), 1234 (m), 1171 (m), 1034 (br vs, ν_{B-F}), 931 (w), 908 (w), 881 (w), 777 (s). ^{1}H NMR (298 K; CD_3OD): δ 8.30 (2H, br s, *6*-py), 7.77 (2H, br t, *4*-py), 7.18 (2H, br s, *m*-Mes C-*H*), 7.16 (2H, br t, *5*-py), 6.55 (2H, br d, *3*-py), 5.05 (2H, m, *H*C=C*H*), 2.37 (3H, s, *p*-CH_3), 2.00 (4H, m, CHCH_2), 1.96 (6H, s, *o*-CH_3), 1.37 (4H, m, CH_2CH_2CH$_3$), 1.02 [3H, t, *J*(H-H) = 7.4 Hz, CHCH$_2$CH_3], 0.90 [3H, t, *J*(H-H) = 7.1 Hz, CH$_2$CH$_2$CH_3]. ^{13}C NMR (298 K; CD_3OD): δ 156.29, 149.84, 141.98, 141.69, 141.06, 138.04, 132.47, 119.84, 116.49, 113.19 (*C*HEt), 110.51 (*C*HCH$_2$), 34.05, 33.87, 27.38, 23.24, 21.33, 17.95, 15.48, 14.36.

[Cu{(2-^{i}PrPh)-dpa}(η^2-*cis*-3-octene)]BF_4 (4.9) This compound was prepared in an analogous manner to that of (**4.7**), using the ligand (2-^{i}PrPh)-dpa. Yield: 49 %. MP (TGA; decomp.) 133 - 135 °C. FTIR (neat, ATR, cm^{-1}): 3120 (w, aromatic ν_{C-H}), 3073 (w, aromatic ν_{C-H}), 3027 (w, alkene ν_{C-H}), 2963 (w, alkene ν_{C-H}), 2931 (w, alkyl ν_{C-H}), 2870 (w, alkyl ν_{C-H}), 1598 (m), 1582 - 1430 (s, aromatic $\delta_{C=C}$), 1328 (s, 3° aromatic ν_{C-N}), 1282 (w), 1243 (m), 1168 (m), 1050 (br vs, ν_{B-F}), 931 (w), 764 (s). ^{1}H NMR (298 K; CD_3OD): δ 8.21 (2H, br s, *6*-py), 7.82 (2H, br t, *4*-py), 7.62 (1H, m, Ph C-*H*), 7.59 (1H, m, Ph C-*H*), 7.45 (1H, br s, Ph C-*H*), 7.43 (1H, br s, Ph C-*H*), 7.21 (2H, br t, *5*-py), 6.87 (2H, br d, *3*-py), 5.02 (2H, m, *H*C=C*H*), 2.92 [1H, br sept, C*H*(CH$_3$)$_2$], 1.95 (4H, m, CHCH_2), 1.36 (4H, m, CH_2CH_2CH$_3$), 1.01 [3H, t, *J*(H-H) = 7.5 Hz, CHCH$_2$CH_3], 0.96 [6H, br d, CH(CH_3)$_2$], 0.89 [3H, t, *J*(H-H) = 7.1 Hz, CH$_2$CH$_2$CH_3]. ^{13}C NMR (298 K; CD_3OD): δ 157.66, 149.88, 148.38, 141.66, 140.05, 132.25, 131.76, 130.52, 129.57,

120.68, 118.94, 106.49 (*C*HEt), 104.47 (*C*HCH$_2$), 33.79, 29.53, 29.05, 23.89, 23.66, 22.61, 15.19, 14.35.

[Cu{(2-^{i}PrPh)-dpa}(η^2-*trans*-3-octene)]BF$_4$ (4.10) This compound was prepared in an analogous manner to that of (**4.7**), using the ligand (2-^{i}PrPh)-dpa and olefin *trans*-3-octene. Yield: 39 %. MP (TGA; decomp.) 123 - 125 °C. FTIR (neat, ATR, cm^{-1}): 3123 (w, aromatic $\nu_{C\text{-}H}$), 3094 (w, aromatic $\nu_{C\text{-}H}$), 3071 (w, aromatic $\nu_{C\text{-}H}$), 3037 (w, alkene $\nu_{C\text{-}H}$), 2961 (w, alkene $\nu_{C\text{-}H}$), 2927 (w, alkyl $\nu_{C\text{-}H}$), 2870 (w, alkyl $\nu_{C\text{-}H}$), 1598 (m), 1582 - 1431 (s, aromatic $\delta_{C=C}$), 1324 (s, 3° aromatic $\nu_{C\text{-}N}$), 1281 (w), 1242 (m), 1170 (m), 1052 (br vs, $\nu_{B\text{-}F}$), 930 (w), 783 (m), 772 (m), 764 (m). ^{1}H NMR (298 K; CD_3OD): δ 8.22 (2H, br s, *6*-py), 7.80 (2H, br t, *4*-py), 7.63 (1H, m, Ph C-*H*), 7.60 (1H, m, Ph C-*H*), 7.42 (2H, br m, Ph C-*H*), 7.18 (2H, br t, *5*-py), 6.78 (2H, br d, *3*-py), 5.09 (2H, m, *H*C=C*H*), 2.91 [1H, br sept, C*H*(CH$_3$)$_2$], 1.99 (4H, m, CHC*H*$_2$), 1.36 (4H, m, C*H*$_2$C*H*$_2$CH$_3$), 1.02 [3H, t, *J*(H-H) = 7.3 Hz, CHCH$_2$C*H*$_3$], 0.97 [6H, br d, C*H*(CH$_3$)$_2$], 0.91 [3H, t, *J*(H-H) = 7.2 Hz, CH$_2$CH$_2$C*H*$_3$]. ^{13}C NMR (298 K; CD_3OD): δ 157.73, 149.64, 148.44, 141.54, 140.18, 132.04, 131.80, 130.55, 129.80, 120.37, 118.55, 116.59 (*C*HEt), 114.03 (*C*HCH$_2$), 33.93, 33.85, 29.45, 27.32, 23.88, 23.28, 15.31, 14.38.

[Cu{(2-^{i}PrPh)-dpa}(η^2-*cis*-4-octene)]BF$_4$ (4.11) This compound was prepared in an analogous manner to that of (**4.7**), using the ligand (2-^{i}PrPh)-dpa and olefin *cis*-4-octene. Yield: 65 %. MP (TGA; decomp.) 132 - 134 °C. FTIR (neat, ATR, cm^{-1}): 3127 (w, aromatic $\nu_{C\text{-}H}$), 3068 (w, aromatic $\nu_{C\text{-}H}$), 2959 (m, alkyl $\nu_{C\text{-}H}$), 2930 (w, alkyl $\nu_{C\text{-}H}$), 2869 (w, alkyl $\nu_{C\text{-}H}$), 1599 (m), 1582 - 1431 (s, aromatic $\delta_{C=C}$), 1327 (s, 3° amine $\nu_{C\text{-}N}$), 1242 (m), 1167 (w), 1057 (br vs, $\nu_{B\text{-}F}$), 1025 (br vs), 783 (s). ^{1}H NMR (298 K; CD_3OD): δ 8.28 (2H, br s, *6*-py), 7.82 (2H, br t, *4*-py), 7.64 (1H, m, Ph C-*H*), 7.60 (1H, m, Ph C-*H*), 7.53 (1H, br s, Ph C-*H*), 7.49 (1H, br s, Ph C-*H*), 7.23 (2H, br t, *5*-py), 6.88 (2H, br d, *3*-py), 5.08 (2H, m, *H*C=C*H*), 2.97 [1H, br s, C*H*(CH$_3$)$_2$], 1.93 (4H, m, CHC*H*$_2$), 1.42

[4H, sext, J(H-H) = 7.4 Hz, CH_2CH$_3$], 0.97 [6H, br s, CH(CH_3)$_2$], 0.92 [6H, t, J(H-H) = 7.4 Hz, CH$_2$CH_3]. ^{13}C NMR (298 K; CD$_3$OD): δ 157.40, 149.75, 148.42, 141.62, 139.92, 132.66, 131.83, 130.53, 129.53, 120.57, 118.60, 107.40 (*C*H=*C*H), 31.46, 29.52, 24.69, 23.94, 14.35.

[Cu{(2-^{i}PrPh)-dpa}(η^2-*trans*-4-octene)]BF$_4$ (4.12) This compound was prepared in an analogous manner to that of (**4.7**), using the ligand (2-^{i}PrPh)-dpa and olefin *trans*-4-octene. Yield: 59 %. MP (TGA; decomp.) 124 - 125 °C. FTIR (neat, ATR, cm^{-1}): 3121 (w, aromatic $\nu_{C\text{-}H}$), 3069 (w, aromatic $\nu_{C\text{-}H}$), 2960 (m, alkyl $\nu_{C\text{-}H}$), 2928 (w, alkyl $\nu_{C\text{-}H}$), 2868 (w, alkyl $\nu_{C\text{-}H}$), 1596 (m), 1580 - 1429 (s, aromatic $\delta_{C=C}$), 1325 (s, 3° amine $\nu_{C\text{-}N}$), 1243 (m), 1168 (w), 1052 (br vs), 1025 (br vs, $\nu_{B\text{-}F}$), 783 (s). ^{1}H NMR (298 K; CD$_3$OD): δ 8.18 (2H, br s, *6*-py), 7.81 (2H, br t, *4*-py), 7.64 (1H, m, Ph C-*H*), 7.59 (1H, m, Ph C-*H*), 7.42 (2H, br m, Ph C-*H*), 7.19 (2H, br t, *5*-py), 6.81 (2H, br s, *3*-py), 5.06 (2H, m, *H*C=C*H*), 2.92 [1H, br s, C*H*(CH$_3$)$_2$], 1.96 (4H, m, CHCH_2), 1.44 [4H, sext, J(H-H) = 7.4 Hz, CH_2CH$_3$], 0.98 [6H, br s, CH(CH_3)$_2$], 0.93 [6H, t, J(H-H) = 7.4 Hz, CH$_2$CH_3]. ^{13}C NMR (298 K; CD$_3$OD): δ 157.80, 149.67, 148.42, 141.54, 140.26, 132.01, 131.75, 130.54, 129.73, 120.55, 118.73, 113.75 (*C*H=*C*H), 36.38, 29.47, 24.96, 23.88, 14.04.

Crystallographic Study. General procedures for X-ray data collection was performed as described in Chapter 1, for compounds **4.1 - 4.5,** and **4.8**. All were collected at room temperature, and **4.1** was collected again at 213 K. The program PLATON was employed for structure validation,[9] which revealed solvent accessible voids in the crystal lattice of structures **4.3**, **4.4**, and **4.8**. The CALC SQUEEZE instruction was used to correct data of density in voids, and all subsequent refinement was performed on the corrected data set. Compounds **4.2**, **4.4**, and **4.8** were all found to crystallize with 2 unique conformers in their respective asymmetric unit. In compound **4.2,** the two conformers are related by a non-crystallographic glide-plane. The second conformer in

4.4 differs from the first by the orientation of the naphthyl group, which is rotated 180° about the N_a - C_{naph} bond.

Some disorder is apparent in C(23) of **4.8**a, which required treatment of the atom as having approximately isotropic behavior (ISOR), with rigid bond restraints (DELU) for carbon atoms C(21)-C(24), as well as a fixed distance restraint for the Cu(1)-C(23) bond distance (DFIX = 2.010). BUMP and DAMP restraints were used in preliminary refinement, but lifted for the final cycles. The disorder observed in C(23), and for that matter, the generally low data quality in the crystal structure of compound **4.8**, is more than likely a result of a non-crystallographic symmetry element seen between the two independent cations. Specifically, the first conformer can be fitted to the second conformer through rota-inversion about (pseudo)axis [l, m, n] by 179.22° (direction cosines with orthogonal cell l, m, n = -0.001519, -0.99994, -0.010847), giving weighted and unit weight RMS-fit values of 0.442 and 0.355 Å, respectively, for all 31 non-hydrogen atoms (per cation). This global pseudo-symmetry is known to cause systematic errors, which can lead to geometric distortions and/or problems with anisotropic refinement.[10]

Finally, refinement of the noncentrosymmetric structure of compound **4.8** (space group $P2_1$) was performed using TWIN and BASF commands as previously described (Flack, 2000). This treatment (i.e., modeling the structure as having an inversion twin) refined the absolute structure with a fractional presence (the Flack x parameter) equal to 0.45(2), with 6210 (79.9 %) Friedel pairs measured. Details concerning the refinement of disordered tetrafluoroborate anions in compounds **4.1**, **4.2**, and **4.3**, in addition to the hexafluorophosphate anion in **4.5**, are given in Chapter 7. A brief examination of the effects of collection temperature on overall data quality in compound **4.1** can be found in Appendix C.

Table 4.5. X-ray data for compounds **4.1** - **4.5**, and **4.8**.

Compound	**4.1**	**4.2**	**4.3**
empir. formula	$CuC_{26}H_{27}N_3OBF_4$	$CuC_{27}H_{27}N_3BF_4$	$CuC_{27}H_{27}N_3BF_4$
M_W	547.86	543.87	543.87
cryst. system	monoclinic	monoclinic	monoclinic
space group	$P2_1/c$	$P2_1/n$	$P2_1/c$
a, Å	13.238(3)	13.001(3)	14.174(3)
b, Å	11.178(2)	17.616(4)	14.040(3)
c, Å	17.418(4)	23.608(5)	14.366(3)
α, deg.	-	-	-
β, deg.	103.54(3)	105.69(3)	110.07(3)
γ, deg.	-	-	-
V, $Å^3$	2505.7(9)	5205(1)	2685(1)
Z	4	8	4
D_{calc}, g/cm^3	1.452	1.388	1.345
μ, mm^{-1}	0.926	0.888	0.861
2θ range, deg.	3.16 - 58.00	2.92 - 56.62	3.06 - 55.72
No. collected	30328	63241	32100
No. ind. (R_{int})	6246 (0.0495)	12690 (0.1166)	6303 (0.1004)
No. obsd. ($\|F_o\| > 4.0\sigma \|F_o\|$)	4852	4306	2391
R	0.0411	0.0616	0.0609
R_w	0.1133	0.1381	0.1407
$\Delta\rho_{max/min}$ ($eÅ^{-3}$)	0.497, -0.752	0.358, -0.269	0.298, -0.207
weights	0.0672, 0.9725	0.0975, 0	0.0764, 0
CCDC Dep. No.	724010	724009	740151

Table 4.5. contd.

Compound	**4.4**	**4.5**	**4.8**
empir. formula	$CuC_{28}H_{23}N_3BF_4$	$CuC_{27}H_{33}N_3PF_6O$	$CuC_{27}H_{35}N_3BF_4$
M_W	551.84	624.07	551.93
cryst. system	monoclinic	monoclinic	monoclinic
space group	$P2_1/c$	$P2_1/c$	$P2_1$
a, Å	25.745(5)	10.770(2)	9.943(2)
b, Å	13.345(3)	14.380(3)	21.275(4)
c, Å	15.876(3)	18.831(4)	13.874(3)
α, deg.	-	-	-
β, deg.	102.30(3)	102.61(3)	107.19(3)
γ, deg.	-	-	-
V, $Å^3$	5329(1)	2846(1)	2804(1)
Z	8	4	4
D_{calc}, g/cm^3	1.376	1.456	1.308
μ, mm^{-1}	0.869	0.888	0.825
2θ range, deg.	3.24 - 55.54	3.60 - 56.72	3.08 - 58.34
No. collected	65597	34349	68486
No. ind. (R_{int})	12485 (0.0792)	6948 (0.0452)	13982 (0.0885)
No. obsd.			
($\|F_o\| > 4.0\sigma \|F_o\|$)	5082	3747	6381
R	0.0602	0.0496	0.0937
R_w	0.1657	0.1305	0.2139
$\Delta\rho_{max/min}$ ($eÅ^{-3}$)	0.590, -0.378	0.384, -0.391	2.449, -0.624
weights	0.0956, 0	0.0776, 1.4546	0.0926, 0
CCDC Dep. No.	743482	728875	733204

References

1 N. Yasuda, H. Uekusa, and Y. Ohasi, *Acta Cryst.,* 2001, **E57**, o1189.

2 H. Masuda, K. Machida, M. Munakata, S. Kitagawa, and H. Shimono, *J. Chem. Soc., Dalton Trans.,* 1988, 1907.

3 J. Min, J. Benet-Buchholz, and R. Boese, *Chem. Comm.,* 1998, 2751.

4 M. Pasquali, C. Floriani, A. Gaetani-Manfredotti, and A. Chiesi-Villa, *J. Am. Chem. Soc.,* 1978, **100**, 4918.

5 L. Brammer, D. Zhao, F. T. Lapido, and J. Braddock-Wilking, *Acta Cryst*, 1995, **B51**, 632.

6 (a) D. Petrovic, L. M. R. Hill, P. G. Jones, W. B. Tolman, and M. Tamm, *Dalton Trans*., 2008, 887. (b) J. W. Steed and J. L. Atwood, *Supramolecular Chemistry*, John Wiley and Sons, LTD., West Sussex, England, 2005, 22-30.

7 M. B. Power, J. R. Nash, M. D. Healy, and A. R. Barron, *Organometallics*, 1992, **11**, 1830.

8 Infrared Characteristic Group Frequencies, 2nd Ed., Edited by George Socrates, 1994, John Wiley and Sons, Inc.

9 (a) A. L. Spek, *PLATON, Molecular Geometry Program*, 2008, Utrecht, The Netherlands. (b) A. L. Spek, *J. Appl. Cryst*., 2003, **36**, 380-388.

10 P. Müller, *Crystal Structure Refinement, A Crystallographer's Guide to SHELXL*, Oxford University Press, UK, (2006).

Chapter 5

Synthesis and Structural Characterization of [Ag(H-dpa)(η^2-styrene)]BF_4

Introduction

In the preceding chapters, the structural and spectroscopic characterization of olefin coordination in copper(I) complexes incorporating the H-dpa ligand, i.e., [Cu(H-dpa)(olefin)]$^+$ (see **I** and **II** from Introduction), in addition to ligand design and synthesis, were examined. Moreover, the ligand distortion about the copper center, resulting from remote substitution on the ligand (see **I** and **II** from Chapter 4), was indeed observed to create a steric preference in olefin binding. More specifically, the presence of the substituted aryl (i.e., where R' and/or R" are alkyl substituents) results in folding of the *bis*-(2-pyridyl)amine ligand, causing a subsequent distortion of the pyridyl rings from coplanar, and thus a variance in the intramolecular steric interactions between the olefin and ligand. These studies, in conjunction with an examination of the ligand geometries in previously prepared complexes,[1] led us to the question as to whether similar changes in ligand geometries, and therefore olefin differentiation, would be observed in complexes of other metals. The attention that silver(I) salts have received as promising agents for olefin/paraffin separation via π-complexation,[2] as well as the surprising paucity of structural reports on simple ligand-chelate silver(I)-olefin complexes,[3,4] prompted the study of the complex [Ag(H-dpa)(η^2-styrene)]BF_4 (**5.1**).

Results and Discussion

The structure for the [Ag(H-dpa)(η^2-styrene)]$^+$ cation in compound **5.1** is shown in Figure 5.1; selected bond lengths and angles can be found in Table 5.1. The coordination sphere about the silver center is consistent with similar Group 11 metal olefin complexes,[1] having a distorted trigonal planar geometry; the three coordination

sites are occupied by the two pyridyl nitrogen atoms and the midpoint of the alkene double bond.

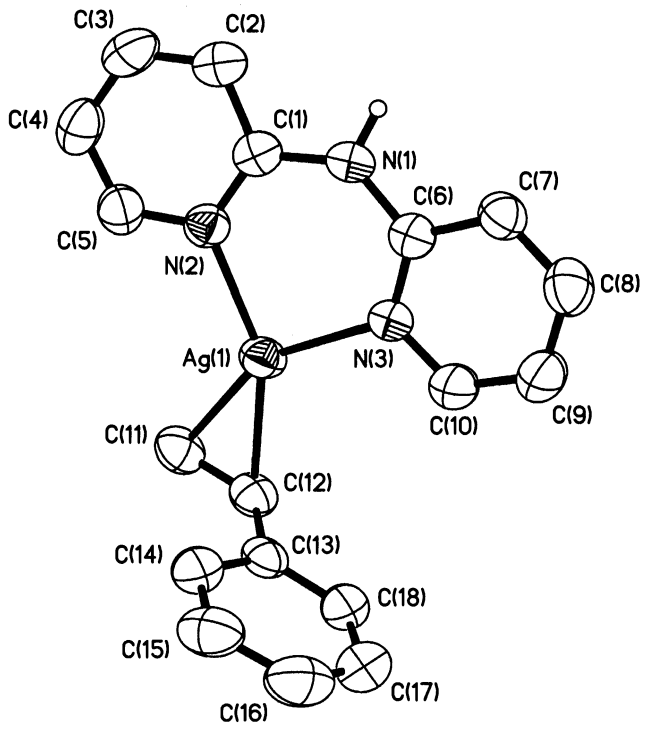

Figure 5.1. Molecular structure of the $[Ag(H\text{-}dpa)(\eta^2\text{-}styrene)]^+$ cation in compound **5.1**. Thermal ellipsoids are set at the 40% probability level, and all hydrogen atoms attached to carbon are omitted for clarity.

The geometries of $[Ag(H\text{-}dpa)(\eta^2\text{-}styrene)]^+$ and the analogous copper cation (i.e., Chapter 1, compound **1.12**) differ primarily in close proximity to the metal center, which is likely a result of size difference between metal ions (Figure 5.2). More specifically, the metal-nitrogen and metal-carbon bond lengths are notably larger for the case of silver, while the corresponding N-M-N and C-M-C angles are smaller. In comparison to their respective copper analogs, silver complexes nominally exhibit much longer M-N and M-C bond distances.[5] For example, the silver-ethylene complex of $MeB\{3\text{-}(CF_3)pz\}_3$ was reported to have Ag-C distances 2.285(1) and 2.279(1) Å, and Ag-N distances 2.268(1)

and 2.319(1) Å,[3] whereas the Cu-C [2.033(3) & 2.043(3) Å] and Cu-N [2.032(1) & 2.034(2) Å][6] distances in the corresponding copper complex are notably shorter.

Shorter C=C bond lengths in olefin complexes (i.e., lengths closer to that of free ligand) indicate a lesser degree of π^* back-bonding. Unfortunately, while the styrene C=C distance in **5.1** is longer than in free styrene [1.325(2) Å],[7] and therefore consistent with binding to the metal and a minor degree of π^* back-bonding, it is within experimental error of that in its copper analogue (Table 5.1).

Table 5.1. Selected bond lengths (Å) and angles (°) for [M(H-dpa)(η^2-styrene)]BF_4.

M	Ag (**5.1**)	Cu (**1.12**)
M - C	2.239(4)	1.990(6)
M - C'	2.277(4)	2.044(5)
M - N	2.220(4)	1.959(5)
M - N'	2.220(3)	1.967(5)
C = C'	1.366(6)	1.387(8)
C' - C_{Ph}	1.475(6)	1.489(8)
$N_a \cdots F$	2.877(9)	2.882(6)
N - M - N'	86.9(1)	96.7(2)
C - M - C'	35.2(1)	40.2(2)
M - C' - C_{Ph}	104.9(3)	108.6(4)
C_{py} - N_a - $C_{py'}$	135.7(4)	133.5(5)
C = C' - C_{Ph}	126.0(4)	124.1(6)
N' ··· N ··· C = C'	4.6(3)	6.8(4)
$\Delta MPLN_{[py\cdots py']}$	11.2(2)	12.3(3)

Moreover, the C=C bond length in **5.1** is within the range reported for several other copper(I)-styrene complexes [1.35(1) - 1.387(8) Å].[8,9,10] As a result, it is difficult to make a meaningful comparison of olefin···metal bonding interactions based upon the C=C distance alone. In addition to change in C = C distances, the pyramidalization of the olefin sp^2 carbon atoms can indicate the extent of π back-bonding.

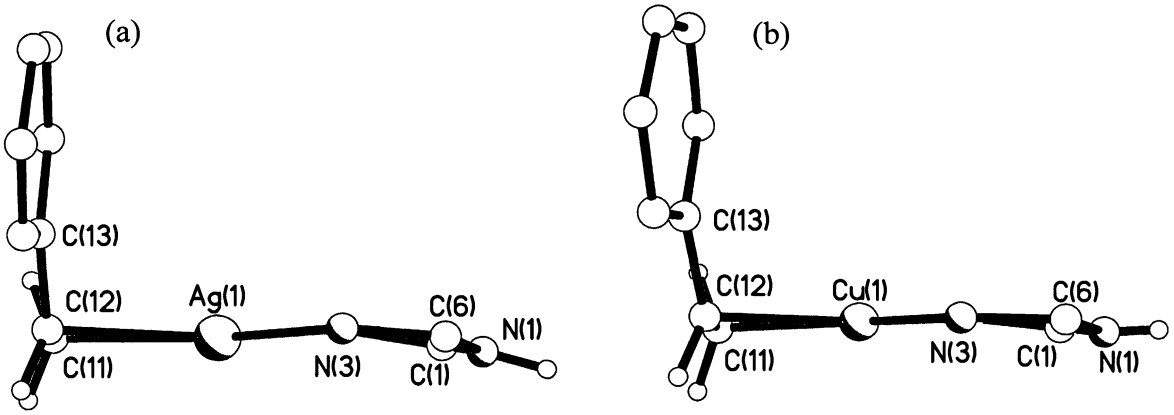

Figure 5.2. Comparison of the partial coordination sphere in the cation of (a) compound **5.1** and (b) the analogous copper(I) complex (**1.12**).

As may be seen from Figure 5.2 and the C(11)-C(12)-C(13) bond angle (Table 5.1), the styrene C(12) atom, in compound **5.1** is less pyramidalized than in its copper counterpart. This is consistent with previous structural reports,[3,4] as well as computational studies[2d], that silver(I)-olefin complexes exhibit very little π^* back-bonding. Interestingly, the gold complexes [Au(R-bipy)(η^2-styrene)]PF_6 are reported to exhibit a high degree of π^* back-bonding, with C=C lengths of 1.384(8) and 1.409(4) Å.[11] Moreover, the M - C bond lengths in these gold complexes [2.098(5) - 2.118(2) Å] lie between those found in **5.1** [2.239(4) and 2.277(4) Å] and its copper analogue, **1.12** [1.990(6) and 2.044(5) Å].[12]

As our interest in [Ag(H-dpa)(olefin)]$^+$ complexes is primarily concerned with potential olefin···ligand interactions allowing for steric differentiation, the structure of compound **5.1** is suggestive that, with regard to our ligand system (and basis for

separation), silver complexes would not be effective candidates as compared to their copper analogs. This is in part because of the increased size of Ag^+ [r_{ion} = 1.45(5) Å] over Cu^+ [r_{ion} = 1.32(2) Å][13] resulting in longer M - C and M - N bond lengths, and as a consequence, greater intramolecular ligand···ligand contact distances. For example, the shortest pyridyl 6-py···styrene distance in compound **5.1** is 3.721(7) Å [C(10)···C(18)], while that in [Cu(H-dpa)(η^2-styrene)]$^+$ is 3.521(9) Å [C(10···C14)].

A consequence of the smaller size of copper and the more intimate interaction of the ligands is also seen from the twist of the styrene C=C bond with regard to the plane of the H-dpa ligand [6.8(4)°] versus that in compound **5.1** [4.6(3)°], see Figure 5.2. The larger values observed in the copper complex are indicative that the coordination sphere about the metal center is more heavily crowded than that of the silver center, forcing the phenyl ring of styrene to twist away from the neighboring pyridyl ring. The lack of π^* back-donation in **5.1** also manifests in the ^{1}H NMR olefin resonances (see Table 5.2).

Table 5.2. Comparison of ^{1}H NMR Δδ values in compounds **5.1** and **1.12**.[a]

M =	Ag (**5.1**)	Cu (**1.12**)
	Δδ, ppm	Δδ, ppm
H_a	-0.01	+0.67
H_b	-0.02	+0.84
H_c	-0.04	+0.54
3-py	+0.38	+0.42
4-py	-0.26	-0.19
5-py	-0.23	-0.14
6-py	-0.04	+0.11

[a] See Figure 1.12 for numbering scheme of protons H_a, H_b, H_c and *3*-py through *6*-py.

The ^{1}H NMR signals for [Cu(H-dpa)(η^2-styrene)]$^+$ (**1.12**) exhibit large *upfield* shifts in the olefin signals as compared to free styrene ($\Delta\delta$ = 0.54 - 0.84 ppm). In stark contrast, the analogous signals found in spectra taken for compound **5.1** are shifted slightly *downfield* ($\Delta\delta$ = -0.01 to -0.04 ppm) from that of free styrene. This is consistent with a weak metal-ligand interaction and/or significant dissociation in solution.[14] Further consideration of ^{1}H NMR spectral data reveals a moderate difference in the electron distribution in the pyridyl rings. Most notably, the $\Delta\delta(^1H)$ value observed at the *6*-py position shifts upfield 0.11 ppm in **1.12**, while the corresponding shift in **5.1** is downfield 0.04 ppm.

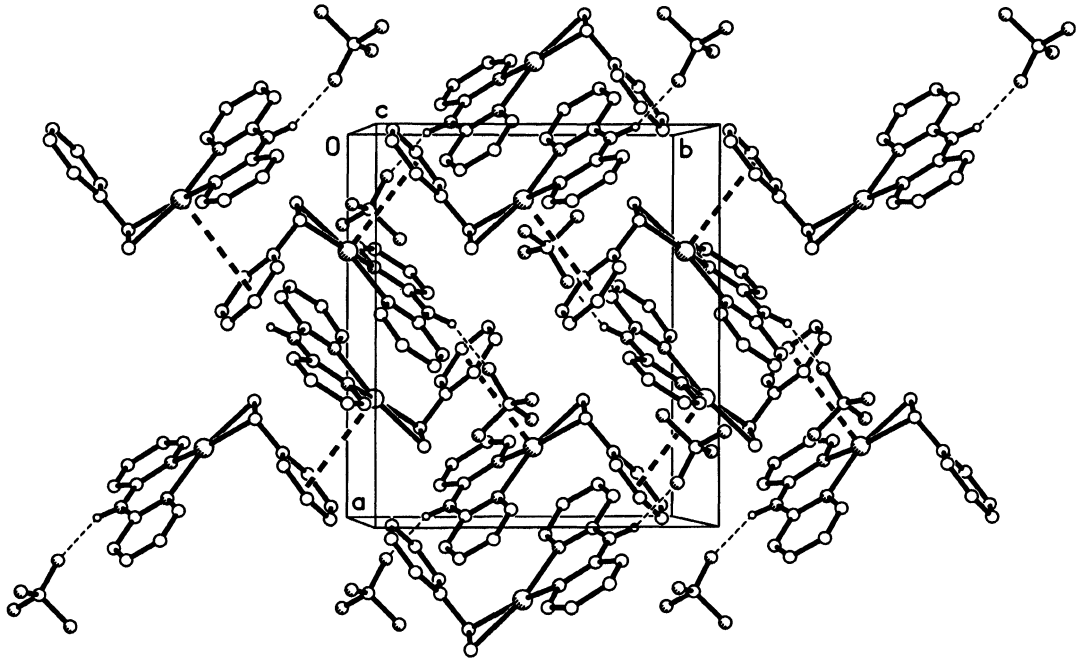

Figure 5.3. Crystal packing of compound **5.1** viewed down the *c*-axis, showing intermolecular interactions present in the lattice.

The molecular packing diagram of compound **5.1** (Figure 5.3) shows that the "L-shaped" cations pack in head-to-tail pairs, with what appears to be a π-stacking interaction between pyridyl rings. However, the distance between the stacked-ring centers

[4.008(3) Å] is larger than any expected π-stacking interaction (3.70 Å).[15] The analogous distance in copper compound **1.12** does exhibit a π-π stacking interaction, with stacked ring distances of 3.651(7) Å, and a mean-plane angle difference of 5.1(3)°.

There exists a close intermolecular contact between the phenyl ring of styrene in one pair of cations and the silver center from another pair. The metal to ring center-of-gravity distance ($M^{\cdots}Cg_{[sty]}$) = 3.573(5) Å is well within the sum of expected van der Waals' radii for Ag^+ and an aromatic half nucleus [2.03 Å and 1.85 Å].[16] In **1.12**, however, the distance is slightly longer [3.586(7) Å].

The head-to-tail arrangement of molecules appears to be linked together by hydrogen bonding interactions between the BF_4^- anions and the amine's hydrogen of the cations in the pair [N(1)···F(2A) = 2.877(9) Å]. The presence of an N-H···F hydrogen bond interaction is confirmed in the FTIR spectrum of compound **5.1**. The N-H stretching and bending modes shifted to higher wavenumber (3316 and 1604 cm^{-1}, respectively) as compared to those in free H-dpa (3263 and 1592 cm^{-1}), in which the amine hydrogen is strongly associated through intermolecular N-H···N interactions. This indicates that the N-H···F interaction with the BF_4^- anion in compound **5.1** is not as strongly associative as that observed for the N-H···N interaction present between the "head-to-tail dimers" in the in the free ligand. The interaction does appear, however, to be stronger than that observed in compound **1.12**, which yielded stretching and bending bands $\nu_{N\text{-}H}$ = 3346 cm^{-1} and $\delta_{N\text{-}H}$ = 1641 cm^{-1}.

Experimental

General experimental procedures are described in Chapters 1 - 4. Additionally, as a precautionary measure against product and/or starting material decomposition, the silver salt was shaded from direct light through the reaction period as well as while in storage.

[Ag(H-dpa)(η^2-styrene)]BF_4 (5.1). $AgBF_4$ (0.194 g, 1.00 mmol) and 2,2'-dipyridylamine (0.172 g, 1.00 mmol) were charged to separate 100 mL Schlenk flasks in a dry box. MeOH (10 mL) was added to the flask containing the H-dpa, which was stirred to dissolve the solids. To the flask containing the silver complex was added styrene (*ca.* 5 mL) in MeOH (5 mL) and *sec*-BuOH (10 mL). The mixture was allowed to stir for 1 hr at room temperature before adding the H-dpa solution. The combined solutions were stirred another three hours at room temperature, after which, the solution volume was reduced to approximately half under vacuum. The solution was gently warmed with a water bath to dissolve the product, and then filtered through a medium porosity glass frit to remove insoluble impurities. The solution was gently warmed to dissolve any precipitate, and upon cooling to –12 °C for several days, the solution yielded colorless crystals. Yield: 0.270 g (57%). MP (TGA; decomp.) 202 - 204 °C. FT-IR (ATR, cm^{-1}): 3316 (m, ν_{N-H}), 3194 (w, aromatic ν_{C-H}), 3173 (w, aromatic ν_{C-H}), 3118 (w, aromatic ν_{C-H}), 3042 (w, alkene ν_{C-H}), 3023 (w, alkene ν_{C-H}), 1605 (s, δ_{N-H}), 1568 (s), 1519 (s), 1485 - 1325 (s, aromatic $\delta_{C=C}$), 1256 (m, aromatic $\delta_{C=N}$), 1169 (m), 1019 (br vs, ν_{B-F}). ^1H NMR (298 K; CD_3OD): δ 8.22 (2H, br s, C*H*, *6,6'*-py), 7.88 (2H, br s, C*H*, *4,4'*-py), 7.43 (2H, m, C*H*, Ph), 7.31 (2H, m, C*H*, Ph), 7.25 (1H, m, *p*- C*H*, Ph), 7.19 (2H, br d, C*H*, *3,3'*-py), 7.09 (2H, br s, C*H*, *5,5'*-py), 6.75 [1H, dd, *J*(H-H) = 17.6 Hz, *J*(H-H) = 10.9 Hz, H_2CCH], 5.77 [1H, dd, *J*(H-H) = 17.6 Hz, *J*(H-H) = 1.0 Hz, *cis*-C*H*], 5.21 [1H, dd, *J*(H-H) = 10.9 Hz, *J*(H-H) = 1.0 Hz, *trans*-C*H*]. ^{13}C NMR (298 K; CD_3OD): δ 158.01, 155.59, 142.60, 137.75, 129.90, 129.13, 127.48, 119.14, 115.75, 112.84, 100.53.

Crystallographic Study. X-ray data for compound **5.1** was collected as described in Chapter 1. Selected bond lengths and angles are given in Table 5.1. Pertinent details of data collection and refinement are given in Table 5.3. See Chapter 7 for details concerning refinement of the disordered BF_4^- anion.

Table 5.3. Summary of X-ray diffraction data for compound (**5.1**).

empir. formula	$AgC_{18}H_{17}N_3BF_4$
M_W	470.03
cryst. system	monoclinic
space group	$P2_1/n$
a, Å	12.764(3)
b, Å	10.590(2)
c, Å	13.624(3)
β, deg.	91.17(3)
V, $Å^3$	1841.3(7)
Z	4
D_{calc}, g/cm^3	1.696
μ, mm^{-1}	1.140
2θ range, deg.	4.32 - 56.58
no. collected	21782
no. ind. (R_{int})	4455 (0.0591)
no. obsd. ($\|F_o\| > 4.0\sigma \|F_o\|$)	2543
R	0.0453
R_w	0.1098
$\Delta\rho_{max/min}$ ($eÅ^{-3}$)	0.653, -0.842
weights	0.0710, 0
CCDC Deposit No.	692442

References

1 (a) J. S. Thompson and J. F. Whitney, *Inorg. Chem.* 1984, **23**, 2813. (b) J. J. Allen and A. R. Barron, *Dalton Trans.* 2009, 878.

2 (a) S. U. Rege, J. Padin, and R. T. Yang, *AIChE J.* 1998, **44**, 799; (b) H. W. Quinn, *Progress in Separation and Purification*, Vol. 4, Perry, E. S. ed., Interscience, New York, 1977; (c) D. J. Safarik, and R. B. Eldridge, *Ind. Eng. Chem. Res.* 1998, **37**, 2571; (d) H. Y. Huang, J. Padin, and R. T. Yang, *J. Phys. Chem. B*, 1999, **103**, 3206.

3 H. V. R. Dias, J. Wu, X. Wang, and R. Krishnan, *Inorg. Chem.* 2007, **46**, 1960.

4 H. V. R. Dias and X. Wang, *Dalton Trans.* 2005, 2985.

5 H. V. R. Dias and M. Fianchini, *Angew. Chem. Int. Ed.*, 2007, **46**, 2188.

6 H. V. R. Dias, X. Wang, and H. V. K. Diyabalanage, *Inorg. Chem.* 2005, **44**, 7322.

7 N. Yasuda, H. Uekusa, and Y. Ohasi, *Acta Cryst.,* 2001, **E57**, o1189.

8 W. A. Braunecker, T. Pintauer, N. V. Tsarevsky, G. Kickelbick, and K. Matyjaszewski, *J. Organomet. Chem.* 2005, **690**, 916.

9 X. Dai and T. H. Warren, *Chem. Comm.* 2001, 1998.

10 H. Masuda, K. Machida, M. Munakata, S. Kitagawa, and H. Shimono, *J. Chem. Soc., Dalton Trans.* 1988, 1907.

11 Cinellu, M. A.; Minghetti, G.; Cocco, F.; Stoccoro, S.; Zucca, A.; Manassero, M.; Arca, M. *Dalton Trans.* 2006, 5703.

12 M. A. Cinellu, G. Minghetti, F. Cocco, S. Stoccoro, A. Zucca, M. Manassero, and M. Arca, *Dalton Trans.* 2006, 5703.

13 B. Cordero, V. Gomez, A. E. Platero-Prats, M. Reves, J. Echeverria, E. Cremades, F. Barragan, and S. Alvarez, *Dalton Trans.*, 2008, 2832-2838.

14 M. B. Power, J. R. Nash, M. D. Healy, and A. R. Barron, *Organometallics* 1992, **11**, 1830.

15 *CRC Handbook of Chemistry and Physics.* 60th Ed. CRC Press, Inc. Boca Raton, FL, 1980, D-194.

16 A. Bondi, *J. Phys. Chem.* 1964, **68**, 441.

Chapter 6

Molecular Structure of $[Cu_2(MeCN)_2(\mu\text{-tpy})_2][BPh_4]_2$

Introduction

Since the first reported cuprous terpyridyl complex,[1] much work has been devoted to the study of its solution redox chemistry,[2] but past structural characterizations have focused on complexes of functionalized terpyridines. Complexes bearing bornyl groups[3] and phenyl groups[4] in the 6-position have been characterized as helical, bridged-bimetallic structures, while sterically larger mesityl groups in the 6-position were found to produce monometallic complexes[5] having distorted square planar geometry.

As part of our study of olefin complexation to copper centers we have investigated the effects of ligand chelate size and dentate number. The reaction of $[Cu(MeCN)_4]X$ with an olefin in the presence of 2,2':6',2"-terpyridine (tpy) did not yield an olefin complex, while reactions performed under analogous conditions using the ligand 2,2'-dipyridylamine instead of tpy were found to complex a wide variety of olefins.[6] Instead, complexes with the formula $[Cu(MeCN)(tpy)]_2X_2$, are isolated that show no propensity for olefin coordination. We have structurally characterized the tetraphenylborate derivative in order to determine the structure type and understand the reason for the lack of olefin complexation.

Results and Discussion

The molecular structure of the complex cation of $[Cu_2(MeCN)_2(\mu\text{-tpy})_2][BPh_4]_2$ (**6.1**) is shown in Figure 6.1; selected bond lengths and angles are given in Table 6.1. The structure consists of discrete bimetallic $[Cu_2(MeCN)_2(\mu\text{-tpy})_2]^{2+}$ units and $[BPh_4]^-$ anions. All bond lengths and angles are within the ranges previously reported for chemically similar complexes.[5,6] Complexes formed with bornyl- and phenyl- functionalized terpyridines are reported to have terpyridine Cu-N bond lengths for the terminal pyridyl

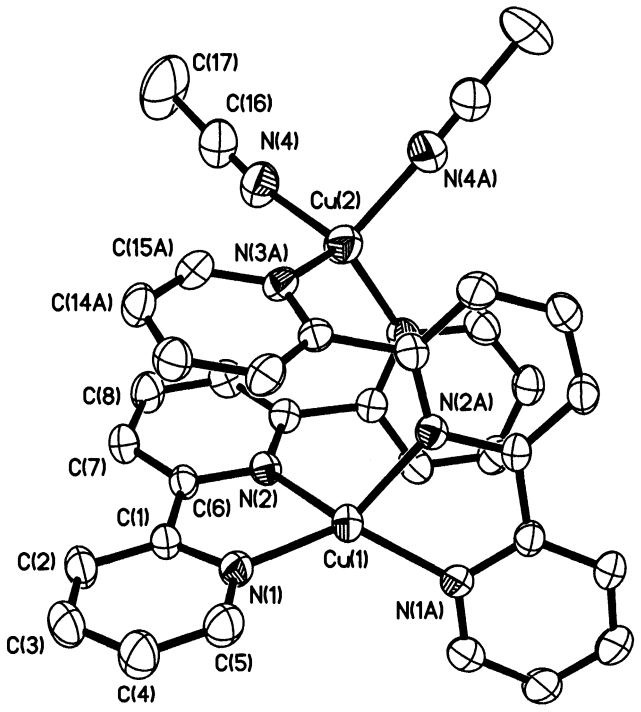

Figure 6.1. Structure of the $[Cu_2(MeCN)_2(\mu\text{-tpy})_2]^{2+}$ cation in **6.1**. Thermal ellipsoids are shown at the 30% level, and all hydrogen atoms are omitted for clarity.

ligands [1.940(3) - 1.959(6) Å], which are significantly shorter than those to the central pyridine rings [2.431(2) Å and 2.224(7) Å]. In contrast, the Cu-N distances in $[Cu_2(MeCN)_2(\mu\text{-tpy})_2]^{2+}$ span a much smaller range. As a result, the Cu-N bonds for the terminal pyridyl ligands are longer in $[Cu_2(MeCN)_2(\mu\text{-tpy})_2]^{2+}$ [1.995(3) Å and 2.045(3) Å] than seen in the 6-py substituted analogs. Moreover, the bond length to the central pyridine in $[Cu_2(MeCN)_2(\mu\text{-tpy})_2]^{2+}$ [2.036(3) Å] is shorter. The observed C-N bond distances of the coordinated acetonitrile ligands [1.108(5) Å] in $[Cu_2(MeCN)_2(\mu\text{-tpy})_2]^{2+}$ are slightly shortened from values reported for the free ligand (1.157 Å),[7] but are within the values expected for acetonitrile complexes (*ca.* 1.13 Å).[8,9]

The asymmetric unit for the complex is comprised of one anion and half of the complex cation, with the copper atoms lying on a two-fold rotation axis. Each terpyridine

ligand chelates one copper center, Cu(1), in a bidentate configuration, resulting in the copper adopting a distorted tetrahedral geometry.

Table 6.1. Selected bond lengths (Å) and angles (°) in compound (**6.1**)

Cu(1)-N(1)	1.994(3)	Cu(1)-N(2)	2.036(3)
Cu(2)-N(3)	2.045(3)	Cu(2)-N(4)	2.038(4)
N(4)-C(16)	1.109(5)	C(16)-C(17)	1.489(6)
N(1)-Cu(1)-N(2)	81.1(1)	N(1)-Cu(1)-N(1A)	130.2(1)
N(1)-Cu(1)-N(2A)	130.0(1)	N(2)-Cu(1)-N(2A)	109.1(1)
N(3)-Cu(2)-N(4)	119.0(1)	N(3)-Cu(2)-N(3A)	110.6(1)
N(3)-Cu(2)-N(4A)	105.5(1)	N(4)-Cu(2)-N(4A)	97.3(2)
Cu(2)-N(4)-C(16)	168.7(5)		
N(1A)-Cu(1)-N(1)-C(5)	43.9(3)	N(2)-Cu(1)-N(1)-C(5)	180.0(3)
N(4)-Cu(2)-N(3)-C(11)	-77.4(3)	N(3A)-Cu(2)-N(3)-C(11)	45.0(2)
N(1)-C(1)-C(6)-N(2)	5.4(4)	N(2)-C(10)-C(11)-N(3)	-113.2(3)

The third ring of each terpyridine ligand forms a bridge with a second copper atom, Cu(2), whose distorted tetrahedral coordination sphere is completed by two MeCN ligands. As a consequence of the 6-membered CuN_2C_3 metallocycles formed by chelating terpyridine ligands, Cu(1) has a geometry more distorted from tetrahedral than does Cu(2) (see Figure 6.2). Additionally, the use of the third pyridine ring as a ligand to Cu(2) results in the closing of the N(2)-Cu(1)-N(2A) angle [109.0(1)°] versus N(1)-Cu(1)-N(1A) [130.2(1)°]. As with complexes bearing substituents in the 6-position the overall geometry resembles a section of a double helix structure.[5,6] The pyridyl rings of a terpyridine ligand bidentate to the same Cu are coplanar, N(2)-Cu(1)-N(1)-C(5) = 180°,

and the third pyridyl ring monodentate to Cu(2) is twisted out of this plane [N(2)-C(10)-C(11)-N(3) = -113.2°] to form half of the double helical structure.

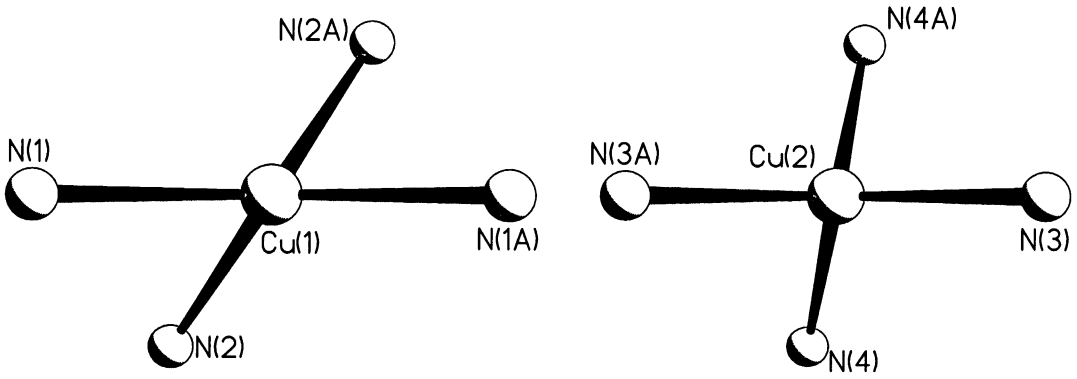

Figure 6.2. Partial coordination spheres about copper atoms showing distortion from tetrahedral geometry about Cu(1) relative to Cu(2).

It is worth noting here that the N(2) and N(3a) pyridyl rings are almost coplanar, with a 9.0° angle between the mean plane of each ring. Moreover, the distance between the centers of these rings (3.73 Å) is within the range expected for π···π stacking interaction (i.e. sum of the van der Waals' aromatic half-nucleus = 3.70 Å).[10] The presence of this π···π stacking interaction dramatically influences the coordination sphere about Cu(1) relative to Cu(2).

While Cu(2) maintains a relatively tetrahedral geometry, the π···π stacking between N(2) and N(3A) pyridyl rings causes the N(1)/N(2) pyridyl rings to bend towards the plane of the N(1A)/N(2A) pyridyl rings. This distortion in the coordination sphere is about Cu(1) relative to Cu(2) is shown in Figure 6.2.

Based upon the overall structure of the $[Cu_2(MeCN)_2(\mu\text{-tpy})_2]^{2+}$ cation, it would be expected that the MeCN ligands could be replaced by an olefin, however, this is not observed. In contrast, dipyridyl derivatives of copper(I) readily form a variety of olefin complexes, in a wide range of solvents, to form complexes [Cu(dpa)(olefin)]X.[11] The chelate bite of the dipyridylamine ligand [96.4(1) - 97.6(2)°] provides a favorable

geometry for the coordination of olefins and the formation of a pseudo square planar geometry.

In spite of this initial appearance, the chelate "bite angle" of the two bridging terpyridine ligands on Cu(2) [110.5(1)°] results in a geometry more suitable for tetrahedral coordination. We propose that despite the electronic similarities of two pyridine ligands, it is this difference in "chelate angle" that disfavors olefin complexation for the terpyridine complexes. The packing diagram of $[Cu_2(MeCN)_2(\mu\text{-tpy})_2][BPh_4]_2$ shows packing of cation and anions in alternating layers. The columns of cations adopt alternating right and left hand helical structures (Figure 6.3).

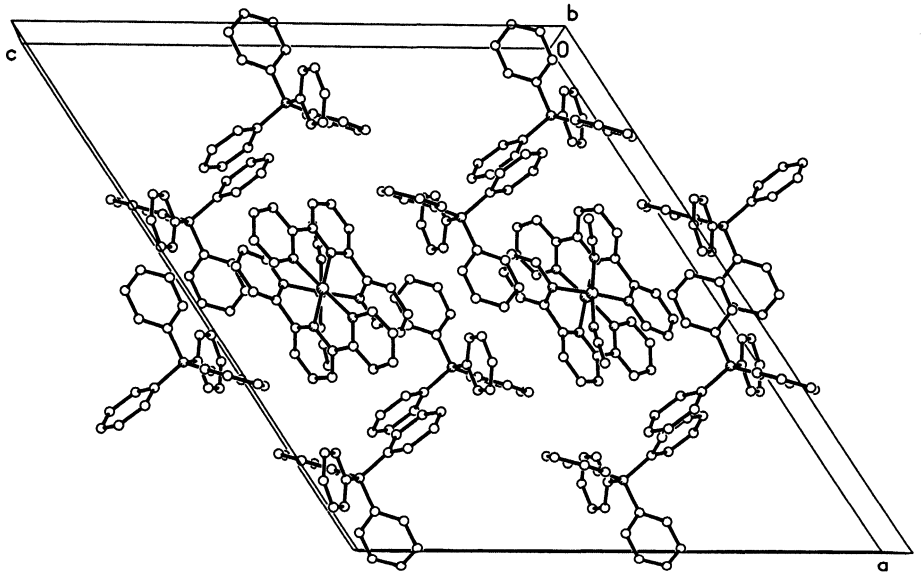

Figure 6.3. Packing diagram of $[Cu_2(MeCN)_2(\mu\text{-tpy})_2][BPh_4]_2$, viewed along the *b*-axis, showing packing of cation and anions in alternating rows. Hydrogen atoms are omitted for clarity.

Experimental

$[Cu_2(MeCN)_2(\mu\text{-tpy})_2][BPh_4]_2$ (**6.1**) The original synthesis of $[Cu_2(MeCN)_2(\mu\text{-tpy})_2][BPh_4]_2$ was performed in the presence of 1-octene; however, once it was

discovered that complexes exhibit no 1-octene coordination, the experimental procedure was modified. CuCl (1.01 g, 10.2 mmol), 2,2':6',2"-terpyridine (2.30 g, 9.86 mmol), and $NaBPh_4$ (3.45 g, 10.1 mmol) were added together to a 100 mL schlenk flask in a drybox. To this was added dry degassed MeCN (25 mL) and the resulting dark red mixture was allowed to stir at room temperature for two hours. After the reaction period the solvent volume was reduced by approximately half under vacuum. CH_2Cl_2 (10 mL) was then added to the mixture, and the flask was then allowed to cool at –12 °C overnight. The solution was filtered cold, yielding dark red powder as the crude product, which was washed with MeOH (2 x 10 mL). The product was then washed through the frit with MeCN (10 mL) and allowed to crystallize overnight at -12 °C, affording dark red prisms. Yield: 4.32 g (67%). IR (ATR, cm^{-1}): 3055, 3037, 3002 (m, arom. $\nu_{C\text{-}H}$), 2925 (w, alkyl $\nu_{C\text{-}H}$), 2265 (w, $\nu_{C\equiv N}$), 1595, 1577, 1472, 1442 (vs). ^1H NMR (298 K; CD_2Cl_2): δ 8.49 [2H, br d, *J*(H-H) = 4.8 Hz, *m*-C*H*, tpy], 8.03-7.93 (5H, m, *o*-C*H*, *m*-C*H*, *p*-C*H*, tpy), 7.89 [2H, ddd, *J*(H-H) = 9.6 Hz, *J*(H-H) = 8.0 Hz, *J*(H-H) = 1.6 Hz, *p*-C*H*], 7.64 (8H, br dd, *o*-C*H*, BPh_4), 7.41 [2H, ddd, *J*(H-H) = 6.0 Hz, *J*(H-H) = 4.8 Hz, *J*(H-H) = 1.2 Hz, *m*-C*H*], 6.95 [8H, t, *J*(H-H) = 7.6 Hz, *m*-C*H*, BPh_4], 6.73 [4H, t, *J*(H-H) = 7.6 Hz, *p*-C*H*, BPh_4], 1.97 (6H, br s, NCCH_3).

Crystallographic Study. General procedures for X-ray data collection are described in Chapter 1. From structural validation using the program PLATON, apparent solvent accessible were found to contain residual electron density. This led to use of the SQUEEZE function in order to obtain the data set free of this residual electron density in these voids. However, subsequent refinement using the resulting corrected data set did not result in any improvement amongst the agreement factors; thus, the original data set was used for final refinement cycles. Pertinent details concerning data collection and structure refinement are given in Table 6.2.

Table 6.2. Summary of X-ray diffraction data for compound **6.1**.

compound	**6.1**
empir. formula	$C_{82}H_{68}B_2Cu_2N_8$
M_W	1314.14
cryst. system	Monoclinic
space group	C2/c
a, Å	27.202(5)
b, Å	12.995(3)
c, Å	23.409(5)
β, deg.	123.13(3)
V, $Å^3$	6930(2)
Z	4
D_{calc}, $g.cm^{-3}$	1.260
μ, mm^{-1}	0.665
2θ range, deg.	3.58 - 56.74
No. collected	41850
No. ind. (R_{int})	8445 (0.1352)
No. obsd. ($\|F_o\| > 4.0\sigma \|F_o\|$)	3144
R	0.0613
R_w	0.0946
$\Delta\rho_{max/min}$ ($eÅ^{-3}$)	0.490, -0.274
CCDC deposit No.	CCDC 683241

References

1 R. T. Pflaum and W. W. Brandt, *J. Am. Chem. Soc.* 1955, **77**, 2019.

2 (a) A. L. Crumbliss and A. T. Poulos, *Inorg. Chem.* 1975, **14**, 1529. (b) M. Munakata, S. Nishibayashi, and H. Sakamoto, *J. Chem. Soc., Chem. Comm.* 1980, 219. (c) A. K. Y. Lam, B. F. Abrahams, M. J. Grannas, W. McFadyen, and R. A. J. O'Hair, *Dalton Trans.* 2006, 5051.

3 E. C. Constable, T. Kulke, M. Neuburger, and M. Zehnder, *J. Chem. Soc., Chem. Comm.* 1997, 489.

4 E. C. Constable, A. J. Edwards, M. J. Hannon, and P. R. Raithby, *J. Chem. Soc., Chem. Commun.*, 1994, 1991.

5 A. Onoda, K. Kawakita, T. Okamura, H. Yamamoto, and N. Ueyama, *Acta Cryst. Sec. E.* 2003, m266.

6 J. J. Allen and A. R. Barron, *Dalton Trans.*, 2009, 878.

7 *Tables of Interatomic Distances and Configuration in Molecules and Ions*. Eds. L. E. Sutton and D. Phil, The Chemical Society, Burlington House, London, W.1; 1958, M128.

8 A. R. Barron, G. Wilkinson, M. Motevalli, and M. B. Hursthouse, *Polyhedron* 1985, **4**, 1131-1134.

9 A. R. Barron, G. Wilkinson, M. Motevalli, and M. B. Hursthouse, *Polyhedron* 1987, **6**, 1089-1095.

10 *CRC Handbook of Chemistry and Physics*. 60th Ed. CRC Press, Inc. Boca Raton, FL, 1980, D-194.

11 M. Munakata, S. Kitagawa, S. Kosome, and A. Asahara, *Inorg. Chem.* 1986, **25**, 2622.

Chapter 7

Refinement of Crystallographic Disorder in the Tetrafluoroborate Anion

Introduction

Through the course of our structural characterization of various tetrafluoroborate salts, the complex cation has nominally been the primary subject of interest. Concerning the present data sets having BF_4^- anions, disordered anions are actually observed to be more common than not (13 out of 23). Furthermore, a consideration of the Cambridge Structural Database as of December 14, 2010 yielded 8,370 structures in which the tetrafluoroborate anion is present; of these, 1044 (12.5%) were refined as having some kind of disorder associated with the BF_4^- anion. Table 7.1 summarizes the compounds in which a disordered anion model was used for refinement, in addition to their corresponding disordered atoms, the type of disorder, any non-crystallographic symmetry element that relates the two parts of the disorder, the site occupancy factors for each part of the disorder, and the $U_{(eq)}$ range for each set of disordered fluorine atoms. Moreover, the PF_6^- anion in the [Cu(Mes-dpa)(η^2-norbornene)]PF_6 complex (**4.5**) [1] is another example of a common[2] anionic disorder of F-atoms. These fluoro-anion disorders[3] break down into several different types, which will be discussed in this chapter.

In crystallography, the observed atomic displacement parameters are an average of millions of unit cells throughout entire volume of the crystal, in addition to thermally induced motion over the time used for data collection. A disorder of atoms/molecules in a given structure can manifest as flat or non-spherical shapes of the ADP's in a given structure. Such cases of disorder are nominally the result of either the aforementioned thermally induced motion (*i.e.*, dynamic disorder), or the static disorder of the atoms/molecules throughout the lattice. The latter is defined as the situation in which certain atoms, or groups of atoms, occupy slightly different orientations from molecule to molecule over the large volume (relatively speaking) covered by the crystal lattice.

Table 7.1. List of disordered anions and relevant data concerning refinement.

compound	disordered atoms	description of the disorder	s.o.f.	U_{eq}(F) range (Å^2)
3.1	F(2)-F(4)	C_2-rotation about axis of B(1)-F(1) bond vector	75:25	0.100(1) - 0.23(1)
3.4	F(2)-F(4)	C_2-rotation about axis of B(1)-F(1) bond vector	45:55	0.164(7) - 0.262(1)
4.3	F(2)-F(4)	C_2-rotation about axis of B(1)-F(1) bond vector	65:35	0.124(6) - 0.288(7)
5.1	F(2)-F(4)	C_2-rotation about axis of B(1)-F(1) bond vector	75:25	0.10(1) - 0.23(2)
4.5 [a]	F(3)-F(6)	C_4-rotation about axis of F(1)-P(1)-F(2) bond vector	50:50	0.163(6) - 0.212(8)
4.1 [b]	F(1)-F(4)	C_2-rotation about axis tilted 6.5(9)° off B(1)-F(2A) bond	50:50	0.061(2) - 0.134(3)
4.1	F(1)-F(4)	C_2-rotation about axis tilted 12(1)° off B(1)-F(2A) bond	50:50	0.117(4) - 0.206(5)
4.2(a)	F(1)-F(4)	C_2-rotation about axis tilted 9(1)° off B(1)-F(4A) bond	50:50	0.105(5) - 0.25(1)
3.11	F(1)-F(4)	C_2-rotation about axis tilted 13(1)° off B(1)-F(1A) bond	60:40	0.100(4) - 0.238(9)
3.2	F(1)-F(4)	C_2-rotation about axis tilted 13.9(8)° off B(1)-F(4) bond	50:50	0.149(3) - 0.255(7)
3.5	F(1)-F(4)	C_2-rotation about axis tilted 13.9(9)° off B(1)-F(1A) bond	50:50	0.138(3) - 0.31(1)
1.8	F(1)-F(4)	C_2-rotation about axis tilted 26.4(8)° off B(1)-F(3) bond	50:50	0.14(1) - 0.30(1)
3.12·MeOH [c]	F(1)-F(4)	C_2-rotation about axis tilted 42(1)° off B(1)-F(4) bond	50:50	0.156(3) - 0.263(7)
1.11 [d]	F(1)-F(4)	σ_m across plane defined by Cu(1)···N(1)···B(1)	50:50	0.195(8) - 0.30(1)
4.2(b)	F(1)-F(4)	*i* centered on atom B(1)	50:50	0.148(5) - 0.34(2)

[a] PF_6^- anion. [b] collection T = 213 K; [c] symmetry operator: y, x, 1-z; [d] symmetry operator x, 3/2-y, z.

Some ambiguity arises between these two causal factors, as the static displacement of atoms can simulate the effect of thermal vibration on the scattering power of the "average" atom.[45] Consequently, differentiation between thermal motion and static disorder can be difficult, if not impossible, unless data collection is performed at low temperature. In other words, low temperature data collection negates much of the thermal motion that would be seen at room temperature.[6] Thus, the presence of disorder in a low temperature structure should largely be the result of a static disorder.

Unfortunately, the very property that makes fluoro-anions such good candidates as counter-ions in coordination complexes (i.e. weak intermolecular interactions) also creates the presence of disorder in crystal structures. In other words, the appearance of disorder is intensified with the presence of a weakly coordinating anion, e.g., BF_4^- or PF_6^- which lack the strong intermolecular interactions needed to keep a regular, repeating anion orientation throughout the crystal lattice. Essentially, these weakly coordinating anions are loosely defined electron-rich spheres. All considered, it seems that fluoro-anions, in general, have a propensity to exhibit apparently large atomic displacement parameters (ADP's), and thus, are appropriately refined as having fractional site-occupancies.[7] Several different methods are reported for the treatment of these disorders, but the majority were refined as a non-crystallographic C_2-rotation along the axis of one of the B-F bonds.[8]

Treatment of disorder in Refinement. In most cases, this disorder is easily resolved as some non-crystallographic symmetry element acting locally on the weakly-coordinating anion. The atomic site occupancies can be refined using the FVAR instruction on the different parts (PART 1 and PART 2) of the disorder, having s.o.f. of x and 1-x, respectively. This is accomplished by replacing 11.000 (on the F-atom lines in the .ins file) with 21.000 or -21.000 for each of the different parts of the disorder. For instance, the "name.ins" file would look something like that seen below in Figure 7.1.

Note that for more heavily disordered structures, i.e., those with more than two disordered parts, the SUMP command can be used to determined the s.o.f. of parts 2, 3, 4, the combined sum of which is set at s.o.f. = 1.0 (esd of 0.01). These are designated in FVAR as the second, third, and fourth terms.

ISOR	$F					
DELU	$F					
SADI	B(1) F(1A)	B(1) F(2A)	B(1) F(3A)	B(1) F(4A)		
SADI	B(1) F(1B)	B(1) F(2B)	B(1) F(3B)	B(1) F(4B)		
SADI	F(1A) F(2A)	F(1A) F(3A)	F(1A) F(4A)	etc.		
SADI	F(1B) F(2B)	F(1B) F(3B)	F(1B) F(4B)	etc.		
FVAR [a]	0.1	0.5				
B(1)	3	x^1	y^1	z^1	U_{eq}	11.00
PART 1						
F(1A)	6	x^2	y^2	z^2	U_{eq}	21.00
F(2A)	6	x^3	y^3	z^3	U_{eq}	21.00
F(3A)	6	x^4	y^4	z^4	U_{eq}	21.00
F(4A)	6	x^5	y^5	z^5	U_{eq}	21.00
PART 2						
F(1B)	6	x^6	y^6	z^6	U_{eq}	-21.00
F(2B)	6	x^7	y^7	z^7	U_{eq}	-21.00
F(3B)	6	x^8	y^8	z^8	U_{eq}	-21.00
F(4B)	6	x^9	y^9	z^9	U_{eq}	-21.00
PART 0						

Figure 7.1 General layout of the SHELXTL "name.ins" file for treatment of disordered tetrafluoroborate.[a] for more than two site occupancies, SUMP = 1.0 0.01 1.0 2 1.0 3 1.0 4 in addition to the FVAR instruction.

Figure 7.1 also introduces some examples of using restraints. In small molecule refinement, the case will inevitably arise in which some kind of restraints or constraints

must be used to achieve convergence of the data. A restraint is any additional information concerning a given structural feature, i.e. limits on the possible values that parameters may have, that may be added into the refinement, thereby increasing the number of refined parameters.[9] For example, aromatic systems are essentially flat, so for refinement purposes, a troublesome ring system could be restrained to lie in one plane. Restraints are not exact, i.e. they are tied to a probability distribution, whereas constraints, are exact mathematical conditions.

Restraints can be regarded as falling into one of several general types: (1) geometric restraints, which relates distances that should be similar (2) rigid group restraints; (3) Anti-bumping restraints; (4) linked parameter restraints; (5) similarity restraints; (6) ADP restraints; (7) sum and average restraints; (8) origin fixing; and finally, shift limiting restraints.[8] Figure 7.2[10] illustrates the utility of three different ADP-type restraints.

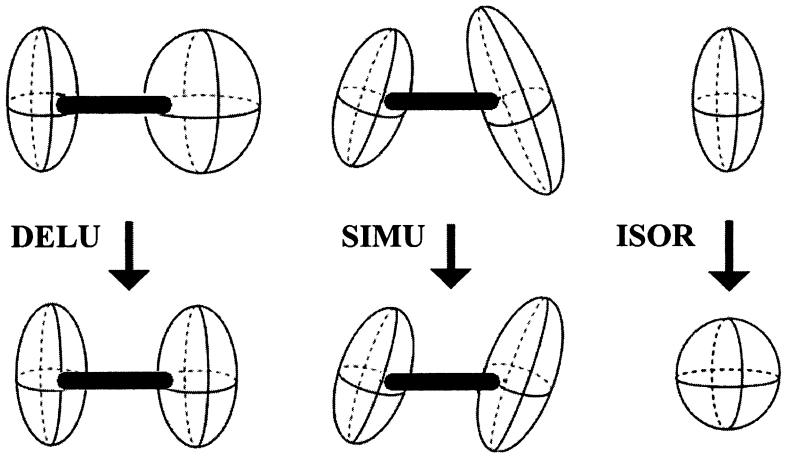

Figure 7.2. Consequence of DELU, SIMU, and ISOR restraints on the shape and directionality of atomic displacement parameters. Adapted from P. Müller, *Crystal Structure Refinement, A Crystallographer's Guide to SHELXL*, Oxford University Press, UK, 2006, 66.

Geometric restraints:

- SADI - similar distance restraints for named pairs of atoms.
- DFIX - defined distance restraint between covalently bonded atoms.
- DANG - defined non-bonding distance restraints, e.g. between fluorine atoms belonging to the same PART of a disordered BF_4^-.
- FLAT - restrains group of atoms to lie in a plane.

Anisotropic Displacement Parameter Restraints:

- DELU - rigid bond restraints.
- SIMU - similar ADP restraints on corresponding U_{ij} components to be approximately equal for atoms in close proximity.
- ISOR - treat named anisotropic atoms to have approximately isotropic behavior.

Constraints (different than "restraints"):

- EADP - equivalent atomic displacement parameters.
- AFIX - fitted group; e.g. AFIX 66 would fit the next six atoms into a regular hexagon.
- HFIX - places H atoms in geometrically ideal positions; e.g. HFIX 123 would place two sets of methyl H atoms disordered over two sites, 180° from each other.

Results and Discussion

Rotation about NCS-axis of a B-F bond. Seemingly, the most common case of disorder is a rotation about a C_2-axis, the simplest of which involves a non-crystallographic symmetry related C_2-rotation axis about the vector made by one of the B-F bonds (Scheme 7.1); this operation leads to three of the four F-atoms having two site occupancies. This is a disorder similar to that seen for ^{t}Bu and CF_3 groups. Specifically, this type of rotational disorder is observed in [H(Mes-dpa)]BF_4 (**3.1**), [H(2-^{i}PrPh-

dpa)]BF_4 (**3.4**), [Cu(2-^{i}PrPh-dpa)(η^2-styrene)]BF_4 (**4.3**), [Ag(H-dpa)(η^2-styrene)]BF_4 (**5.1**), and [Cu(Mes-dpa)(η^2-norbornene)]PF_6 (**4.5**), see Figure 7.3 and Figure 7.4.

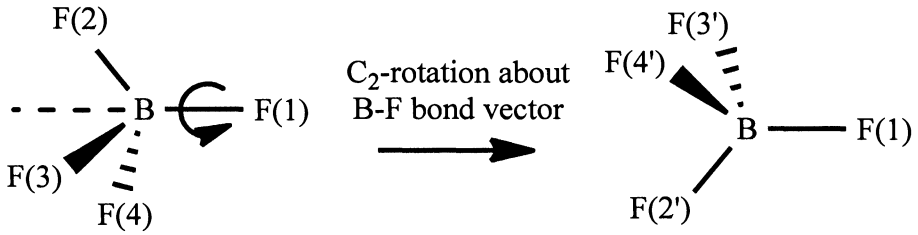

Scheme 7.1. Illustration of the C_2-rotational disorder about the B(1)-F(1) bond vector.

The BF_4^- anion present in the crystal structure of **3.1** was found to have a 75:25 site occupancy disorder for three of the four fluorine atoms. The disorder, shown below in Figure 7.3, is a C_2-rotation about the axis of the B(1)-F(1) bond. For initial refinement cycles, similar distance restraints (SADI) were placed on all B - F and F - F distances, in addition to similar ADP restraints (SIMU) and rigid bond restraints (DELU) for all fluorine atoms. Restraints were lifted for final refinement cycles.

Similarly, the BF_4^- anion present in the crystal structure of **3.4** was found to have a site occupancy disorder (45:55) for three of the four fluorine atoms. The disorder, shown in Figure 7.3, is a C_2-rotation about the axis of the B(1)-F(1) bond. For initial refinement cycles, similar distance restraints (SADI) were placed on all B - F and F···F distances, in addition to similar ADP restraints (SIMU) and rigid bond restraints (DELU) for all fluorine atoms. All restraints were lifted for final refinement cycles.

The disordered BF_4^- anion in **4.3** exhibits a 65:35 site occupancy disorder for three of the four fluorine atoms about a C_2-rotation along the B(1)-F(1) bond. Refinement of the disorder was performed similarly to that in compound **3.1**, with the exception that only SADI and DELU restraints were lifted in final refinement cycles (Figure 7.3), while SIMU restraints were retained.

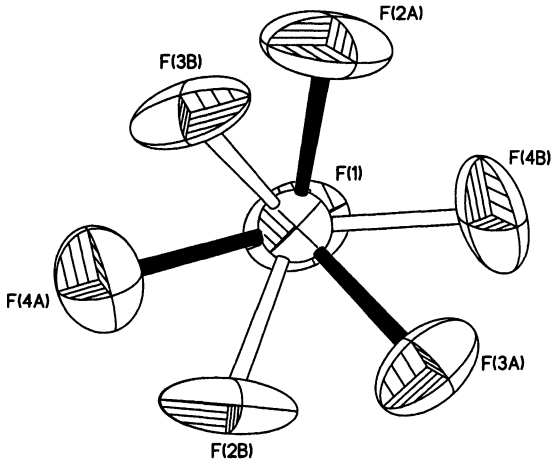

3.1

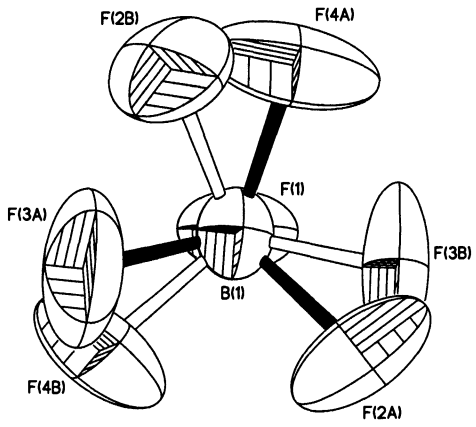

3.4

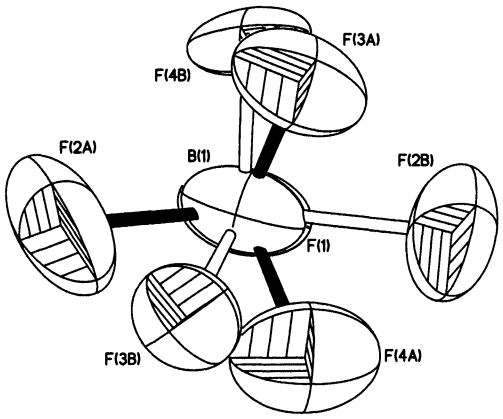

4.3

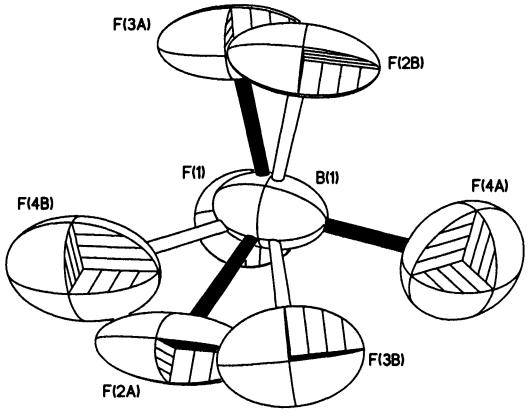

5.1

Figure 7.3. Structures determined for the tetrafluoroborate anions in [H(Mes-dpa)]BF_4 (**3.1**), [H(Mes-pqa)]BF_4 (**3.4**), [Cu(2-^{i}PrPh-dpa)(η^2-styrene)]BF_4 (**4.3**), and [Ag(H-dpa)(η^2-styrene)]BF_4 (**5.1**), which are disordered about a C_2-rotation axis coincident with the B(1)-F(1) bond vector.

In the complex, [Ag(H-dpa)(η^2-styrene)]BF_4 (**5.1**), use of the free variable (FVAR) led to refinement of disordered fluorine atoms F(2A) - F(4A) and F(2B) - F(4B) as having a 75:25 site-occupancy disorder (Fig. 1). For initial refinement cycles, all B - F

bond lengths were given similar distance restraints (SADI). Similar distance restraints (SADI) were also placed on F···F distances for each part, i.e., F(2A)···F(3A) = F(2B)...F(3B), etc. Additionally, similar ADP restraints (SIMU) and rigid bond restraints (DELU) were placed on all fluorine atoms. All restraints, with the exception of SIMU, were lifted for final refinement cycles. BF_4^-

Closely related to the C_2-rotational disorders about a B-F bond, the PF_6^- anion in compound **4.5** exhibits a 50:50 site occupancy disorder for four of the six fluorine atoms about a C_4-rotation coincident with the F(1)-P(1)-F(2) vector. Figure 7.4 illustrates this disorder, as viewed down the axis of rotation.

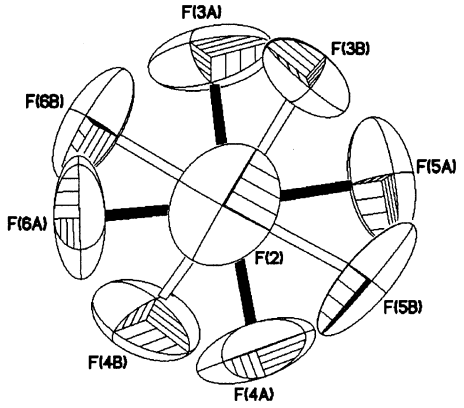

Figure 7.4. PF_6^- anion in compound **4.5** [disordered 50:50 along a C_4-rotation-axis defined by the F(1)···P(1)···F(2) vector]. For clarity, thermal ellipsoids are shown at the 20% level.

Rotation about NCS-axis tilted off B-F bond. The second type of disorder is closely related to the first, with the only difference being that the C_2-axis is tilted slightly off the B-F bond vector. As a result, all four fluorine atoms exhibit two site occupancies. (e.g., Scheme 7.2). This type of disorder was determined to be present in compounds **1.8**, **4.2**(a), **3.2**, **3.5**, and **4.1** (at both low and room temperature data collection). See Figure 7.5 and Figure 7.6. Tilt angles are listed in Table 7.1.

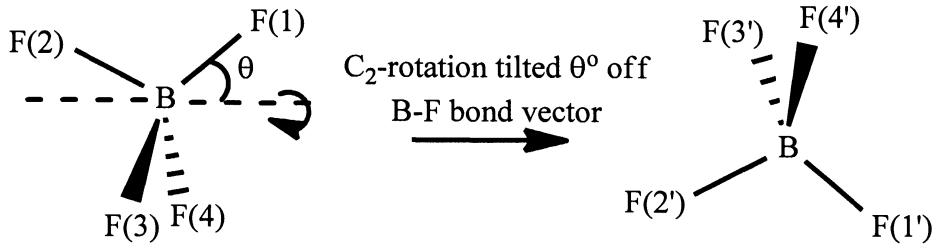

Scheme 7.2. Illustration of the C_2-rotational disorder about an axis tilted θ° off the appropriate B-F bond.

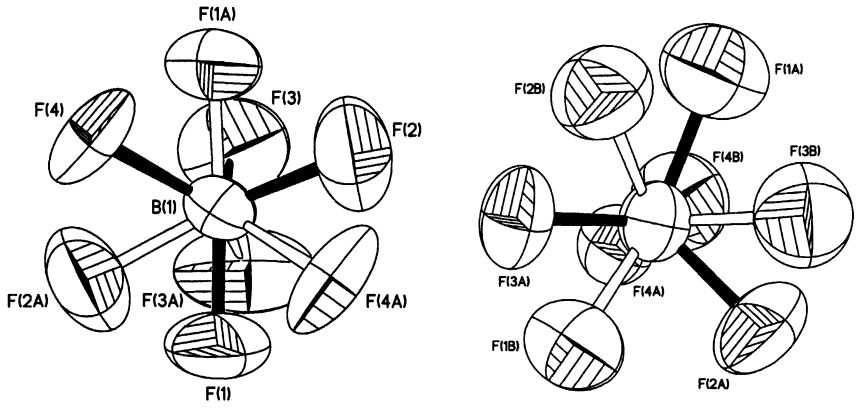

1.8 **4.2(a)**

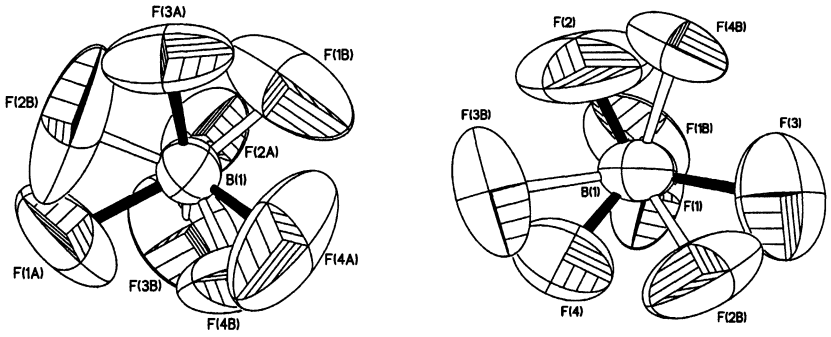

3.2 **3.5**

Figure 7.5. Structures determined for the tetrafluoroborate anions in [Cu(H-dpa)(η^2-*cis*-3-octene)]BF_4 (**1.8**), [H(2-^{i}PrPh-dpa)]BF_4 (**3.2**), [H(2,6-^{i}Pr$_2$Ph-dqa)]BF_4 (**3.5**), and , [Cu(Mes-dpa)(η^2-styrene)] [**4.2(a)**], which are disordered about a C_2-rotation axis tilted θ° off the appropriate B-F bond vector.

The BF_4^- anion in compound **1.8** shows a disorder of the fluorine atoms [F(1) through F(4)] rotated about an arbitrary C_2-axis of local NCS to yield 50:50 site occupancies [F(1)-F(4):F(1A)-F(4A)]. The BF_4^- anion present in the crystal structure of **3.2** was found to have a 50:50 site occupancy disorder for all four fluorine atoms. The disorder is a C_2-rotation slightly tilted off the axis of the B(1)-F(1A) bond. The BF_4^- anion present in the crystal structure of compound **3.5** was found to have a 50:50 site occupancy disorder for all four fluorine atoms. The disorder, shown in Figure 7.5, is a C_2-rotation about an axis slightly tilted off the B(1)-F(1) bond. For initial refinement cycles, similar distance restraints (SADI) were placed on all B - F and F - F distances, in addition to similar ADP restraints (SIMU) and rigid bond restraints (DELU) for all fluorine atoms. Similar distance restraints were lifted for final refinement cycles.

The disordered BF_4^- anion present in the crystal structure of **4.1** was refined having fractional site occupancies for all four fluorine atoms about a C_2-rotation slightly tilted off the B(1)-F(2A) bond (Figure 7.6).

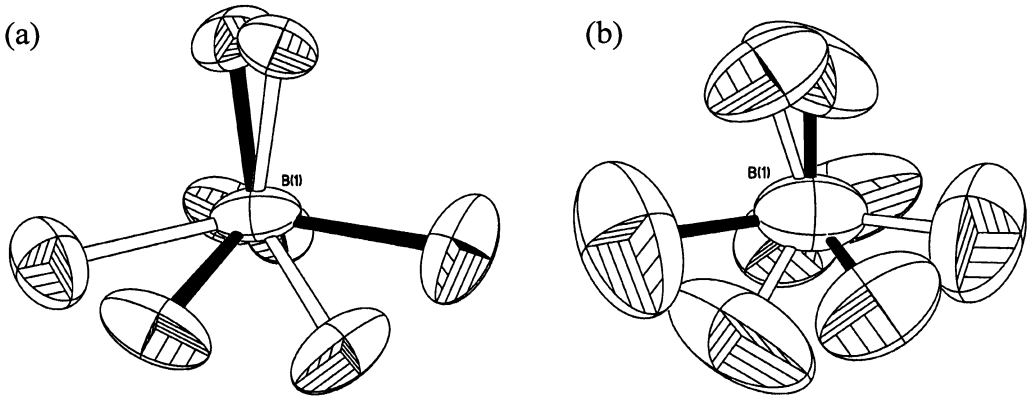

Figure 7.6. Comparison of the atomic displacement parameters observed in the disordered tetrafluoroborate anion from [Cu(Ph-dpa)(η^2-styrene)]BF_4 (**4.1**) at data collection temperature T = 213 K (a) and T = 298 K (b). For clarity, thermal ellipsoids are set at the 25 % level.

Note the difference in the $U_{(eq)}$ values determined for **4.1** collected at each temperature (Table 7.1). The low temperature data is roughly half that of that found at room temperature. This can be clearly seen on inspection of the sizes and shapes of fluorine atoms in Figure 7.6. Site occupancies refined to 50:50 in each case. An extreme example of rotation off-axis is observed where refinement of more that two site occupancies (Figure 7.7) with as many as thirteen different fluorine atom locations on only one boron atom.[11]

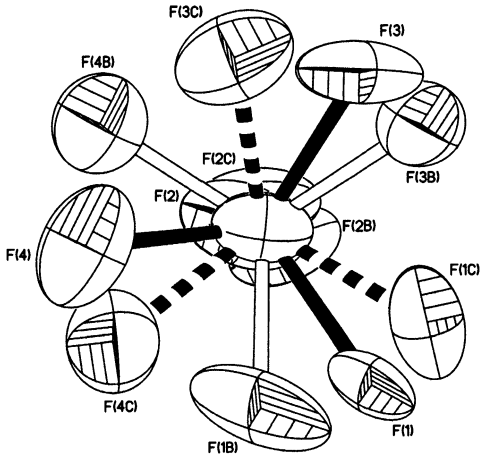

Figure 7.7. Structure for the tetrafluoroborate anion with 12 F atom locations. Adapted from S. Martinez-Vargas *et al.*, *Acta Cryst.*, 2007, **E63**, m1975.

Constrained rotation about an axis not along a B-F bond. Although a wide range of tilt angles are possible, in some systems the angle is constrained by the presence of hydrogen bonding. For example, the BF_4^- anion present in $[Cu(Mes\text{-}dpa)(\mu\text{-}OH)(H_2O)]_2[BF_4]_2$ (**3.11**) was found to have a 60:40 site occupancy disorder of the four fluorine atoms. While the disorder is an NCS C_2-rotation slightly tilted off the axis of the B(1)-F(1A) bond, this angle is restricted by the presence of two B-F···H-O interactions for one of the disordered parts (Figure 7.8).

(a)

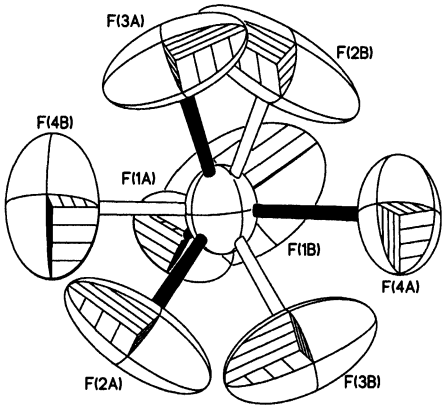

(b)

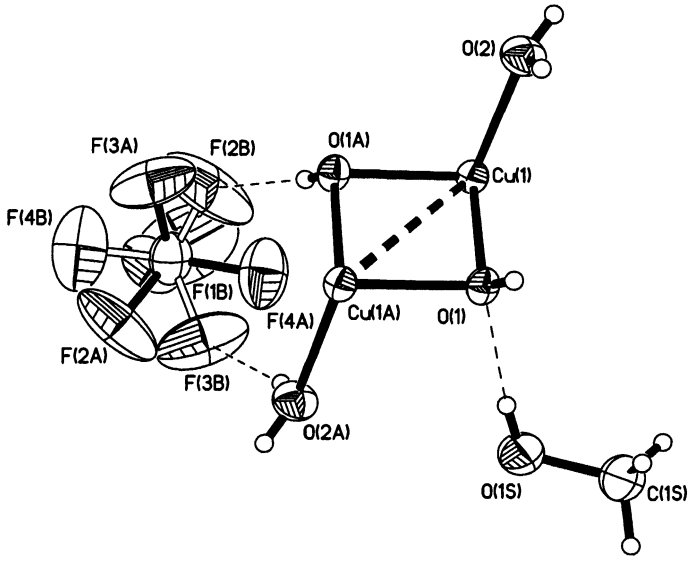

Figure 7.8. (a) Structure of the disordered BF_4^- in compound **3.11**; (b) showing interaction with methanol solvent. For clarity, thermal ellipsoids are shown at the 20 % level.

Similarly, the BF_4^- anion present in $[Cu\{2,6\text{-}^iPr_2C_6H_3\text{-}dqa\}_2]BF_4 \cdot MeOH$ (**3.12**; Figure 7.9), which exhibits a hydrogen-bonding interaction with a methanol solvent molecule, is another example of constrained rotational disorder. By crystallographic symmetry, the carbon atom from methanol and the boron atom from the BF_4^- anion lie on a C_2-axis. fluorine atoms [F(1)-F(4)], the methanol oxygen atom, and the hydrogen atoms

attached to methanol O(1S) and C(1S) atoms were refined as having 50:50 site occupancy disorder.

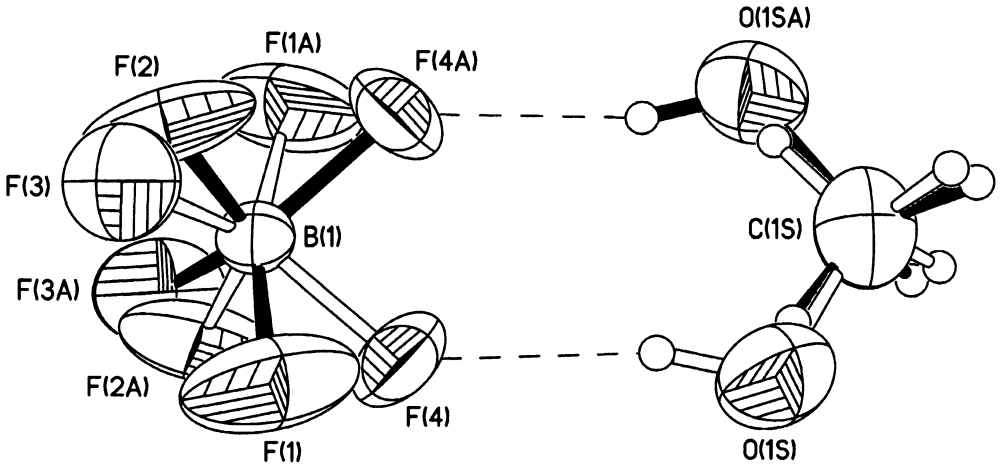

Figure 7.9. H-bonding interaction in compound **3.12** between anion and solvent of crystallization, both disordered about a crystallographic C_2-rotation axis running through the B(1) ··· C(1S) vector..

Disorder on a crystallographic mirror plane. Another instance in which the BF_4^- anion is observed to be disordered about a crystallographic symmetry element is that of **1.11**. Only fluorine atoms F(1) through F(4) are present in the asymmetric unit of the complex. Disordered atoms F(1A)-F(4A) were refined with 50% site occupancies, as B(1) lies on a mirror plane (Scheme 7.3 and Figure 7.10). For initial refinement cycles, similar distance restraints (SADI) were placed on all B - F and F - F distances, in addition to similar ADP restraints (SIMU) and rigid bond restraints (DELU) for all fluorine atoms. Restraints were lifted for final refinement cycles.

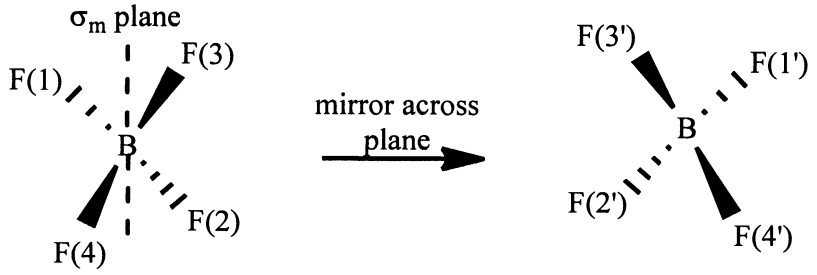

Scheme 7.3. Illustration of the σ_m disorder across a plane on which the boron atom lies.

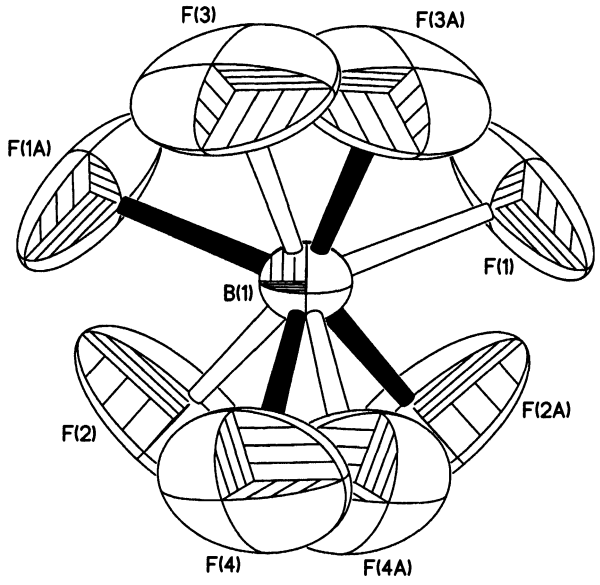

Figure 7.10. Molecular structure for the anion in (**1.11**) with both parts of the disordered BF_4^- present. For clarity, thermal ellipsoids are shown at the 20 % level.

Disorder on a non-crystallographic mirror plane. It has been observed that the BF_4^- anion can exhibit site occupancy disorder of the boron atom and one of the fluorine atoms across an NCS mirror plane defined by the plane of the other three fluorine atoms (Figure 7.11).[12].

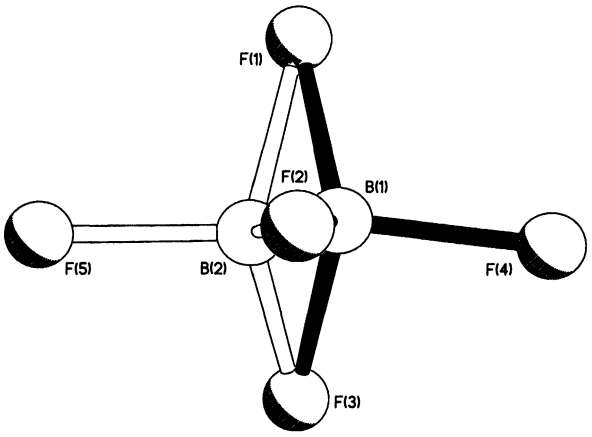

Figure 7.11. Disordered anion across the plane of 3 fluorine atoms. Adapted from J. T. Mague and S. W. Hawbaker, *J Chem. Cryst*, 1997, **27**, 603.

Disorder through an inversion center. Multiple disorders can be observed within a single unit cell of a given structure. For example, the two BF_4^- anions in [Cu(Mes-dpa)(styrene)]BF_4 (**4.2**) both exhibited 50:50 site occupancy disorders, the first of which manifests as a C_2-rotation tilted off one of the B-F bonds.

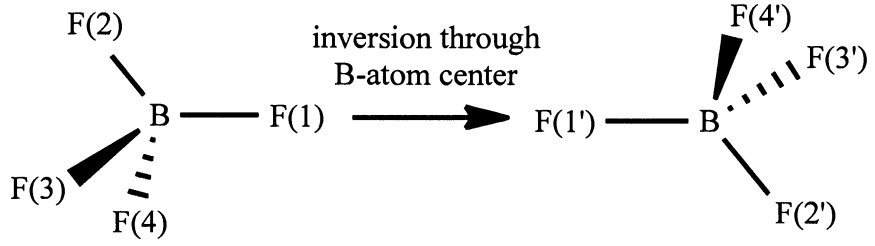

Scheme 7.4. Illustration of the disorder of fluorine atoms through the boron atom as an inversion center.

The second BF_4^- anion in **4.2** exhibited fluorine atoms that were seemingly inverted through the boron atom center. Refinement was carried out similarly to the aforementioned cases, with the exception that fixed distance restraints for non-bonded atoms (DANG) were left in place for all fluorine atoms (Figure 7.12).

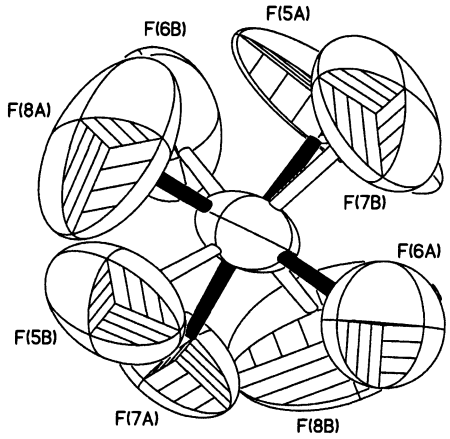

Figure 7.12. Structure for the BF_4^- anion disordered about a non-crystallographic inversion center (centered on the boron atom) in compound 4.2. For clarity, thermal ellipsoids are shown at the 20 % level.

Disorder of the boron atom core. The extreme case of a disorder involves refinement of the entire anion, with all boron and all fluorine atoms occupying more than two sites (Figure 7.13).[13] In fact, some disorders of the latter types must be refined isotropically, or as a last-resort, not at all, to prevent one or more atoms from turning non-positive definite.

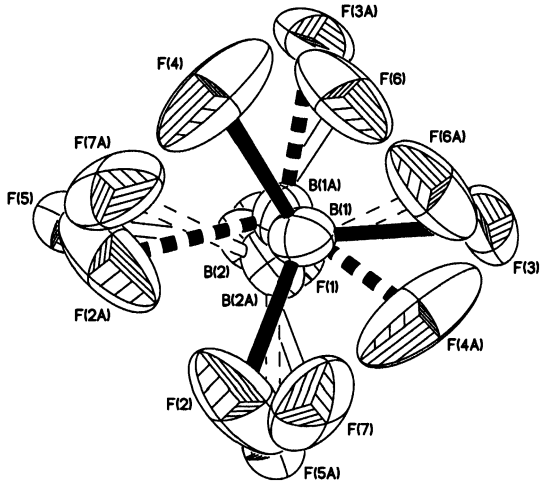

Figure 7.13. Structure of a highly disordered BF_4^- anion refined with four site occupancies for all boron and fluorine atoms. Adapted from P. Szklarz et al., *J. Mol. Struct.*, 2009, **929**, 48-57.

References

1 J. J. Allen, C. E. Hamilton, and A. R. Barron, *Dalton Trans.*, 2010, **39**, 11451.

2 (a) E. C. Alyea, G. Ferguson, and A. Somogyvari, *Inorg. Chem.*, 1982, **21**, 1369. (b) C. S. Campos-Fernandez, B. L. Schottel, H. T. Chifotides, J. K. Bera, J. Basca, J. M. Koomen, D. H. Russel, and K. R. Dunbar, *J. Am. Chem. Soc.*, 2005, **127**, 12909. (c) D. H. Gibson, M. S. Mashuta, and J. G. Andino, *Acta Cryst.*, 2005, **E61**, m341. (d) F. X. Chen, Y. Kong, H. J. Han, Y. Q. Zhang, and M. R. Xie, *Acta Cryst.*, 2007, **E63**, o1136. (e) J. C. Fettinger, H.-B. Kraatz, and R. Poli, *Acta Cryst.*, 1995, **C51**, 364. (f) E. C. Constable, A. J. Edwards, M. J. Hannon, and P. R. Raithby, *J. Chem. Soc., Chem. Commun.*, 1994, 1991.

3 (a) P. O. Lumme and U. Turpeinen, *Acta Cryst*, 1989, **C45**, 559. (b) P. Kolle and R. Dronskowski, *Eur. J. Inorg. Chem.*, 2004, 2313.

5 (a) *Accurate Molecular Structures: Their determination and Importance*, IUCr Monographs on Crystallography.1, ed. by E. Domenicano and I. Hargittai, Oxford University Press, NY, 1992, 200-216. (b) A. L. Spek, "Treating Disorder and Solvent Molecules" in *Crystallographic computing 6: A Window on Modern Crystallography*, ed. by H. D. Flack, L. Parkanyi, and K. Simon, Oxford University Press, NY, 1993, 123-131.

6 (a) "Accurate Molecular Structures: Their determination and Importance." *IUCr Monographs on Crystallography*.1, ed. by E. Domenicano and I. Hargittai, Oxford University Press, NY, 1992, 200-216. (b) A. L. Spek, "Treating Disorder and Solvent Molecules" in *Crystallographic computing 6: A Window on Modern Crystallography*, ed. by H. D. Flack, L. Parkanyi, and K. Simon, Oxford University Press, NY, 1993, 123-131.

7 (a) F. L. Hirshfield, *Acta Cryst*, 1976, **A32**, 239. (b) W. Clegg, *Crystal Structure Determination*, Oxford University Press, NY, 1998, 70.

8 (a) D. Watkin, *J. Appl. Cryst.*, 2008, **41**, 491-522. (b) H. A. Chiong and and O. Daugulis, *Organomet.*, 2006, **25**, 4054.

9 J. P. Glusker and K. N. Trueblood, *Crystal Structure Analysis: A Primer*, Oxford University Press, UK, 2010, 167.

10 P. Müller, *Crystal Structure Refinement, A Crystallographer's Guide to SHELXL*, Oxford University Press, UK, 2006, 66.

11 (a) D. F. Mullica, S. L. Gibson, E. L. Sappenfield, Chen C. Lin, and D. H. Leschnitzer, *Inorg. Chim. Acta*, 1990, **177**, 89. (b) S. Martinez-Vargas, R. Toscano, and J. Valdez-Martinez, *Acta Cryst.*, 2007, **E63**, m1975.

12 J. T. Mague,and S. W. Hawbaker, *J Chem. Cryst*, 1997, **27**:603.

13 P. Szklarz, M. Owczarek, G. Bator, T. Lis, K. Gatner, and R. Jakubas, *J. Mol. Struct.*, 2009, **929**, 48-57.

Appendix A

List of Compounds Structurally Characterized and CCDC Deposit No.'s.

The CIF data contain complete details of structure solution and refinement, full tables of bond lengths and angles, atomic coordinates and equivalent isotropic displacement parameters, anisotropic displacement parameters (all non-H atoms), and hydrogen atom coordinates and isotropic displacement parameters. These data can be obtained free of charge via www.ccdc.cam.ac.uk/conts/retrieving.html or from the Cambridge Crystallographic Data Centre, 12, Union Road, Cambridge CB2 1EZ, United Kingdom; fax: (+44)-1223-336-033; e-mail: deposit@ccdc.cam.ac.uk.

Table A.1. Summary of compounds characterized crystallographically with the corresponding CCDC deposit number.

	Compound	CCDC no.
1.5	[Cu(H-dpa)(η^2-1-octene)]BF_4	692443
1.6	[Cu(H-dpa)(η^2-*cis*-2-octene)]BF_4	692444
1.8	[Cu(H-dpa)(η^2-*cis*-3-octene)]BF_4	693280
1.1	[Cu(H-dpa)(η^2-norbornylene)]BF_4	692446
1.11	[Cu(H-dpa)(η^4-1,5-cyclooctadiene)]BF_4	698583
1.12	[Cu(H-dpa)(η^2-styrene)]BF_4	692447
1.13	[Cu(H-dpa)(η^2-*cis*-stilbene)]BF_4	692445
2.1	MesN(H)py	697653
2.2	2,6-$Et_2C_6H_3$N(H)py	697654
2.3	2-^{i}PrC_6H_4N(H)py	720342
2.4	Ph_3CN(H)py	697655

Table A.1. contd.

	Compound	CCDC no.
2.5	$MesN(py)_2$	720335
2.6	$2,6\text{-}Et_2C_6H_3N(py)_2$	720338
2.7	$2\text{-}^iPrC_6H_4N(py)_2$	720339
2.8	$2,6\text{-}^iPr_2C_6H_3N(py)_2$	720340
2.9	$1\text{-}naphN(py)_2$	720337
2.1	HN(py)quin	720334
2.11	PhN(py)quin	723245
2.12	MesN(py)quin	720336
2.13	$2,6\text{-}^iPr_2C_6H_3N(py)quin$	779677
2.14	$MesN(quin)_2$	741964
2.15	$2,6\text{-}^iPr_2C_6H_3N(quin)_2$	720341
2.16	MesN{2-quin-[N-(2'-quin)]}	683242
3.1	$[H(Mes\text{-}dpa)]BF_4$	720347
3.2	$[H(2\text{-}^iPrC_6H_4\text{-}dpa)]BF_4$	735399
3.3	$[H\{PhN(py)quin\}]BF_4$	720348
3.4	$[H\{MesN(py)quin\}]BF_4$	779678
3.5	$[H\{2,6\text{-}^iPr_2C_6H_3N(quin)_2\}]BF_4$	779679
3.6	$[Cu\{MesN(H)py\}_2]BF_4$	697652
3.7	$[Cu\{PhN(py)_2\}Cl_2]_2$	720344
3.8	$[Cu\{2\text{-}^iPrC_6H_4N(py)_2\}Cl_2]_2$	733833
3.9	$[Cu\{naphN(py)_2\}Cl_2]_2$	720343
3.1	$[Cu\{PhN(py)quin\}Cl_2]$	732508
3.11	$[Cu\{MesN(py)_2\}(\mu\text{-}OH)(H_2O)]_2[BF_4]_2$	720346
3.12·MeOH	$[Cu\{2,6\text{-}^iPr_2C_6H_3N(quin)_2\}_2]BF_4$·MeOH	720345

Table A.1. contd.

	Compound	CCDC no.
3.12·tol	$[Cu\{2,6\text{-}^{i}Pr_2C_6H_3N(quin)_2\}_2]BF_4$·tol	721175
4.1	$[Cu(Ph\text{-}dpa)(\eta^2\text{-styrene})]BF_4$	724010
4.2	$[Cu(Mes\text{-}dpa)(\eta^2\text{-styrene})]BF_4$	724009
4.3	$[Cu(2\text{-}^{i}PrC_6H_4\text{-}dpa)(\eta^2\text{-styrene})]BF_4$	740151
4.4	$[Cu(1\text{-naph-}dpa)(\eta^2\text{-styrene})]BF_4$	743482
4.5	$[Cu(Mes\text{-}dpa)(\eta^2\text{-norbornylene})]PF_6$	728875
4.8	$[Cu(Mes\text{-}dpa)(\eta^2\text{-}$*trans*$\text{-3-octene})]BF_4$	733204
5.1	$[Ag(H\text{-}dpa)(\eta^2\text{-styrene})]BF_4$	692442
6.1	$[Cu_2(\mu\text{-tpy})_2(MeCN)_2][BPh_4]_2$	683241
D.1	Methylated Meerwin's Ester: $C_{18}H_{22}O_{10}$	703400

Appendix B

Atomic Coordinates for Calculated Structures

Table B.1. Atomic coordinates for the $[Cu(H\text{-}dpa)(1\text{-}oct)]^+$ cation calculated using the RB3LYP method at the LANL2DZ/6-311++G*, with electron core potentials for copper.

atom	x	y	z	atom	x	y	z
Cu	0.8861	-0.4554	0.5388	C	-0.4317	-1.9552	1.1753
C	5.0838	-2.3711	-0.8653	C	-1.1557	-0.7675	1.1751
C	1.8812	4.2146	-0.098	C	-2.1492	-0.3793	0.0942
C	2.8222	3.2498	-0.4516	C	-3.6116	-0.6372	0.5579
C	2.5259	1.8734	-0.2513	C	-4.6494	-0.2026	-0.4996
C	4.0506	-3.188	-0.3503	C	-6.1046	-0.4701	-0.0574
C	0.6466	3.8056	0.4581	C	-7.1471	-0.0249	-1.1067
C	0.4195	2.4426	0.622	C	-8.5984	-0.3005	-0.6623
N	1.3333	1.4802	0.2719	H	-0.5435	-2.6677	0.3581
C	2.8667	-2.5756	0.0513	H	0.0241	-2.3299	2.0912
C	4.8875	-0.9936	-0.9481	H	-1.2223	-0.2057	2.1117
N	3.5162	0.9548	-0.6186	H	-1.9543	-0.9511	-0.8241
C	3.6536	-0.4353	-0.5164	H	-2.0545	0.6863	-0.1624
N	2.6577	-1.2221	-0.0293	H	-3.7987	-0.0953	1.4981
H	6.0227	-2.8077	-1.1917	H	-3.734	-1.7068	0.7816
H	2.0993	5.2679	-0.2456	H	-4.4539	-0.7336	-1.4448
H	3.7799	3.5417	-0.8735	H	-4.5261	0.8716	-0.7128
H	4.1652	-4.2626	-0.2669	H	-6.3012	0.0528	0.8922
H	-0.1095	4.5246	0.7517	H	-6.2333	-1.5449	0.1466
H	-0.5098	2.0797	1.0443	H	-6.9501	-0.5443	-2.0573
H	2.0445	-3.1573	0.451	H	-7.0233	1.0505	-1.3081
H	5.6699	-0.3469	-1.3355	H	-9.3172	0.0269	-1.424
H	4.335	1.4007	-1.0174	H	-8.8339	0.2299	0.2705
				H	-8.761	-1.3728	-0.4874

Table B.2. Atomic coordinates for the $[Cu(H\text{-}dpa)(1\text{-}oct)]^+$ cation calculated using the RMP2-FC method at the LANL2DZ/6-311++G*, with electron core potentials for copper.

atom	x	y	z	atom	x	y	z
Cu1	-0.9145	-0.5348	-0.5506	C24	0.2884	-2.1183	-1.0972
C2	-5.2584	-2.0639	0.8978	C25	1.0200	-0.8953	-1.1616
C3	-1.5106	4.2302	-0.0479	C26	2.0208	-0.4842	-0.0695
C4	-2.4455	3.3384	0.5182	C27	3.4975	-0.7149	-0.5429
C5	-2.2675	1.9242	0.3459	C28	4.5363	-0.3036	0.5457
C6	-4.3624	-2.9452	0.2138	C29	6.0110	-0.5178	0.0825
C7	-0.4097	3.7047	-0.7960	C30	7.0535	-0.1037	1.1679
C8	-0.2881	2.3082	-0.9247	C31	8.5246	-0.3221	0.6941
N9	-1.1959	1.4170	-0.3514	H32	0.4186	-2.7932	-0.2410
C10	-3.1130	-2.4464	-0.2016	H33	-0.1212	-2.5570	-2.0156
C11	-4.8700	-0.7264	1.1229	H34	1.1693	-0.4351	-2.1528
N12	-3.2116	1.0604	0.9580	H35	1.8385	-1.0788	0.8485
C13	-3.5821	-0.2797	0.6733	H36	1.9077	0.5861	0.1972
N14	-2.7123	-1.1309	0.0324	H37	3.6826	-0.1287	-1.4677
H15	-6.2371	-2.4136	1.2332	H38	3.6310	-1.7859	-0.7978
H16	-1.6384	5.3079	0.0742	H39	4.3530	-0.8976	1.4657
H17	-3.3098	3.7139	1.0729	H40	4.3861	0.7655	0.8078
H18	-4.6270	-3.9849	0.0155	H41	6.1904	0.0703	-0.8421
H19	0.3290	4.3605	-1.2591	H42	6.1572	-1.5875	-0.1760
H20	0.5286	1.8513	-1.4829	H43	6.8666	-0.6933	2.0881
H21	-2.3878	-3.0713	-0.7224	H44	6.8988	0.9637	1.4260
H22	-5.5446	-0.0260	1.6231	H45	9.2440	-0.0230	1.4773
H23	-3.8785	1.5472	1.5578	H46	8.7339	0.2752	-0.2126
				H47	8.7009	-1.3866	0.4527

Table B.3. Atomic coordinates for the [Cu(H-dpa)(*cis*-2-oct)]$^+$ cation calculated using the RMP2-FC method at the LANL2DZ/6-311++G*, with electron core potentials for copper.

atom	x	y	z	atom	x	y	z
Cu1	-0.3139	-0.1716	-0.3825	C24	1.6982	0.2012	-0.6228
C2	-2.7205	3.9905	0.0761	C25	1.4662	-1.2103	-0.6131
C3	-4.0202	-3.2136	0.19	H26	1.3657	-1.6886	-1.6009
C4	-4.1292	-1.8723	0.6187	H27	1.7907	0.6752	-1.6157
C5	-3.029	-0.976	0.4125	C28	1.7772	-2.162	0.5549
C6	-1.449	3.9545	-0.578	H29	1.0332	-2.9754	0.6168
C7	-2.8205	-3.6442	-0.4588	H30	2.7691	-2.6254	0.3997
C8	-1.7739	-2.7156	-0.6257	H31	1.7955	-1.641	1.5264
N9	-1.8615	-1.3991	-0.1799	C32	2.3032	1.01	0.5375
C10	-0.7936	2.714	-0.71	H33	2.1655	0.4845	1.5013
C11	-3.2893	2.7859	0.5454	H34	1.791	1.9888	0.6185
N12	-3.1459	0.3597	0.8862	C35	3.8361	1.2623	0.3067
C13	-2.5725	1.5559	0.3731	H36	4.2026	1.9407	1.103
N14	-1.3345	1.5258	-0.2257	H37	3.98	1.7789	-0.6655
H15	-3.2583	4.9333	0.1975	C38	4.6882	-0.0448	0.3203
H16	-4.8528	-3.9047	0.3378	H39	4.373	-0.7075	-0.5117
H17	-5.0478	-1.5082	1.0869	H40	4.5048	-0.591	1.2698
H18	-0.9825	4.8614	-0.9659	C41	6.2164	0.2381	0.1839
H19	-2.7028	-4.6682	-0.8167	H42	6.3985	0.7924	-0.7589
H20	-0.836	-2.9853	-1.1117	H43	6.538	0.8939	1.0176
H21	0.1784	2.624	-1.1956	C44	7.0637	-1.0725	0.1929
H22	-4.2748	2.7803	1.0191	H45	6.9105	-1.6289	1.1363
H23	-3.9693	0.5172	1.4687	H46	6.7737	-1.7308	-0.6473
				H47	8.1412	-0.8495	0.0976

Table B.4. Atomic coordinates for the [Cu(H-dpa)(*trans*-2-oct)]$^+$ cation calculated using the RMP2-FC method at the LANL2DZ/6-311++G*, with electron core potentials for copper.

atom	x	y	z	atom	x	y	z
Cu(1)	0.4836	-0.3493	0.4241	C(24)	-0.9496	-1.8713	1.1302
C(2)	4.5691	-2.2627	-1.2242	C(25)	-1.6139	-0.6796	1.0711
C(3)	1.6016	4.312	0.1334	C(26)	-0.3519	-2.4157	2.39
C(4)	2.5287	3.3751	-0.2421	C(27)	-2.496	-0.2971	-0.0896
C(5)	2.1927	1.9672	-0.161	C(28)	-3.9734	-0.5241	0.2824
C(6)	3.4828	-3.0895	-0.8411	C(29)	-4.9143	-0.1058	-0.8541
C(7)	0.3269	3.8986	0.5981	C(30)	-6.3836	-0.3483	-0.4792
C(8)	0.0576	2.5324	0.659	C(31)	-7.3313	0.0692	-1.6027
N(9)	0.9368	1.5498	0.2966	H(32)	-1.0065	-2.6009	0.3087
C(10)	2.3243	-2.4784	-0.3655	H(33)	-1.7273	-0.0386	1.9568
C(11)	4.4591	-0.9017	-1.1228	H(34)	-1.0024	-3.2093	2.7927
N(12)	3.1782	1.0691	-0.5604	H(35)	-0.2382	-1.6673	3.1873
C(13)	3.2283	-0.3227	-0.6209	H(36)	0.639	-2.8672	2.2301
N(14)	2.1519	-1.1297	-0.2346	H(37)	-2.2508	-0.8761	-1.0035
H(15)	5.4798	-2.7244	-1.6001	H(38)	-2.3419	0.7673	-0.3646
H(16)	1.828	5.3761	0.0798	H(39)	-4.2187	0.0434	1.2011
H(17)	3.5086	3.6664	-0.5998	H(40)	-4.1335	-1.5902	0.5347
H(18)	3.557	-4.1623	-0.9228	H(41)	-4.6671	-0.6624	-1.7783
H(19)	-0.4113	4.6285	0.8929	H(42)	-4.7619	0.9629	-1.0994
H(20)	-0.9214	2.1912	1.0186	H(43)	-6.6334	0.2101	0.4442
H(21)	1.476	-3.1048	-0.0695	H(44)	-6.5389	-1.4182	-0.2383
H(22)	5.2764	-0.2538	-1.4138	H(45)	-8.3735	-0.1061	-1.3236
H(23)	4.0463	1.5225	-0.8764	H(46)	-7.1389	-0.4906	-2.524
				H(47)	-7.2301	1.1343	-1.84

Table B.5. Atomic coordinates for the [Cu(H-dpa)(*cis*-3-oct)]$^+$ cation calculated using the RMP2-FC method at the LANL2DZ/6-311++G*, with electron core potentials for copper.

atom	x	y	z	atom	x	y	z
Cu(1)	0.1877	-0.2775	-0.5303	C(24)	-1.0265	-2.116	-0.6224
C(2)	4.7821	-1.4151	0.3408	C(25)	-1.8579	-1.0278	-0.6624
C(3)	0.4676	4.4881	0.076	H(26)	-0.7094	-2.6053	-1.5595
C(4)	1.5322	3.6964	0.478	C(27)	-0.7367	-2.9411	0.6086
C(5)	1.4776	2.2919	0.2453	H(28)	0.224	-2.6478	1.0818
C(6)	3.9072	-2.3179	-0.2904	H(29)	-1.5119	-2.7478	1.3855
C(7)	-0.6408	3.8874	-0.5476	H(30)	-2.212	-0.6343	-1.6324
C(8)	-0.6391	2.5108	-0.7397	C(31)	-0.7011	-4.4414	0.3199
N(9)	0.3953	1.6858	-0.3491	H(32)	-0.3468	-4.9957	1.2021
C(10)	2.6106	-1.907	-0.5711	H(33)	-1.7014	-4.8276	0.0839
C(11)	4.3349	-0.1415	0.6578	H(34)	-0.0435	-4.7032	-0.5152
N(12)	2.5849	1.5291	0.6993	C(35)	-2.6189	-0.4711	0.5144
C(13)	2.9961	0.2211	0.3365	H(36)	-2.4344	0.6191	0.6161
N(14)	2.1219	-0.6548	-0.2643	H(37)	-2.2736	-0.9149	1.4727
H(15)	5.809	-1.7165	0.5734	C(38)	-4.1355	-0.7325	0.3798
H(16)	0.4872	5.5707	0.2377	H(39)	-4.4706	-1.3802	1.2159
H(17)	2.3993	4.1521	0.9578	H(40)	-4.3608	-1.3159	-0.5335
H(18)	4.2447	-3.3229	-0.5527	C(41)	-4.9472	0.5734	0.3784
H(19)	-1.4861	4.495	-0.8756	H(42)	-4.6942	1.1728	1.2778
H(20)	-1.4927	2.0174	-1.2265	H(43)	-4.6679	1.1945	-0.4941
H(21)	1.9028	-2.5923	-1.068	C(44)	-6.4519	0.3152	0.3515
H(22)	5.0073	0.5682	1.1415	H(45)	-6.7839	-0.2761	1.2131
H(23)	3.2991	2.0773	1.2055	H(46)	-7.0108	1.2607	0.3731
				H(47)	-6.764	-0.2192	-0.5547

Table B.6. Atomic coordinates for the [Cu(H-dpa)(*trans*-3-oct)]$^+$ cation calculated using the RMP2-FC method at the LANL2DZ/6-311++G*, with electron core potentials for copper.

atom	x	y	z	atom	x	y	z
Cu(1)	0.1493	-0.248	0.2228	C(24)	-1.4581	-1.6754	0.581
C(2)	4.2442	-2.3438	-1.2329	C(25)	-1.9998	-0.4181	0.5809
C(3)	1.6911	4.3051	0.6246	C(26)	-1.089	-2.4242	1.8372
C(4)	2.5748	3.3241	0.2068	C(27)	-2.6891	0.1794	-0.6198
C(5)	2.1172	1.9777	0.0892	C(28)	-4.2167	0.0835	-0.4405
C(6)	3.068	-3.091	-1.033	C(29)	-4.9624	0.7069	-1.6283
C(7)	0.3617	3.9518	0.9217	C(30)	-6.4741	0.6055	-1.4556
C(8)	-0.025	2.6251	0.7855	H(31)	-1.508	-2.3134	-0.3165
N(9)	0.8228	1.6145	0.3723	H(32)	-2.1872	0.1244	1.5221
C(10)	1.9224	-2.4358	-0.6017	H(33)	-0.965	-1.7466	2.7114
C(11)	4.2276	-0.9797	-0.996	H(34)	-0.115	-2.9477	1.7218
N(12)	3.0813	1.0352	-0.3456	H(35)	-2.4039	-0.3294	-1.5658
C(13)	3.0166	-0.3638	-0.5568	H(36)	-2.4057	1.2436	-0.7576
N(14)	1.86	-1.0778	-0.3542	H(37)	-4.524	0.5852	0.4978
H(15)	5.1596	-2.84	-1.573	H(38)	-4.5147	-0.9777	-0.3249
H(16)	2.0185	5.3457	0.724	H(39)	-4.6631	0.2087	-2.572
H(17)	3.6078	3.5851	-0.027	H(40)	-4.6729	1.7705	-1.7442
H(18)	3.0601	-4.1678	-1.2161	H(41)	-6.8224	1.1266	-0.5557
H(19)	-0.347	4.715	1.2515	H(42)	-6.8089	-0.4378	-1.3784
H(20)	-1.0589	2.3227	1.0082	C(43)	-2.1783	-3.4519	2.1528
H(21)	0.9909	-2.9967	-0.4361	H(44)	-1.9521	-4.0039	3.0731
H(22)	5.1317	-0.386	-1.1458	H(45)	-3.1574	-2.9793	2.2971
H(23)	4.0126	1.4448	-0.5368	H(46)	-2.2926	-4.1908	1.3502
				H(47)	-6.9974	1.0464	-2.3066

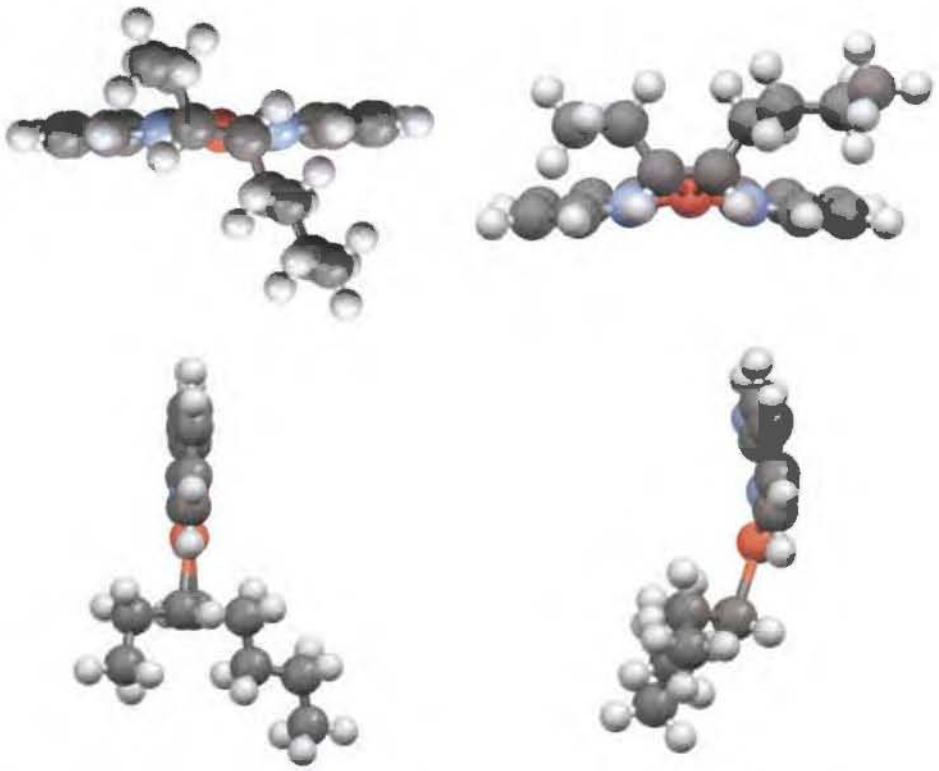

Figure B.1. Calculated structures comparing views down the Cu···N vector (top) and the side-on view (bottom) of cuprous cations of H-dpa incorporating *trans*-3-octene (left column) and *cis*-3-octene (right column).

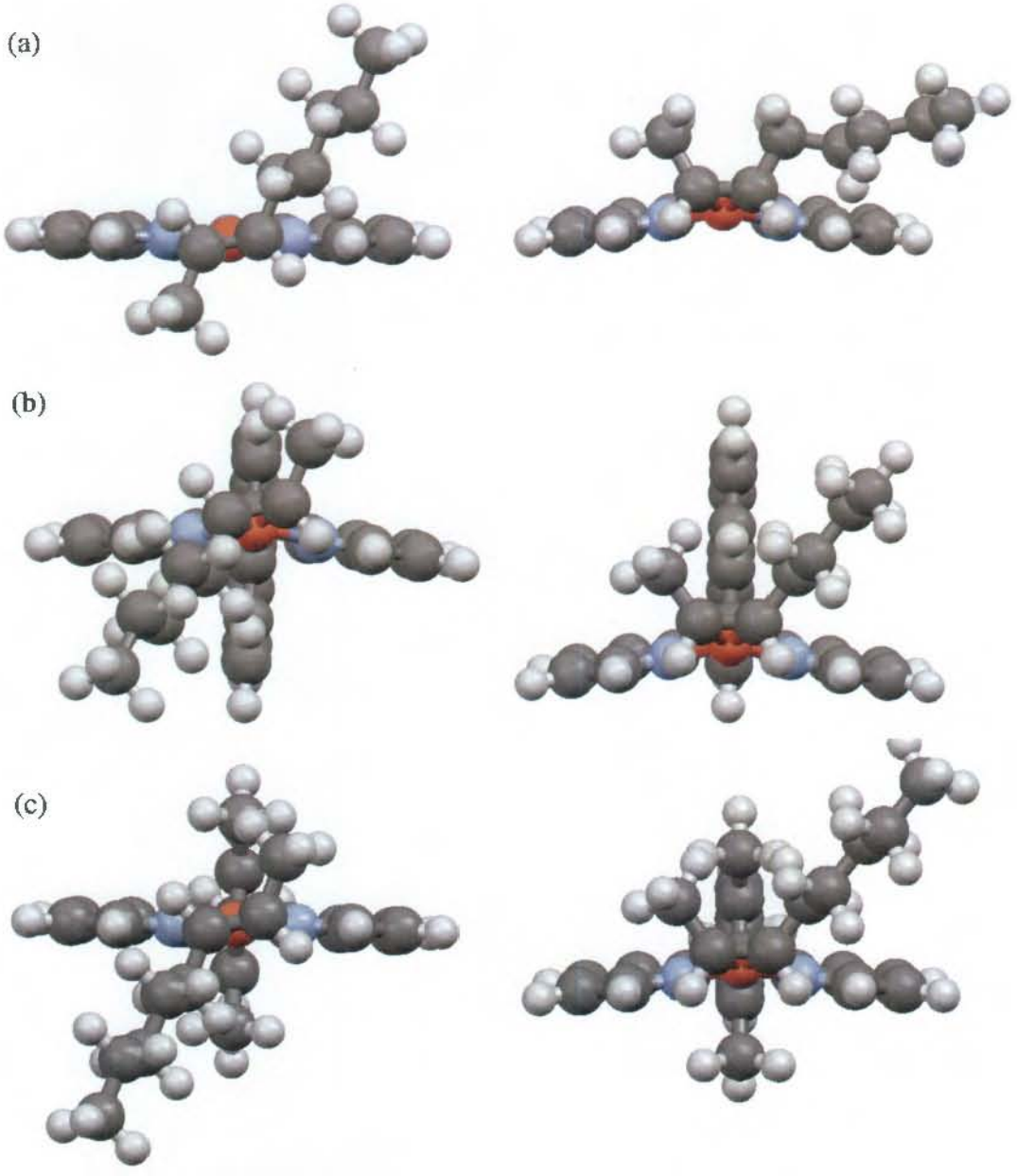

Figure B.2. Illustration demonstrating the ligand distortions in compounds of the type [Cu(Ar-dpa)(*cis*/*trans*-2-octene)]$^+$, where Ar = H (a), 1-naph (b), and Mes (c), as viewed along the Cu‴N vector, of .

Table B.7. Atomic coordinates for the [Cu(Mes-dpa)(*trans*-2-oct)]$^+$ cation calculated using the RMP2-FC method at the LANL2DZ/6-311++G*, with electron core potentials for copper.

atom	x	y	z	atom	x	y	z
Cu(1)	-1.3184	0.7835	-0.5173	H(34)	3.1335	-1.6114	3.4191
C(2)	0.9222	-3.369	-1.3507	H(35)	1.8948	-1.9113	2.1846
C(3)	2.2429	3.4218	1.3034	H(36)	2.1505	-0.2744	2.7945
C(4)	2.5302	2.1387	0.9305	H(37)	8.0135	-0.5054	0.7565
C(5)	1.5019	1.2865	0.3588	H(38)	7.7432	-2.0715	-0.02
C(6)	-0.4639	-3.1908	-1.5891	H(39)	7.5706	-1.9109	1.7312
C(7)	0.9304	3.9327	1.1268	H(40)	4.572	0.5733	-2.8516
C(8)	-0.0178	3.0827	0.5704	H(41)	3.3032	1.4522	-1.9726
N(9)	0.2045	1.7906	0.177	H(42)	2.9723	-0.1595	-2.6164
C(10)	-1.0136	-1.9531	-1.2752	C(43)	-3.4829	0.6458	-0.9471
C(11)	1.6637	-2.339	-0.8379	C(44)	-3.1463	1.9648	-0.8311
N(12)	1.8373	-0.0274	-0.0056	C(45)	-4.0969	-0.1459	0.1783
C(13)	1.0474	-1.059	-0.5372	C(46)	-2.8412	2.8391	-2.0076
C(14)	3.2484	-0.3831	0.1965	C(47)	-5.6175	-0.2591	-0.0341
N(15)	-0.3255	-0.8841	-0.7673	C(48)	-6.2862	-1.0818	1.0735
C(16)	3.6596	-0.952	1.4216	C(49)	-7.8019	-1.1829	0.8487
C(17)	5.0098	-1.2826	1.5991	C(50)	-8.4806	-2.0029	1.9427
C(18)	5.9418	-1.0521	0.5807	H(51)	-3.5388	0.1517	-1.9287
C(19)	5.5241	-0.4855	-0.6329	H(52)	-3.2983	2.5143	0.11
C(20)	4.1832	-0.1455	-0.8414	H(53)	-3.6484	-1.1605	0.2303
C(21)	2.6743	-1.203	2.5119	H(54)	-3.8953	0.314	1.168
C(22)	7.3814	-1.4036	0.7763	H(55)	-3.7024	3.4912	-2.2283
C(23)	3.7484	0.4569	-2.1338	H(56)	-2.6273	2.2809	-2.9298
H(24)	1.3814	-4.3279	-1.5824	H(57)	-1.9824	3.5045	-1.8284
H(25)	3.0071	4.063	1.7381	H(58)	-5.826	-0.7175	-1.0204
H(26)	3.5379	1.7553	1.0607	H(59)	-6.0614	0.7551	-0.0732
H(27)	-1.0631	-3.9885	-2.001	H(60)	-6.0825	-0.6282	2.0626
H(28)	0.6858	4.9427	1.4173	H(61)	-5.8456	-2.0969	1.1136
H(29)	-1.0402	3.4527	0.4264	H(62)	-8.006	-1.6392	-0.1399
H(30)	-2.0863	-1.7924	-1.4387	H(63)	-8.2474	-0.1695	0.8118
H(31)	2.7237	-2.4826	-0.6521	H(64)	-9.5638	-2.0611	1.7792
H(32)	5.332	-1.7225	2.5402	H(65)	-8.3223	-1.5645	2.9348
H(33)	6.2489	-0.3076	-1.4236	H(66)	-8.0988	-3.0298	1.9744

Table B.8. Atomic coordinates for the [Cu(Mes-dpa)(*cis*-2-oct)]$^+$ cation calculated using the RMP2-FC method at the LANL2DZ/6-311++G*, with electron core potentials for copper.

atom	x	y	z	atom	x	y	z
Cu(1)	-1.2404	1.0058	-0.5907	C(34)	-1.0552	-1.5967	-1.7794
C(2)	-3.0877	2.1664	-0.3341	C(35)	1.526	-2.2623	-1.1134
C(3)	-3.4406	0.9093	-0.738	C(36)	1.4155	4.1858	0.1878
C(4)	-3.1428	2.6739	1.072	C(37)	2.6587	3.5692	0.4838
C(5)	-3.9851	-0.1801	0.1492	C(38)	0.3595	3.3601	-0.1834
C(6)	-5.5226	-0.1921	0.0572	C(39)	1.0079	-0.938	-0.8268
C(7)	-6.1336	-1.3291	0.884	N(40)	1.8535	0.0168	-0.2366
C(8)	-7.6658	-1.3268	0.7823	C(41)	2.7921	2.2122	0.3712
C(9)	-8.2876	-2.4552	1.601	C(42)	1.671	1.3986	-0.0635
H(10)	-2.9485	2.9673	-1.0807	N(43)	s0.4237	1.9989	-0.3002
H(11)	-3.5836	0.6956	-1.8103	N(44)	-0.3247	-0.6293	-1.1434
H(12)	-2.3079	3.352	1.3056	C(45)	3.1416	-0.5017	0.2377
H(13)	-3.1359	1.8783	1.8302	C(46)	3.252	-0.9667	1.5651
H(14)	-4.0707	3.2483	1.2298	C(47)	2.0826	-0.9335	2.4914
H(15)	-3.6744	-0.0507	1.206	C(48)	4.4842	-1.4636	2.0117
H(16)	-3.5836	-1.1687	-0.1595	C(49)	5.4721	-1.0356	-0.162
H(17)	-5.8352	-0.2895	-1.001	C(50)	4.2554	-0.5309	-0.6366
H(18)	-5.92	0.7833	0.4002	C(51)	5.5919	-1.5006	1.1562
H(19)	-5.8273	-1.2377	1.9437	C(52)	6.9024	-2.0357	1.6345
H(20)	-5.7371	-2.3048	0.5415	C(53)	4.1338	-0.0379	-2.0366
H(21)	-7.9729	-1.422	-0.278	H(54)	-1.2176	-3.5873	-2.6044
H(22)	-8.0653	-0.3525	1.1265	H(55)	1.1221	-4.1875	-1.9606
H(23)	-9.3811	-2.4444	1.5236	H(56)	-2.0834	-1.3198	-2.04
H(24)	-8.0337	-2.3714	2.6639	H(57)	2.5419	-2.5168	-0.8278
H(25)	-7.9451	-3.4389	1.2599	H(58)	1.3008	5.256	0.2536
H(26)	2.3128	-1.3412	3.4829	H(59)	3.4952	4.1892	0.8017
H(27)	1.7188	0.0969	2.6333	H(60)	-0.6155	3.8104	-0.4046
H(28)	3.3747	-0.6141	-2.593	H(61)	3.7417	1.7403	0.6059
H(29)	5.0727	-0.0961	-2.5988	H(62)	1.2402	-1.5138	2.0814
H(30)	6.9046	-2.2617	2.7089	H(63)	4.5755	-1.8238	3.033
H(31)	7.7179	-1.3213	1.4539	H(64)	6.3332	-1.0686	-0.8255
C(32)	-0.5927	-2.8681	-2.1	H(65)	7.1634	-2.966	1.108
C(33)	0.7403	-3.1931	-1.7366	H(66)	3.7983	1.0127	-2.0603

Table B.9. Atomic coordinates for the [Cu(2-^{i}PrPh)(*cis*-2-oct)]$^{+}$ cation calculated using the RMP2-FC method at the LANL2DZ/6-311++G*, with electron core potentials for copper.

atom	x	y	z	atom	x	y	z
Cu(1)	-0.9541	1.2167	-0.7016	C(34)	-2.7365	2.3501	-0.1443
C(2)	0.8562	-2.7436	-2.705	C(35)	-3.6718	-0.0273	0.0049
C(3)	3.0896	3.4156	0.5887	C(36)	-2.6835	2.6172	1.3256
C(4)	3.1388	2.0761	0.3179	C(37)	-5.2109	0.0185	0.0561
C(5)	1.965	1.3935	-0.1866	C(38)	-5.7955	-1.2338	0.7203
C(6)	-0.4602	-2.3062	-2.9836	C(39)	-7.328	-1.1631	0.7905
C(7)	1.8776	4.132	0.3903	C(40)	-7.9212	-2.4065	1.4482
C(8)	0.7689	3.4235	-0.0564	H(41)	-3.3788	1.1588	-1.8058
N(9)	0.7482	2.0819	-0.3258	H(42)	-2.6246	3.2642	-0.7545
C(10)	-0.8828	-1.1172	-2.3982	H(43)	-3.2652	-0.0948	1.0343
C(11)	1.6699	-1.9937	-1.8944	H(44)	-3.3411	-0.9553	-0.5067
N(12)	2.0448	0.019	-0.5267	H(45)	-3.5697	3.1958	1.6367
C(13)	1.1992	-0.7412	-1.34	H(46)	-1.8019	3.2137	1.6085
C(14)	3.2686	-0.6611	-0.0794	H(47)	-2.6717	1.7073	1.9426
N(15)	-0.1174	-0.3298	-1.5823	H(48)	-5.6182	0.124	-0.9684
C(16)	3.2991	-1.3386	1.1522	H(49)	-5.5336	0.9257	0.6038
C(17)	4.5001	-1.9672	1.5262	H(50)	-5.3797	-1.3539	1.7392
C(18)	5.6253	-1.9192	0.7043	H(51)	-5.4875	-2.1397	0.1629
C(19)	5.5773	-1.2368	-0.5168	H(52)	-7.7484	-1.043	-0.2272
C(20)	4.4007	-0.6048	-0.9138	H(53)	-7.6385	-0.2611	1.3535
C(21)	2.0942	-1.4068	2.0729	H(54)	-9.015	-2.3454	1.4934
H(22)	1.2116	-3.676	-3.1419	H(55)	-7.5574	-2.5345	2.474
H(23)	3.9661	3.9515	0.9478	H(56)	-7.6671	-3.3184	0.8957
H(24)	4.0576	1.5201	0.4766	H(57)	4.3501	-0.0654	-1.8606
H(25)	-1.11	-2.8808	-3.6276	H(58)	6.5455	-2.4126	1.0137
H(26)	1.8289	5.1932	0.5804	C(59)	1.6638	-2.8631	2.2921
H(27)	-0.1765	3.9552	-0.2087	H(60)	0.7502	-2.9137	2.8939
H(28)	-1.902	-0.7575	-2.5857	H(61)	1.4615	-3.3603	1.3364
H(29)	2.6757	-2.3374	-1.676	H(62)	2.4266	-3.4505	2.8136
H(30)	4.5482	-2.4984	2.4772	C(63)	2.3968	-0.7055	3.4021
H(31)	6.4577	-1.1961	-1.1565	H(64)	1.5071	-0.6817	4.0414
H(32)	1.2333	-0.8669	1.5962	H(65)	3.1945	-1.203	3.964
C(33)	-3.1568	1.1839	-0.7272	H(66)	2.7117	0.3348	3.2347

Table B.10. Atomic coordinates for Pd(L)[N(Mes)quin](quin) (L = 1,3-*bis*(2,6-diisopropylphenyl)imidazol-2-ylidene) with the quin rings oriented in the *syn*-conformation.

atom	No.	x	y	z	atom	No.	x	y	z
Pd	107	-0.34379	0.04504	0.15285	H	3	4.48855	1.15833	1.73046
N	24	2.0522	1.87113	-0.39064	H	4	4.23076	2.5176	-0.47781
N	25	2.27966	0.71575	1.47185	H	12	0.88997	2.55229	-4.86999
N	41	-2.78305	1.44755	-0.46435	H	13	-0.03084	5.6199	-2.03049
N	57	-2.37284	-2.32621	-0.06635	H	14	-0.06388	4.77079	-4.35088
N	66	-0.14948	-1.79904	-0.55884	H	21	2.72739	-2.90156	4.3777
C	1	3.59309	1.2773	1.15971	H	22	0.04532	0.25418	5.46418
C	2	3.45847	1.97595	0.02608	H	23	1.0987	-1.92875	5.96201
C	5	1.45016	0.99029	0.44109	H	30	-2.41397	-0.00394	2.53955
C	6	1.49895	2.62386	-1.53058	H	33	-4.74203	0.87636	2.77079
C	7	1.46604	2.12912	-2.85296	H	35	-3.97453	2.76518	-2.35302
C	8	0.98096	3.89636	-1.25508	H	38	-6.30125	3.5872	-2.2495
C	9	0.90891	2.9189	-3.86928	H	39	-6.66838	2.02787	1.72326
C	10	0.3951	4.66555	-2.26354	H	40	-7.65618	3.2192	-0.21356
C	11	0.36816	4.18179	-3.57656	H	46	0.01924	-4.24621	-1.43308
C	15	1.98594	-0.038	2.7014	H	49	-1.90227	-5.79097	-1.67699
C	16	2.59284	-1.27179	2.98783	H	51	-4.79875	-1.78828	0.75189
C	17	1.07671	0.52071	3.60658	H	54	-6.77047	-3.24212	0.414
C	18	2.27199	-1.95553	4.16739	H	55	-4.28344	-6.19352	-1.44492
C	19	0.75119	-0.16577	4.78279	H	56	-6.51723	-5.43768	-0.69011
C	20	1.34708	-1.40463	5.06219	H	64	4.12307	-3.4483	0.01205
C	26	-2.21335	0.75575	0.52604	H	65	3.08585	-2.16615	-3.9298
C	27	-2.88794	0.53131	1.73413	H	68	1.00846	3.65362	0.88122
C	28	-4.02148	1.90791	-0.38482	H	70	1.45985	-0.01828	-2.68841
C	29	-4.19466	1.02298	1.86524	H	72	1.13954	2.4727	2.69155
C	31	-4.56446	2.59758	-1.47362	H	74	3.25814	-2.86108	1.70312
C	32	-4.77498	1.70201	0.77723	H	76	2.27214	-0.47284	-4.98064
C	34	-5.8826	3.0674	-1.41476	H	77	0.86374	0.55817	-5.02872

Table B.10. contd.

atom	No.	x	y	z	atom	No.	x	y	z
C	36	-6.09182	2.18038	0.83861	H	78	2.45596	1.24151	-5.26582
C	37	-6.64894	2.85906	-0.25917	H	80	3.59125	0.82307	-1.75472
C	42	-1.16746	-2.6733	-0.56331	H	81	3.88279	-0.31038	-3.05164
C	43	-0.95948	-3.94694	-1.10929	H	82	4.05194	1.40575	-3.33444
C	44	-3.44034	-3.14533	-0.1986	H	84	2.55569	5.53212	1.32919
C	45	-2.04166	-4.81711	-1.24434	H	85	3.2431	4.41908	0.16771
C	47	-4.69215	-2.73592	0.26016	H	86	2.56054	5.93174	-0.37209
C	48	-3.29543	-4.40227	-0.80853	H	88	0.03642	6.27912	-0.27158
C	50	-5.80801	-3.56246	0.07764	H	89	-0.99043	4.9935	0.31476
C	52	-4.40579	-5.23593	-0.98101	H	90	0.04347	5.8607	1.42503
C	53	-5.66778	-4.81137	-0.54792	H	92	4.47481	-1.40147	0.13377
C	58	1.18198	-2.15441	-1.10937	H	93	2.81756	-0.87663	0.30963
C	59	2.12749	-2.69736	-0.22628	H	94	4.09689	-0.01333	1.12487
C	60	1.52111	-1.96891	-2.46338	H	96	5.31005	-1.0913	3.0618
C	61	3.4078	-3.04063	-0.67313	H	97	4.84315	-2.68946	3.59551
C	62	2.81475	-2.31374	-2.9062	H	98	5.66976	-2.48411	2.07058
C	63	3.75101	-2.85112	-2.01374	H	100	-1.55324	1.19529	3.175
C	67	1.08848	4.45233	0.17851	H	101	-1.28529	2.71978	2.36592
C	69	2.01686	0.73102	-3.21153	H	102	-0.71478	1.23548	1.64195
C	71	0.46671	1.90976	3.30615	H	104	-0.41825	2.10538	5.25502
C	73	3.60546	-1.89707	2.02379	H	105	1.18855	2.77737	5.13944
C	75	1.89291	0.49582	-4.73832	H	106	-0.16802	3.62632	4.4345
C	79	3.49927	0.65528	-2.80734	H	109	5.077	-3.84313	-3.38221
C	83	2.46727	5.13754	0.33874	H	110	5.71285	-2.35107	-2.73219
C	87	-0.04084	5.47468	0.43092	H	111	5.66491	-3.78699	-1.73775
C	91	3.76217	-0.97746	0.80561	H	113	-0.33885	-2.05267	-3.53508
C	95	4.96154	-2.05362	2.7435	H	114	0.16627	-0.43388	-3.11385
C	99	-0.87378	1.75182	2.56636	H	115	0.95701	-1.28381	-4.41977
C	103	0.24951	2.66123	4.63554	H	117	1.5721	-1.97616	1.7196
C	108	5.15886	-3.23756	-2.50387	H	118	0.85658	-3.51429	1.30095
C	112	0.49835	-1.3907	-3.45898	H	119	2.54288	-3.42864	1.75051
C	116	1.74563	-2.92119	1.24874					

Table B.11. Atomic coordinates for Pd(L)[N(Mes)quin](quin) (L = 1,3-*bis*(2,6-diisopropylphenyl)imidazol-2-ylidene) with the quin rings oriented in the *anti*-conformation.

atom	No.	x	y	z	atom	No.	x	y	z
Pd	107	0.53076	0.41936	-0.10444	H	3	-2.47477	-3.13024	2.22943
N	24	-0.58056	-2.41887	-0.38761	H	4	-2.03782	-4.14567	-0.13034
N	25	-0.96204	-1.56037	1.60562	H	12	-0.27332	-2.38838	-5.05494
N	41	3.34061	-0.15132	0.17315	H	13	2.74377	-4.44516	-2.82162
N	57	-2.5559	0.35522	-0.61079	H	14	1.79999	-3.72938	-4.99032
N	66	-0.76619	1.85738	-0.54593	H	21	-2.59608	1.25213	4.94465
C	1	-1.80764	-2.74736	1.48775	H	22	1.51442	0.0668	5.12179
C	2	-1.58101	-3.26812	0.27581	H	23	-0.39338	1.33046	6.06312
C	5	-0.3694	-1.34692	0.41016	H	30	2.35472	2.88812	-0.85458
C	6	0.01554	-2.75765	-1.69223	H	33	4.83472	3.17991	-0.96722
C	7	-0.51655	-2.33299	-2.9296	H	35	5.00154	-2.03885	0.80671
C	8	1.17597	-3.54279	-1.67126	H	38	7.45975	-1.87242	0.63473
C	9	0.1301	-2.69997	-4.1188	H	39	7.08362	2.16833	-0.7364
C	10	1.83694	-3.87684	-2.85593	H	40	8.50843	0.22927	-0.13952
C	11	1.30789	-3.46457	-4.0843	H	46	-2.53354	3.66727	-1.16411
C	15	-0.84628	-0.76003	2.83536	H	49	-4.97883	3.27809	-1.24825
C	16	-1.93286	-0.05205	3.37454	H	51	-3.67702	-1.99138	-0.32704
C	17	0.39634	-0.7293	3.47814	H	54	-6.11407	-2.4079	-0.27405
C	18	-1.76897	0.70392	4.5422	H	55	-6.84678	1.75091	-0.99451
C	19	0.56183	0.0315	4.64196	H	56	-7.69832	-0.5401	-0.59828
C	20	-0.52001	0.74967	5.17277	H	64	1.15448	5.23448	-3.03729
C	26	2.51975	0.84074	-0.18186	H	65	0.48176	6.06444	1.09992
C	27	3.02107	2.08282	-0.59516	H	68	1.50362	-3.34011	0.44416
C	28	4.65764	-0.03921	0.10376	H	70	-1.61412	-0.52572	-2.52026
C	29	4.41207	2.24802	-0.66055	H	72	1.17567	-2.40815	2.37106
C	31	5.45533	-1.13053	0.46248	H	74	-3.60805	0.91248	2.4352
C	32	5.23968	1.1594	-0.32644	H	76	-3.0332	-0.60022	-4.54546
C	34	6.84961	-1.03619	0.36885	H	77	-1.34564	-0.701	-4.98235
C	36	6.63614	1.25588	-0.4116	H	78	-2.33766	-2.1412	-4.98787
C	37	7.44257	0.15659	-0.06905	H	80	-2.70055	-2.3839	-1.29988
C	42	-2.07356	1.61048	-0.72045	H	81	-3.83108	-1.5991	-2.37584

Table B.11. contd.

atom	No.	x	y	z	atom	No.	x	y	z
C	43	-2.93023	2.68314	-1.00157	H	82	-3.12208	-3.13359	-2.81894
C	44	-3.88661	0.11778	-0.63975	H	84	1.33616	-5.75482	0.95841
C	45	-4.30702	2.46277	-1.05092	H	85	-0.07676	-5.20133	0.08794
C	47	-4.36594	-1.17869	-0.45399	H	86	1.16285	-6.10398	-0.74514
C	48	-4.78886	1.17487	-0.84325	H	88	3.43294	-5.02375	-1.17142
C	50	-5.74588	-1.41732	-0.43299	H	89	3.72152	-3.38277	-0.64706
C	52	-6.1678	0.93797	-0.83559	H	90	3.5855	-4.6653	0.53206
C	53	-6.64915	-0.35879	-0.61839	H	92	-4.17985	-0.98404	0.96899
C	58	-0.21432	3.23089	-0.65113	H	93	-2.50728	-0.52324	0.7616
C	59	0.25005	3.65123	-1.90664	H	94	-2.91212	-1.93773	1.70069
C	60	-0.14338	4.10994	0.4466	H	96	-4.04156	-1.67922	3.94637
C	61	0.79738	4.92742	-2.07527	H	97	-4.38832	-0.08039	4.56318
C	62	0.41291	5.39366	0.27025	H	98	-5.2969	-0.71172	3.21159
C	63	0.87679	5.79987	-0.98739	H	100	2.80728	0.13028	2.47492
C	67	1.7045	-4.05868	-0.31836	H	101	3.21584	-1.3004	1.56021
C	69	-1.78908	-1.46077	-3.01059	H	102	1.79955	-0.36889	1.13694
C	71	1.56471	-1.56604	2.90664	H	104	2.82879	-1.23689	4.61345
C	73	-3.30851	-0.08345	2.70197	H	105	1.84607	-2.6747	4.7305
C	75	-2.15487	-1.20587	-4.49484	H	106	3.24739	-2.65504	3.68462
C	79	-2.95039	-2.19988	-2.32377	H	109	0.80798	7.93527	-0.76297
C	83	0.977	-5.38193	0.02222	H	110	2.41914	7.26387	-0.68265
C	87	3.22671	-4.30186	-0.40792	H	111	1.60496	7.39949	-2.22271
C	91	-3.22171	-0.94853	1.43773	H	113	-1.71192	3.4903	1.7773
C	95	-4.3387	-0.68404	3.68149	H	114	-0.1521	2.79368	2.14437
C	99	2.41075	-0.71001	1.94718	H	115	-0.47742	4.46448	2.53891
C	103	2.43905	-2.07032	4.07299	H	117	0.7857	1.85118	-2.94969
C	108	1.47268	7.20699	-1.17851	H	118	-0.86249	2.36492	-3.21916
C	112	-0.66067	3.68194	1.83254	H	119	0.45412	3.20852	-3.99887
C	116	0.14915	2.69609	-3.11044					

Table B.12. Atomic coordinates for Pd(L)[N(2,6-^{i}Pr$_2$Ph)quin](quin) (L = 1,3-*bis*(2,6-diisopropylphenyl)imidazol-2-ylidene) with the quin rings oriented in the *syn*-conformation.

atom	no.	x	y	z	atom	no.	x	y	z
Pd	103	-0.26347	0.18831	0.25871	H	4	3.89107	2.81172	-1.55657
N	24	1.83249	2.07728	-0.92852	H	12	-0.77506	5.52249	-2.72031
N	25	2.54899	1.06149	0.89091	H	13	-0.15321	1.99766	-5.06761
N	41	-2.834	1.48488	0.16272	H	14	-1.14965	4.24302	-4.79967
N	57	-2.34976	-2.14238	0.20156	H	21	2.20914	0.87938	5.53641
N	67	-0.13033	-1.68929	-0.37518	H	22	3.19601	-2.71618	3.43151
C	1	3.7204	1.65798	0.2507	H	23	2.76153	-1.52964	5.55894
C	2	3.28828	2.27185	-0.85735	H	30	-1.76433	0.12413	3.03857
C	5	1.49025	1.22898	0.06816	H	33	-4.02134	0.9245	3.75523
C	6	0.98905	2.72618	-1.94816	H	35	-4.45904	2.71008	-1.44384
C	7	0.43473	4.01659	-1.79945	H	38	-6.73998	3.44905	-0.85115
C	8	0.7443	1.9992	-3.1208	H	39	-6.17436	1.97817	3.13203
C	9	-0.34808	4.55229	-2.83254	H	40	-7.60596	3.08341	1.43636
C	10	-0.0067	2.5501	-4.16214	H	46	-0.04072	-4.17576	-1.14382
C	11	-0.5643	3.8253	-4.01479	H	49	-2.00202	-5.68456	-1.26545
C	15	2.59025	0.38032	2.19494	H	51	-4.73879	-1.51265	1.06173
C	16	2.3327	1.05271	3.40084	H	54	-6.75096	-2.9336	0.8436
C	17	2.88624	-0.98733	2.20651	H	55	-4.38387	-6.02095	-0.94996
C	18	2.39448	0.36169	4.61759	H	56	-6.57791	-5.18084	-0.16814
C	19	2.95419	-1.67677	3.42337	H	64	2.81266	-1.90577	-3.92379
C	20	2.71044	-1.00201	4.62885	H	65	4.10707	-3.68862	-0.26265
C	26	-2.03556	0.83956	1.01714	H	66	4.52206	-3.1125	-2.62462
C	27	-2.42294	0.62123	2.3465	H	69	0.50874	-0.10205	-3.51158
C	28	-4.04372	1.90164	0.50164	H	71	1.62828	4.61216	-0.10853
C	29	-3.68939	1.06807	2.75008	H	74	1.58057	2.83558	2.46564
C	31	-4.8373	2.54333	-0.45461	H	76	0.82884	6.95165	-0.01701
C	32	-4.5188	1.6978	1.8029	H	77	1.42525	6.57573	-1.61446
C	34	-6.12963	2.9661	-0.1187	H	78	-0.29677	6.62791	-1.31405
C	36	-5.80966	2.12922	2.14084	H	80	-0.43242	3.53655	0.73945
C	37	-6.61853	2.7592	1.17908	H	81	-0.27214	5.15893	1.36706
C	42	-1.16705	-2.53895	-0.31255	H	82	-1.38621	4.8317	0.06113
C	43	-1.00292	-3.83984	-0.80677	H	84	2.78068	-0.44454	-4.43047

Table B.12. contd.

atom	no.	x	y	z	atom	no.	x	y	z
C	44	-3.43842	-2.94142	0.1355	H	85	1.95419	0.84779	-5.27144
C	45	-2.10745	-4.68966	-0.87295	H	86	3.17228	1.22197	-4.07911
C	47	-4.66724	-2.4832	0.60998	H	88	2.69251	0.78804	-1.61264
C	48	-3.33878	-4.22697	-0.42158	H	89	1.14186	0.14173	-1.1343
C	50	-5.80582	-3.29074	0.49537	H	90	2.28693	-0.87142	-1.9805
C	52	-4.47174	-5.04132	-0.52599	H	92	0.71474	3.84295	4.54147
C	53	-5.71114	-4.56885	-0.07754	H	93	0.06509	2.23692	4.31465
C	58	1.17666	-2.09942	-0.94591	H	94	1.35235	2.50275	5.46308
C	59	1.42948	-1.77995	-2.28854	H	96	3.67458	3.07101	4.64466
C	60	2.15335	-2.78499	-0.19836	H	97	3.98863	3.16853	2.92745
C	61	2.63394	-2.14965	-2.89623	H	98	3.02845	4.39903	3.71155
C	62	3.36377	-3.15781	-0.81835	H	100	3.83589	-3.5299	1.76898
C	63	3.60241	-2.8366	-2.16063	H	101	4.30402	-3.33215	0.09799
C	68	1.29574	0.56472	-3.23922	H	102	5.09123	-2.39117	1.34203
C	70	0.67783	4.86425	-0.53097	H	104	2.17612	-2.15553	0.5495
C	72	3.10378	-1.72575	0.86516	H	106	3.55482	0.26556	0.1971
C	73	1.9879	2.5449	3.41556	H	107	4.58803	-0.96523	-0.48897
C	75	0.65742	6.37018	-0.89641	H	108	2.94644	-0.78488	-1.05969
C	79	-0.43806	4.57647	0.48814	H	110	2.22536	-2.31749	1.89719
C	83	2.38524	0.54526	-4.3387	H	112	2.76984	-4.4836	2.71533
C	87	1.90096	0.12211	-1.88938	H	113	2.22942	-5.25825	1.24532
C	91	0.95222	2.80273	4.51787	H	114	3.7024	-4.31835	1.24697
C	95	3.26871	3.35897	3.69535	H	116	0.11904	-3.0099	2.46105
C	99	4.16427	-2.82868	1.03258	H	117	-0.15651	-2.91579	0.73818
C	105	3.58498	-0.72632	-0.20311	H	118	0.22493	-4.45145	1.47932
C	109	1.91035	-3.13412	1.28173	H	120	0.3419	0.00922	-2.76926
C	111	2.71434	-4.39477	1.65047	H	122	-1.04751	-2.59865	-3.3826
C	115	0.40998	-3.39795	1.50728	H	123	-1.17534	-1.80338	-1.83203
C	119	0.36905	-1.00913	-3.09657	H	124	-1.77209	-1.01256	-3.27132
C	121	-1.01184	-1.65523	-2.87903	H	126	1.10927	-0.10604	-4.89977
C	125	0.72856	-1.05787	-4.59323	H	127	1.47262	-1.80917	-4.75702
H	3	4.72843	1.61741	0.60283	H	128	-0.14641	-1.29227	-5.16277

Appendix C.

Consequence of Collection Temperature on Overall Data Quality

In addition to collection of data at 213 K (see Chapter 4), data for complex **4.1** was collected at room temperature. This room temperature data is not deposited in the CSD. Consequently, this appendix presents the complete details of structure solution and refinement, full tables of bond lengths and angles (with the exception of those to H atoms, which were constrained to fixed lengths), atomic coordinates and equivalent isotropic displacement parameters, anisotropic displacement parameters (all non-H atoms), and hydrogen atom coordinates and isotropic displacement parameters. Chapter 7 discusses treatment of the disordered tetrafluoroborate anion. It is worth noting here that generally, the $U_{(eq)}$ values are roughly cut in half at the lower collection temperature (see Figure C.1 and Tables C.1-C.2), and the esd's on bond lengths and angles drop noticeably, while the agreement factors, i.e. R_1, R_w, etc... are only slightly lowered.

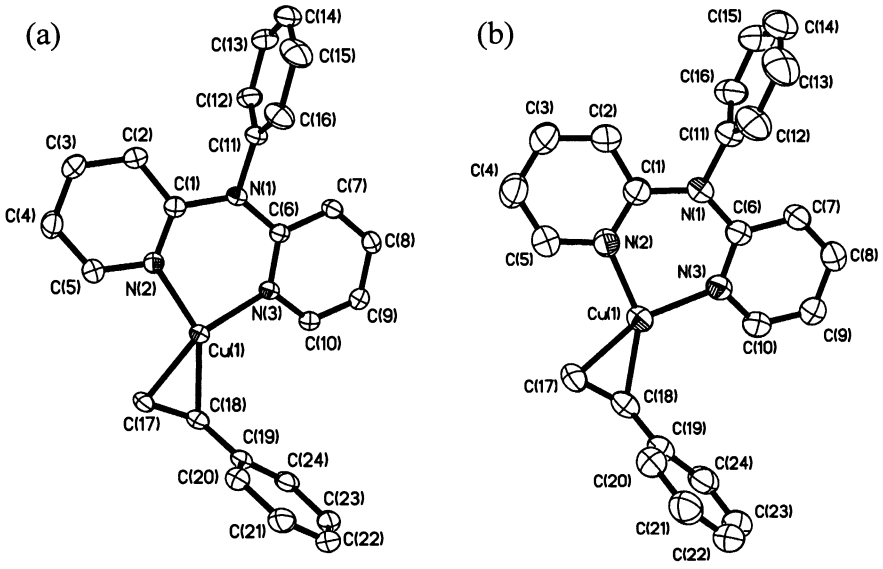

Figure C.1. Comparison of structure of **4.1** at collection temperatures 213 K (a) and 298 K (b). Thermal ellipsoids are set at the 30% level, and all H atoms are omitted for clarity.

Table C.1. Comparison of data collection and refinement details for the two structures determined (at T = 298 K and 213 K) for compound **4.1**.

Compound	**4.1** (298 K)	**4.1** (213 K)
empir. formula	$CuC_{26}H_{27}N_3OBF_4$	$CuC_{26}H_{27}N_3OBF_4$
M_W	547.86	547.86
cryst. system	monoclinic	monoclinic
space group	$P2_1/c$	$P2_1/c$
a, Å	13.340(3)	13.238(3)
b, Å	11.237(2)	11.178(2)
c, Å	17.596(4)	17.418(4)
β, deg.	103.57(3)	103.54(3)
V, $Å^3$	2563.9(9)	2505.7(9)
Z	4	4
D_{calc}, g/cm^3	1.419	1.452
μ, mm^{-1}	0.905	0.926
2θ range, deg.	4.34 - 56.70	3.16 - 58.00
No. collected	30675	30328
No. ind. (R_{int})	6243 (0.0413)	6246 (0.0495)
No. obsd. ($\|F_o\| > 4.0\sigma \|F_o\|$)	3551	4852
R	0.0483	0.0411
R_w	0.1299	0.1133
$\Delta\rho_{max/min}$ ($eÅ^{-3}$)	0.488, -0.287	0.497, -0.752
weights	0.0789, 0.6172	0.0672, 0.9725
CCDC Dep. No.	-	724010

Table C.2. Final coordinates and equivalent isotropic displacement parameters of non-hydrogen atoms of **4.1** at collection temperature of 298 K. Final column lists U_{eq} at 213 K for comparison.

atom	x	y	z	T = 298 K U_{eq}(Å^2)	T = 213 K U_{eq}(Å^2)
Cu1	0.38760(3)	0.40428(3)	0.69367(2)	0.0639(2)	0.0375(1)
N1	0.26311(19)	0.6165(2)	0.59049(14)	0.0627(8)	0.0376(5)
N2	0.24859(19)	0.4676(2)	0.68434(14)	0.0649(9)	0.0369(5)
N3	0.42902(17)	0.5242(2)	0.62707(13)	0.0562(8)	0.0331(4)
C1	0.2108(2)	0.5638(3)	0.64294(18)	0.0667(11)	0.0409(6)
C2	0.1181(3)	0.6137(4)	0.6510(3)	0.115(2)	0.0712(11)
C3	0.0632(3)	0.5603(5)	0.6983(3)	0.120(2)	0.0739(11)
C4	0.1000(3)	0.4596(4)	0.7382(2)	0.0921(16)	0.0554(8)
C5	0.1912(3)	0.4175(3)	0.7302(2)	0.0820(12)	0.0469(7)
C6	0.3659(2)	0.6054(2)	0.58480(15)	0.0539(9)	0.0322(5)
C7	0.4029(2)	0.6812(3)	0.53453(17)	0.0644(10)	0.0397(6)
C8	0.5024(3)	0.6753(3)	0.52883(18)	0.0686(11)	0.0409(6)
C9	0.5682(2)	0.5944(3)	0.57418(17)	0.0635(10)	0.0384(6)
C10	0.5288(2)	0.5226(3)	0.62136(17)	0.0628(10)	0.0358(5)
C11	0.2001(2)	0.7010(3)	0.53581(18)	0.0687(11)	0.0420(6)
C12	0.1450(3)	0.6619(4)	0.4661(2)	0.0947(16)	0.0549(8)
C13	0.0832(3)	0.7438(6)	0.4153(3)	0.115(2)	0.0684(11)
C14	0.0780(4)	0.8582(6)	0.4378(4)	0.118(2)	0.0701(11)
C15	0.1339(4)	0.8953(4)	0.5066(4)	0.117(2)	0.0744(10)
C16	0.1965(3)	0.8175(3)	0.5571(2)	0.0888(14)	0.0588(8)
C17	0.4121(3)	0.2763(3)	0.77313(18)	0.0768(13)	0.0425(6)
C18	0.5020(3)	0.2889(3)	0.74809(17)	0.0692(11)	0.0411(6)
C19	0.5381(2)	0.2068(3)	0.69538(18)	0.0675(11)	0.0412(6)
C20	0.4754(3)	0.1164(3)	0.6547(2)	0.0802(12)	0.0489(7)

Table C.2. contd.

atom	x	y	z	T = 298 K $U_{eq}(Å^2)$	T = 213 K $U_{eq}(Å^2)$
C21	0.5143(4)	0.0385(4)	0.6080(3)	0.109(2)	0.0650(10)
C22	0.6142(5)	0.0491(5)	0.6009(3)	0.116(2)	0.0715(11)
C23	0.6753(4)	0.1352(5)	0.6390(3)	0.110(2)	0.0685(11)
C24	0.6382(3)	0.2153(4)	0.6868(2)	0.0886(16)	0.0541(8)
*F1A	0.1932(7)	0.0979(10)	0.7876(7)	0.153(4)	0.090(3)
*F1B	0.1442(7)	0.1236(8)	0.7188(10)	0.178(5)	0.065(2)
*F2A	0.1218(11)	-0.0671(16)	0.7143(10)	0.173(8)	0.0610(18)
*F2B	0.2747(8)	-0.0014(11)	0.7125(7)	0.117(4)	0.105(5)
*F3A	0.1867(9)	0.1142(10)	0.6641(7)	0.206(5)	0.096(2)
*F3B	0.2031(6)	0.0045(11)	0.8149(4)	0.162(4)	0.116(3)
*F4A	0.2765(9)	-0.0197(15)	0.7289(9)	0.153(5)	0.107(2)
*F4B	0.1039(10)	-0.0315(15)	0.6945(8)	0.118(5)	0.134(4)
B1	0.1877(4)	0.0248(5)	0.7316(4)	0.097(2)	0.0667(12)
O1S	0.2616(8)	0.2483(8)	0.5564(6)	0.330(6)	0.1306(16)
C1S	0.1791(8)	0.2938(9)	0.5009(7)	0.232(6)	0.0889(16)
C2S	0.1726(9)	0.2253(8)	0.4328(6)	0.265(6)	0.1031(16)

Table C.3. Idealized positions and isotropic displacement parameters of H-atoms.

Atom	x	y	z	$U_{iso}(Å^2)$
H2AA	0.0936	0.6831	0.6242	0.138
H3AA	0.0009	0.5928	0.7031	0.144
H4AA	0.0633	0.4213	0.7699	0.11
H5AA	0.2168	0.3492	0.758	0.098
H7AA	0.3587	0.7364	0.5046	0.077
H8AA	0.5261	0.7253	0.4947	0.082
H9AA	0.6372	0.5896	0.5723	0.076
H10A	0.5731	0.4682	0.6521	0.075
H12A	0.1477	0.5825	0.4519	0.114
H13A	0.046	0.7192	0.3663	0.138
H14A	0.0349	0.9114	0.405	0.142
H15A	0.1308	0.9747	0.5207	0.141
H16A	0.2357	0.844	0.6049	0.106
H17A	0.3742	0.2029	0.7585	0.092
H17B	0.4148	0.3005	0.8265	0.092
H18A	0.5579	0.3273	0.7864	0.083
H20A	0.4076	0.1088	0.6591	0.096
H21A	0.4725	-0.0216	0.5813	0.131
H22A	0.6396	-0.0038	0.5693	0.139
H23A	0.7429	0.1417	0.6338	0.132
H24A	0.6812	0.2748	0.7129	0.106
H1SA	0.24	0.2081	0.588	0.495
H1SB	0.1906	0.377	0.4908	0.279
H1SC	0.1159	0.2873	0.5189	0.279
*H2SA	0.1174	0.2547	0.3919	0.398
*H2SB	0.1596	0.1437	0.4435	0.398
*H2SC	0.2364	0.2309	0.4167	0.398
*H2SD	0.2249	0.1648	0.4428	0.398
*H2SE	0.1826	0.2758	0.3912	0.398
*H2SF	0.1058	0.1886	0.418	0.398

Table C.4. Anisotropic Displacement parameters.

Atom	U(1,1)	U(2,2)	U(3,3)	U(2,3)	U(1,3)	U(1,2)
Cu1	0.0747(3)	0.0559(2)	0.0629(3)	0.0106(2)	0.0198(2)	0.0073(2)
N1	0.066(2)	0.0612(15)	0.0608(14)	0.0121(11)	0.0147(12)	0.0086(11)
N2	0.073(2)	0.0627(15)	0.0612(14)	0.0037(12)	0.0211(12)	0.0004(12)
N3	0.062(1)	0.0512(13)	0.0542(13)	0.0008(10)	0.0109(10)	0.0022(10)
C1	0.063(2)	0.074(2)	0.0633(18)	0.0055(15)	0.0149(14)	0.0036(15)
C2	0.087(3)	0.141(4)	0.130(4)	0.066(3)	0.049(3)	0.046(3)
C3	0.077(3)	0.168(5)	0.128(4)	0.057(3)	0.050(3)	0.035(3)
C4	0.074(2)	0.117(3)	0.092(3)	0.013(2)	0.033(2)	-0.004(2)
C5	0.088(2)	0.079(2)	0.084(2)	0.015(2)	0.030(2)	0.0025(18)
C6	0.062(2)	0.0502(15)	0.047(1)-0.003(1)	0.007(1)	0.0023(12)	
C7	0.071(2)	0.0594(17)	0.0617(17)	0.0106(14)	0.0126(14)	0.0071(14)
C8	0.081(2)	0.0643(18)	0.0624(17)	0.0050(15)	0.021(2)-0.007(2)	
C9	0.064(2)	0.0632(18)	0.064(2)-0.006(1)	0.017(1)-0.004(1)		
C10	0.064(2)	0.0575(17)	0.064(2)-0.001(1)	0.0088(14)	0.0022(14)	
C11	0.063(2)	0.074(2)	0.067(2)	0.0143(15)	0.0126(15)	0.0098(15)
C12	0.094(3)	0.098(3)	0.079(2)	0.011(2)	-0.006(2)	-0.009(2)
C13	0.087(3)	0.152(5)	0.087(3)	0.031(3)	-0.016(2)	-0.013(3)
C14	0.080(3)	0.142(5)	0.131(4)	0.066(4)	0.023(3)	0.031(3)
C15	0.116(4)	0.096(3)	0.152(5)	0.036(3)	0.056(4)	0.047(3)
C16	0.098(3)	0.079(2)	0.090(2)	0.0108(19)	0.023(2)	0.030(2)
C17	0.100(3)	0.073(2)	0.0615(18)	0.0209(15)	0.0270(17)	0.0139(18)
C18	0.078(2)	0.0651(19)	0.0586(16)	0.0154(14)	0.0043(15)	0.0060(15)
C19	0.073(2)	0.0627(19)	0.0662(18)	0.0216(15)	0.0149(15)	0.0104(15)
C20	0.090(2)	0.074(2)	0.080(2)	0.0069(17)	0.0267(19)	0.0057(18)

Table C.4. contd.

Atom	U(1,1)	U(2,2)	U(3,3)	U(2,3)	U(1,3)	U(1,2)
C21	0.161(5)	0.077(3)	0.097(3)	0.005(2)	0.049(3)	0.013(3)
C22	0.156(5)	0.101(3)	0.110(4)	0.034(3)	0.069(4)	0.054(3)
C23	0.103(3)	0.120(4)	0.120(4)	0.055(3)	0.052(3)	0.046(3)
C24	0.074(2)	0.088(3)	0.103(3)	0.037(2)	0.019(2)	0.0130(19)
O1S	0.353(11)	0.281(9)	0.357(11)	0.052(8)	0.088(9)	0.093(8)
C1S	0.225(10)	0.188(9)	0.310(14)	0.082(9)	0.115(10)	0.049(8)
C2S	0.379(15)	0.137(6)	0.208(9)	-0.041(6)	-0.074(9)	-0.010(7)
F1A	0.144(7)	0.171(8)	0.153(8)	-0.071(7)	0.055(6)	-0.015(6)
F1B	0.146(7)	0.116(5)	0.275(14)	0.078(8)	0.054(8)	0.041(5)
F2A	0.129(11)	0.130(9)	0.296(19)	-0.087(11)	0.123(10)	-0.060(8)
F2B	0.079(7)	0.146(7)	0.146(7)	-0.048(6)	0.064(6)	-0.036(6)
F3A	0.185(9)	0.193(9)	0.211(10)	0.097(8)	-0.014(7)	-0.049(7)
F3B	0.129(5)	0.261(11)	0.090(4)	0.026(6)	0.015(3)	-0.012(7)
F4A	0.077(7)	0.185(10)	0.172(9)	0.012(7)	-0.018(6)	0.046(6)
F4B	0.060(3)	0.173(13)	0.112(4)	-0.021(5)	0.004(3)	-0.010(5)
B1	0.068(3)	0.091(4)	0.128(4)	-0.022(3)	0.016(3)	0.003(3)

Table C.5. Bond distances (Å) at 298 K.

atoms		dist.	atoms		dist.
Cu1	C17	1.979(3)	C6	C7	1.399(4)
Cu1	C18	2.059(4)	C7	C8	1.356(5)
F1A	B1	1.272(13)	C8	C9	1.380(5)
F1B	B1	1.249(11)	C9	C10	1.350(4)
F2A	B1	1.344(18)	C11	C12	1.347(5)
F2B	B1	1.315(13)	C11	C16	1.366(5)
F3A	B1	1.553(13)	C12	C13	1.407(7)
F3B	B1	1.450(10)	C13	C14	1.352(9)
F4A	B1	1.297(14)	C14	C15	1.331(9)
F4B	B1	1.317(16)	C15	C16	1.380(7)
O1S	C1S	1.386(15)	C17	C18	1.379(6)
C1S	C2S	1.410(15)	C18	C19	1.467(5)
N1	C6	1.404(4)	C19	C24	1.382(5)
N1	C11	1.468(4)	C19	C20	1.401(5)
N1	C1	1.411(4)	C20	C21	1.382(6)
N2	C5	1.358(5)	C21	C22	1.373(9)
N2	C1	1.335(4)	C22	C23	1.339(8)
C1	C2	1.395(5)	C23	C24	1.399(7)
C2	C3	1.369(7)	N3	C10	1.358(4)
N3	C6	1.342(3)			

Table C.6. Bond angles (°) at 298 K.

atoms			angle (°)	atoms			angle (°)
N2	CU1	N3	95.45(10)	N1	C1	C2	118.9(3)
N2	CU1	C17	108.65(14)	N2	C1	C2	120.0(3)
N2	CU1	C18	148.45(13)	N1	C1	N2	121.0(3)
N3	CU1	C17	154.72(14)	C1	C2	C3	119.9(4)
N3	CU1	C18	115.54(13)	C2	C3	C4	119.9(4)
C17	CU1	C18	39.86(16)	C3	C4	C5	117.7(4)
C1	N1	C6	130.6(2)	N2	C5	C4	124.5(3)
C6	N1	C11	115.4(2)	N3	C6	C7	119.7(3)
C1	N1	C11	113.9(2)	N1	C6	C7	119.1(2)
Cu1	N2	C5	117.0(2)	N1	C6	N3	121.2(2)
Cu1	N2	C1	124.7(2)	C6	C7	C8	120.9(3)
C1	N2	C5	117.8(3)	C7	C8	C9	119.4(3)
Cu1	N3	C6	125.02(19)	C8	C9	C10	117.6(3)
C6	N3	C10	117.8(2)	N3	C10	C9	124.6(3)
Cu1	N3	C10	117.2(2)	N1	C11	C16	119.5(3)
C17	C18	C19	125.2(3)	N1	C11	C12	119.5(3)
Cu1	C18	C19	114.8(2)	C12	C11	C16	121.0(3)
Cu1	C18	C17	66.9(2)	C11	C12	C13	118.6(4)
C18	C19	C24	119.6(3)	C12	C13	C14	119.9(5)
C20	C19	C24	118.1(3)	C13	C14	C15	120.5(6)
Cu1	C17	C18	73.2(2)	C14	C15	C16	120.8(5)
C11	C16	C15	119.1(4)	C1S	O1S	H1SA	110

Appendix D

Molecular Structure of Methylated Meerwin's Ester

The structural characterization of tetramethyl-(1-methyl-2-oxo-6-hydroxy-(bicyclo[1.3.3]-nonane))-1,3,5,7-tetracarboxylate (**D.1**) was performed via single crystal X-ray diffraction.[1] General procedures for the collection of X-ray data are described in chapter 1. Selected bond lengths and angles are given in Table D.1; pertinent details of data collection and refinement are given in Table D.2.

Table D.1. Selected bond lengths (Å) and angles (°) in conformers of **D.1**.

	(a)		(b)
O(1)-C(4)	1.342(4)	O(11)-C(22)	1.347(4)
O(6)-C(13)	1.227(5)	O(16)-C(31)	1.227(5)
O(2)-C(7)	1.205(4)	O(12)-C(25)	1.209(4)
O(5)-C(13)	1.329(5)	O(15)-C(31)	1.322(5)
O(5)-C(14)	1.454(5)	O(15)-C(32)	1.449(6)
C(8)-C(10)	1.541(5)	C(26)-C(28)	1.544(5)
C(4)-C(5)	1.347(5)	C(22)-C(23)	1.345(5)
C(2)-C(1)-C(6)	108.7(3)	C(20)-C(19)-C(24)	109.4(3)
C(1)-C(7)-C(8)	118.6(3)	C(19)-C(25)-C(26)	118.4(3)
C(3)-C(4)-C(5)	122.7(3)	C(21)-C(22)-C(23)	122.2(3)

Refinement of the noncentrosymmetric structure was performed using TWIN and BASF instructions, and merging Friedel pairs, MERG 4 (all atoms with Z < Si), as previously described (Flack, 2000).

Table D.2. Summary of X-ray diffraction data for compound **D.1**.

compound	(**D.1**)
empir. formula	$C_{18}H_{22}O_{10}$
M_W	398.36
cryst. system	Orthorhombic
space group	$Pna2_1$
a, Å	16.400(3)
b, Å	11.699(2)
c, Å	19.703(4)
V, $Å^3$	3780(1)
Z	8
D_{calc}, g/cm^3	1.400
μ, mm^{-1}	0.115
2θ range, deg.	4.04 - 56.70
no. collected	38032
no. ind. (R_{int})	4807 (0.0441)
no. obsd. ($\|F_o\| > 4.0\sigma \|F_o\|$)	3320
R	0.0433
R_w	0.0969
$\Delta\rho_{max/min}$ ($eÅ^{-3}$)	0.233, -0.169
weights	0.0366 1.4845
CCDC no.	703400

The program PLATON was employed for structure validation,[2,3] Each of the two independent molecules in the asymmetric unit exhibit an intramolecular H-bonding interaction between the alcoholic proton and the neighboring carbonyl oxygen from one

of the ester groups [O(1)-H(1A)···O(6) and O(11)-H(11A)···O(16)]. The O···O distances were found to be 2.602(4) and 2.591(4) Å, while the O-H···O angles were both 144°.

(a)

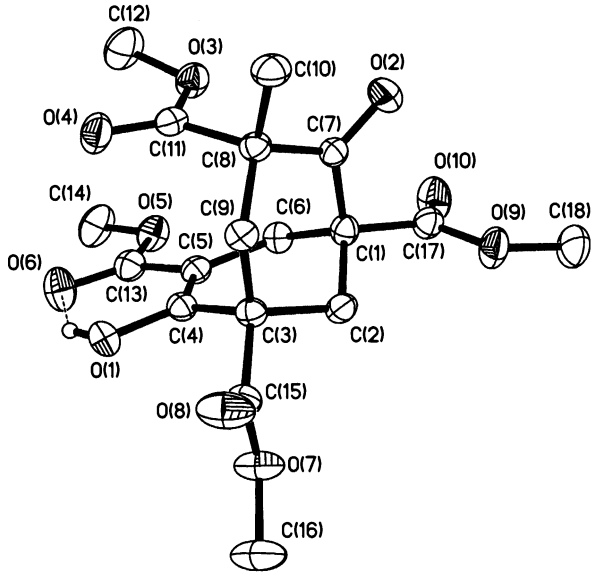

(b)

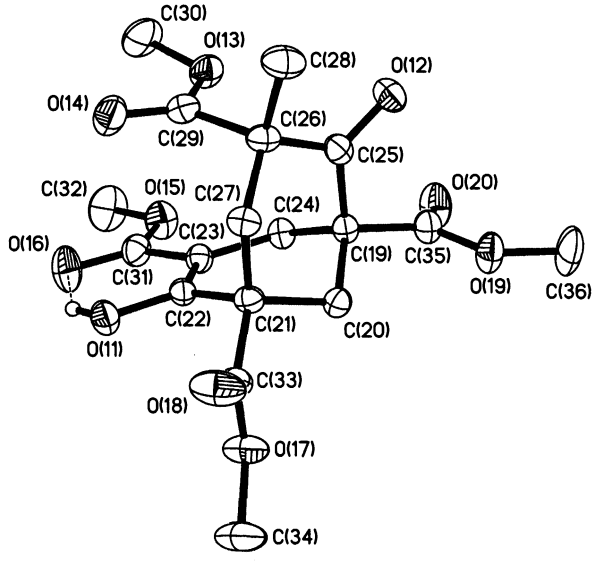

Figure D.1. Molecular structures of the two unique conformers of **D.1** present in the asymmetric unit. Thermal ellipsoids are set at the 30% level, and hydrogen atoms attached to carbon are omitted for clarity.

References

1 V. Russo, J. J. Allen, and Z. T. Ball, *Chem Comm*, 2009, 595-596.

2 A. L. Spek, *PLATON, Molecular Geometry Program*, 2008, Utrecht, The Netherlands.

3 A. L. Spek, *J. Appl. Cryst.*, 2003, **36**, 380-388.

Appendix E

Publications List

1. "Unusual Co-Crystallization of both Monomeric and Dimeric Forms of Cu[PhN(py)(quin)]Cl2, J. J. Allen and A. R. Barron, J. Chem. Cryst., DOI. 10.1007/s10870-010-9947-8.
2. "Demonstration of Remote Steric Differentiation of *cis/trans* Alkene Coordination in Copper(I) Complexes of Aryl-substituted *Bis*(2-pyridyl)amine. J. J. Allen and A. R. Barron, *Dalton Trans.*, 2011, **40**, 1189 - 1194.
3. "Synthesis and Characterization of Aryl Substituted *Bis*(2-pyridyl)amines and their Copper Olefin Complexes: Investigation of Remote Steric Control Over Olefin Binding." J. J. Allen, C. E. Hamilton, and A. R. Barron. *Dalton Trans.*, 2010, **39**, 11451-11468..
4. "Cross coupling of substituted anilines with quinoline: Synthesis and Structural Characterization of HN(py)quin, PhN(py)quin, MesN(py)quin, and [H(PhN(py)quin]BF_4" J. J. Allen, C. E. Hamilton, and A. R. Barron, *J. Chem. Cryst.*, 2010, **40**, 137-144.
5. "Synthesis and Structural Characterization of (2,6-$^{i}Pr_2C_6H_3$)N(quin)$_2$ and [Cu{(2,6-$^{i}Pr_2C_6H_3$)-N(quin)$_2$}$_2$]BF_4" J. J. Allen, C. E. Hamilton, and A. R. Barron, *J. Chem. Cryst.*, 2010, **40**, 130-136.
6. "Synthesis and Structural Characterization of [Ag(H-dpa)(η^2-styrene)]BF_4: Comparing Silver and Copper for Olefin Binding" J. J. Allen and A. R. Barron, *J. Chem. Cryst.*, 2009, **39**, 935-939.
7. "Molecular Structures of RN(H)Py (R = 2,4,6-$Me_3C_6H_3$, 2,6-$Et_2C_6H_3$, Ph_3C), and the Copper Complex [Cu{(2,4,6-$Me_3C_6H_3$)N(H)Py}$_2$]BF_4" J. J. Allen, C. E. Hamilton, and A. R. Barron, *J. Chem. Cryst.*, 2009, **39**, 573-580.

8. "Olefin Coordination in Copper(I) Complexes of *Bis*(2-pyridyl)amine" J. J. Allen and A. R. Barron. *Dalton Trans.*, 2009, 878-890.

9. "Synthesis and Isotopic Labeling of a Naturally-occurring Alkyl-thiadiamondoid by Selective Mono-methylation of Meerwein's Ester" V. Russo, J. J. Allen, and Z. T. Ball. *Chem. Commun.*, 2009, 595.

10. "Molecular Structure of Quinolin-1-(2-quinolyl)-2-one-mesitylimine: An Unusual Amination Product of 2,4,6-Trimethylaniline and 2-Chloroquinoline." J. J. Allen, C. E. Hamilton, and A. R. Barron, *J. Chem. Cryst.*, 2008, **38**, 873.

11. "Molecular Structure of $[Cu_2(MeCN)_2(\mu\text{-tpy})_2][BPh_4]_2$: A Helical Di-Cuprous Terpyridine Complex." J. J. Allen and A. R. Barron, *J. Chem. Cryst.*, 2008, **38**, 879-882.

12. "Refinement of Crystallographic Disorder in the Tetrafluoroborate Anion" J. J. Allen and A. R. Barron, Connexions module: m36687, 2011; http://cnx.org/content/m36687/1.1/.

13. A. R. Barron, J. J. Allen, C. E. Hamilton, R. C. Schucker, and M. F. Lynch, *Olefin Separation Agents and Methods of Designing, Preparing, and Utilizing Same*, Application for United States Letters Patent.